

SPATIAL AND SEASONAL VARIABILITY OF WATERSHED RESPONSE TO  
ANTHROPOGENIC NITROGEN LOADING IN A MOUNTAINOUS WATERSHED

by

Kristin Kiara Gardner

A dissertation submitted in partial fulfillment  
of the requirements for the degree

of

Doctor of Philosophy

in

Ecology and Environmental Science

MONTANA STATE UNIVERSITY  
Bozeman, Montana

November, 2010

©COPYRIGHT

by

Kristin Kiara Gardner

2010

All Rights Reserved

APPROVAL

of a dissertation submitted by

Kristin Kiara Gardner

This dissertation has been read by each member of the dissertation committee and has been found to be satisfactory regarding content, English usage, format, citation, bibliographic style, and consistency and is ready for submission to the Division of Graduate Education.

Dr. Brian L. McGlynn

Approved for the Department of Land Resources and Environmental Sciences

Dr. Tracy M. Sterling

Approved for the Division of Graduate Education

Dr. Carl A. Fox

## STATEMENT OF PERMISSION TO USE

In presenting this dissertation in partial fulfillment of the requirements for a doctoral degree at Montana State University, I agree that the Library shall make it available to borrowers under rules of the Library. I further agree that copying of this dissertation is allowable only for scholarly purposes, consistent with “fair use” as prescribed in the U.S. Copyright Law. Requests for extensive copying or reproduction of this dissertation should be referred to ProQuest Information and Learning, 300 North Zeeb Road, Ann Arbor, Michigan 48106, to whom I have granted “the exclusive right to reproduce and distribute my dissertation in and from microform along with the non-exclusive right to reproduce and distribute my abstract in any format in whole or in part.”

Kristin Kiara Gardner

November, 2010

## ACKNOWLEDGEMENTS

First and foremost, I would like to thank my advisor Dr. Brian McGlynn for his continuous support, encouragement, and brilliance throughout my long, winding graduate program; a program, which transformed from a couple of research ideas to grant proposals to a well-funded research study. I greatly appreciate Brian's patience and willingness to adapt to my non-traditional graduate program as I moved through major milestones in my life, which included a move to Big Sky, marriage, employment, and most recently my first child, Elijah. I am thankful for the support and guidance from the rest of my committee members, Dr. Wyatt Cross, Dr. Rick Lawrence, Dr. Lucy Marshall, and Dr. Duncan Patten. A special thank you to Lucy for her modeling guidance and patience mentoring a novice Bayesian modeler. I am appreciative of the support, conversations, companionships, and help with large sampling events from Watershed Hydrology labmates: Tim, Becca, Galena, Diego, Vince, Kelsey, John, Austin, Trish, and Luke. Other folks at MSU, who helped with my field-work include: Kristy Segal, Natalie Campos, Greg Pederson, and Todd and Julie Kipfer. A special thank you to the community of Big Sky for actively supporting my research project. I would like to dedicate this dissertation to my Mom, who's spirit of adventure has brought me to where I am today and who taught me that the world is my oyster with a little hard work and perseverance. Finally, to my beloved husband, Jeremy, son, Elijah, dog, Thailer, and cat, Narnia – thank you for making our home a harmonious and peaceful retreat, for putting up with my crazy work hours, for continuous and generous support, and for always bringing a smile to my heart after a long day.

## TABLE OF CONTENTS

1. INTRODUCTION .....	1
Site Description.....	3
Dissertation Organization .....	5
References Cited.....	8
2. SEASONALITY IN SPATIAL VARIABILITY AND INFLUENCE OF LAND USE/LAND COVER AND WATERSHED CHARACTERISTICS ON STREAMWATER NITRATE CONCENTRATIONS IN A DEVELOPING WATERSHED IN THE ROCKY MOUNTAIN WEST .....	12
Contribution of Authors and Co-Authors .....	12
Manuscript Information .....	13
Abstract.....	14
Introduction.....	15
Methods.....	18
Study Area .....	19
Synoptic Streamwater Sampling and Chemistry Analysis .....	21
Terrain Analysis.....	22
Statistical Analysis.....	25
Potential Predictor Variables .....	25
Spatial Linear Models.....	25
Semivariogram Plots.....	31
Results.....	31
Discussion.....	33
Is there Seasonality in the Spatial Patterns of Streamwater N? .....	34
What is the influence of LULC and Watershed Characteristics on Streamwater N and Do the Influences Change Seasonally?.....	36
What is the Role of Spatial Location of N Loading?.....	40
Conclusions.....	42
Acknowledgements.....	43
References Cited.....	44
3. A MULTI-ANALYSIS APPROACH TO ASSESS THE SPATIO-TEMPORAL PATTERNS OF WATERSHED RESPONSE TO LOCALIZED INPUTS OF NITROGEN .....	63
Contribution of Authors and Co-Authors .....	63
Manuscript Information .....	64

## TABLE OF CONTENTS - CONTINUED

Abstract.....	65
Introduction.....	66
Methods.....	74
Study Area .....	74
Watershed Streamwater and Snow Sampling.....	75
Chemistry Analysis of Streamwater and Snow Samples.....	75
Stream Discharge Measurements.....	77
N Export, Load, and Retention Calculations .....	77
Isotopic Separation of Streamwater NO <sub>3</sub> <sup>-</sup> Sources .....	79
Results.....	80
Spatial and Seasonal Patterns of NO <sub>3</sub> <sup>-</sup> , DON, and DOC Concentrations .....	80
Annual and Seasonal NO <sub>3</sub> <sup>-</sup> , DON, and DOC Export .....	84
Annual Watershed N Loading and Watershed N Retention.....	86
Isotopic Separation of Streamwater NO <sub>3</sub> <sup>-</sup> Sources .....	87
Discussion.....	89
Does Anthropogenic N Loading Influence the Spatio-Temporal Patterns of NO <sub>3</sub> <sup>-</sup> , DON, and DOC Export, Concentrations, and Stoichiometric Ratios? .....	89
Annual NO <sub>3</sub> <sup>-</sup> , DON, and DOC Export.....	89
Seasonal NO <sub>3</sub> <sup>-</sup> , DON, and DOC Export .....	94
Seasonal NO <sub>3</sub> <sup>-</sup> , DON, and DOC Concentration Patterns.....	96
Do Localized Inputs of Anthropogenic N Lead to Similar Stages of Watershed Saturation Observed at the Catchment Outlet as Spatially Distributed Inputs From Atmospheric Deposition?.....	101
Are There Spatially and Seasonal Variations in the Impact of Anthropogenic N Loading on Streamwater NO <sub>3</sub> <sup>-</sup> ? .....	106
Spatio-Temporal Sources of Streamwater NO <sub>3</sub> <sup>-</sup> .....	106
Seasonal Sources of Streamwater NO <sub>3</sub> <sup>-</sup> .....	108
Conclusions.....	111
Acknowledgements.....	113
References Cited .....	114
 4. QUANTIFYING WATERSHED SENSITIVITY TO SPATIALLY VARIABLE NITROGEN LOADING AND THE RELATIVE IMPORTANCE OF NITROGEN RETENTION MECHANISMS .....	 144
Contribution of Authors and Co-Authors .....	144
Manuscript Information .....	145
Abstract.....	146
Introduction.....	147
Study Area .....	150
Methods.....	152

## TABLE OF CONTENTS - CONTINUED

Streamwater Sampling and Chemistry Analysis.....	153
Geologic Weathering Experiments.....	155
Atmospheric Deposition.....	156
Watershed Characteristics.....	157
Terrain Analysis.....	157
Land Cover Analysis.....	159
Big Sky Nutrient Export Model.....	161
BiSN Model Specification and Parameter Estimation.....	163
BiSN Inference and Markov Chain Monte Carlo Methods.....	163
BiSN Implementation.....	165
Prior Densities.....	165
Model Convergence.....	166
Model Uncertainty.....	167
Results.....	167
Model Performance and Model Uncertainty.....	168
Parameter Estimates.....	169
Drivers of the Spatial Heterogeneity of Streamwater NO <sub>3</sub> <sup>-</sup> Export.....	172
Discussion.....	173
Model Performance and Model Uncertainty.....	173
Drivers of the Spatial Heterogeneity of Streamwater NO <sub>3</sub> <sup>-</sup> Export.....	175
Spatial Distribution of NO <sub>3</sub> <sup>-</sup> Loading, Retention and Export Across Land Use/Land Cover and Landscape Position.....	182
Conclusions.....	187
Acknowledgements.....	188
References Cited.....	189
 5. SUMMARY.....	 214
References Cited.....	222
 APPENDICES.....	 223
APPENDIX A: Atmospheric Deposition Calculation for the Big Sky Nutrient Export Model (BiSN).....	224
APPENDIX B: Instream Nitrogen Decay Model Description.....	226

## LIST OF TABLES

Table	Page
2.1 Synoptic sampling event dates and corresponding hydrological condition and biological activity potential.....	53
2.2 Potential explanatory variables of streamwater NO <sub>3</sub> <sup>-</sup> in the West Fork watershed .....	53
2.3 Spatial linear models fitted to streamwater NO <sub>3</sub> <sup>-</sup> for each synoptic campaign (see Table 2.2 for variable descriptions).....	54
2.4 Spatial covariance parameters for the spatial linear models fitted to streamwater NO <sub>3</sub> <sup>-</sup> for each synoptic sampling campaign (see Table 2.2 for variable descriptions).....	55
3.1 Watershed characteristics for the West Fork watershed and five subwatersheds. Location of subwatersheds is illustrated in Figure 3.1B ....	126
3.2 Median C and N concentrations and ratios from three synoptic campaigns representing a range in hydrological conditions and biological activity potential.....	126
3.3 Annual streamwater N and C export in the West Fork watershed and five subwatersheds. Location of subwatersheds is illustrated in Figure 3.1B .....	127
3.4 N loading and export, and retention in the West Fork watershed and five subwatersheds. Location of subwatersheds is illustrated in Figure 3.1B .....	128
3.5 Estimated source of N loading to West Fork watershed and five subwatersheds. Table 3.1 describes the subwatershed abbreviations. Location of subwatersheds is illustrated in Figure 3.1B.....	128
3.6 Comparison of NO <sub>3</sub> <sup>-</sup> , DON, and DOC export from Rocky Mountain watersheds.....	129
3.7 Sources of streamwater NO <sub>3</sub> <sup>-</sup> and their uncertainty estimated from a three component mixing model. Location of subwatersheds is illustrated in Figure 3.1B .....	129

## LIST OF TABLES – CONTINUED

Table	Page
4.1 Prior distributions of BiSN parameters and corresponding references used to determine the range of possible prior values.....	201
4.2 The 5 <sup>th</sup> and 95 <sup>th</sup> percentile of sampled parameter values and the parameter values corresponding to the maximum log-likelihood of BiSN runs. Abbreviations for parameters are described in Table 4.1 .....	202
4.3 Modeled sources of N loading for subwatersheds corresponding to Figures 4.9 and 4.10. Map codes correspond to sites depicted in Figure 4.10A. Abbreviations for N sources are described in Table 4.1 .....	203
4.4 Prior distributions of BiSN parameters and corresponding references used to determine the range of possible prior values. Percent retention excluding upland retention is in parenthesis. Map codes correspond to sites depicted in Figure 4.10A.....	204

LIST OF FIGURES

Figure	Page
1.1 A) Location of the West Fork watershed (212 km <sup>2</sup> ) in southwestern Montana. (B) Map of the West Fork watershed (212 km <sup>2</sup> ) in the Gallatin and Madison Mountain ranges of southwestern Montana showing the locations of ski resorts, structures, and Big Sky Water and Sewer boundaries. (C) An expanded view of the wastewater storage ponds and the Big Sky Resort Golf Course. Wastewater effluent is stored in the ponds and irrigated onto the golf course from mid-May through early October.....	11
2.1 (A) Location of the West Fork watershed (212 km <sup>2</sup> ) in southwestern Montana. (B) Map of the West Fork watershed showing locations of 50 synoptic sampling sites, building structures, and the Big Sky Water and Sewer District boundaries. The West Fork (WF) drains into the Gallatin River (a tributary of the Upper Missouri River) and is comprised of three main tributaries: the Middle Fork (MF), the North Fork (NF), and the South Fork (SF). (C) An expanded view of the wastewater storage ponds and the Big Sky Resort Golf Course. Wastewater effluent is stored in the ponds and irrigated onto the golf course from mid-May through early October.....	56
2.2 A simplified example of watershed E and subwatersheds A-D to illustrate modeled spatial dependence in a stream network. (a) Spatial dependence of stream sites is considered only if sites are flow connected. If water flows downstream between two sites, than they are considered “flow connected”. a and c and b and c are “ <i>flow connected</i> ” sites, while a and b are “ <i>not flow connected</i> ” sites. (b)The proportional influence ( <i>PI</i> ) matrix represents the influence of an upstream location on a downstream location. The <i>PI</i> matrix - the <i>PI</i> for a pair of sites is equal to the product of the segment PIs found in the path between them (modified <i>Peterson et al.</i> , 2007 – Figure 2).....	57
2.3 Streamwater NO <sub>3</sub> <sup>-</sup> concentrations for 6 synoptic sampling campaigns capturing a range of seasonal hydrological and biological conditions (Table 2.1). Elevated NO <sub>3</sub> <sup>-</sup> concentrations persist in streams draining Lone Mountain across seasons (grey ovals), while elevated concentrations downgradient from the Big Sky Golf Course are elevated only in the winter months during periods of low potential biologic activity (grey rectangles) .....	58

## LIST OF FIGURES – CONTINUED

Figure	Page
2.4 Synoptic $\text{NO}_3^-$ concentrations for the 6 synoptic sampling campaigns conducted between September 2005 and August 2007. Each boxplot consists of 46-50 data points. Streamwater $\text{NO}_3^-$ concentrations and variability are highest during late fall, winter, and early spring during periods of low streamflow and limited biologic activity. The weekly time series for two sites with varying levels of N loading are included for context and are represented by squares (Middle Fork – high N loading), crosses (South Fork – medium N loading) and triangles (North Fork – low N loading) .....	59
2.5 Median streamwater $\text{NO}_3^-$ concentrations of sites located downgradient from the Big Sky Golf Course (black circles) and Lone Mountain (black triangles) for each synoptic event (grey boxplots). Streamwater $\text{NO}_3^-$ at sites draining Lone Mountain remain relatively elevated throughout the year, while streamwater $\text{NO}_3^-$ concentrations at sites downgradient from the Big Sky Golf Course exhibit a more amplified seasonal pattern.....	60
2.6 Semivariograms of unmodeled synoptic streamwater $\text{NO}_3^-$ . Seasonality exists in the degree autocovariance variance between “flow connected” sites (black circles) and is not apparent in “not-flow connected” sites (grey circles). Dormant season semivariograms (February -winter, October - late fall and March early spring) illustrate a greater autocorrelated variance than growing season (June - late spring, August - summer, and September -late summer). This difference in autocorrelated variability suggests the importance of a biologic component in streamwater $\text{NO}_3^-$ patterns during periods of high potential biologic activity. Symbol size is proportional to the number of pairs at each lag distance .....	61
2.7 Semivariograms of spatial model residuals of synoptic streamwater $\text{NO}_3^-$ . Seasonality exists in the range of spatial dependence between “ <i>flow connected</i> ” sites (black circles) and is not apparent in “ <i>not-flow connected</i> ” sites (grey circles). The range of spatial dependency is longer in the dormant season (February -winter, October - late fall and March - early spring) as compared to the growing season (June - late spring, August - summer, and September -late summer). The shorter range in the growing season suggests the importance of a biologic component in streamwater $\text{NO}_3^-$ patterns during periods	

LIST OF FIGURES – CONTINUED

Figure	Page
of high potential biologic activity. Symbol size is proportional to the number of pairs at each lag distance .....	62
3.1 A) Location of the West Fork watershed (212 km <sup>2</sup> ) in southwestern Montana, with locations of the atmospheric deposition data sites. (B) Map of the West Fork watershed showing locations of 50 synoptic sampling sites, 6 weekly sampling sites, building structures, and the Big Sky Water and Sewer District boundaries. The West Fork (WF) drains into the Gallatin River (a tributary of the Upper Missouri River) and is comprised of three main tributaries: the Middle Fork (MF), the North Fork (NF), and the South Fork (SF). (C) An expanded view of Meadow Village with wastewater storage ponds and the Big Sky Resort Golf Course. Wastewater effluent is stored in the ponds and irrigated onto the golf course from mid-May through early October .....	126
3.2 In the West Fork watershed, residential development and annual average streamwater NO <sub>3</sub> <sup>-</sup> -N concentrations in the West Fork have followed a similar upward trend since resort development. [ <i>NSF, 1976; Blue Water Task Force, and Big Sky Water and Sewer District, unpublished data</i> ].....	127
3.3 Streamwater NO <sub>3</sub> <sup>-</sup> concentrations and DIN:DON and DOC:DON ratios for 3 synoptic sampling campaigns capturing a range of seasonal hydrological and biological conditions (Table 3.2). (A) Elevated NO <sub>3</sub> <sup>-</sup> concentrations persist in streams draining Lone Mountain across seasons (grey ovals), while elevated concentrations downgradient of Meadow Village are elevated only in the winter months during periods of low potential biologic activity (grey rectangles). (B) DIN:DON ratios were highest during the summer at sites draining alpine areas (black rectangles), and lowest during snowmelt corresponding with peak DON concentrations. DIN:DON was elevated downstream of Meadow Village during winter and snowmelt (black ovals) (C) DOC:DON ratios were smallest during the winter when groundwater flowpaths dominate. During the summer, DOC:DON ratios were smaller in the lower reaches of the South Fork and West Fork (black-dashed ovals) suggesting an instream source of DOM. Otherwise, the West Fork watershed exhibited a high degree of spatial variability in DOC concentrations across seasons .....	128

## LIST OF FIGURES – CONTINUED

Figure	Page
<p>3.4 Weekly time series for the main tributaries of the West Fork (WF) represented by squares (Middle Fork), crosses (South Fork), and triangles (North Fork). Grey boxplots illustrate synoptic <math>\text{NO}_3^-</math>, DOC, and DON concentrations and DIN:DON and DOC:DON ratios for the 6 synoptic sampling campaigns conducted between September 2005 and August 2007. Each boxplot consists of 46-50 data points. (A) Streamwater <math>\text{NO}_3^-</math> concentrations and variability are highest during late fall, winter, and early spring during periods of low streamflow and limited biologic activity. (B) Streamwater DON and (C) DOC concentrations peaked on the ascending limb of the hydrograph and exhibited a high degree of variability the rest of the year. (D) Streamwater DIN:DON ratios were highest during the winter when biological activity is at a minimum. (E) Streamwater DOC:DON ratios were highest just prior to snowmelt, corresponding to peak DOC concentrations and otherwise, exhibit a high degree of variability the rest of the year.....</p>	129
<p>3.5 Concentration-discharge relationships for the lower Middle Fork (LMF) and the Upper North Fork (UNF), two streams with contrasting land use and watershed characteristics (Table 3.1). Relationships between discharge and (A) <math>\text{NO}_3^-</math>, (C) DOC, (D) DIN:DON, and (E) DOC:TDN exhibit clockwise hysteresis at both sites, while the relationship between (B) DON and discharge exhibited clockwise hysteresis at UNF and counterclockwise hysteresis at LMF. This difference may be due to either deeper and/ or longer flowpath source of N (A) <math>\text{NO}_3^-</math> concentration and (D) DIN:DON sharply declined with initial increase in discharge followed by a gradual decline until discharge reached a near minimum and concentration began to rise suggesting biological control of the concentration discharge relationship. DOC (C) and DOC:TDN increased with increasing discharge peaked prior to peak snowmelt indicating a flushing mechanism controlling the concentration discharge relationship. The magnitude of <math>\text{NO}_3^-</math>, DON, and DOC concentrations and DIN:DON DOC:TDN ratios were greater at LMF than UNF throughout snowmelt.....</p>	130
<p>3.6 Cumulative flux of TDN, DON, <math>\text{NO}_3^-</math>, and DOC for 6 stream reaches in the West Fork watershed: (A) upper North Fork (UNF), (B) lower North Fork (LNF), (C) South Fork (SF), (D) West Fork</p>	

## LIST OF FIGURES – CONTINUED

Figure	Page
(WF), (E) upper Middle Fork (UMF) and the (F) lower Middle Fork. The majority of C and N flux occurs at snowmelt during the months of May and June. (B) LMF exported $\text{NO}_3^-$ at twice the rate of the other main West Fork tributaries on the descending limb of the snowmelt hydrograph.....	131
3.7 Annual and seasonal streamwater export of $\text{NO}_3^-$ and DON with corresponding DIN:DON ratios on top of each stacked column. (A) DON was the dominant form of N exported from all subwatersheds, except for LMF. (B) $\text{NO}_3^-$ was the most abundant form of TDN exported in the winter for all subcatchments, while DON dominated TDN during snowmelt (C) and summer (D), except for LMF, where $\text{NO}_3^-$ was more abundant throughout the year .....	132
3.8 Annual and seasonal export of TDN and DOC with corresponding DOC:TDN ratios on top of each stacked column. (C) The majority of DON and DOC export occurred during snowmelt. (A) Annual DON and DOC export was highest at LMF, just downstream from an extensive wetland complex. (D) Generally, DOC:TDN ratios were lowest during the summer except for LMF and the WF. ....	133
3.9 Estimated sources of N loading to the West Fork watershed and five subwatersheds. Atmospheric deposition was the biggest source of N to all subwatersheds. Total N loading varied from $3.39 \text{ kg ha}^{-1}\text{yr}^{-1}$ at LNF to $4.46 \text{ kg ha}^{-1}\text{yr}^{-1}$ at UMF. The highest N loading (UMF) corresponded with the highest TDN and DON export (Table 3.3), while the highest wastewater loading corresponded to the highest $\text{NO}_3^-$ export .....	134
3.10 Watershed retention of (A) TDN, (B) $\text{NO}_3^-$ , and (C) DON increased linearly with N loading. The linear relationship was significant and signified that the West Fork watershed was well below N saturation according to the Michaelis-Menten kinetics model [ <i>Earl et al.</i> , 2006]. As expected in an N limited system, watershed $\text{NO}_3^-$ retention increased at a higher rate than retention of TDN or DON as evident by the slope of the regression line; the slope of $\text{NO}_3^- = 0.93$ versus 0.83 for TDN and 0.90 for DON.....	135
3.11 $\delta^{15}\text{N}$ of $\text{NO}_3^-$ of snow (black triangles), wastewater effluent (black squares), mineral weathering experiment slurries (grey triangles	

## LIST OF FIGURES – CONTINUED

Figure	Page
<p>[<i>Ackerman et al.</i>, in prep.], and a subset of the (A) February and (B) August synoptic samples from the West Fork watershed (black outlined circles) (Figure 3.4A). Streamwater <math>\text{NO}_3^-</math> concentration represented by circle size, ranged from <math>0.04 \text{ mg L}^{-1}</math> to <math>0.045 \text{ mg L}^{-1}</math> in February and <math>0.01 \text{ mg L}^{-1}</math> to <math>0.21 \text{ mg L}^{-1}</math> in August. <math>\delta^{15}\text{N}</math> of <math>\text{NO}_3^-</math> values at sites located downgradient from Meadow Village had enriched <math>\delta^{15}\text{N}</math> of <math>\text{NO}_3^-</math> values in August and February, indicating a significant contribution from wastewater. Other sites appeared to be more influenced by a mixture of geologic weathering, soil water [<i>Kendall and McDonnell</i>, 1998], or precipitation.....</p>	136
<p>3.12 <math>\delta^{15}\text{N}</math> and <math>\delta^{18}\text{O}</math> of <math>\text{NO}_3^-</math> values for a subset of August (A) and February (B) synoptic streamwater samples. <math>\delta^{15}\text{N}</math> of <math>\text{NO}_3^-</math> values at sites located downgradient from Meadow Village had enriched <math>\delta^{15}\text{N}</math> of <math>\text{NO}_3^-</math> values in August and February, indicating a significant contribution from wastewater. Light <math>\delta^{15}\text{N}</math> of <math>\text{NO}_3^-</math> values indicated that sites draining Lone Mountain with high <math>\text{NO}_3^-</math> concentrations were not influenced by wastewater. Median <math>\delta^{18}\text{O}</math> of <math>\text{NO}_3^-</math> was lower suggesting less contribution from atmospheric <math>\text{NO}_3^-</math> [<i>Kendall and McDonnell</i>, 1998] .....</p>	137
<p>3.13 <math>\text{NO}_3^-</math> isotope data from the main West Fork tributaries illustrated seasonal variability in the sources of streamwater <math>\text{NO}_3^-</math>. During snowmelt, enriched <math>\delta^{18}\text{O}</math> of <math>\text{NO}_3^-</math> values at all sites pointed to higher contributions of atmospheric <math>\text{NO}_3^-</math> than other times of year; however, contributions from atmospheric <math>\text{NO}_3^-</math> were less than soil water contributions as evident from <math>\delta^{18}\text{O}</math> of <math>\text{NO}_3^-</math> signatures more similar to soil water <math>\text{NO}_3^-</math>. During summer and winter baseflow, <math>\delta^{15}\text{N}</math> of <math>\text{NO}_3^-</math> values indicated a significant contribution from wastewater to streamwater <math>\text{NO}_3^-</math> concentrations in the Middle Fork and to a lesser degree during snowmelt. In the South Fork, small wastewater contributions were evident in winter and summer baseflow .....</p>	138
<p>3.14 Seasonal variability of streamwater <math>\text{NO}_3^-</math> sources to the three main tributaries of the West Fork estimated through mixing model analysis of <math>\delta^{15}\text{N}</math> and <math>\delta^{18}\text{O}</math> of <math>\text{NO}_3^-</math> values. Seasonal fluctuations occurred in the influences of anthropogenic N on streamwater <math>\text{NO}_3^-</math>. Wastewater influence on streamwater <math>\text{NO}_3^-</math> concentrations was evident in the Middle Fork throughout the year and in the South</p>	

## LIST OF FIGURES – CONTINUED

Figure	Page
	<p>Fork only during winter (“W”) and summer (“W”) baseflow. While in the pristine North Fork, soil water NO<sub>3</sub><sup>-</sup> contributed most to streamwater NO<sub>3</sub><sup>-</sup> concentrations throughout the year. For all three tributaries, soil water NO<sub>3</sub><sup>-</sup> was the most significant source of streamwater NO<sub>3</sub><sup>-</sup> during spring runoff (“SN”) when melt water contributed 69, 86, and 83% of streamwater NO<sub>3</sub><sup>-</sup> in the Middle Fork, South Fork, and North Fork, respectively.....</p>
4.1	139
	<p>(A) Location of the West Fork watershed (212 km<sup>2</sup>) in southwestern Montana, with locations of atmospheric deposition data collection sites. (B) Map of the West Fork watershed showing locations of 50 synoptic sampling sites (black triangles), building structures (grey circles), and the Big Sky Water and Sewer District boundaries (grey hatched lines). The West Fork (WF) drains into the Gallatin River (a tributary of the Upper Missouri River) and is comprised of three main tributaries: the Middle Fork (MF), the North Fork (NF), and the South Fork (SF). (C) An expanded view of the wastewater storage ponds and the Big Sky Resort Golf Course. Wastewater effluent is stored in the ponds and irrigated onto the golf course from mid-May through early October.....</p>
4.1	205
	<p>(A) Location of the West Fork watershed (212 km<sup>2</sup>) in southwestern Montana, with locations of atmospheric deposition data collection sites. (B) Map of the West Fork watershed showing locations of 50 synoptic sampling sites (black triangles), building structures (grey circles), and the Big Sky Water and Sewer District boundaries (grey hatched lines). The West Fork (WF) drains into the Gallatin River (a tributary of the Upper Missouri River) and is comprised of three main tributaries: the Middle Fork (MF), the North Fork (NF), and the South Fork (SF). (C) An expanded view of the wastewater storage ponds and the Big Sky Resort Golf Course. Wastewater effluent is stored in the ponds and irrigated onto the golf course from mid-May through early October.....</p>
4.2	206

## LIST OF FIGURES – CONTINUED

Figure	Page
4.3 (A) Watershed modeling units of the Big Sky Nutrient Model (BiSN) were 231 non-nested stream reach contributing areas ranging in size from 0.01 km <sup>2</sup> to 3.7 km <sup>2</sup> . The stream network was delineated into stream reaches of approximately 500m in length. A 500 m stream reach length was chosen because 97% of measured NO <sub>3</sub> <sup>-</sup> uptake lengths were less than 500m [McNamara <i>et al.</i> , in prep.]. (B) Conceptual model of processes controlling N loading and retention West Fork watershed. Stream reach NO <sub>3</sub> <sup>-</sup> is as function of upstream N inputs and lateral loading from the reach contributing area (A). N can be immobilized instream and in the upland and riparian areas as it travels along hydrological flowpaths to the stream .....	206
4.4 (A) Observed spatial NO <sub>3</sub> <sup>-</sup> concentrations (black bars) from August 7, 2010. NO <sub>3</sub> <sup>-</sup> concentration is greatest in the headwaters of the Middle Fork and elevated in the South Fork and West Fork compared to other streams. (B) Observed streamwater NO <sub>3</sub> <sup>-</sup> export (black bars) generally increased in a downstream direction. (C) When N export is normalized for watershed area, NO <sub>3</sub> <sup>-</sup> export pattern mirrors the patterns of concentrations; NO <sub>3</sub> <sup>-</sup> export is greatest in the headwaters of the Middle Fork and elevated in the South Fork and West Fork compared to other streams. Height of the black bars corresponds to NO <sub>3</sub> <sup>-</sup> export values .....	207
4.5 The spatial variability of observed streamwater NO <sub>3</sub> <sup>-</sup> export (black x's) was well captured by BiSN over a wide range of land use/ land cover and landscape positions with 90% prediction intervals (grey lines). 93% of observed data falls within the 90% prediction intervals. Data is ordered to depict network organization. From the headwaters, the Middle Fork flows into the West Fork (grey squares). Tributaries to the Middle Fork and West Fork include the South Fork and Beehive (grey circles). Yellow mule is a tributary to the South Fork (black outlined circle).....	208
4.6 BiSN was a good predictor of streamwater NO <sub>3</sub> <sup>-</sup> export (Nash-Sutcliffe model efficiency coefficient = 0.90). Model residuals were normally distributed and did not appear to have a pattern about the 1:1 line or to be spatially correlated (Figure 4.7).....	209
4.7 Spatial distribution of NO <sub>3</sub> <sup>-</sup> export model residuals. Model	

## LIST OF FIGURES – CONTINUED

Figure	Page
residuals do not exhibit spatial correlation: Model under-predictions (grey circles) and over-predictions (black circles) appear to be randomly dispersed across the West Fork watershed. The spatial variability of streamwater $\text{NO}_3^-$ export was well captured by the N export model over a wide range of land use/ land cover and landscape positions .....	210
4.8 (A-G) Histograms of model posterior distributions (grey) with corresponding prior distributions (black). Parameters vary in their identifiability: the wastewater (B) and travel parameters (G) were most identifiable, while the vegetation (A) and septic (C) parameters were least identifiable.....	211
4.9 Modeled N loading across the West Fork watershed (A) compared to N loading after travel time decay is applied (B). N originating from soil storage release dominated the $\text{NO}_3^-$ signal. Excluding N loading from soil storage release (C, D – see Figure 4.10), localized small inputs of anthropogenic N from wastewater were responsible for elevated streamwater $\text{NO}_3^-$ export in the lower section of the West Fork (D). Wastewater inputs, which occurred “hydrologically close” to the stream and were smaller relative to other N inputs, had a disproportionate impact on the watershed $\text{NO}_3^-$ export.....	212
4.10 Modeled upland, instream, and riparian $\text{NO}_3^-$ retention across the West Fork watershed. (A) Most N loading was retained in the upland (by either biological processes or lack of a physical transport mechanism (hydrological connectivity). (B) Excluding upland retention, instream processes were responsible for more $\text{NO}_3^-$ immobilization than riparian areas in the majority of the watershed. Numbers correspond to Map codes in Tables 4.3 and 4.4 .....	213

## ABSTRACT

Anthropogenic activity has greatly increased watershed export of bioavailable nitrogen. Escalating levels of bioavailable nitrogen can deteriorate aquatic ecosystems by promoting nuisance algae growth, depleting dissolved oxygen levels, altering biotic communities, and expediting eutrophication. Despite these potential detrimental impacts, there is notable lack of understanding of the linkages between anthropogenic nitrogen inputs and the spatial and seasonal heterogeneity of stream network concentrations and watershed nitrogen export. This dissertation research seeks to more accurately define these linkages by investigating the roles of landscape position and spatial distribution of anthropogenic nitrogen inputs on the magnitude and speciation of watershed nitrogen export and retention and how these roles vary seasonally across contrasting landscapes in a 212 km<sup>2</sup> mountainous watershed in southwest Montana. Results indicate localized inputs of anthropogenic nitrogen occurring in watershed areas with quick transport times to streams had disproportionate effects on watershed nitrogen export compared to spatially distributed or localized inputs of nitrogen to areas with longer transport times. In lower elevation alluvial streams, these effects varied seasonally and were most evident during the dormant winter season by amplified nitrate peaks, elevated dissolved organic nitrogen:dissolved organic nitrogen (DIN:DON) ratios and lower dissolved organic carbon (DOC):total dissolved nitrogen (DOC:TDN). During the summer growing season, biologic uptake of nitrogen masked anthropogenic influences on watershed nitrogen export; however, endmember mixing analysis of nitrate isotopes revealed significant anthropogenic influence during the growing season, despite low nitrate concentrations and DIN:DON ratios. In contrast, streams draining alpine environments consisting of poorly developed, shallow soils and small riparian areas exhibited yearlong elevated nitrate concentrations compared to other sites, suggesting these areas were highly nitrogen enriched. Watershed modeling revealed the majority of watershed nitrogen retention occurred in the upland environment, most likely from biological uptake or lack of hydrologic connectivity. This work has critical implications for watershed management, which include: 1) developing flexible strategies that address varying landscape characteristics and nitrogen loading patterns across a watershed, 2) avoiding clustering nitrogen loading in areas with quick travel times to surface waters, 3) seasonal monitoring to accurately gauge watershed nitrogen saturation status, and 4) incorporating spatial relationships into streamwater nitrogen models.

## CHAPTER 1

## INTRODUCTION

Human impacts on the nitrogen cycle (N) have profoundly affected the natural functioning of world's ecosystems through the addition of bioavailable nitrogen (N) [Vitousek, 1997]. Although N is the most common limiting nutrient in North American forested ecosystems [Cole and Rapp, 1981; Vitousek and Howarth, 1991], research has shown that chronic spatially uniform inputs of N from anthropogenic deposition can saturate biological requirements resulting in "nitrogen saturation" [Aber *et al.*, 1989; 1998]. When N saturation is reached additional N inputs are in excess of biological requirements and are "leaked" to streams and groundwater, commonly as nitrate ( $\text{NO}_3^-$ ) [Gundersen *et al.*, 1998]. Escalating inputs of  $\text{NO}_3^-$  to surface waters can lead to nuisance algal growth, altered biological communities, and in extreme cases, eutrophication [Bisson and Bilby, 2001; Folke *et al.*, 2002].

Identifying the controls of the spatial heterogeneity of streamwater N is critical to preventing the potential adverse effects from watershed N enrichment; however, because of the complex coupling of biological and hydrologic processes that control N transport and immobilization [Lohse *et al.*, 2009], there is still very poor understanding of the linkages between watershed N loading and the resultant patterns of streamwater N. Major sources of watershed N include atmospheric deposition, mineral weathering, N fixation, human and animal waste, and fertilizer application.

Biogeochemical and hydrologic processes can prohibit direct transfer of N inputs from source areas to streams. Biogeochemical processes that immobilize N include vegetation and microbial uptake, adsorption to soils, and denitrification [Chapin, 2002]. In addition to biogeochemical process, patterns of hydrologic connectivity can determine whether N is transported from N source areas to streams [Creed and Band, 1998; Pacific *et al.*, 2009]. In some environments, a hydrologic connection between most of the landscape and the stream exists for a very limited time of year [Jencso *et al.*, 2009]. Without a hydrologic connection, N inputs are stored within watershed soils and vegetation.

For N that is ultimately transported to streams, similar biogeochemical processes as terrestrial ecosystems transform, transport and retain streamwater N [Allan, 1995]. Instream N processing can account for a substantial portion of watershed N budgets [Burns *et al.*, 1998]; however, streamwater N removal magnitude and efficiency can vary throughout the network depending on factors such as stream order and discharge [Alexander *et al.*, 2000; Peterson *et al.*, 2001], carbon availability [Bernhardt and Likens, 2002; Groffman *et al.*, 2005], N concentration [Earl *et al.*, 2006], hyporheic storage [Runkel, 2007], or on how much N is imported from an upstream reach [Mulholland *et al.*, 2008].

Given the spatial and seasonal complexity of the processes controlling N cycling in stream and terrestrial ecosystems, it is no surprise that streamwater N patterns are equally as complex. This research aimed to characterize these spatial and seasonally variable patterns of watershed nitrogen export and retention and improve knowledge of

the influence anthropogenic N loading has on these patterns. Specifically, this research sought to: 1) assess how the magnitude, corresponding landscape position, spatial distribution of anthropogenic N sources influences the timing, magnitude, and speciation of watershed N export, 2) determine whether localized inputs of anthropogenic N result in the same N saturation dynamics as spatially distributed inputs [Aber *et al.*, 1989; 1998] and if so, whether N saturation varies across space and time, and 3) quantify the relative importance of watershed N retention processes (i.e. terrestrial, riparian, and instream) and how they may vary along the stream network. To do this, I analyzed multiple sources of contemporary field data, including synoptic and temporal sampling for N and C species and  $\delta^{15}\text{N}$  and  $\delta^{18}\text{O}$  ratios of  $\text{NO}_3^-$  with a combination of approaches that included mass balances, endmember mixing analysis, geostatistical modeling, and Bayesian hybrid mechanistic modeling.

### Site Description

The study site was the West Fork of the Gallatin (“West Fork”) watershed (212  $\text{km}^2$ ) located in the Gallatin and Madison mountain ranges of southwestern Montana (Figure 1.1A). The West Fork drains into the Gallatin River, which is a tributary to the Missouri River and is fed by three main tributaries, the Middle Fork, South Fork, and North Fork (Figure 1.1B). The watershed is characterized by well-defined steep topography and shallow soils. Elevation in the drainage ranges from approximately 1800 to 3400 m and average annual precipitation exceeds 127 cm at higher elevations and is

less than 50 cm near the watershed outlet. Sixty percent of precipitation falls during the winter and spring months [*USDA NRCS*, 2008].

Streams in the West Fork watershed range from first-order, high gradient, boulder dominated mountain streams in the upper elevations to fourth-order, alluvial streams near the watershed outlet. Stream productivity is generally low due to cold temperatures and short growing seasons [*USDA FS*, 2004]. Hydrographs of streams in the watershed indicate peak flows during spring snowmelt typically occurring in late May and early June followed by a general recession throughout the summer, autumn, and winter months.

Diverse geologic materials are present in the West Fork watershed, including metamorphosed volcanics of Archean age, sedimentary and meta-sedimentary formations of various ages, and colluvium and glacial deposits that dominate the surficial geology in valley bottoms. Carbonaceous minerals such as limestones and shales are present in the mineralogy of some but not all headwater catchments, and quartzite, biotite, gneiss, gabbros, and sandstones are also present [*Alt and Hyndman*, 1986; *Kellog and Williams*, 2006]. Vegetation below tree line consists of coniferous forest (lodgepole pine, blue and Engelmann spruce, and Douglas-fir), grasslands, shrublands, and willow and aspen groves in the riparian areas. The watershed has a brief growing season from mid-June through mid-September (75 – 90 frost free days), decreasing with elevation [*USDA FS*, 1994].

Big Sky Resort was established in the early 1970s and since then, the West Fork watershed has seen a rapid increase in growth with the addition of three new ski resorts

(Moonlight Basin, Spanish Peaks, and the Yellowstone Club) and golf courses with associated residential development. The Big Sky Water and Sewer District services the two village areas with public water supply and sewer in the West Fork watershed. Public wastewater receives secondary treatment and is released into three lined sewer detention ponds and stored until mid-spring when it is released as irrigation water onto the Big Sky Golf Course. Areas outside of the sewer district are on individual or community septic systems and private wells [*R. Edwards*, personal comm., 2007].

The West Fork watershed is an ideal location to examine the spatial and seasonal influences of land use and watershed characteristics on N export due to the wide range in topographic gradients, development densities and strong seasonality in hydrologic and biologic dynamics. Furthermore, high elevation ecosystems can have faster response times to anthropogenic N loading due to increased precipitation, steep slopes, limited vegetation, large areas of exposed bedrock, and shallow soils, often resulting in rapid hydrological flushing during snowmelt and rainfall [*Williams et al.*, 1993; *Forney et al.*, 2001; *Kopacek et al.*, 2005]. Therefore, even modest levels of anthropogenic N loading can have disproportionately large effects on N dynamics in mountainous headwater ecosystems. Because of this sensitivity to nutrient perturbation and quick response times, mountain environments can be ideal field laboratories to study anthropogenic impacts on watershed N cycling.

### Dissertation Organization

This dissertation outlines increased understanding of the linkages between

anthropogenic loading on emergent patterns of watershed N export and retention.

Specifically, the objectives of this research were to:

1. Examine the seasonal and spatial heterogeneity in watershed N export, concentration, speciation, and retention across landscape positions and development intensities.
2. Assess the primary drivers of streamwater  $\text{NO}_3^-$  concentrations and how these drivers may vary across space and time.
3. Determine whether localized inputs of anthropogenic N result in the same N saturation dynamics as spatially distributed inputs of N, and if so, are these saturation dynamics spatially and seasonally variable across watersheds.

The work presented in this dissertation addresses important gaps in understanding anthropogenic impacts on watershed N as well as presents an example of a creative multi-analysis approach towards understanding solute export at the watershed scale. As a starting point, an exploratory spatial analysis of land use impacts on streamwater  $\text{NO}_3^-$  concentrations is presented in Chapter 2, “Seasonality in spatial variability and influence of land use/land cover and watershed characteristics on streamwater  $\text{NO}_3^-$  concentrations in a developing watershed in the Rocky Mountain West.” This chapter examines the spatio-temporal patterns of streamwater  $\text{NO}_3^-$  concentrations and develops geostatistical relationships between streamwater  $\text{NO}_3^-$  concentrations land use and terrain indices across periods of varying potential of hydrologic and biological activity.

Chapter 3, “A multi-analysis approach to assess the spatio-temporal patterns of watershed response to localized inputs of anthropogenic nitrogen” is an empirical

analysis of the extensive spatial and seasonal streamwater chemistry data sets collected in the West Fork watershed. The combination of both spatial and high-resolution temporal chemistry from the catchment outlet is a unique and valuable data set to explore anthropogenic impacts on spatio-temporal trends in streamwater N export. A mass balance approach was combined with exploratory data analysis and a three component mixing model to provide insight into N export and retention processes occurring across watersheds with varying development intensities and spatial patterns of N loading.

In Chapter 4, “Quantifying watershed sensitivity to spatially variable N loading and the relative importance of watershed N retention mechanisms”, I introduce the Big Sky Nutrient Model (BiSN), which is a hybrid mechanistic model run with a Bayesian framework. BiSN is applied to summer synoptic streamwater  $\text{NO}_3^-$  data to examine 1) how spatial patterns and landscape position of anthropogenic N loading influence streamwater  $\text{NO}_3^-$  concentrations, and 2) the relative importance of watershed N retention occurring in the uplands, riparian areas, and instream.

Finally, Chapter 5 is a synthesis of the main findings of this research and its implications. Here I suggest recommendations for future study that will address questions highlighted from this research.

References Cited

- Alexander, R.B., R.A. Smith, G.E. Schwarz (2000). Effect of stream channel size on the delivery of nitrogen to the Gulf of Mexico. *Nature*, 403: 758-761.
- Aber, J., McDowell, W., Nadelhoffer, K., Magill, A., Berntson, G., Kamakea, M., McNulty, S., Currie, W., Rustad, L., and I. Fernandez (1998). N saturation in temperate forest ecosystems *Hypothesis revisited*. *BioScience*, 48(11): 921-933.
- Aber, J.D., Nadelhoffer, K.J., Steudler, P., and J.M. Melillo (1989). Nitrogen saturation in northern forest ecosystems: excess nitrogen from fossil fuel combustion may stress the biosphere. *BioScience*. 39(60): 378-385.
- Alt, D., and D.W. Hyndman (1986). *Roadside geology of Montana*. Mountain Press Publishing Company. Missoula MT.
- Allan, J.D. (1995). *Stream Ecology: Structure and function of running waters*. Klewer Academic Publishers, Norwell, MA.
- Bernhardt, E.E., and G.E. Likens (2002). Dissolved organic carbon enrichment alters nitrogen dynamics in a forest stream. *Ecology*, 83: 1689-1700.
- Bisson, P. A. and R. E. Bilby (2001). Organic Matter and Trophic Dynamics. In Naiman, Robert J. and Robert E. Bilby, eds. *River Ecology and Management: Lessons from the Pacific Coastal Ecoregion*. Springer, New York. p 373-398. Bollman, W. 2003. *A Biological Assessment of Sites in the Gallatin River Watershed: Gallatin County, Montana- 2001-2003*. Final Report to the Montana Water Center.
- Burns, D.A. (1998). Retention of NO<sub>3</sub><sup>-</sup> in an upland stream environment: A mass balance approach. *Biogeochemistry*, 40: 73-96.
- Chapin III, S.F., P.A. Matson, and H.A. Mooney (2002). *Principles of Terrestrial Ecosystem Ecology*. Springer, New York, New York.
- Cole, D.W. and M. Rapp (1981). In *Dynamic Properties of Forest Ecosystems*. Reichle, D.E., Ed. Cambridge University Press: New York.
- Creed, I.F. and L.E. Band (1998). Exploring functional similarity in the export of nitrate-N from forested catchments: A mechanistic modeling approach. *Water Resources Research*, 34(11): 3079-3093.

- Earl, S. R., H. M. Valett, and J. R. Webster (2006). Nitrogen saturation in streams. *Ecology*, 87(12): 3140-3151.
- Edwards, R. (2007). Personal Communications. *Big Sky Water and Sewer District Operations*. General Manager Big Sky Water and Sewer District.
- Folke, C., Folke Carpenter, S., Elmqvist, T., Gunderson, L., Holling, C.S., Walker, B., Bengtsson, J., Berkes, F., Colding, J., Danell, K., Falkenmark, M., Gordon, L., Kasperson, R., Kautsky, N., Kinzig, A., Simon, L., Mäler, K., Moberg, F., Ohlsson, L., Olsson, P., Ostrom, E., Reid, W., Rockström, J., Savenije, H. and U. Svedin. Resilience and Sustainable Development: Building Adaptive Capacity in a World of Transformations. April 16, 2002 Scientific Background Paper on Resilience for the process of the World Summit on Sustainable Development on behalf of The Environmental Advisory council to the Swedish Government URL: <http://www.sou.gov.se/mvb/pdf/resiliens.pdf>.
- Forney, W., Richards, L., Adams, K.D., Minor, T.B., Rowe, T.G., LaRue Smith, J., and Raumann, C.G (2001). *Land Use Change and Effects on Water Quality and Ecosystem Health in the Lake Tahoe Basin, Nevada California*. U.S.G.S. Open File Report 01-418.
- Groffman, P.M., A.M. Dorsey, and P.M. Mayer (2005). N processing within geomorphic structures in urban streams. *Journal of the North American Benthological Society*, 24: 613-625.
- Gunderson, P., Emmett, B.A., Kjonaas, O.J., Koopmans, C.J., and A. Tietema (1998). Impact of nitrogen deposition on nitrogen cycling in forests: a synthesis of NITREX data. *Forest Ecology and Management*, 101: 37-55.
- Kellog, K.S. and V.S. Williams (2005). *Geologic Map of the Ennis 30' X 60' Quadrangle, Madison and Gallatin counties, Montana and Park County, Wyoming*. Montana Bureau of Mines and Geology Open File No. 529.
- Kopacek, J., E. Stuchlik, and R.F. Wright (2005). Long-term trends and spatial variability in nitrate leaching from alpine catchment-lake ecosystems in the Tatra Mountains, *Environmental Pollution*, 136, 89-101.
- Lohse, K.A., P.D. Brooks, J.C. McIntosh, T. Meixner, and T.E. Huxman (2009). Interactions between biogeochemistry and hydrologic systems. *Annual Review of Environment and Resources*, 34: 65-96.
- Mulholland, P.J., A.M. Helton, G.C. Poole, R.O. Hall, S.K. Hamilton, B.J. Peterson, J.L. Tank, L.R. Ashkenas, L.W. Cooper, C.N. Dahm, W.K. Dodds, S.E.G. Findlay, S.V. Gregory, N.B. Grimm, S.L. Johnson, W.H. McDowell, J.L. Meyer, H.

Valett, J.R. Webster, C. P. Arango, J.J. Beaulieu, M.J. Bernot, A.J. Burgin, C.L. Crenshaw, L.T. Johnson, B.R. Niederlehner, J.M. O'Brien, J.D. Potter, R. W. Sheibley, D.J. Sobota, and S.M. Thomas (2008). Stream denitrification across biomes and its response to anthropogenic nitrate loading. *Nature*, 452(13):doi:10.1038/nature06686.

Pacific, V., K. Jencso, and B.L. McGlynn (2010). Variable flushing mechanisms and landscape structure control stream DOC export during snowmelt in a set of nested catchments. *Biogeochemistry*. DOI: 10.1007/s10533-009-9401-1.

U.S. Department of Agriculture (USDA) Forest Service (FS) (2004). *Gallatin National Forest: Streams*  
<http://www.fs.fed.us/r1/gallatin/?page=resources/fisheries/streams>.

USDA Forest Service (FS) (1994). *Ecoregions of the United States*:  
<http://www.fs.fed.us/land/pubs/ecoregions/>.

USDA Natural Resource Conservation Service (NRCS) (2008). Snotel Precipitation Data.  
<http://www.wcc.nrcs.usda.gov/cgi-bin/wygraphmulti.pl?stationidname=11D19S-LONE+MOUNTAIN&state=MT&wateryear=2008>.

Vitousek, P.M., and R.W. Howarth (1991). Nitrogen limitation on land and in the sea.: How does it occur? *Biogeochemistry*, 13: 87-115.

Williams, M. W., Brown, A. and J. M. Melack (1993). Geochemical and hydrologic controls on the composition of surface water in a high-elevation basin, Sierra Nevada, *Limnology and Oceanography*, 38: 775-797.

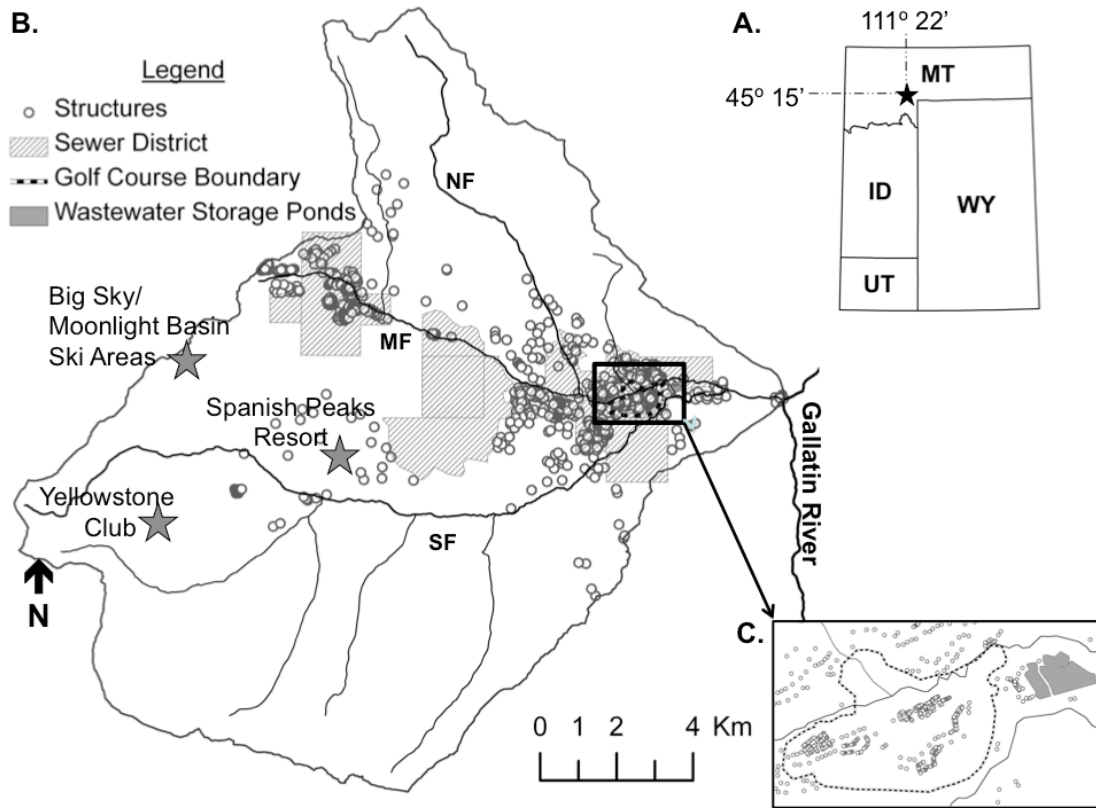


Figure 1.1: A) Location of the West Fork watershed (212 km<sup>2</sup>) in southwestern Montana. (B) Map of the West Fork watershed (212 km<sup>2</sup>) in the Gallatin and Madison mountain ranges of southwestern Montana showing the locations of ski resorts, structures, and Big Sky Water and Sewer District (public sewer system) boundaries. (C) An expanded view of the wastewater storage ponds and the Big Sky Resort Golf Course. Wastewater effluent is stored in the ponds and irrigated onto the golf course from mid-May through early October.

Contribution of Authors and Co-Authors

Manuscript in Chapter 2: Seasonality in Spatial Variability and Influence of Land Use/  
Land Cover and Watershed Characteristics on Streamwater Nitrogen Export in a  
Developing Watershed in the Rocky Mountain West

Chapter 2:

Author: Kristin K. Gardner

Contributions: co-developed and implemented the project, collected  
and analyzed output data, and wrote the manuscript.

Co-author: Dr. Brian L. McGlynn

Contributions: co-developed the study, discussed the results and implications, and  
commented on the manuscript at all stages.

Manuscript Information Page

Kristin K. Gardner and Brian L. McGlynn

Journal Name: Water Resources Research

Status of Manuscript:

Prepared for submission to a peer-reviewed journal

Officially submitted to a peer-reviewed journal

Accepted by a peer-reviewed journal

Published in a peer-reviewed journal

Publisher: American Geophysical Union

Issue in which manuscript appears in: Volume 45, W08411,  
doi:10.1029/2008WR007029.

## CHAPTER 2

SEASONALITY IN SPATIAL VARIABILITY AND INFLUENCE OF LAND  
USE/LAND COVER AND WATERSHED CHARACTERISTICS ON  
STREAMWATER NITROGEN EXPORT IN A DEVELOPING  
WATERSHED IN THE ROCKY MOUNTAIN WESTAbstract

In recent decades, the Rocky Mountain West has been one of the fastest growing regions in the United States. Headwater streams in mountain environments may be particularly susceptible to nitrogen enrichment from residential and resort development. We utilized streamwater chemistry from six synoptic sampling campaigns combined with land use/land cover (LULC) and terrain analysis in geostatistical modeling to examine the spatial and seasonal variability of LULC impacts on streamwater nitrate. Streamwater nitrate was spatially correlated for longer distances during the dormant season than during the growing season, suggesting the importance of biological retention. Spatial linear models indicated anthropogenic sources best predicted streamwater nitrate in the dormant season, while variables describing biological processing were the best predictors in the growing season. This work demonstrates the importance of 1) incorporating spatial relationships into water quality modeling, and 2) investigating streamwater chemistry across seasons to gain a more complete understanding of development impacts on streamwater quality.

## Introduction

Human alteration of the patterns of land use/land cover (LULC) on the Earth surface is one of the most profound impacts on the functioning of natural ecosystems [Steffen *et al.*, 2004]. Impacts on water quality, commonly viewed as an integrated environmental indicator of ecosystem function, are of particular concern in high-elevation ecosystems due to the combined effects of increased precipitation, steep slopes, limited vegetation, large areas of exposed bedrock, and shallow soils, often resulting in rapid hydrological flushing during snowmelt and rainfall [Williams *et al.*, 1993; Forney *et al.*, 2001]. Streamwater nitrogen (N) concentrations and yields across the U.S. have generally increased with anthropogenic development and have been well documented [Eckhardt and Stackelberg, 1995; Nolan, 2000; Whitehead *et al.*, 2002; Biggs *et al.*, 2004; Groffman *et al.*, 2004; Gardner and Vogel, 2005; U.S.G.S., 2006]; however, the extent and magnitude of development impacts on streamwater N concentrations vary.

Spatial and seasonal variability in headwater stream N is primarily a function of watershed hydrology [Fisher *et al.*, 2004; Meixner *et al.*, 2007], physical and chemical properties of the landscape (e.g. climate, geology) [Holloway, 1999; Howarth *et al.*, 2006], N loading (e.g. atmospheric, fertilizer, wastewater) [Galloway *et al.*, 2004], physical sorption [Triska *et al.*, 1994] and the net result of uptake, retention, and release by biota [Stumm and Morgan, 1996]. Identifying the spatial and seasonal variability of LULC impacts on streamwater N represents a significant challenge and highlights a fundamental gap in understanding of LULC impacts on watershed N export. Addressing

this need is critical to assessing the potential risk of development and effectively managing water quality at the watershed scale.

Anthropogenic development can increase watershed N export by adding N from septic and wastewater effluent, fertilizer, and animal waste [Puckett, 1994] and by increasing impervious surfaces, clearing vegetation and disturbing soils [Vitousek *et al.*, 1979]. The relationship between terrestrial N loading and stream N concentration is complicated because N is not conservative; there is potential for N loading to be immobilized in terrestrial and stream ecosystems. N immobilization alters the timing, magnitude, and form of N transported creating complex spatial patterns in streamwater N. Mechanisms for N immobilization include: (1) microbial denitrification [Brooks *et al.*, 1996; Burt *et al.*, 1999], (2) plant or microbial assimilation [Hadas, 1992; Wetzel, 2001], (3) physical sorption [Triska *et al.*, 1994], and (4) biotic and abiotic retention through iron and sulfur reduction [Brunet and Garcia-Gil, 1996; Davidson *et al.*, 2003].

Stream and riparian ecosystems can be hot spots for N immobilization [Lowrance *et al.* 1984; Meyer *et al.*, 1988; Groffman *et al.* 1996; Hill, 1996; Alexander *et al.* 2000; Peterson *et al.*, 2001; Bernhardt *et al.*, 2005]. The potential for N immobilization in riparian zone can be limited if: (1) hydrological flowpaths bypass the riparian zone, (2) cold temperatures limit assimilation/denitrification, or (3) there is a lack of labile carbon required for microbial denitrification [Burt *et al.*, 1999; Dent *et al.*, 2007]. Research has suggested that the magnitude of instream N immobilization is controlled by stream order, concentration, and seasonality. Headwater streams are important sites for N processing and retention [Alexander *et al.*, 2000; Peterson *et al.*, 2001]; however, as uptake

efficiency in small streams decreases, there is a rise in the relative role of  $\text{NO}_3^-$  removal in larger streams [Mulholland *et al.*, 2008]. Although there can be substantial processing of N in streams, there may also be concentration and seasonal thresholds, that when exceeded, the system loses its ability to remove/retain dissolved inorganic N [Alexander *et al.*, 2000; Dodds *et al.*, 2002; Earl *et al.*, 2006] similar to terrestrial environments [Aber *et al.*, 1989]. Increased watershed N loading can lead to greater N export to the stream ecosystem with instream uptake velocity decreasing as the stream approaches N saturation [Earl *et al.*, 2006], all leading to greater watershed N export. Shortest nutrient uptake lengths and highest uptake velocities generally occur in spring and summer [Simon, *et al.*, 2005].

Research in the Rocky Mountain West has indicated peak inorganic N concentrations occur throughout the winter and decline considerably during the growing season, suggesting the importance N immobilization [Williams and Melack, 1991; Baron and Campbell, 1996; Campbell *et al.*, 2000; Kaushal and Lewis, 2003]. There is potential to increase winter N delivery to streams in mountain resort areas because human activity often peaks during the winter ski season [Kaushal *et al.*, 2006]. In the winter increased septic system effluent can leach into shallow, cold soil that has little or no capacity to transform and assimilate nutrients or retain large inputs of subsurface water; N may then directly enter shallow groundwater and be readily transported to streams [Firestone, 1982].

Over the past decade, the Rocky Mountain West has been one of the fastest growing regions in the country [Hobbs and Stoops, 2002]. With future development,

there is the potential to increase watershed N loading to sensitive mountain environments, which may already be showing signs of nitrogen enrichment [*Kaushal et al.*, 2006]. Identifying the spatial and seasonal variability of LULC impacts on streamwater N represents a significant challenge; however, addressing this need is critical to accurate modeling and prediction of streamwater N concentrations under changing landscape and/or climatic conditions. In this study, we investigated the spatial and seasonal variability of LULC and watershed characteristics influence on streamwater N concentrations in a developing, high-elevation, mountain watershed. We utilized streamwater chemistry from six spatial snapshots in time combined with LULC mapping and terrain analysis in a 212 km<sup>2</sup> northern Rocky Mountain watershed undergoing significant LULC change to address the following questions: (1) is there seasonality in the spatial pattern of streamwater N?, (2) What is the influence of LULC and watershed characteristics on streamwater N and do the influences change seasonally?, and (3) What is the role of the spatial location of N loading?

## Methods

### Study Area

The West Fork of the Gallatin River in the northern Rocky Mountains of southwestern Montana (Figure 2.1A) drains Big Sky, Moonlight Basin, Yellowstone Club, and Spanish Peaks resort areas (Figure 2.1B). The West Fork watershed (212 km<sup>2</sup>) is characterized by well-defined steep topography and shallow soils. Elevation in the drainage ranges from approximately 1800 to 3400 m and average annual precipitation

exceeds 127 cm at higher elevations and is less than 50 cm near the watershed outlet. Sixty percent of precipitation falls during the winter and spring months [*USDA NRCS*, 2008]. Hydrographs of the West Fork River indicate peak flows during spring snowmelt typically occurring in late May/early June followed by a general recession throughout the summer, autumn, and winter months.

Streams in the West Fork watershed range from first-order, high-gradient, boulder dominated mountain streams in the upper elevations to fourth-order, alluvial streams near the watershed outlet. Stream productivity is generally low due to cold temperatures and short growing seasons [*USDA FS*, 2004], however in recent years, increased algal growth has been noted in streams draining developed subwatersheds near the watershed outlet. Chlorophyll a data collected in September 2005 suggest that algal growth is elevated above natural background levels in streams draining developed subwatersheds. Median Chlorophyll a ranges from 2.5 mg/m<sup>2</sup> in pristine low order streams, 20 mg/m<sup>2</sup> in pristine higher order streams to 360 mg/m<sup>2</sup> in higher order streams draining more developed watersheds [*PBS&J*, 2005].

Diverse geologic materials are present in the West Fork watershed, including metamorphosed volcanics of Archean age, sedimentary and meta-sedimentary formations of various ages, and colluvium and glacial deposits that dominate the surficial geology in valley bottoms. Carbonaceous minerals such as limestones and shales are present in the mineralogy of some but not all headwater catchments, and quartzite, biotite, gneiss, gabbros, and sandstones are also present [*Alt and Hyndman*, 1986; *Kellog and Williams*, 2006]. The chemical weathering potential of different minerals found throughout the

study watershed is the focus of a current investigation; however, previous research has shown that inorganic N can be weathered from layered silicates such as biotite and muscovite, and sedimentary rocks such as shale [*Holloway et al.*, 1999; 2001].

Vegetation below tree line consists of coniferous forest (lodgepole pine, blue and Engelmann spruce, and Douglas-fir), grasslands, shrublands, and willow and aspen groves in the riparian areas. The watershed has a brief growing season from mid-June through mid-September (75 – 90 frost free days), decreasing with elevation [*USDA FS*, 1994].

Big Sky Resort was established in the early 1970s and since then, the West Fork watershed has seen a rapid increase in growth with the addition of three new ski resorts and golf courses with associated residential development. Since resort development, streamwater N concentrations in the West Fork of the Gallatin River have followed a similar upward trend as development [*NSF*, 1976; *Blue Water Task Force, and Big Sky Water and Sewer District*, unpublished data]. The Big Sky Water and Sewer District services the two village areas with public water supply and sewer in the West Fork watershed (Figure 2.1B). Public wastewater receives secondary treatment and is released into 3 sewer detention ponds and stored until mid-spring when it is released as irrigation water onto the Big Sky Golf Course (Figure 2.1C). Golf course irrigation begins in mid-spring when the ground thaws and continues through mid-fall, when the ground again freezes. Areas outside of the sewer district are on individual or community septic systems and private wells [*R. Edwards*, personal comm., 2007].

### Synoptic Streamwater Sampling and Chemistry Analysis

The spatial distribution of watershed N export was explored through synoptic, or “snapshot-in-time,” sampling in which streamwater was collected in 250 mL high-density polyethylene (HDPE) bottles from 50 sites across the West Fork watershed within 2-3 hours time (Figure 2.1B). Six repeated synoptic sampling campaigns were conducted to capture varying hydrological conditions and potential for biological activity (Table 2.1). Potential biological activity was assumed to be a function of streamwater and air temperature. Synoptic sampling campaigns conducted in the growing season, mid June through mid September, were considered “high potential”, while the mid winter synoptic sampling campaign was considered “low potential”. Synoptic sampling sites were randomly selected to represent a range of subwatershed characteristics including: LULC, number of wastewater disposal units, geology, stream order, elevation, and discharge (Figure 2.1B).

Streamwater samples were chilled and transported to the laboratory where they were filtered within 24 hours of collection with 0.45  $\mu\text{m}$  Millipore Isopore Polycarbonate membranes. Filtered water samples were preserved in HDPE bottles at 0 – 4°C until analysis. Aqueous nitrogen species analyzed included nitrite ( $\text{NO}_2^-$ ), nitrate ( $\text{NO}_3^-$ ), ammonium ( $\text{NH}_4^+$ ), and organic forms. Water samples collected for this study were analyzed for all major N species; however, most samples contained  $\text{NO}_2^-$  and  $\text{NH}_4^+$  levels near or below detection limits (5-10  $\mu\text{g/L}$ ). We focused on  $\text{NO}_3^-$  in this study.  $\text{NO}_3^-$  was analyzed by ion-exchange chromatography (IC) using a Metrohm Peak model 820

interface equipped with a 4-mm anion-exchange column [Metrohm, Herisau, Switzerland]. Detection limits for  $\text{NO}_3^-$  were 0.011 mg/L  $\text{NO}_3\text{-N}$ . Accuracy was within 10% for certified 0.1 ppm  $\text{NO}_3^-$ -N standards ( $0.09 \pm 0.009 \text{ mg} \cdot \text{L}^{-1} \text{NO}_3\text{-N}$ ), as measured every 11<sup>th</sup> sample. Coefficients of variation (CVs) for  $\text{NO}_3^-$  standard peak areas were 2% or less.

A subset of the filtered streamwater samples were frozen until delivery to the Woods Hole Whole Marine Microbial Biogeochemistry Lab for isotopic analysis.  $\delta^{15}\text{N}$  and  $\delta^{18}\text{O}$  of  $\text{NO}_3^-$  were analyzed by the Sigman-Casciotti microbial denitrifier method [Sigman *et al.*, 2001; Casciotti *et al.*, 2001]. Nitrate  $\delta^{15}\text{N}$  and  $\delta^{18}\text{O}$  were calibrated against USGS32, USGS34, and USGS35 [Casciotti *et al.*, 2007].

### Terrain Analysis

The potential impact of LULC along hydrologic flowpaths is partially controlled by landscape characteristics [Dunne, 1978; Newson, 1997]. LULC change can alter water flow and biogeochemical processes, which together mediate N movement and transformation in watersheds [Findlay, 2001; Biggs *et al.*, 2004; Zimmerman *et al.*, 2006]. Definition of hydrological flowpaths, potential travel times along each flowpath and the concomitant spatial pattern of N loading across the West Fork watershed are necessary to explain variability in streamwater N. Hydrological flowpaths can be estimated by a Digital Elevation Model (DEM) terrain analysis. The West Fork watershed has steep slopes and predominately shallow soils with high hydraulic conductivities [USDA SCS, 1978; USDA SCS, 1982]. These conditions often promote shallow runoff pathways that can result in rapid  $\text{NO}_3^-$  delivery to riparian zones and

streams. Consequently, flowpaths are likely to be well represented by surface topography. For this study, the  $MD^\infty$  flow accumulation algorithm [Seibert and McGlynn, 2007] was used to define the hydrological flowpaths in the West Fork watershed using a 10m DEM developed by parsing a 1-m resolution Airborne Laser Swath Mapping data set. The spatial resolution of the 1-m DEM was reduced to improve computational time and to prevent the terrain analysis software from terminating before completion.

Our terrain analysis extracted relevant terrain characteristics from the 10m DEM to use as potential predictor variables for modeling streamwater ( $\text{NO}_3^-$ ) concentrations. First, an approximation of water residence time for each grid cell was calculated [McGuire *et al.*, 2005]. We will refer to this approximation as water travel time ( $TT$ ).  $TT$  has been shown to have a correlation of 0.91 with mean water residence time [McGuire *et al.*, 2005].  $N$  export has been shown to be inversely related to watershed residence time by increasing the potential reaction time for immobilization [Seitzinger *et al.*, 2002]. For each grid cell,  $TT$  is the hydrological flowpath distance to the stream divided by the gradient over the flowpath. Assuming a constant hydraulic conductivity throughout the watershed,  $TT$  can be viewed as a first approximation of Darcy's Law:

$$\bar{V} = K * I \quad \rightarrow \quad K = \text{a constant} \quad \rightarrow \quad \bar{V} \cup I \quad \rightarrow \quad TT \approx \frac{D}{I} \quad (2.1)$$

where,  $\bar{V}$  is the average velocity,  $K$  is the hydraulic conductivity,  $I$  is the gradient (slope) along the flowpath to the stream,  $D$  is the flowpath distance to the stream, and  $TT$

is the travel time from each grid cell to the stream following the topographically driven flow routing algorithm. Assuming this first-order approximation,  $TT$  is a measure of the travel time from a grid cell to the stream channel.

Riparian areas were computed from the DEM by an automated method in which all area less than three meters above the stream along each flowpath was delineated as a riparian zone [McGlynn and Seibert, 2003]. The method has been field-tested by comparing terrain based riparian delineation to riparian field surveys performed in Tenderfoot Creek, Montana ( $R^2=0.97$ ) [Jencso *et al.*, 2010]. Once riparian areas were delineated, riparian hillslope area ratios (riparian buffering potential) were computed as the ratio of local riparian area associated with each stream pixel divided by the local contributing area (lateral upslope inflows) [Beven and Kirkby, 1979]. Stream reach to stream reach assessment of riparian buffering potential of lateral hillslope inputs is pertinent in LULC change-water quality analyses because it allows for assessment of potential riparian buffering down-gradient (along each flowpath) of N inputs.

The subwatersheds for each of 50 synoptic stream sampling sites were delineated from the flowpath model. The 50 subwatersheds of the West Fork ranged in size from  $0.04 \text{ km}^2$  to  $207 \text{ km}^2$ . Subwatershed characteristics were extracted to employ as potential predictor variables in spatial linear models of synoptic streamwater  $\text{NO}_3^-$  concentrations (Table 2.2).

## Statistical Analysis

Potential Predictor Variables: Potential predictor variables were extracted for each subwatershed to describe subwatershed characteristics and LULC upstream of each synoptic sampling site (Table 2.2). Septic locations were mapped by masking the Big Sky Water and Sewer District boundary GIS layer over a 2006 structure layer supplied by the Gallatin County Planning District. To test the impact of septic location on watershed N export, septic locations were also weighted by inverse  $TT$  and flowpath distance to the stream ( $D$ ). Sites influenced by wastewater input from the golf course were identified through terrain analysis and confirmed by isotopic analysis of  $\delta^{15}\text{N}$  and  $\delta^{18}\text{O}$  of  $\text{NO}_3$  [Kendall and McDonnell, 1998].

Forest cover was delineated from a cloud-free QuickBird scene acquired on July 21, 2005. Geologic maps, acquired from the Montana Bureau of Mines and Geology [Kellogg and Williams, 2005] were used to determine the percent of geology with higher potential for N weathering in each subwatershed. The Strahler stream order classification system was used to assess stream order [Strahler, 1952]. Median slope, median aspect, site elevation, and area of each subwatershed were computed through terrain analysis. Aspect was converted from a circular variable to a linear variable by computing the medians of the sine and cosine of the aspect and then converting back to an angle with arctangent.

Spatial Linear Models: The unidirectional flow of water in stream networks dictates that each sampling site is influenced by upstream sites; therefore, streamwater

$\text{NO}_3^-$  concentrations may not be spatially independent. The presence of spatial dependence violates the assumption of independently and identically distributed (i.i.d.) errors of most standard statistical procedures. Potentially this can encumber analyses and threatens statistical and inferential interpretation by leading to: 1) a confidence interval that is too narrow, 2) underestimation of the sample variance, and 3) inaccurate parameter estimates [Cressie, 1993; Legendre, 1993]. Although spatial dependency violates standard statistical techniques, it can be used as a source of information in spatial models, rather than something to be ignored or corrected [Carroll and Pearson, 2006].

A spatial linear model is an extension of a general linear model (GLM) in which the errors are allowed to be spatially correlated. Consider the GLM:  $Y = \beta X + \epsilon$ , where  $Y$  is a  $n \times 1$  vector of observations,  $X$  is a  $n \times p$  matrix of predictor variables,  $\beta$  is a  $p \times 1$  vector of best-fit parameters, and  $\epsilon$  is a  $n \times 1$  vector of random errors. Typically, the random errors,  $\epsilon$ , are assumed to be independent, so  $\text{var}(\epsilon) = \sigma^2 I$ , where  $I$  is the  $n \times n$  identity matrix; however, in spatial models, the independence assumption of  $\epsilon$  is relaxed and the values are allowed to be spatially correlated so  $\text{var}(\epsilon) = \Sigma$ , where  $\Sigma$  is the covariance matrix [Cressie, 1993].  $\Sigma$  is a function of the autocovariance parameters, which are determined by fitting an autocovariance function to the modeled residuals. In order for the modeled autocovariance function to be statistically valid, it must produce a symmetric and positive-definite covariance matrix [Cressie, 1993].

Typically, spatial models are based on Euclidean distance to quantify spatial dependence [Cressie, 1993]. However, Euclidean distance may not best represent distance in stream networks, and consequently, recent research has begun to use instream distance

to model stream characteristics [*Dent and Grimm, 1999; Gardner et al., 2003; Legleiter et al., 2003; Ganio et al., 2005*]. Concurrently, new geostatistical methodologies to model stream characteristics have incorporated the unidirectional flow of water by developing statistically valid covariance measures based on directional hydrologic flowpath distance [*Cressie et al., 2006; Ver Hoef et al., 2006; Peterson et al., 2007*]. Directional hydrologic flowpath distance may be more representative of the unidirectional flow of water and solutes in a stream network.

We applied a geostatistical method, which incorporates spatial dependence of the data, using a weighted hydrologic flowpath distance developed for stream networks [*Ver Hoef et al., 2006*]. Spatial weights are generated using metrics that represent relative influence of one site on another, such as proportion watershed area at a confluence, to create more ecologically representative distance measures [*Ver Hoef et al., 2006*]. To implement this method, a flow network was derived from the 10m DEM with the Functional Linkage of Waterbasins and Streams (FLoWS) toolset [*Theobald et al., 2005*]. The flow network described whether or not a synoptic sampling site was connected to other synoptic sampling sites by streamflow. In order for two sites to be considered “flow-connected”, water must flow from one site to another. If water does not flow from one site to another site (e.g. an adjacent tributary), then the sites are considered “not flow connected” (Figure 2.2a).

For the purpose of this study, we quantified how much influence an upstream site had on a downstream site by considering the downstream flow distance (*DFD*) between sites and the proportional influence (*PI*) of streamflow contributed from one site to

another site. *DFD* is the total downstream distance between sampling sites along the flow network and the *PI* is the influence of an upstream location on a downstream location based on discharge volume. For this study, watershed area was used as a surrogate for discharge volume. Watershed area has been shown to be highly correlated to annual stream discharge ( $R^2$  values ranging from 0.92-0.99) in all 18 water resource regions of the United States [Vogel *et al.*, 1999]. Calculation of the *PI* of one sample site on another involves two steps [Peterson *et al.*, 2007]. First, the *PI* of each segment on the segment directly downstream is computed by dividing its watershed area by the total incoming area to the downstream segment (Figure 2.2b). The *PIs* of the incoming segments are proportions and will always sum to one. The second step uses the segment *PIs* to calculate the *PI* for each pair of flow-connected sites (Figure 2.2b). The *PI* for a pair of sites is equal to the product of the segment *PIs* found in the downstream path between them, excluding the segment *PI* that the downstream site lies on [Peterson *et al.*, 2007]. For this study, the *DFD* and *PI* matrices for each synoptic sampling campaign were computed from the flow network using the FLoWS toolset. The *DFD* and *PI* matrices must be reformatted before they can be used to create a statistically valid covariance matrix [Peterson *et al.*, 2007]. The *DFD* and *PI* matrices must be forced into symmetry by adding their respective transposes. Matrix *A* is created by taking the square root of the symmetric *PI* matrix. The symmetric *DFD*, functions as the lag distance, and *A*, as a spatial weights matrix, in development of a spatial linear model.

Spatial linear models for each of six synoptic campaigns were constructed by: (1) developing a spatial autocovariance model through moving average constructions on

streams, (2) estimating the autocovariance parameters using restricted maximum likelihood (REML) [Cressie *et al.*, 1993], (3) applying the covariance matrix to estimate the fixed effects by generalized least squares, and (4) making predictions using universal kriging [Ver Hoef *et al.*, 2006]. Statistically valid spatial autocovariance models for stream networks can be developed using moving average constructions based on weighted hydrologic distances [Cressie *et al.*, 2006; Ver Hoef *et al.*, 2006]. The spatial autocovariance functions fitted and compared for each set of modeled parameters included the linear-with-sill, spherical, Mariah, and exponential autocovariance functions. For example, a spherical autocovariance model is:

$$CI(h|\theta_0, \theta_1, \theta_2) = \begin{cases} \theta_0 + \theta_1 & \text{If } h = 0 \\ \theta_1 \left[ 1 + \frac{1}{2} \left( \frac{h}{\theta_2} \right)^3 - \left( \frac{3}{2} \right) \left( \frac{h}{\theta_2} \right) \right] & \text{If } 0 < h < \theta_2 \\ 0 & \text{If } \theta_2 \leq h \end{cases} \quad (2.2)$$

where  $CI$  is an unweighted covariance matrix not guaranteed to be statistically valid at this point [Ver Hoef *et al.*, 2006],  $h$  is hydrologic flowpath distance, and  $\theta_0$ ,  $\theta_1$ , and  $\theta_2$  are the estimated autocovariance parameters. The autocovariance covariance parameters must be estimated in order to fit the covariance function to the empirical covariances. The estimated autocovariance parameters (and  $\theta_0$ ,  $\theta_1$ , and  $\theta_2$ ) describe how the variability between data points changes with increasing separation distance.  $\theta_0$  is the “range”, which is an indication of the spatial scale at which streamwater N concentrations are spatially autocorrelated; beyond the range streamwater  $\text{NO}_3^-$  concentrations are considered spatially independent.  $\theta_1 + \theta_2$  is the “sill”, which represents the variance found among

uncorrelated data.  $\theta_2$  is the “nugget effect”, which represents differences relating to fine-scale variability as the distance between locations approaches zero, which can result from experimental error or from variability that is occurring at a scale finer than the study scale. Finally, the partial sill, which is the difference between the sill and the nugget is the autocorrelated variation. The autocovariance parameters,  $\theta_0$ ,  $\theta_1$ , and  $\theta_2$ , were estimated by REML.

Finally, the covariance matrix,  $\Sigma$  is computed by applying the Hadamard (element-wise) product of the unweighted covariance matrix,  $CI$ , and the spatial weights matrix,  $A$  [Ver Hoef *et al.*, 2006; Cressie *et al.*, 2006; Peterson *et al.*, 2007]:

$$\Sigma = CI \odot A \quad (2.3)$$

$\Sigma$  was used in the general linear model to estimate the fixed effects by generalized least squares. Model residuals were assessed to identify outliers. Extreme outliers at the 0.01 significance level were identified by studentized residuals and removed. Leave-one-out cross-validation predictions were generated to calculate the Root Mean Square Prediction Error (RMPSE) for each model [Hastie *et al.*, 2001]

The “best” model for each synoptic event was selected by forward and backward stepwise selection by minimizing the RMSPE (Hastie *et al.*, 2001). RMSPE was used in model selection because information criteria are invalid when REML is used to estimate the autocovariance parameters (Verbeke and Molenberghs, 2000). If alternative models had the same RMSPE then model selection was based on maximizing the  $r^2$  value for the observations and the cross-validation predictions.

Semivariogram Plots: For visual interpretation, we computed semivariogram plots of the raw data and the fitted model residuals of streamwater  $\text{NO}_3^-$  concentrations. Raw data semiovariograms provided insight onto whether spatial processes might be controlling streamwater  $\text{NO}_3^-$  concentrations; while the fitted model residual semiovariograms were used to estimate autocovariance parameters for the spatial linear model. Semivariograms were computed to compare the degree of similarity among samples as a function of the instream distance between them:

$$\hat{\gamma}(h) = \frac{1}{2N(h)} \sum_{i=1}^{N(h)} (z(x_i) - z(x_i + h))^2 \quad (2.4)$$

where  $\hat{\gamma}(h)$  is the estimated semivariance at a separation distance  $h$ ,  $N(h)$  is the number of paired data with a range of distances (or lag) of  $h$ ,  $z(x_i)$  and  $z(x_i + h)$  are the data at two locations, and  $h$  is the distance between pairs. [Cressie, 1993]. If spatial correlation does exist, the semivariance increases as the distance between the sites increases.

Semivariograms for flow-connected models should be interpreted with caution because there is no weighting for flow volume [Ver Hoef *et al.*, 2006].

## Results

Spatial variability of streamwater  $\text{NO}_3^-$  concentrations within and across synoptic sampling campaigns is illustrated in Figures 2.3, 2.4 and 2.5. Seasonal synoptic concentrations were within the range of weekly  $\text{NO}_3^-$  time series of two streams, one draining a pristine watershed and the other a more developed watershed (Figure 2.4). Streamwater  $\text{NO}_3^-$  concentrations were highest in the winter months with median

concentrations in February and March of 0.17 and 0.14 mg/L-NO<sub>3</sub><sup>-</sup>-N, respectively. Greatest variability of streamwater NO<sub>3</sub><sup>-</sup> occurred in late fall, winter, and early spring, when the variance of streamwater NO<sub>3</sub><sup>-</sup> in October, February and March was 0.01, 0.15 and 0.08 mg/L NO<sub>3</sub><sup>-</sup>-N, respectively (Figure 2.4 and 3.5). NO<sub>3</sub><sup>-</sup>-N concentrations remained elevated at sites draining Lone Mountain (major mountain of Big Sky Resort) compared to other streams across a range of hydrologic conditions and biological potential (Figure 2.5). Sites downgradient from wastewater loading were significantly elevated compared to other sites during the winter/late fall (Figure 2.5). Isotopic analysis of δ<sup>15</sup>N and δ<sup>18</sup>O of NO<sub>3</sub><sup>-</sup> indicate elevated δ<sup>15</sup>N values, similar to the wastewater signature [Kendall and McDonnell, 1998], at sites located downgradient from the Big Sky golf course as compared to other sites. Semivariograms of raw streamwater NO<sub>3</sub><sup>-</sup> concentrations at “flow-connected” sites versus “not flow connected” sites illustrate seasonality in the autocorrelated variation at “flow connected sites” (Figure 2.6). The sill variance of “flow connected sites” was greater in the late fall, winter, and early spring semivariograms as compared to late spring, summer, and late summer. The residuals from linear models fit to the raw streamwater concentrations illustrated spatial structure (Figure 2.7); therefore, spatial linear models were applied to incorporate spatial relationships into the modeling process.

Spatial linear models indicate seasonal differences in the influential roles of LULC and terrain characteristics on streamwater NO<sub>3</sub><sup>-</sup> (Table 2.3). During the late spring (June), summer (August), and late summer (September), predictor variables representative of biological processing (riparian buffer potential and percent forest) were

significant predictors of streamwater  $\text{NO}_3^-$  concentrations. In the late fall (October), winter (February), and early spring (March), N loading variables (i.e. septic, wastewater and geology) had the highest explanatory power of the streamwater  $\text{NO}_3^-$  signal. In mid summer (August), only one of the N loading variables was significant in predicting streamwater  $\text{NO}_3^-$ , while in the mid winter (February) all of the N loading variables were significant (Table 2.3).

The autocovariance models fit to the linear model residual semiovariograms varied by synoptic sampling event (Table 2.4; Figure 2.7); however, the model choice had little effect on the estimated autocovariance parameters. Seasonality existed in the range parameter. The range was longest in October and February at 5.03 and 5.51 km respectively, and lowest in the August and June, when the range was 2.18 and 1.88, respectively. The nugget was generally low for all models, ranging from 0.00007 to 0.002.

## Discussion

The extensive spatial streamwater chemistry data collected over six time periods covering a range of hydrological conditions and potential biological activity in the West Fork watershed is a valuable and unique data set for exploring spatio-temporal trends in streamwater N export and assessing water quality impacts of mountain resort development. Furthermore, this study is the first study to use extensive spatial data sets across time employing geostatistical models based on flow-connected hydrologic

distance measures to examine trends in spatial patterns and seasonal controls of streamwater chemistry.

Spatial and temporal data indicated that peak streamwater  $\text{NO}_3^-$  concentrations in both pristine and developed watersheds occur throughout the winter and decline during the growing season (Figure 2.3, 3.4, and 3.5), which is consistent with other research in mountainous areas throughout the Rocky Mountain West [*Williams and Melack, 1991; Baron and Campbell, 1996; Campbell et al., 2000; Kaushal and Lewis, 2003; Kaushal et al., 2006*]. The magnitude of the winter peak was greater in developed watersheds and highest at sites downgradient from wastewater loading on the Big Sky Golf Course (Figure 2.3, 3.4, and 3.5).

#### Is There Seasonality in the Spatial Pattern of Streamwater N?

Spatial heterogeneity of streamwater  $\text{NO}_3^-$  concentrations existed within and across synoptic events (Figure 2.3, 3.4, and 3.5). Streamwater  $\text{NO}_3^-$  concentrations remained elevated at sites draining Lone Mountain (Big Sky Resort/Moonlight Basin resort areas) throughout a range of hydrological conditions and potential biological potential activity (all 6 synoptic campaigns), while sites downgradient from wastewater loading at the Big Sky Golf Course were only elevated during the winter and late fall synoptics (Figures 2.3 and 2.5). Much of Lone Mountain is an alpine environment above treeline with steep slopes, consisting mainly of talus and scree. There is limited vegetation below treeline as a result of ski runs and resort development. Riparian areas are small in these subwatersheds. Conversely, the Big Sky Golf Course is situated in an

alluvial valley with abundant vegetation, deeper more developed soils, and wider riparian areas providing an environment more likely to immobilize N loading during the growing season. Elevated inorganic N concentrations draining talus and scree fields have been noted in other research [*Williams and Tonnessen, 2000; Clow and Sueker, 2000; Hood and Williams, 2003; Seastedt et al., 2004*]. At these high elevations, there is increased precipitation and potential for increased deposition of inorganic N in areas with shallow soils, steep talus/scree slopes, and little riparian area with limited potential for N processing. These spatial and seasonal patterns suggest that N may be immobilized along upland and riparian flow paths and in the stream network during the late spring, summer, and late summer in the valley bottom; while at higher elevations on Lone Mountain, there may be limited N processing and thus, streamwater  $\text{NO}_3^-$  concentrations remain elevated throughout the year (Figures 2.3 and 2.5).

The distance, or range, over which streamwater  $\text{NO}_3^-$  concentrations were spatially correlated differed between seasons (Table 2.4; Figure 2.7). The range of the semivariograms in the dormant season varied from 3.17 in March to 5.51 km in February, while during the growing season the range of the semivariograms varied from 1.88 in June to 2.70 km in September. These differences in spatial dependence, suggest that streamwater  $\text{NO}_3^-$  concentrations are influenced by ecological and hydrological processes acting at different spatial and temporal scales.

Peterson et al., 2006 found ranges to vary between 20 and 73 km in streamwater  $\text{NO}_3^-$  data collected statewide in Maryland streams during the spring and summers of 1995-1997. Modeled ranges were 20.78, 45.13, and 73.30 depending on the type of

distance measure used (i.e. Euclidian, symmetric hydrologic flowpath distance, and weighted asymmetric hydrologic flowpath distance, respectively). In another study using the same Maryland data set, *Yuan* [2004] used Euclidian distance measures in geostatistical models and found the range of streamwater  $\text{NO}_3^-$  to be 49 km. The difference in range values found between *Peterson et al.* [2006] and *Yuan* [2004] may be a result of the differences in the methods used to fit the autocovariance functions: *Yuan* [2004] used weighed least squares, while *Peterson et al.* [2006] used maximum likelihood *Peterson et al.* [2006]. In an N-limited desert stream in Arizona, range values for streamwater  $\text{NO}_3^-$  decreased with post-flood successional time from >3000 m during the first succession to 359 m during the succession survey [*Dent and Grimm*, 1999]. It is difficult to compare the results of this study to those of other studies because there are regional differences in the ecological processes that affect water chemistry [*Johnes and Butterfield*, 2002; *Clark et al.*, 2004].

#### What is the Influence of LULC and Watershed Characteristics on Streamwater N and Do the Influences Change Seasonally?

Spatial linear models indicated seasonal shifts in the relationships between LULC and terrain variables on streamwater  $\text{NO}_3^-$  concentrations (Table 2.3). During the dormant season, predictor variables describing the major sources of N loading (septic, wastewater, and geology) had positive relationships and were significant in predicting streamwater  $\text{NO}_3^-$  concentrations. The strongest relationships occurred in the mid-winter synoptic (February) when 90% of the variability in streamwater  $\text{NO}_3^-$  was explained by septic, wastewater and geology, and p-values for all predictor variables were significant at the

10% level (Table 2.3). Although wastewater was not significant in the early spring (March) synoptic model (Table 2.3), there was elevated streamwater  $\text{NO}_3^-$  at most sites downgradient of the Big Sky Golf Course (Figure 2.3). The March synoptic was complicated by a period of above freezing temperatures, melting snowpack at lower elevations, and slightly elevated discharge. More snowmelt was likely occurring in watersheds drained by higher-order valley bottom streams, than in the watersheds drained by low-order high-elevation headwater streams (personal observation).

During the growing seasons, the fitted modeling results suggest the importance of a biological component in predicting streamwater  $\text{NO}_3^-$  (Table 2.3). The significance of riparian and upland vegetation in the growing season spatial models supports other research that has shown vegetation to be effective at processing watershed nutrients. Percent forest, which may be representative of upland N processing, had a significant negative relationship with streamwater  $\text{NO}_3^-$  during the growing season. Riparian buffering potential was a significant predictor variable of streamwater  $\text{NO}_3^-$ , with an inverse relationship in the late spring (June) and late summer (September) (Table 2.3). Riparian buffering potential was not a significant predictor of August, October, February, and March streamwater  $\text{NO}_3^-$  concentrations; which may result from a lack of hydrologic connection between the riparian buffer and the water table [*Jencso et al.*, 2008] and/or limited biological retention (i.e. microbial and plant assimilation and microbial denitrification) occurring in riparian areas in the winter.

Investigations of microbial dynamics in alpine tundra and dry meadows revealed a seasonal pattern wherein plant uptake dominates the summer growing season and

maximal microbial assimilation takes place in autumn and winter under snowpack [Brooks *et al.*, 1998; Lipson *et al.*, 1999; Sickman, 2003]; however, microbial activity is isolated in shallow soil from groundwater and deeper soil [Brooks *et al.*, 1996; 1998; 1999]. These studies found that microbial biomass gradually increased through the autumn and winter, peaking at the initiation of snowmelt and declining as snowmelt progressed. Perhaps, microbial assimilation was occurring during the winter, but a lack of hydrologic connectivity between the shallow soils and the stream network may have prevented the riparian buffer from immobilizing detectable amounts of N. This may explain why riparian buffering potential was not found to be a significant predictor in spatial linear models in October, February and March streamwater  $\text{NO}_3^-$ . On the other hand, in September there was a small rain event just prior and during the September synoptic sampling campaign, which may have created a riparian/upland connection and thus the potential for riparian buffering of N along hydrological flowpaths.

Spatial models of June and March synoptic  $\text{NO}_3^-$  concentrations had the least amount of predictive ability.  $R^2$  was 0.06 and 0.37, respectively, while RMSPE was 0.045 and 0.059, respectively. Both of these synoptic events occurred during significant snowmelt events. In March, snowmelt was only occurring at lower elevations, and in June, snowmelt was only occurring at higher elevations, while the lower elevations were drying out. During these hydrologic transitional periods, it may be difficult to model the watershed as a whole since elevational differences exist in hydrological and ecological processes as a result of temperature, radiation, and snow cover gradients [Seastedt *et al.*, 2004].

In the West Fork watershed, development impacts were most apparent in the winter months when streamwater  $\text{NO}_3^-$  concentrations downstream of N loading sources were two to three times greater than streamwater  $\text{NO}_3^-$  concentrations in pristine areas (Figure 2.3, 3.4, and 3.5). The spatial linear models confirmed the importance of N loading on streamwater  $\text{NO}_3^-$  concentrations in the dormant season. *Aber et al.* [1989], proposed a hypothetical timeline for a watershed response to chronic, spatially distributed N loading from atmospheric deposition. Although N loading in the West Fork watershed is localized, we propose that it exhibits the same characteristics as spatially distributed N loading. According to *Aber et al.* [1989], a sequence of four recognizable stages emerges in response to long-term loading and leads to seasonal patterns of streamwater  $\text{NO}_3^-$  concentrations. Stage characteristics range from Stage 0, in which there is a slight seasonal pattern in streamwater  $\text{NO}_3^-$  to Stage 3, in which chronic year-long elevated  $\text{NO}_3^-$  concentrations persist with no recognizable seasonal pattern. Streamwater  $\text{NO}_3^-$  concentrations in the North Fork, draining a relatively pristine subwatershed, exhibit slight winter peaks and low concentrations at baseflow (Stage 0). Slightly amplified streamwater  $\text{NO}_3^-$  winter peaks in the South Fork are characteristic of Stage 1, while amplified winter and summer streamwater  $\text{NO}_3^-$  concentrations downstream of wastewater loading in the Middle Fork suggest Stage 2 conditions (Figure 2.4). We propose a modified N saturation conceptual model whereby localized N saturation along upland flowpaths leads to heterogeneity in N saturation state. In addition, this flowpath saturation and watershed N saturation state heterogeneity results in N dilution during snowmelt and highest concentrations during winter baseflow.

Results from this study indicate the importance of investigating across seasons to elucidate the seasonal impacts of development on streamwater chemistry. Water quality studies, which focus on water quality during the “critical period” or summer baseflow, may miss the early characteristics of N enrichment. Without seasonal monitoring of streamwater N, watershed managers would not be aware of amplified  $\text{NO}_3^-$  peaks in the winter. Streams with low  $\text{NO}_3^-$  concentrations in the growing season may still be exhibiting signs of N enrichment with an amplified winter peak. Knowledge of an amplified seasonal N pattern, would inform watershed managers of the early stages of N enrichment, and the future potential of water quality degradation with continued or increased N loading. Moreover, a complete understanding of the nutrient status of headwater streams is critical to understand larger scale nutrient issues. For example, the West Fork of the Gallatin flows into the Mississippi River and eventually the Gulf of Mexico, which is already experiencing water quality problems due to nutrient enrichment.

#### What is the Role of Spatial Location of N Loading?

Fitted spatial linear models indicate that spatial location of septic along hydrological flowpaths (i.e. weighted by inverse  $TT$ ) were significant in predicting streamwater  $\text{NO}_3^-$  concentrations during seasonal transitions (Table 2.3). One would expect travel time to have an inverse relationship with streamwater  $\text{NO}_3^-$  concentrations because the more time it takes N to travel to the stream, the more reaction time available for N immobilization to occur. Septic locations weighted by  $TT$  was a better predictor of

streamwater  $\text{NO}_3^-$  than unweighted septic locations in March, June, and October; while unweighted septic was a better predictor during mid-winter (February) (Table 2.3). During August and September N loading from septic (weighted or not weighted) was not a significant explanatory variable of streamwater  $\text{NO}_3^-$  concentrations. These results suggest biological processing of terrestrial N loading may be occurring during the growing season. In mid winter, when there is low potential for biological activity, terrestrial N loading leaches through cold soils to groundwater and is readily transported to the stream, while during the growing period with highest potential for biological activity (August and September), N immobilization (assimilation and denitrification) along hydrological flowpaths mediates N transport to the stream. In August and September, septic N loading may be immobilized along hydrological pathways before it reaches the stream network.

Another way to examine the role of spatial location of N loading is to focus on the stream network. In other words, does N loading along the stream network have cascading impacts on streamwater  $\text{NO}_3^-$  concentrations downstream? Similar to the terrestrial impacts of N loading on streamwater  $\text{NO}_3^-$ , the impact of spatial location of N loading along the stream network depends on the time of year. During the growing season, semivariograms indicate that N loading along the stream network had less downstream impact on streamwater  $\text{NO}_3^-$  concentrations than during the dormant season (Figure 2.7; Table 2.4). These results suggest N immobilization along upland and riparian flow paths and/or in the stream network may lead to a breakdown in spatial

pattern and a lack of spatial correlation, therefore partially mitigating potential downstream impacts of N loading during the growing season.

Ongoing research in the West Fork watershed will further explore the spatial and seasonal patterns of LULC and watershed characteristics influences on streamwater  $\text{NO}_3^-$  by: (1) quantifying instream biological immobilization through space, seasons, and ambient N concentration via instream N additions across the West Fork watershed, (2) determining N weathering potential of geologic materials in the West Fork watershed, and (3) conducting spatially semi-distributed analyses and modeling.

### Conclusion

Synoptic sampling approaches in the West Fork watershed of southwestern Montana provided evidence that spatial and seasonal variability exists in the influences of LULC and watershed characteristics on streamwater quality. This research suggests that at lower elevations during periods of high biological potential, N immobilization may lead to a breakdown of spatial streamwater N patterns, therefore masking or potentially inhibiting LULC impacts on streamwater  $\text{NO}_3^-$  concentrations; however, in high-elevation alpine environments, N concentrations remained elevated year-long.

Spatial linear models indicate that there are seasonal differences in the range of spatial autocorrelation of synoptic streamwater  $\text{NO}_3^-$  concentrations: streamwater  $\text{NO}_3^-$  concentrations are spatially correlated at a larger scale during the dormant season as compared to the growing season. Spatial linear models of streamwater  $\text{NO}_3^-$  revealed seasonal shifts in the influence of LULC and watershed characteristics on streamwater

$\text{NO}_3^-$ . In the dormant season, N loading variables explained the most variability in streamwater  $\text{NO}_3^-$  concentrations, while during the growing season, riparian buffering potential and percent forest most strongly influenced streamwater  $\text{NO}_3^-$ . This study provides valuable insight into the spatial and seasonal influences of LULC impacts on streamwater  $\text{NO}_3^-$  concentrations and variability in mountain streams. As populations in the Rocky Mountain West continue to rise, incorporating spatial dependence and seasonality into water quality models will be critical to accurately predict the impact of future development scenarios and the ramifications of changing climatic conditions.

#### Acknowledgements

Financial support was provided by the Environmental Protection Agency (EPA) STAR Grant #R832449, EPA 319 funds administered by the Montana Department of Environmental Quality, the U.S. National Science Foundation BCS 0518429, and the USGS 104(b) Grant Program administered by the Montana Water Center. We appreciate the critical reviews of Erin Peterson, Mark Williams, and an anonymous reviewer. K.K.G. acknowledges support from the EPA STAR Fellowship and NSF GK-12 Fellowship programs. We thank the Big Sky community for allowing access to sampling sites and in particular the Big Sky Water and Sewer District, and Big Sky and Moonlight ski resort areas.

References Cited

- Aber, J.D., K.J. Nadelhoffer, P. Steudler, and J.M. Melillo (1989). Nitrogen saturation in northern forest ecosystems: excess nitrogen from fossil fuel combustion may stress the biosphere. *BioScience*. 39(6): 378-385.
- Alexander, R.B., R.A. Smith, G.E. Schwarz (2000). Effect of stream channel size on the delivery of nitrogen to the Gulf of Mexico. *Nature*, 403: 758-761.
- Alt, D., and D.W. Hyndman (1986). *Roadside geology of Montana*. Mountain Press Publishing Company. Missoula MT.
- Baron, J.S., and Campbell, D.H. (1996), Nitrogen fluxes in a high elevation Colorado Rocky Mountain basin: *Hydrological Processes*, v. 11, p. 783-799.
- Bernhardt, E.S., G.E. Likens, R.O. Hall, D.C. Buso, S.G. Fisher, T.M. Burton, J.L. Meyer, W.H. McDowell, M.S. Mayer, W.B. Bowden, S.E.G. Findlay, K.H. Macneale, R.S. Stelzer and W.H. Lowe (2005). Can't see the forest for the stream? Instream processing and terrestrial nitrogen exports. *BioScience*, 55(3): 219- 230.
- Beven, K.J. and M.J. Kirkby (1979). *A physically-based variable contributing area model of basin hydrology*. *Hydrological Sciences Bulletin*, 24(1): 43-69.
- Biggs, T.W., T. Dunne, and L.A. Martinelli (2004). Natural controls and human impacts on stream nutrient concentrations in a deforested region of the Brazilian Amazon basin. *Biogeochemistry*, 68: 227-257.
- Brooks, P.D. and M.W. Williams (1999). Snowpack controls on nitrogen cycling and export in seasonally snow-covered catchments. *Hydrological Processes*, 13: 2177-2190.
- Brooks P.D., Williams M.W. and Schmidt S.K. (1998). Inorganic nitrogen and microbial biomass dynamics before and during spring snowmelt. *Biogeochemistry*, 43: 1-15.
- Brooks, P.D., M.W. Williams, S.K. Schmidt (1996). Microbial Activity under Alpine Snowpacks, Niwot Ridge, Colorado. *Biogeochemistry*, 32(2): 93-113.
- Brunet, R.C. and L.J. Garcia-Gil (1996). Sulfide-induced dissimilatory nitrate reduction to ammonia in anaerobic freshwater sediments, *FEMS Microbiology Ecology*, 21: 131-138.

- Burt, T.P., L.S. Matchett, K.W.T. Goulding, C.P. Webster, and N.E. Haycock (1999). Denitrification in riparian buffer zones: the role of floodplain hydrology. *Hydrological Processes*, 13: 1451-1463.
- Campbell, D.H., Baron, J.S., Tonnessen, K.A., Brooks, P.D., and P.F. Schuster (2000). Controls on nitrogen flux in alpine/subalpine watersheds of Colorado. *Water Resources Research*, 36(1): 37-47.
- Carroll, S.S. and D.L. Pearson (2000). Detecting and Modeling Spatial and Temporal Dependence in Conservation Biology. *Conservation Biology*, 14(6): 1893-1897.
- Casciotti, K.L., J.K. Bohlke, M.R. Mellvin, S.J. Mroczkowski, and J.E. Hannon (2007). Oxygen Isotopes in Nitrite: Analysis, Calibration, and Equilibration. *Analytical Chemistry*, 79 (6): 2427-2436.
- Casciotti, K.L., D.M. Sigman, M.G. Hastings, J.K. Bohlke, and A. Hilkert (2001). Measurement of the oxygen isotopic composition of nitrate in seawater and freshwater using the denitrifier method. *Analytical Chemistry*, 74(19): 4905-4912.
- Clark, G.M., D.K. Mueller, and M.A. Mast (2000). Nutrient concentrations and yields in undeveloped stream basins of the United States. *Journal of the American Water Resources Association*, 36(4): 849-860.
- Clow, D. W. and J.K. Sueker (2000), 'Relations between basin characteristics and stream-water chemistry in alpine/subalpine basins in Rocky Mountain National Park, Colorado, *Water Resources Research* 36, 49-61.
- Cressie, N. J. Frey, B. Harch, and M. Smith (2006). Spatial prediction on a river network. *Journal of Agricultural Biological and Environmental Statistics*, 11(2): 127-150.
- Cressie, N (1993). *Statistics for Spatial Data*. John Wiley & Sons, Inc, New York.
- Davidson, E.A., J. Chorover, and D.B. Dail (2003). A mechanism of abiotic immobilization of nitrate in forest ecosystems: the ferrous wheel hypothesis. *Global Change Biology*, 9: 228-236.
- Dent, C.L., N.B Grimm, E. Marti, J.W. Edmonds, J.C. Henry, and J.R. Welter (2007). Variability in surface-subsurface hydrologic interactions and implications for nutrient retention in an arid-land stream. *Journal of Geophysical Research*, 112, G04004, doi:10.1029/2007JG000467.
- Dent, C.L. and N.B. Grimm (1999). Spatial heterogeneity of stream water nutrient concentrations over successional time. *Ecology*, 80: 2283-2298.

- Dodds, W.K., A.J. Lopez, W.B. Bowden, S. Gregory, N.B. Grimm, S.K. Hamilton, A.E. Hershey, E. Marti, W.H. McDowell, J.L. Meyer, D.D. Morrall, P.J. Mulholland, B.J. Peterson, J.T. Tank, H.M. Valett, J.R. Webster, and W.M. Wolheim (2002). N uptake as a function of concentration in streams. *Journal of the North American Benthological Society*, 21:206-220.
- Dunne, T. (1978). *Field studies of hillslope processes. In: Hillslope Hydrology*, Kirkby MJ (ed.). John Wiley and Sons, Ltd: New York: 227– 289.
- Earl, S. R., H. M. Valett, and J. R. Webster (2006). Nitrogen saturation in streams. *Ecology*, 87(12): 3140-3151.
- Eckhardt, D.A, and P.E. Stackelberg (1995). Relation of Ground-Water Quality to Land Use on Long Island, New York. *Ground Water*, 33(6): 1019-1033.
- Edwards, R. (2007). Personal Communications. *Big Sky Water and Sewer District Operations*. General Manager Big Sky Water and Sewer District.
- Findlay, S., J.M. Quinn, C.W. Hickey, G. Burrell, and M. Downes (2001). Effects of land use and riparian flowpath on delivery of dissolved organic carbon to streams. *Limnology and Oceanography*, 46(2): 345-355.
- Firestone, M.K. (1982). *Biological denitrification, Nitrogen in Agricultural Soils—* Agronomy Monograph no. 22, ASA-CSSA-SSSA, Madison, Wisconsin, USA, pp. 289–326.
- Fisher, S., R. Sponseller, and J. Heffernan (2004). Horizons in stream biogeochemistry: flowpaths to progress. *Ecology*, 85:2369-2379.
- Forney, W., Richards, L., Adams, K.D., Minor, T.B., Rowe, T.G., LaRue Smith, J., and Raumann, C.G. (2001). *Land Use Change and Effects on Water Quality and Ecosystem Health in the Lake Tahoe Basin, Nevada California*. U.S.G.S. Open File Report 01-418.
- Galloway, J. N., F. J. Dentener, D. G. Capone, E. W. Boyer, R. W. Howarth, S. P. Seitzinger, G. P. Asner, C. C. Cleveland, P. A. Green, E. A. Holland, D. M. Karl, A. F. Michaels, J. H. Porter, A. R. Townsend, and C. J. Vorosmarty (2004). Nitrogen cycles: past, present, and future. *Biogeochemistry* 70:153-226.
- Ganio, L.M., C.E. Torgersen, And R.E. Gresswell (2005). A geostatistical approach for describing spatial pattern in stream networks. *Frontiers in Ecology*, 3(3): 138-144.

- Gardner, B., P.J. Sullivan, and A.J. Lembo (2003). Predicting stream temperatures: geostatistical model comparison using alternative distance metrics. *Canadian Journal of Aquatic Science*, 60: 344-351.
- Gardner K., and R.M. Vogel (2005). Predicting Ground water nitrate concentrations from land use. *Ground water*, 43(3): 343-352.
- Groffman, P.M., N.L. Law, K.T. Belt, L.E. Band, and G.T. Fisher (2004). Nitrogen fluxes and retention in urban watershed ecosystems. *Ecosystems*, 7: 393-403.
- Groffman, P.M., G.C. Hanson, E. Kiviat, and G. Stevens (1996). Variation in microbial biomass and activity in four different wetland types. *Soil Science Society of America Journal*, 60(2): 622-629.
- Hadas, A., M. Sofer, J.A. E. Molina, P. Barak, and C.E. Clapp (1992). Assimilation of nitrogen by soil microbial population:  $\text{NH}_4$  versus organic N. *Soil Biology & Biochemistry*, 24: 137-143.
- Hastie, T., R. Tibshirani, and J. Friedman (2001). *The Elements of Statistical Learning*. Springer-Verlag, New York, New York.
- Hill, A. R. (1996). Nitrate removal in stream riparian zones, *Journal of Environmental Quality*, 25, 743–755.
- Hobbs, F. and N. Stoops (2002). *Demographic Trends in the 20th Century: Census 2000 Special Reports*. <http://www.census.gov/prod/2002pubs/censr-4.pdf>.
- Holloway, J.M., R.A. Dahlgren, B. Hansen, and W.H. Casey (1999). Contribution of bedrock nitrogen to high nitrate concentrations in streamwater. *Nature*, 395, 785-788.
- Holloway, J.M., R.A. Dahlgren, and W.H. Casey (2001). Nitrogen release from rock and soil under simulated field conditions. *Chemical Geology*, 174, 403-413.
- Hood, E.W., M.W. Williams; and N. Caine (2003). Landscape Controls on Organic and Inorganic Nitrogen Leaching across an Alpine/Subalpine Ecotone, Green Lakes Valley, Colorado Front Range. *Ecosystems*, 6: 31-45.
- Howarth, R.W., D.P. Swaney, E.W. Boyer, R. Marino, N. Jaworski, and C. Goodale (2006). The influence of climate on average nitrogen export from large watersheds in the Northeastern United States, *Biogeochemistry*, 79 (1-2): 163-186, doi:10.1007/s10533-006-9010-1.

- Jencso, K. J., B. L. McGlynn, M. N. Gooseff, S. M. Wondzell, and K. E. Bencala. In Review. Hydrologic Connectivity Between Landscapes and Streams: Transferring Reach and Plot Scale Understanding to the Catchment Scale, *Water Resources Research*.
- Johnes, P.J. and D. Butterfield (2002). Landscape, regional and global estimates of nitrogen flux from land to sea: Errors and uncertainties. *Biogeochemistry*, 57/58: 429-476.
- Kaushal, S.S., W.M. Lewis, and J.H. McCutchan (2006). Land use change and nitrogen enrichment of a Rocky Mountain Watershed. *Ecological Applications*, 16(1):299-312.
- Kaushal, S.S., and W.M. Lewis (2003). Patterns in the chemical fractionation of organic nitrogen in Rocky Mountain streams. *Ecosystems*, 6: 483-492.
- Kellog, K.S. and V.S. Williams (2005). *Geologic Map of the Ennis 30' X 60' Quadrangle, Madison and Gallatin counties, Montana and Park County, Wyoming*. Montana Bureau of Mines and Geology Open File No. 529.
- Kendall, C and McDonnell J.J. (1998). *Isotope Tracers in Catchment Hydrology*. Elsevier, New York.
- Legendre, P. (1993). Spatial Autocorrelation: Trouble or New Paradigm. *Ecology*, 74(6): 1659-1673.
- Legleiter, C.J., R.L. Lawrence, M.A. Fonstad, W.A. Marcus and R. Aspinall (2003). Fluvial response a decade after wildfire in the northern Yellowstone ecosystem: a spatially explicit analysis. *Geomorphology*, 54: 119-136.
- Lipson D.A., Raab T.K., Schmidt S.K. and Monson R.K. (1999). Variation in competitive abilities of plants and microbes for specific amino acids. *Biology and Fertility of Soils* 29: 257–261.
- Lowrance, R., R. Todd, J. Fail, Jr., O. Hendrickson, Jr., R. Leonard, and L Asmussen (1984). Riparian forests as nutrient filters in agricultural watersheds. *Bioscience*, 34: 374-377.
- McGlynn, B.L., and J. Seibert (2003). Distributed assessment of contributing area and riparian buffering along stream networks. *Water Resources Research*, 39(4), 1082, doi:10.1029/2002WR001521.

- McGuire, K. J., J. J. McDonnell, M. Weiler, C. Kendall, B. L. McGlynn, J. M. Welker, and J. Seibert. 2005. The role of topography on catchment-scale water residence time. *Water Resources Research*, 41, W05002, doi:10.1029/2004WR003657.
- Meixner, T., A. K. Huth, P. D. Brooks, M. H. Conklin, N. B. Grimm, R. C. Bales, P. A. Haas, and J. R. Petti (2007). Influence of shifting flow paths on nitrogen concentrations during monsoon floods, San Pedro River, Arizona. *Journal of Geophysical Research*, 112, G03S03, doi:10.1029/2006JG000266.
- Meyer, J.L., W.H. McDowell, T.L. Bott, J.W. Elwood, C. Ishizaki, J.M. Melack, B.L. Peckarsky, B.J. Peterson, P.A. Rublee (1988). Elemental Dynamics in Streams. *Journal of the North American Benthological Society*, 7(4): 410-432.
- Mulholland, P.J., A.M. Helton, G.C. Poole, R.O. Hall, S.K. Hamilton, B.J. Peterson, J.L. Tank, L.R. Ashkenas, L.W. Cooper, C.N. Dahm, W.K. Dodds, S.E.G. Findlay, S.V. Gregory, N.B. Grimm, S.L. Johnson, W.H. McDowell, J.L. Meyer, H. Valett, J.R. Webster, C. P. Arango, J.J. Beaulieu, M.J. Bernot, A.J. Burgin, C.L. Crenshaw, L.T. Johnson, B.R. Niederlehner, J.M. O'Brien, J.D. Potter, R. W. Sheibley, D.J. Sobota, and S.M. Thomas (2008). Stream denitrification across biomes and its response to anthropogenic nitrate loading. *Nature*, 452(13):doi:10.1038/nature06686.
- National Science Foundation (NSF) (1976) *Impacts of Large Recreational Development Upon Semi-Primitive Environments*. NSF RANN Program Final Report.
- Newson, M.D. (1997). *Land, Water and Development: Sustainable Management of River Basin Systems*. Routledge: London.
- Nolan, B. (2000). Relating Nitrogen Sources and Aquifer Susceptibility to Nitrate in Shallow Ground Waters of the United States. *Ground Water*, 39(2), 290-299.
- Peterson, B. J., W. M. Wolheim, P. J. Mulholland, J. R. Webster, J. L. Meyer, J. L. Tank, E. Marti, W. B. Bowden, H. M. Valett, A. E. Hershey, W. H. McDowell, W. K. Dodds, S. K. Hamilton, S. Gregory, and D. D. Morrall (2001). Control of nitrogen export from watersheds by headwater streams. *Science*, 292:86-90.
- Peterson, E.E., D.M. Theobald, and J.M. Ver Hoef (2007). Geostatistical modeling on stream networks: developing valid covariance matrices based on hydrologic distance and stream flow. *Freshwater Biology*. 52: 267-279.
- Peterson, E.E., A.A. Merton, D.M. Theobald, and N.S. Urquhart (2006). Patterns of spatial autocorrelation in stream water chemistry. *Environmental Monitoring and Assessment*, 121(1-3): 571-596.

- Peterson, E.E. and N.S. Urquhart (2006). Predicting water quality impaired stream segment using landscape-scale data and a regional geostatistical model: A case study in Maryland. *Environmental Monitoring and Assessment*, 121(1-3): 615-638.
- Post, Buckley, Schuh, and Jernigan, Inc. (PBS&J) (2005). *2005 Biological Monitoring Chlorophyll A Data Summary Upper Gallatin Water Quality Restoration Planning Areas*. TMDL Report prepared for the Montana Department of Environmental Quality.
- Puckett, L. (1994). Nonpoint and point sources of nitrogen in major watersheds of the United States. U.S. Geological Survey Water-Resources Investigations Report 94-4001.
- Seastedt, T.R., W.D. Bowman, N. Caine, D. McKnight, A. Townsend and M.W. Williams (2004) The landscape continuum: A model for high-elevation ecosystems. *BioScience*, 54(2): 111-120.
- Seibert, J. and B.L. McGlynn (2007). A new triangular multiple flow-direction algorithm for computing upslope areas from gridded digital elevation models. *Water Resources Research*, 43, W04501, doi:10.1029/2006WR005128.
- Seitzinger, S.P., R.V. Styles, E.W. Boyer, R.B. Alexander, G. Billen, R.W. Howarth, B. Mayer, and N. Van Breemen (2002). Nitrogen retention in rivers: model development and application to watersheds in the northeastern U.S.A. *Biogeochemistry*, 57/58: 199-237.
- Sickman, J.O., A.L. Leydecker, C.C.Y. Chang; C. Kendall, J.M. Melack, D.M. Lucero and J. Schimel (2003). Mechanisms underlying export of N from high-elevation catchments during seasonal transitions. *Biogeochemistry*, 64: 1-24.
- Sigman, D.M., K.L. Casciotti, M. Andreani, C. Barford, M. Galanter, and J.K. Bohlke (2001). A bacterial method for the nitrogen isotopic analysis of nitrate in seawater and freshwater. *Analytical Chemistry*, 73 (17): 4145-4153.
- Simon, K.S., C.R. Townsend, and B.J.F. Biggs, and W. B. Bowden (2005). Temporal variation of N and P uptake in 2 New Zealand streams. *Journal of the North American Benthological Society*, 24(1):1-18.
- Steffen, W, A. Sanderson, P. Tyson, J. Jager, P. Matson, B. Moore , III, F. Oldfield, K. Richardson, H.J. Schellnhuber, B.L. Turner II, and R. Wasson (2004). *Global Change and the Earth System: A Planet Under Pressure*, Springer, Berlin.
- Strahler, A. N. (1952). Hypsometric (area altitude) analysis of erosional topology. *Geological Society of America Bulletin*, 63: 1117 - 1142.

- Stumm, W. and J.J. Morgan (1996). *Aquatic Chemistry, Chemical Equilibria and Rates in Natural Waters, 3rd ed.* John Wiley & Sons, Inc., New York.
- Theobald, D.M., J.B. Norman, E.E Peterson, and S.B. Ferraz (2005). FLoWS v1: Functional Linkage of Watersheds and Streams tools for ArcGIS v9. Natural Resource Ecology Lab, Colorado State University.
- Triska, F.J., A.P. Jackman, J.H. Duff, and R.J. Avanzino (1994). Ammonium sorption to channel and riparian sediments: A transient storage pool for dissolved inorganic nitrogen. *Biogeochemistry*, 26: 67-83.
- U.S. Department of Agriculture (USDA) Forest Service (FS) (1994). *Ecoregions of the United States*: <http://www.fs.fed.us/land/pubs/ecoregions/>.
- USDA FS. (2004). *Gallatin National Forest: Streams*  
<http://www.fs.fed.us/r1/gallatin/?page=resources/fisheries/streams>
- USDA Natural Resource Conservation Service (NRCS) (2008). Snotel Precipitation Data. <http://www.wcc.nrcs.usda.gov/cgi-bin/wygraph-multi.pl?stationidname=11D19S-LONE+MOUNTAIN&state=MT&wateryear=2008>.
- USDA Soil Conservation Service (USDA SCS) (1982). Soils of Montana, Bulletin 744, November, Montana State University, Bozeman, MT.
- USDA S.C.S. (1978). General Soil Map, Montana, Ext. Misc. Publication No. 16.
- U.S. Geological Survey (U.S.G.S.) (2006). *Nutrients in Streams and Rivers Across the Nation 1992-2001*. Scientific Investigations Report 2006-5107.
- Ver Hoef, J.M., E.E. Peterson, and D.M. Theobald (2006). Spatial statistical models that use flow and stream distance. *Environmental and Ecological Statistics*, 13: 449-464.
- Vitousek, P.M., J.R. Gosz, C.C. Grier, J.M. Melillo, W.A. Reiners, and R.L. Todd (1979). Nitrate Losses from Disturbed Ecosystems, *Science*, 204(4392): 469-474.
- Vogel, R.M., I. Wilson and C. Daly (1999). Regional regression models of annual streamflow of the United States. *Journal of Irrigation and Drainage Engineering*, 125, 148-157.
- Wetzel R.G. (2001). *Limnology, 3rd ed.* San Diego: Academic Press.

- Whitehead, P.G., P.J. Johnes, and D. Butterfield (2002). Steady state and dynamic modelling of nitrogen in River Kennet: Impacts of land use change since 1930s. *The Science of the Total Environment*, 282: 417-434.
- Williams, M.W. and K.A. Tonnessen (2000). Critical loads for inorganic nitrogen deposition in the Colorado Front Range, USA. *Ecological Applications*, 10: 1648-1665.
- Williams, M.W., A.D. Brown, and J.M. Melack (1993): Geochemical and hydrologic controls in the composition of surface water in a high-elevation catchment, Sierra Nevada, California. *Limnology and Oceanography*, 38(4): 775-797.
- Williams, M.W, and J.M. Melack (1991). Solute Chemistry of Snowmelt and Runoff in an Alpine Basin, Sierra Nevada. *Water Resources Research*, 27: 1576-1588.
- Yuan, L.L. (2004). Using spatial interpolation to estimate stressor levels in unsampled streams. *Environmental Monitoring and Assessment*, 94: 23-38.
- Zimmerman, B., H. Elsenbeer, and J.M. De Moraes (2006) The influence of land-use changes on soil hydraulic properties: Implications for runoff generation. *Forest Ecology and Management*, 222 (1-3): 29-38.

Table 2.1: Synoptic sampling event dates and corresponding hydrological condition and biological activity potential.

Synoptic Date	Hydrological Conditions	Biological Activity
September 10, 2005	Baseflow	High Potential
February 12, 2006	Baseflow	Low Potential
June 11, 2006	Snowmelt	Medium Potential
October 16, 2006	Baseflow	Med-Low Potential
March 25, 2007	Pre-snowmelt	Low Potential
August 7, 2007	Baseflow	High Potential

Table 2.2: Potential explanatory variables of streamwater  $\text{NO}_3^-$  in the West Fork watershed.

Variable	Description
# Septic	# of septic
# Septic $TT$	# of septic weighed by travel time ( $TT$ )
#Septic $D$	# of septic weighed by distance to the stream ( $D$ )
Wastewater	Indicator variable (1 or 0) of wastewater irrigation
Area	Area of subwatershed (km)
Geology	Percent geology with higher N weathering potential
Riparian Buffer	Ratio of riparian area to hillslope area
Forest	Percent forest coverage
Order	Strahler stream order
Slope	Median slope
Aspect	Median aspect
Elevation	Elevation at synoptic sampling site

Table 2.3: Spatial linear models fitted to streamwater  $\text{NO}_3^-$  for each synoptic sampling campaign (see Table 2.2 for variable descriptions).

Synoptic Month	Explanatory Variables	Coefficient	p-value	$r^2$	RMPSE
October 2006 (Late Fall)	Intercept	0.033	0.023	0.75	0.047
	Septic $TT$	2.379	0.002		
	Wastewater	0.092	< 0.001		
February 2006 (Winter)	Intercept	0.085	< 0.001	0.90	0.037
	Septic	0.0005	< 0.001		
	Wastewater	0.221	< 0.001		
	Geology	40.0	0.008		
March 2007 (Early Spring)	Intercept	0.083	< 0.001	0.37	0.059
	Septic $TT$	1.942	< 0.001		
June 2006 (Late Spring)	Intercept	0.209	< 0.001	0.06	0.045
	Septic $TT$	1.437	0.002		
	Riparian Buffer Potential	-1.441	0.004		
	Stream Order	-0.033	0.006		
	Forest	-0.135	0.027		
August 2007 (Summer)	Geology	53.5	<0.0001	0.53	0.0203
	Forest	-0.117	0.003		
September 2005 (Late Summer)	Intercept	0.139	< 0.001	0.45	0.028
	Geology	45.42	< 0.001		
	Wastewater	0.058	< 0.001		
	Forest	-0.018	< 0.001		
	Riparian Buffer Potential	-0.626	0.077		

Table 2.4: Spatial covariance parameters for the spatial linear models fitted to streamwater  $\text{NO}_3^-$  for each synoptic sampling campaign (see Table 2.2 for variable descriptions).

Synoptic Month	Autocovariance Model	Nugget	Partial Sill	Range (km)
October 2006 (Late Fall)	Spherical	0.002	0.003	5.03
February 2006 (Winter)	Exponential	0.00043	0.00098	5.505
March 2007 (Early Spring)	Linear-with-sill	0.0008	0.002	3.17
June 2006 (Late Spring)	Mariah	0.00016	0.00228	1.88
August 2007 (Summer)	Linear-with-sill	0.00007	0.0005	2.18
September 2005 (Late Summer)	Linear-with-sill	0.0004	0.0002	2.70

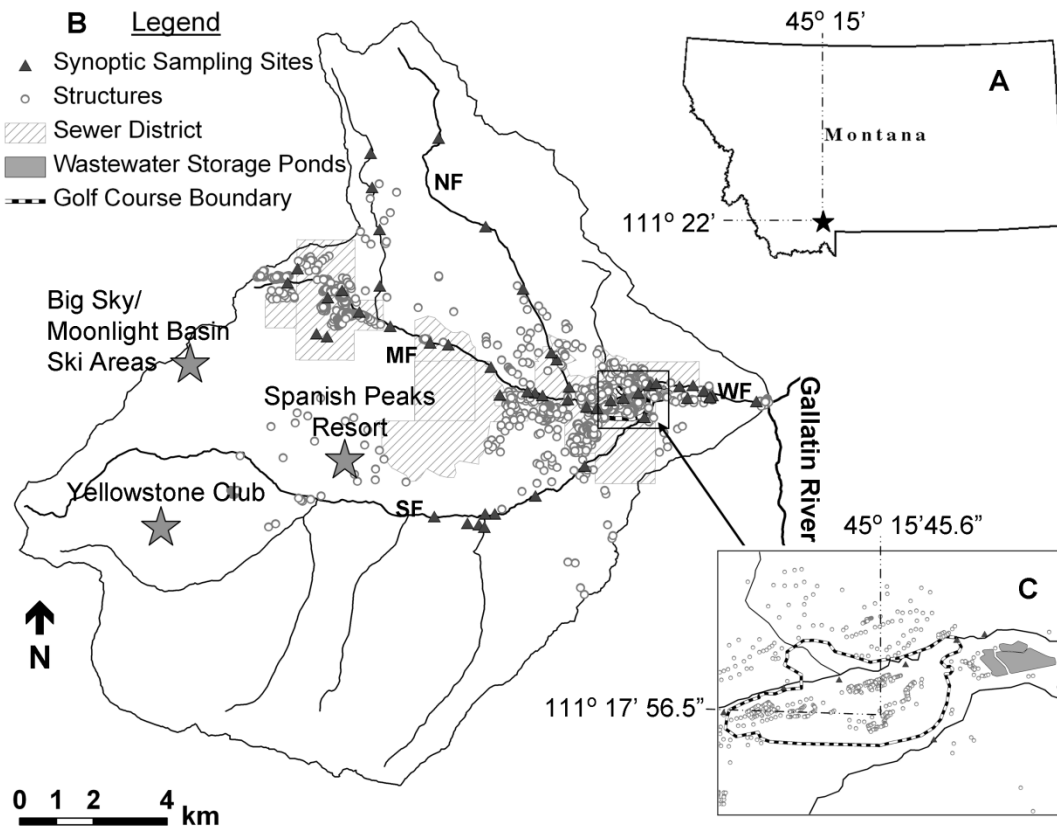


Figure 2.1: (A) Location of the West Fork watershed (212 km<sup>2</sup>) in southwestern Montana. (B) Map of the West Fork watershed showing locations of 50 synoptic sampling sites, building structures, and the Big Sky Water and Sewer District boundaries. The West Fork (WF) drains into the Gallatin River (a tributary of the Upper Missouri River) and is comprised of three main tributaries: the Middle Fork (MF), the North Fork (NF), and the South Fork (SF). (C) An expanded view of the wastewater storage ponds and the Big Sky Resort Golf Course. Wastewater effluent is stored in the ponds and irrigated onto the golf course from mid-May through early October.

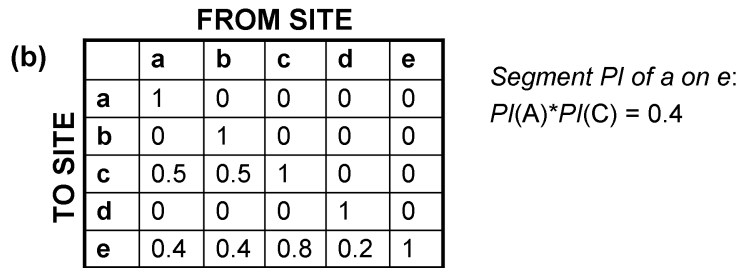
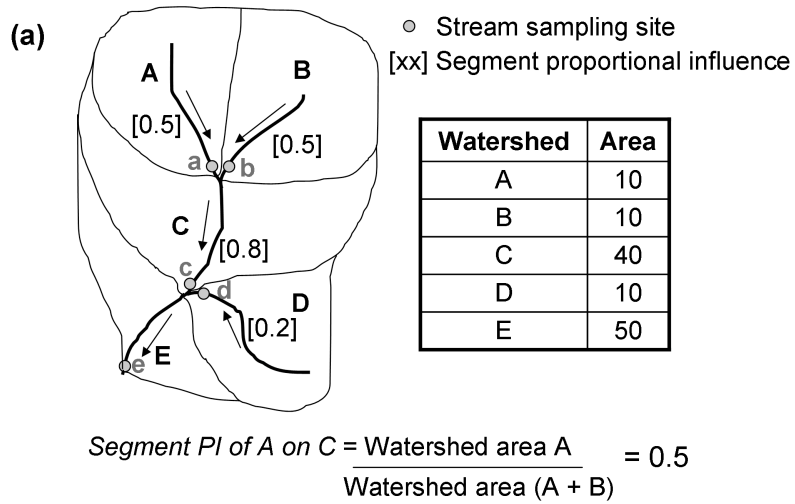


Figure 2.2: A simplified example of watershed E and subwatersheds A-D to illustrate modeled spatial dependence in a stream network. (a) Spatial dependence of stream sites is considered only if sites are flow connected. If water flows downstream between two sites, then they are considered “flow connected”. a and c and b and c are “flow connected” sites, while a and b are “not flow connected” sites. (b) The proportional influence (PI) matrix represents the influence of an upstream location on a downstream location. The PI matrix - the PI for a pair of sites is equal to the product of the segment PIs found in the path between them (modified Peterson et al., 2007 – Figure 2).

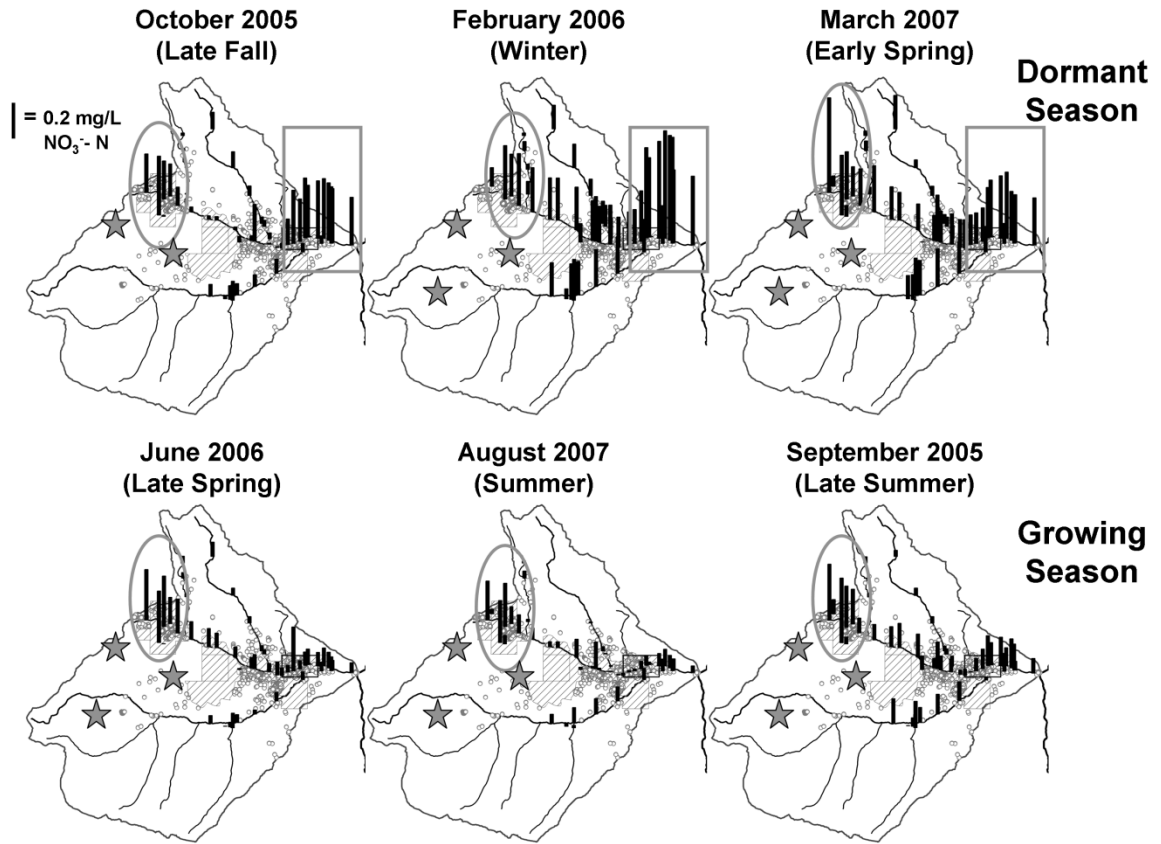


Figure 2.3: Streamwater NO<sub>3</sub><sup>-</sup> concentrations for 6 synoptic sampling campaigns capturing a range of seasonal hydrological and biological conditions (Table 1). Elevated NO<sub>3</sub><sup>-</sup> concentrations persist in streams draining Lone Mountain across seasons (grey ovals), while elevated concentrations downgradient from the Big Sky Golf Course are elevated only in the winter months during periods of low potential biologic activity (grey rectangles).

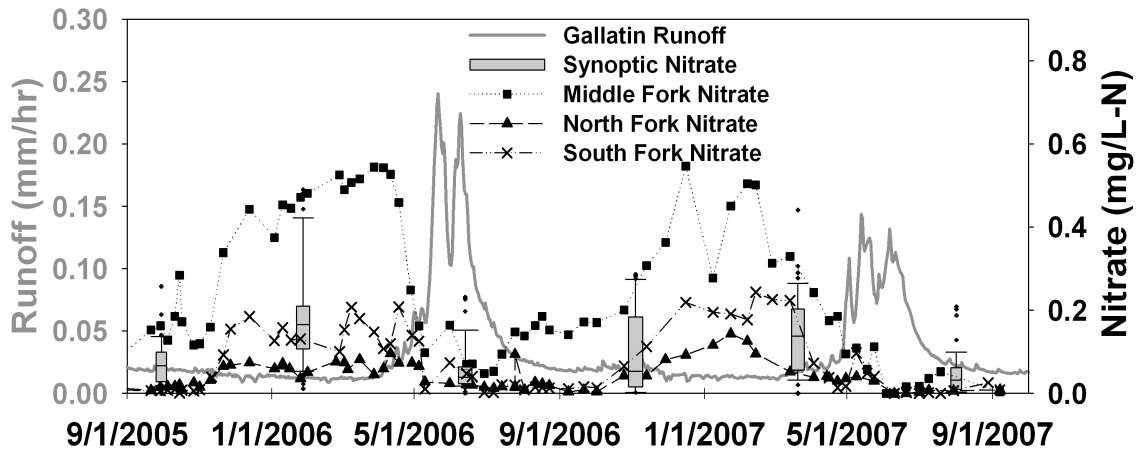


Figure 2.4: Synoptic  $\text{NO}_3^-$  concentrations for the 6 synoptic sampling campaigns conducted between September 2005 and August 2007. Each boxplot consists of 46-50 data points. Streamwater  $\text{NO}_3^-$  concentrations and variability are highest during late fall, winter, and early spring during periods of low streamflow and limited biologic activity. The weekly time series for two sites with varying levels of N loading are included for context and are represented by squares (Middle Fork – high N loading), crosses (South Fork – medium N loading) and triangles (North Fork – low N loading).

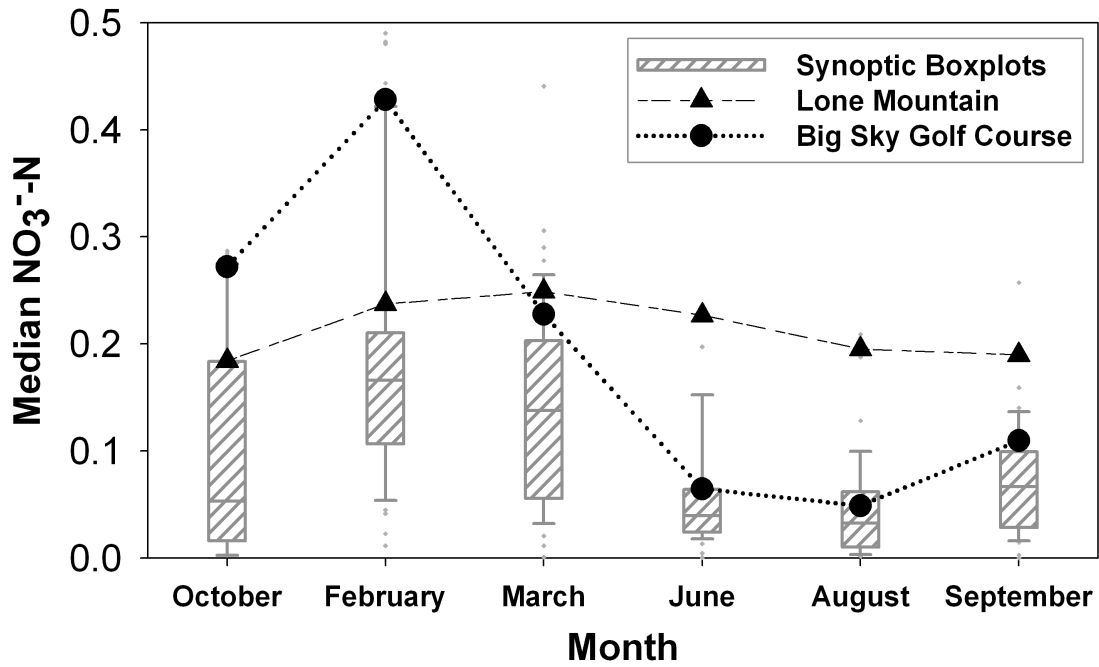


Figure 2.5: Median streamwater  $\text{NO}_3^-$  concentrations of sites located downgradient from the Big Sky Golf Course (black circles) and Lone Mountain (black triangles) for each synoptic event (grey boxplots). Streamwater  $\text{NO}_3^-$  at sites draining Lone Mountain remain relatively elevated throughout the year, while streamwater  $\text{NO}_3^-$  concentrations at sites downgradient from the Big Sky Golf Course exhibit a more amplified seasonal pattern.

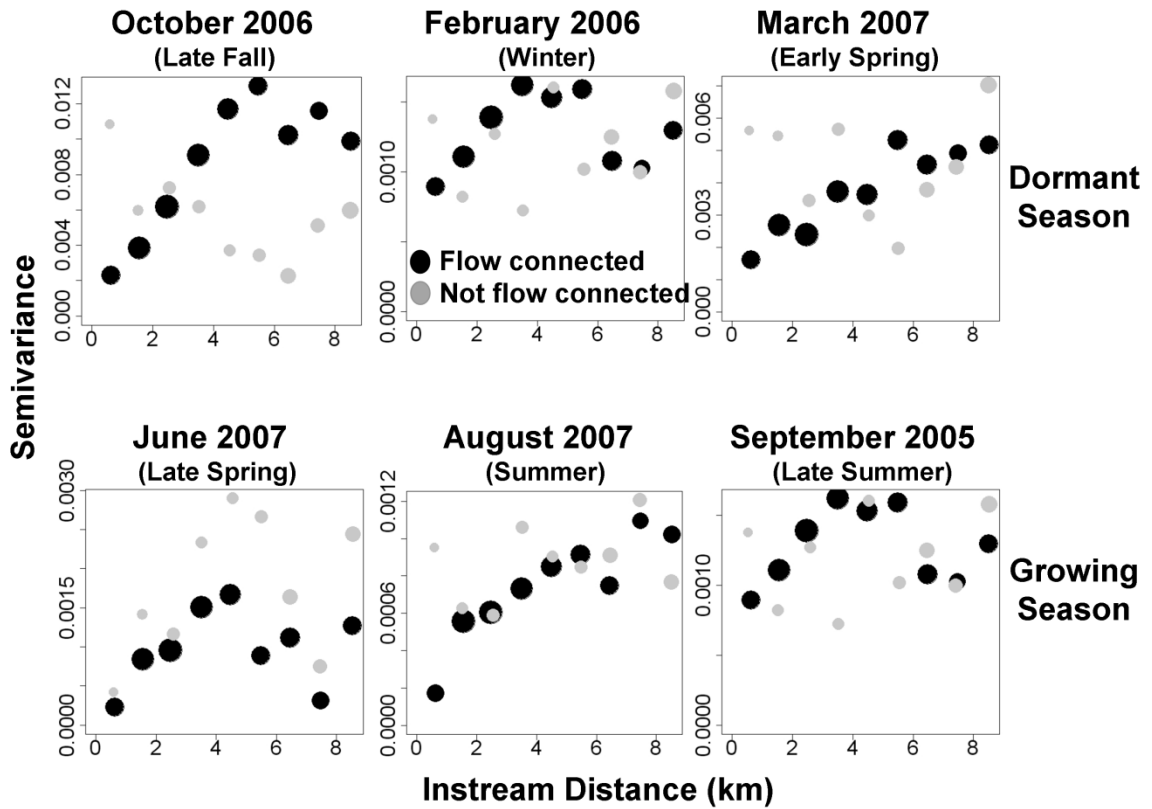


Figure 2.6: Semivariograms of unmodeled synoptic streamwater  $\text{NO}_3^-$ . Seasonality exists in the degree autocovariance variance between “flow connected” sites (black circles) and is not apparent in “not-flow connected” sites (grey circles). Dormant season semivariograms (February -winter, October - late fall and March - early spring) illustrate a greater autocorrelated variance than growing season (June - late spring, August - summer, and September -late summer). This difference in autocorrelated variability suggests the importance of a biologic component in streamwater  $\text{NO}_3^-$  patterns during periods of high potential biologic activity. Symbol size is proportional to the number of pairs at each lag distance.

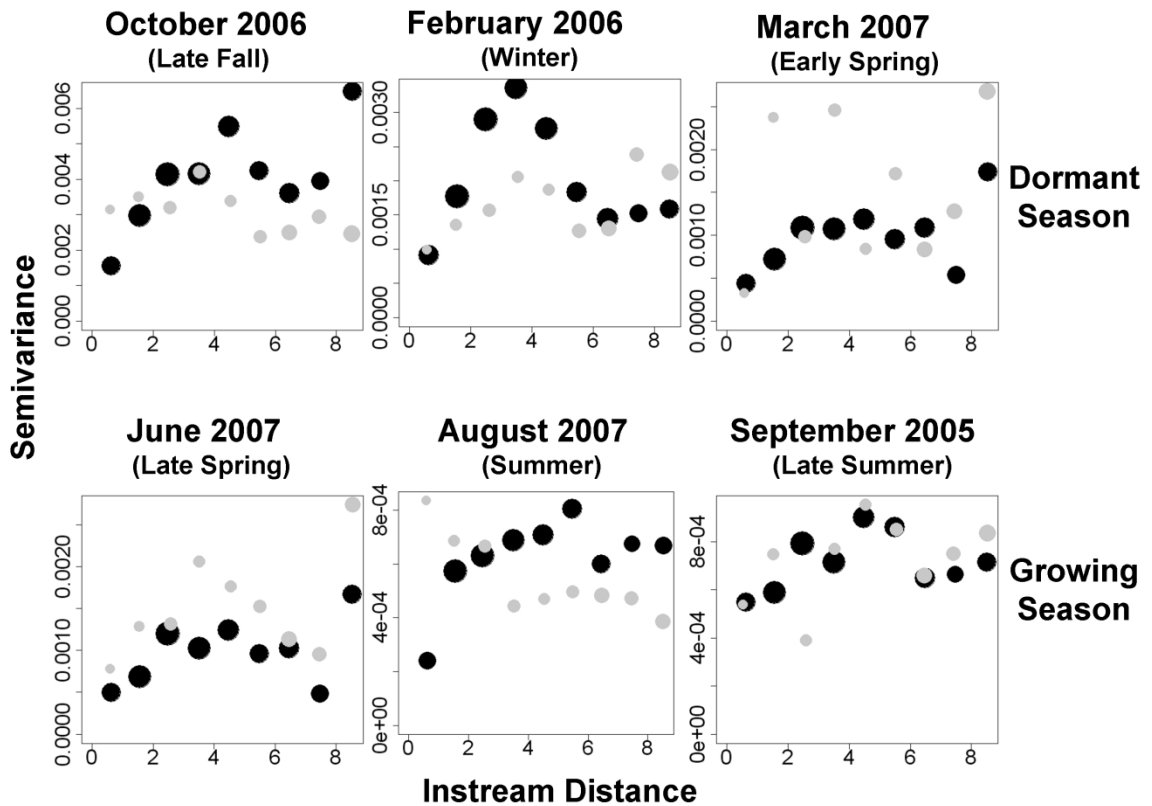


Figure 2.7: Semivariograms of the spatial model residuals of synoptic streamwater  $\text{NO}_3^-$ . Seasonality exists in the range of spatial dependence between “*flow connected*” sites (black circles) and is not apparent in “*not-flow connected*” sites (grey circles). The range of spatial dependency is longer in the dormant season (February -winter, October - late fall and March - early spring) as compared to the growing season (June - late spring, August - summer, and September -late summer). The shorter range in the growing season suggests the importance of a biologic component in streamwater  $\text{NO}_3^-$  patterns during periods of high potential biologic activity. Symbol size is proportional to the number of pairs at each lag distance.

Contribution of Authors and Co-Authors

Manuscript in Chapter 3: A Multi-analysis Approach to Assess the Spatio-temporal Patterns of Watershed Response to Localized Inputs of Nitrogen

Author: Kristin K. Gardner

Contributions: co-developed and implemented the project, collected and analyzed output data, and wrote the manuscript.

Co-author: Dr. Brian L. McGlynn

Contributions: co-developed the study, discussed the results and implications, and commented on the manuscript at all stages.

Manuscript Information Page

Kristin K. Gardner and Brian L. McGlynn

Journal Name: Water Resources Research

Status of Manuscript:

Prepared for submission to a peer-reviewed journal

Officially submitted to a peer-reviewed journal

Accepted by a peer-reviewed journal

Published in a peer-reviewed journal

Publisher: American Geophysical Union

Issue in which manuscript appears in: NA

## CHAPTER 3

## A MULTI-ANALYSIS APPROACH TO ASSESS THE SPATIO-TEMPORAL PATTERNS OF WATERSHED RESPONSE TO LOCALIZED INPUTS OF NITROGEN

Abstract

Understanding the impacts of anthropogenic nitrogen (N) on aquatic ecosystems and how it may vary across space and time is critical for effectively managing watershed nitrogen. This research analyzed spatial and seasonal streamwater nitrogen and carbon concentration data with mass balance calculations and endmember mixing analysis of nitrate ( $\text{NO}_3^-$ ) isotopes to examine the effects of anthropogenic N loading on the timing, magnitude and speciation of watershed nitrogen export and retention. Localized N loading from development lead to similar N saturation characteristics as spatially distributed loading from atmospheric deposition. Spatial and seasonal heterogeneity of watershed N saturation characteristics were exhibited by increased streamwater  $\text{NO}_3^-$  export and concentrations, elevated dissolved inorganic N:dissolved organic N (DIN:DON) ratios, lower dissolved organic carbon:total dissolved N (DOC:TDN) ratios, enriched  $\delta^{15}\text{N}$  of  $\text{NO}_3^-$  values, and sustained DON concentrations through snowmelt; however, biological uptake of N masked enrichment signs during the summer growing season when N concentrations were relatively low. Endmember mixing analysis of  $\text{NO}_3^-$  isotopes demonstrated that despite low  $\text{NO}_3^-$  concentrations and loads in the summer, wastewater was the most significant source of streamwater  $\text{NO}_3^-$ . Anthropogenic N

loading that occurred in areas with quick transport and hydrologic connections to the stream were more apt to display N saturation signals than those areas disconnected or connected to streams via longer flowpaths for only a small portion of the year.

Watershed N retention estimates confirmed that it is not only the amount of N loading that controls watershed N export but where on the landscape it occurs and whether it is localized or spatially distributed. The results of this study provide key insights into effectively managing watershed N by 1) developing flexible strategies across developing watershed to address the spatial and seasonally variable influences of anthropogenic N, and 2) using metrics other than N concentration during periods of high biologic potential to assess N saturations dynamics.

### Introduction

Human activities have greatly increased the amount of bioavailable N over the past century [Vitousek, 1997] through the addition of fertilizer, manure, wastewater, and atmospheric deposition [Puckett, 1994], and disturbance and/or removal of soil and vegetation [Likens, 1970; Vitousek, 1979]. Despite this, N is still the most common limiting nutrient in North American forested ecosystems [Cole and Rapp, 1981; Vitousek and Howarth, 1991]. Escalating inputs of anthropogenic N can saturate ecosystems so that N is no longer the limiting nutrient. Long term spatially distributed inputs (e.g. atmospheric deposition) of anthropogenic N across the U.S. and northern Europe have moved numerous ecosystems towards “N saturation” [Aber et al., 1989; Murdoch and Stoddard, 1992; Lovett et al., 2000; Magill et al., 2000; Baron et al., 2000; Burns, 2003].

When N saturation is reached, N is no longer the limiting nutrient and additional N inputs in excess of biological requirements are “leaked” to streams and groundwater, commonly as nitrate ( $\text{NO}_3^-$ ) [Gundersen *et al.*, 1998b]. This human induced addition of N to aquatic ecosystems has led to increased productivity, reduction in species diversity, and in the most severe cases, eutrophication [Bisson and Bilby, 2001; Folke *et al.*, 2002].

Related to the accepted catchment-wide N saturation concept, N saturation can also occur as a result of localized human inputs of anthropogenic N associated with development (e.g. wastewater effluent, fertilizer, animal waste from pets/feedlots/corrals). In these scenarios, N inputs are concentrated to localized areas where they can quickly saturate hydrological flowpaths, transporting excess N directly to streams and groundwater. Mountain resort development has the potential to exacerbate these effects by adding N to sensitive, strongly seasonal high elevation ecosystems. A growing body of evidence has documented increased N export due to mountain resort development [Coats and Goldman, 2001; Kaushal *et al.*, 2006; Wemple *et al.*, 2007; Burt and Rice, 2009; Gardner and McGlynn, 2009].

Mountainous watersheds can be particularly susceptible to N enrichment from resort development because of greater precipitation and the potential for increased loading of inorganic N in areas with shallow soils, steep talus/scree slopes, and limited potential for riparian buffering and N processing [Seastedt *et al.*, 2004; Gardner and McGlynn, 2009]. Furthermore, mountain resort development is frequently concentrated in riparian areas and valleys, with enhanced opportunity for N transport to aquatic systems [Hill *et al.*, 1996; Gardner and McGlynn, 2009] or on mountain ridges with steep slopes

and shallow soils that have little capacity to assimilate N [Seastedt *et al.*, 2004].

Therefore, even modest levels of anthropogenic N loading can have disproportionately large effects on N dynamics in mountainous headwater ecosystems [Gardner *et al.*, in review]. Because of this sensitivity to nutrient perturbation, mountain environments can be ideal field laboratories to study anthropogenic impacts on watershed N cycling.

The degree to which anthropogenic N inputs impact streamwater N can depend upon the extent and magnitude of nutrient loading and the ecosystem's ability to retain N [Aber *et al.*, 1989 and 1998; Burt and Rice, 2009]. Terrestrial retention of N can be influenced by vegetation [Lovett *et al.*, 2002], flowpath travel time [Seitzinger *et al.*, 2002; Gardner and McGlynn, 2009], riparian area [Hill, 1996; McGlynn and Seibert, 2003; Gardner and McGlynn, 2009], seasonality [Chapin *et al.*, 2002; Gardner and McGlynn, 2009], and hydrologic connectivity [Creed *et al.*, 1996; Jencso *et al.*, 2009; Pacific *et al.*, 2010]. Once delivered to the aquatic ecosystem, additional N can also be immobilized instream via both physical and biological processes [Covino *et al.*, 2010a]. Instream N retention can be a function stream order [Alexander *et al.*, 2000; Peterson *et al.*, 2001], N concentration [Earl *et al.*, 2006; Covino *et al.*, 2010a, b], seasonality [Simon, *et al.*, 2005], and upstream retention dynamics [Mulholland *et al.*, 2008].

In addition, terrestrial and instream retention and release of N can be affected by the relative abundance or “stoichiometric ratios” of carbon (C) and nitrogen (N) due to the tight coupling of C and N cycles for many biological processes [Sturner and Elser, 2002; Gunderson *et al.*, 1998; Lovett *et al.*, 2002; Dodds *et al.*, 2004; Brookshire *et al.*, 2005; Goodale, 2005; Aitkenhead-Peterson *et al.*, 2007; Arango *et al.*, 2007] and the

different ecological and hydrological controls that govern the export of C and N species. In snowmelt-dominated systems, the majority of DIN, DON, and DOC export occurs during snowmelt [*Baron and Campbell, 1997; Boyer et al., 1997; Campbell et al., 2000a; Williams et al., 2001; Kaushal and Lewis, 2005; Pacific et al., 2010*]. During the rest of the year, watershed DIN export is largely a function of biotic demand [*Aber et al., 1989*] and/or a lack of mobilization [*Creed and Band, 1998*]. The mechanisms of DOC and DON (i.e. dissolved organic matter (DOM)) loss can be more complex. DOM is comprised of a mixture of compounds varying in bioavailability [*Findlay and Sinsabaugh, 1999*]. Export of bioavailable DOM is most likely influenced by biotic demand, while export of less labile DOM is controlled mainly by mobilization [*Kaushal and Lewis, 2003*]; however, bioavailable DOM export can occur less readily than DIN because it is readily adsorbed by mineral soils [*Qualls and Haines, 1992*]. Since bioavailability greatly influences DIN uptake and to a lesser extent DON and DOC uptake, as N limited watersheds become N enriched, additional N inputs should increase the ratio of DIN to DON and decrease the ratio of C:N. Therefore, the stoichiometric ratios of C:N and DIN:DON have been suggested as indices of watershed N saturation status from N limited (low DIN:DON, high C:N) to N saturated (high DIN:DON, low C:N) [*Campbell et al., 2000b; Williams et al., 2001*].

Another documented sign of watershed N enrichment is altered seasonal patterns of streamwater  $\text{NO}_3^-$  concentrations [*Aber et al., 1989; 1998*]. Seasonal patterns of  $\text{NO}_3^-$  have been attributed to increased N loading during certain times of the year [*Kaushal et al., 2006; Sobota et al., 2009*] or seasonal differences in biological retention [*Aber et al.,*

1989; Goodale *et al.*, 2000; Gardner and McGlynn, 2009]. In the Rocky Mountain West, streamwater  $\text{NO}_3^-$  concentrations are often highest throughout the winter and decline considerably during the growing season, suggesting the importance biological N retention [Williams and Melack, 1991; Baron and Campbell, 1997; Campbell *et al.*, 2000a; Kaushal and Lewis, 2003]. According to Aber *et al.* [1989; 1998], with increasing watershed N enrichment, seasonal streamwater  $\text{NO}_3^-$  patterns can eventually exhibit chronically high  $\text{NO}_3^-$  concentrations with no distinguishable seasonal pattern [Aber *et al.*, 1989; 1998].

Research focused on the anthropogenic impacts on streamwater N has largely focused on  $\text{NO}_3^-$ , despite DON representing the majority of N loss from many systems [Scott *et al.*, 2007]. Studies that have examined anthropogenic impacts on streamwater DON show conflicting results. Those studies that have found little anthropogenic influence on streamwater DON include: Goodale *et al.* [2000] and Pellerin *et al.* [2004]. Contrastingly, Van Kessel *et al.* [2009] documented that DON can be an important vector of N loss from agricultural land and Stanley and Maxted [2008] documented increased DON export with urban land, although human impacts on DON export occurred to a lesser degree than inorganic N.

Identification of watershed N sources and their relative contributions to streamwater N is critical for implementing effective management strategies that minimize N loading impacts on streams. Dual isotopic analysis of  $\delta^{15}\text{N}$  and  $\delta^{18}\text{O}$  of  $\text{NO}_3^-$  can be used successfully to identify N sources and determine their relative contributions to streamwater  $\text{NO}_3^-$  [Spoelstra *et al.*, 2001; Chang *et al.*, 2002; Campbell *et al.*, 2002;

*Kaushal et al.*, 2006; *Burns et al.*, 2009] when the isotopic signatures of primary sources of  $\text{NO}_3^-$  are sufficiently distinct [*Kendall and McDonnell*, 1998]. Research has shown that  $\delta^{15}\text{N}$  of  $\text{NO}_3^-$  alone can distinguish a domestic wastewater signature from other  $\text{NO}_3^-$  sources [*Aravena*, 1993; *Kaushal et al.*, 2006] because wastewater is enriched in  $\delta^{15}\text{N}$  relative to other N sources (soil, precipitation, mineral weathering). Typically  $\delta^{15}\text{N}$  of  $\text{NO}_3^-$  values of wastewater (+10 to +20‰) are higher than other N sources (<5‰)[*Kendall and McDonnell*, 1998].  $\delta^{18}\text{O}$  values of  $\text{NO}_3^-$  have also worked well to separate atmospheric  $\text{NO}_3^-$  from other N sources [*Spoelstra et al.*, 2001; *Campbell et al.*, 2002; *Chang et al.*, 2002; *Burns*, 2009], because the  $\delta^{18}\text{O}$  values of atmospheric  $\text{NO}_3^-$  are typically quite high (>+60‰) [*Elliot et al.*, 2007] relative to other sources that are often <25‰.

Although identifying the spatial and seasonal variability of anthropogenic impacts on streamwater N represents a significant challenge, isotopic data can add significant analysis power when combined with spatial and temporal streamwater chemistry, and mass balance export calculations. Mass balance approaches can provide insight into ecological controls on N retention and export at the watershed scale [*Baron and Campbell*, 1997; *Burns*, 1998; *Sickman et al.*, 2001; *Groffman et al.*, 2004; *Judd et al.*, 2007; *Claessens et al.*, 2009]. Therefore, multi-analysis approaches can aid assessment of watershed N saturation state and assist identification of watershed N sources contributing to its N status. This is critical to recognizing early signs of N enrichment.

Here we present multiple sources of contemporary field data, including synoptic and temporal sampling for  $\text{NO}_3^-$ , DON and DOC streamwater chemistry and isotopic

ratios of  $\text{NO}_3^-$ , analyzed by mass balance calculations and endmember mixing analysis to examine the effects of anthropogenic N loading on the timing, magnitude, and speciation of watershed N export and retention in watersheds exhibiting varying degrees of watershed N saturation. We address the following research questions: 1) Does anthropogenic N loading influence the spatio-temporal patterns of watershed N and C export, retention, concentrations, and stoichiometric ratios? 2) Do localized inputs of anthropogenic N lead to similar stages of watershed saturation observed at the watershed outlet as spatially distributed inputs from atmospheric deposition?, and 3) Are there spatial and/or seasonal variations in the impact of anthropogenic N loading on streamwater  $\text{NO}_3^-$ ?

## Methods

### Study Area

The West Fork of the Gallatin River in the northern Rocky Mountains of southwestern Montana (Figure 3.1A) drains the Big Sky, Moonlight Basin, Yellowstone Club, and Spanish Peaks resort areas (Figure 3.1B). The West Fork watershed (212 km<sup>2</sup>) is characterized by well-defined steep topography and shallow soils. Elevation in the drainage ranges from approximately 1800 to 3400 meters and average annual precipitation exceeds 1270 mm at higher elevations and is less than 500 mm near the watershed outlet. Sixty percent of precipitation falls during the winter and spring months [USDA NRCS, 2008]. Hydrographs of the West Fork River exhibit peak flows during spring snowmelt typically occurring in late May/early June followed by a general

recession throughout the summer, autumn, and winter months.

The West Fork watershed has steep slopes and predominately shallow soils with high hydraulic conductivities [*USDA SCS, 1978; USDA SCS, 1982*]. These conditions often promote shallow runoff pathways that can result in rapid  $\text{NO}_3^-$  delivery to riparian zones and streams. Shallowest soil depths are in alpine areas, where soil depth can range from zero to less than one meter. Deeper soils exist near the watershed outlet where soil depths can be up to two meters.

Streams in the West Fork watershed range from first-order, high gradient, boulder dominated mountain streams in the upper elevations to fourth-order, alluvial streams near the watershed outlet (Table 3.1). Stream productivity is generally low due to cold temperatures and short growing seasons [*USDA FS, 2004*], however in recent years, increased algal growth has been noted in streams draining developed subwatersheds near the watershed outlet. Chlorophyll a data collected in September 2005 suggest that algal growth is elevated above natural background levels in streams draining developed subwatersheds. Median Chlorophyll a ranged from  $2.5 \text{ mg m}^{-2}$  in pristine low order streams,  $20 \text{ mg m}^{-2}$  in pristine higher order streams to  $360 \text{ mg m}^{-2}$  in higher order streams draining more developed watersheds [*PBS&J, 2005*].

Diverse geologic materials are present in the West Fork watershed, including metamorphosed volcanics of Archean age, sedimentary and meta-sedimentary formations of various ages, and colluvium and glacial deposits that dominate the surficial geology in valley bottoms. Carbonaceous minerals such as limestones and shales are present in the mineralogy of some but not all headwater catchments, and quartzite, biotite, gneiss,

gabbros, and sandstones are also present [Alt and Hyndman, 1986; Kellog and Williams, 2006]. Chemical weathering experiments of different rock types found throughout the study watersheds showed that Cretaceous carbonate rocks produced enough nitrogen to be considered an important source of inorganic nitrogen to certain streams in the watershed [Ackerman *et al.*, in prep.]. Other research has shown that inorganic N can be weathered from layered silicates such as biotite and muscovite, and sedimentary rocks such as shale [Holloway *et al.*, 1999; 2001]. Vegetation below tree line consists of coniferous forest (Lodgepole pine, Blue and Engelmann spruce, and Douglas fir), grasslands, shrublands, and willow and aspen groves in the riparian areas. The watershed has a brief growing season from mid June through mid September (75 – 90 frost free days), decreasing with elevation [USDA FS, 1994].

Big Sky Resort was established in the early 1970's and since then, the West Fork watershed has grown rapidly with the addition of three new ski resorts and golf courses with associated residential development. Since resort development, streamwater  $\text{NO}_3^-$  concentrations in the West Fork of the Gallatin River have followed a similar upward trend as development (Figure 3.2). The Big Sky Water and Sewer District services the two village areas with public water supply and sewer in the West Fork watershed (Figure 3.1B). Public wastewater receives secondary treatment and is released into three lined sewer detention ponds and stored until mid-spring when it is released as irrigation water onto the Big Sky Golf Course (Figure 3.1C). Golf course irrigation begins in mid spring when the ground thaws and continues through mid fall, when the ground again freezes.

Areas outside of the sewer district are on individual or community septic systems and private wells [R. *Edwards*, personal comm., 2007].

### Watershed Streamwater and Snow Sampling

The spatial distribution of watershed  $\text{NO}_3^-$ , DON and DOC concentrations and export was measured through synoptic, or “snapshot-in-time,” sampling in which streamwater was collected in 250 mL high-density polyethylene (HDPE) bottles from 50 sites across the West Fork watershed within 2-3 hours time (Figure 3.1B). Six repeated synoptic sampling campaigns were conducted to represent a range of hydrological conditions and potential biological activity. In addition, weekly samples were collected at 7 sites between September 2005 and August 2007 (Figure 3.1B). Sampling sites were selected to represent a range of subwatershed characteristics including: development intensity, number of wastewater disposal units, geology, stream order, elevation, and discharge (Figure 3.1B). In addition to the streamwater samples, wastewater and snow samples were collected for solute and isotopic analysis. Wastewater was collected from Big Sky Water and Sewer effluent. Snow cores were collected at five sites across the watershed in 2006 and 2007. Snow was transferred from the cores into plastic bags and transferred to the laboratory for solute and isotopic analysis.

### Chemical Analysis of Water and Snowpack Samples

Streamwater and snowpack samples were filtered within 24 hours of collection with 0.45  $\mu\text{m}$  Millipore Isopore Polycarbonate membranes. Filtered water samples were preserved in HDPE bottles and frozen until analysis. Aqueous nitrogen species analyzed

included nitrite ( $\text{NO}_2^-$ ),  $\text{NO}_3^-$ , ammonium ( $\text{NH}_4^+$ ), and total dissolved nitrogen (TDN). DON was computed as the difference between TDN and DIN. In this study, we focus on  $\text{NO}_3^-$  and DON since most samples contained  $\text{NO}_2^-$  and  $\text{NH}_4^+$  levels near or below detection limits (0.005-0.01  $\text{mg L}^{-1}$ ).  $\text{NO}_3^-$  was analyzed by ion-exchange chromatography (IC) using a Metrohm Peak model 820 interface equipped with a 4-mm anion-exchange column [Metrohm, Herisau, Switzerland]. Detection limits for  $\text{NO}_3^-$  were 0.011  $\text{mg L}^{-1} \text{NO}_3^- \text{-N}$ . Accuracy was within 10% for certified 0.4  $\text{mg L}^{-1} \text{NO}_3^- \text{-N}$  standards ( $0.09 \pm 0.009 \text{ mg L}^{-1} \text{NO}_3^- \text{-N}$ ), as measured every 11<sup>th</sup> sample. Coefficients of variation (CVs) for  $\text{NO}_3^-$  standard peak areas were 2% or less.

Concentrations of DOC and TDN were measured simultaneously by oxidative combustion at 720 °C on a Shimadzu TOC-V<sub>CSH</sub> Carbon Analyzer attached to a TNM-1 total nitrogen measuring unit (Shimadzu Corp., Kyoto, Japan). Detection of DOC was by a non-dispersive infrared  $\text{CO}_2$  detector and combustible N was detected as excited  $\text{NO}_2$  by chemiluminescence. Samples were acidified to 2% HCl and sparged for 2 minutes prior to analysis. The DOC detection limit was 0.07  $\text{mg L}^{-1} \text{C}$ , while TDN detection was 0.02  $\text{mg L}^{-1} \text{N}$ . Both DOC and TDN accuracy were measured as the percent difference from a deep seawater reference standard purchased from the University of Miami (FL). These values ranged from less than 1% to 11% error for DOC, and less than 1% to 10% error for TDN. Coefficient of variation (%) for both DOC and TDN ranged from 0 - 4%.

A subset of the filtered streamwater, wastewater, and snowpack samples were frozen until delivery to either the Woods Hole Marine Microbial Biogeochemistry Lab or the University of California-Davis Stable Isotope Facility for isotopic analysis.  $\delta^{15}\text{N}$  and

$\delta^{18}\text{O}$  of  $\text{NO}_3^-$  values were analyzed by the Sigman-Casciotti microbial denitrifier method [Sigman *et al.*, 2001; Casciotti *et al.*, 2001].  $\delta^{15}\text{N}$  and  $\delta^{18}\text{O}$  of  $\text{NO}_3^-$  values are reported relative to the standard AIR and VSMOW, respectively.

#### Stream Discharge Measurements

AquaRod® capacitance probes (*Advanced Measurements and Controls*, Washington, USA) recorded continuous stream height at 30-minute intervals between April and October of 2006-2007 with an accuracy of 3 mm. Stream discharge was calculated from stage-discharge rating curves developed from discharge measurements collected over the full range of streamflow. Stream gauging was performed by the velocity area method with a Marsh-McBirney Flo-Mate Model 2000 portable flowmeter. Discharge over the rest of the study period was manually measured weekly.

#### N Export, Loading, and Retention Calculations

Streamwater export was approximated for  $\text{NO}_3^-$ , DON, TDN, and DOC over 2006-2007 by multiplying weekly measured streamwater chemistry by measured discharge. In locations and on dates when discharge was not measured at the time a water chemistry sample was collected, area-weighted discharge was calculated from regression relationships determined for a range of streamflows between measured weekly streamflow at 9 sites distributed across the West Fork watershed and the U.S. Geological Survey streamflow gauge at Gallatin Gateway, Montana. Watershed area was a good predictor of streamflow across a range of streamflows (all  $R^2$  values greater than 0.95). Annual streamwater  $\text{NO}_3^-$ , DON, TDN, and DOC export, reported as  $\text{kg ha}^{-1}\text{yr}^{-1}$ , was

determined by summing daily flux, which was linearly interpolated between weekly flux calculations.

To compute seasonal export, seasons were defined based on the measured hydrograph and observed weather parameters. Winter was defined as October 1<sup>st</sup> through March 31<sup>st</sup> and is a period of minimum streamflow and least potential for biologic activity. Snowmelt, defined as April 1<sup>st</sup> through July 15<sup>th</sup>, is a period of maximum discharge. Summer, defined as July 16<sup>th</sup> through September 31<sup>st</sup>, is a period of declining discharge and maximum potential for biological activity.

Sources of N loading considered for this analysis were wastewater (public wastewater treatment plant effluent and residential septic systems), and dry and wet atmospheric deposition. We recognize that other N sources exist, but were excluded because of lack of data and consequent uncertainty (i.e. N fixation, small-scale fertilizer application, and mineral weathering). Estimates of wastewater and septic effluent and atmospheric deposition N loads were computed by the Big Sky Nutrient Export model (BiSN) [*Gardner et al.*, in review]. BiSN estimated atmospheric N deposition and wastewater N loading by strictly constraining their likelihood distributions by field observation data, while septic N loading was loosely constrained (by an order of magnitude) by reported values in the literature [*EPA, 2002*] (for more details see *Gardner et al.*, in review or Chapter 4, Table 4.1). Annual N retention was calculated by subtracting observed watershed N export from estimated N loading. Since N loading was more likely underestimated than over estimated (absence of N fixation, fertilizer application, and mineral weathering inputs), watershed N retention was also likely

underestimated. On the other hand, a lack storm event sampling likely underestimated N export, which would have overestimated watershed N retention; however, since the majority of N flux occurs during spring runoff in the snowmelt dominated West Fork watershed, storm event N export is most likely a minor proportion of annual N export. Snowmelt exports 70 to 80 percent of the annual flux of solute and water in watersheds like the West Fork [Baron and Campbell, 1997].

### Isotopic Separations of Streamwater NO<sub>3</sub><sup>-</sup> Sources

Three-component tracer separations of  $\delta^{15}\text{N}$  and  $\delta^{18}\text{O}$  values of streamwater NO<sub>3</sub><sup>-</sup> were used to approximate relative sources of streamwater NO<sub>3</sub><sup>-</sup>. The three sources of streamwater NO<sub>3</sub><sup>-</sup> considered for this analysis were wastewater, atmospheric deposition, and soil water and were estimated by the following mass balance equations originally developed for three-component hydrograph tracer separations [DeWalle et. al., 1988]:

$$Q_{\text{streamflow}} = Q_{\text{atmospheric deposition}} + Q_{\text{wastewater}} + Q_{\text{soilwater}} \quad (1)$$

$$A_{\text{streamflow}} = f_{\text{atmospheric deposition}}A_1 + f_{\text{wastewater}}A_{\text{wastewater}} + f_{\text{soilwater}}A_{\text{soilwater}} \quad (2)$$

$$B_{\text{streamflow}} = f_{\text{atmospheric deposition}}B_1 + f_{\text{wastewater}}B_{\text{wastewater}} + f_{\text{soilwater}}A_{\text{soilwater}} \quad (3)$$

where, A represents the “concentrations” of <sup>15</sup>N or  $\delta^{15}\text{N}$  values and B represents the  $\delta^{18}\text{O}$  values. The wastewater  $\delta^{15}\text{N}$  and  $\delta^{18}\text{O}$  of NO<sub>3</sub><sup>-</sup> endmember was determined from Big Sky Water and Sewer treated effluent. The average snowpack  $\delta^{15}\text{N}$  and  $\delta^{18}\text{O}$  values represented the atmospheric deposition endmember. The soil water endmember was not directly measured and was estimated through examination of isotopic values from pristine sites during baseflow and from weathered parent material [Ackerman et al., in prep.]. Uncertainty in the three-component tracer was assessed [Genereux, 1998].

## Results

### Spatial and Seasonal Patterns of NO<sub>3</sub><sup>-</sup>, DON and DOC Concentrations

Spatial and seasonal variability of streamwater NO<sub>3</sub><sup>-</sup>, DON and DOC concentrations existed across the West Fork watershed (Figures 3.3 and 3.4). Synoptically sampled streamwater NO<sub>3</sub><sup>-</sup> concentrations were highest in February (dormant season) when median concentrations were 0.17 mg L<sup>-1</sup> NO<sub>3</sub><sup>-</sup>-N, and lowest in June (snowmelt) and August (growing season), when median concentrations were 0.04 and 0.03 mg L<sup>-1</sup>-N, respectively (Figure 3.3A, Table 3.2). NO<sub>3</sub><sup>-</sup> concentrations remained elevated at sites draining Lone Mountain (major mountain of Big Sky Resort) compared to other streams across a range of hydrologic conditions and biologic potential. Streamwater NO<sub>3</sub><sup>-</sup> concentrations at sites downgradient from wastewater loading in Meadow Village were significantly elevated compared to other sites in the winter (see *Gardner and McGlynn [2009]* for more details).

Watershed DON and DOC concentrations were highest during snowmelt when median concentrations were 0.19 and 2.49 mg L<sup>-1</sup>, respectively (Table 2). Median DON concentration was lowest during the summer growing season (0.03 mg L<sup>-1</sup>-N), while the median DOC concentration was at a minimum during the winter dormant season (0.75 mg L<sup>-1</sup>) when deeper groundwater was the primary source of streamflow. The synoptic sampling events illustrated no apparent spatial patterns in DON and DOC concentrations at any time of year.

Synoptically sampled DIN:DON ratios were highest during the winter dormant season (median=1.31), driven primarily by high DIN concentrations, and lowest during snowmelt (0.22), driven by low DIN concentrations and elevated DON concentrations (Figure 3.3B, Table 3.2). DIN:DON ratios were generally lowest during the summer growing season except for streams draining high-elevation alpine areas. DOC:TDN ratios were highest during the summer growing season (median=124.55), driven by low TDN concentrations, and were lowest during the winter dormant season (median=2.26), driven by low DOC concentrations and high TDN concentrations (Figure 3.3C).

Concentration data from weekly sampling at the outlets of the three main tributaries (the South, Middle, and North Forks) of the West Fork illustrated seasonally dynamic DOC, DON, and  $\text{NO}_3^-$  concentration patterns (Figure 3.4). Maximum  $\text{NO}_3^-$  concentrations in all three tributaries occurred through the winter dormant season until the onset of snowmelt when concentrations declined and remained low through the summer growing season. As the growing season ended, concentrations began increasing towards winter highs. Winter  $\text{NO}_3^-$  concentrations were amplified in developed streams (Middle Fork and South Fork) as compared to the relatively pristine North Fork (Figure 3.4A). Average winter  $\text{NO}_3^-$  concentrations in the Middle Fork were 3.5 times higher than the  $\text{NO}_3^-$  concentrations in the North Fork ( $0.48 \text{ mg L}^{-1}\text{-N}$  vs.  $0.14 \text{ mg L}^{-1}\text{-N}$ ) and twice the  $\text{NO}_3^-$  concentrations in the South Fork ( $0.24 \text{ mg L}^{-1}\text{-N}$ ).

While biologic activity (season) appeared to influence  $\text{NO}_3^-$  concentration patterns, hydrology appeared to control DON and DOC concentration patterns (Figures 4B and 4C). Both DON and DOC concentrations peaked during snowmelt, with

maximum DOC concentrations occurring just prior to the maximum DON concentration. No discernable temporal concentration pattern existed for DON or DOC throughout rest of the year. Comparison of the three main tributaries revealed DON concentrations two times greater in the Middle Fork as compared to the South Fork and the North Fork ( $0.06$  vs.  $0.03 \text{ mg L}^{-1} \text{ -N}$ ) during baseflow.

Time series of stoichiometric ratios illustrated that the relative abundance of DIN:DON and DOC:TDN exhibited a high degree variability throughout the year (Figures 3.4D and 3.4C). In general, DIN:DON ratios were highest during the winter, when potential for biological activity was low. These high ratios were a result of high DIN concentrations and low DON concentrations. DOC:TDN ratios peaked at the onset of snowmelt at the DOC concentration peak and remained low the rest of the year.

$\text{NO}_3^-$ , DON, and DOC concentration-discharge relationships for the upper North Fork (UNF) and lower Middle Fork (LMF) are illustrated in Figure 3.5. These two subwatersheds represent two extremes in watershed and land use characteristics; LMF is a highly-developed, unconfined, valley-bottom stream receiving high anthropogenic N loading, while UNF flows through a relatively narrow confined forested landscape with minimal human impact (Table 3.1). Like their contrasts in landscapes and anthropogenic influence, the N and C hysteresis patterns of the two subwatersheds differ in magnitude and shape. The  $\text{NO}_3^-$  versus stream discharge hysteretic loops were clockwise and banana shaped; concentration sharply declined with initial increase in discharge followed by a gradual decline until the descending limb discharge reached a near minimum and concentration began to rise (Figure 3.5A). Although the general shapes of the LMF and

UNF  $\text{NO}_3^-$  hysteresis loops were similar, streamwater  $\text{NO}_3^-$  concentrations at LMF increased more sharply on the descending limb of the hydrograph. Another difference was the magnitude of streamwater  $\text{NO}_3^-$  concentrations; minimum streamwater  $\text{NO}_3^-$  concentrations at LMF were an order of magnitude higher than UNF ( $0.05 \text{ mg L}^{-1}\text{-N}$  vs.  $0.005 \text{ mg L}^{-1}\text{-N}$ ).

Compared to  $\text{NO}_3^-$ , DON and DOC hysteresis loops were more rounded corresponding to overall less dramatic changes in concentration with discharge (Figures 3.5B and 3.5C). Peak DON preceded peak DOC and increased towards the end of snowmelt at both LMF and UNF, while DOC remained low on the descending limb (Figure 3.5C). The DON concentration loop at LMF was the only loop to exhibit counter-clockwise hysteresis (Figure 3.5B); the highest DON concentrations were sustained for a longer period of time after peak runoff. Though not as large as the difference in  $\text{NO}_3^-$  concentrations, the DOC and DON concentration peaks at LMF were greater than those at UNF: peak DOC at LMF was  $5.5 \text{ mg L}^{-1}$  versus  $3.7 \text{ mg L}^{-1}$  at UNF, while peak DON was  $0.18 \text{ mg L}^{-1}\text{-N}$  at LMF versus  $0.08 \text{ mg L}^{-1}\text{-N}$  at UNF. In addition, at LMF DOC peaked much earlier at the onset of snowmelt, than UNF suggesting a near stream source of high DOC at LMF.

The stoichiometric ratio hysteresis loops at LMF and UNF differed in shape and magnitude (Figures 3.5D and 3.5E). In both streams, DIN:DON generally decreased with increasing discharge (Figure 3.5D); however, DIN:DON increased at LMF on the descending limb of the snowmelt hydrograph, while at UNF, DIN:DON remained relatively constant. The magnitude of DIN:DON was 2.5 times greater at LMF compared

to UNF during at the onset of snowmelt, but that difference waned with increasing discharge. In both streams, DOC:TDN increased with increasing discharge, peaked prior to peak discharge and then decreased to a relatively constant level for the remainder of snowmelt (Figure 5E). At peak discharge, DOC:TDN was 4 times greater at LMF compared to UNF, driven by higher DOC concentrations.

#### Annual and Seasonal NO<sub>3</sub><sup>-</sup>, DON, and DOC export

Annual NO<sub>3</sub><sup>-</sup>, DON and DOC export data are presented in Table 3.3 and Figures 3.6, 3.7A, and 3.8A. Average annual TDN export for streams within the West Fork watershed varied from 0.37 to 0.81 kg ha<sup>-1</sup> yr<sup>-1</sup>. DON was the dominant form of TDN in all watersheds (60% – 70%) except for LMF (Figures 3.6 and 3.7), where DON represented only 40% of annual TDN export. DON export ranged from 0.23 to 0.63 kg ha<sup>-1</sup> yr<sup>-1</sup> from the upper Middle Fork (UMF), which is downstream of an extensive wetland complex. Annual NO<sub>3</sub><sup>-</sup> export varied from 0.14 kg ha<sup>-1</sup> yr<sup>-1</sup> from the lower North Fork (LNF) to 0.48 kg ha<sup>-1</sup> yr<sup>-1</sup> at LMF, which is downstream of significant anthropogenic loading from Meadow Village. Annual DOC export was greatest at UMF (14.12 kg ha<sup>-1</sup> yr<sup>-1</sup>) and lowest at UNF (5.91 kg ha<sup>-1</sup> yr<sup>-1</sup>). Annual DIN:DON ratios varied from 0.29 at UMF to 1.60 at LMF. Annual DOC:TDN ratios were relatively uniform throughout the watershed. DOC:TDN ranged from 12.03 at LMF, driven by high TDN values, to 17.41 at UMF, driven by high DOC values.

The West Fork watershed exhibited a high degree of seasonality in the magnitude and relative abundance of NO<sub>3</sub><sup>-</sup>, DON and DOC export. The majority of NO<sub>3</sub><sup>-</sup>, DON and DOC export occurred during snowmelt when 71, 92, and 93%, respectively was

transported from the basin (Figures 3.7C, and 3.8C). For all tributaries,  $\text{NO}_3^-$ , DON and DOC mass export declined on the descending limb of the snowmelt hydrograph and remained relatively constant for the rest of the year (Figure 3.6B). The watershed was the most retentive of  $\text{NO}_3^-$ , DON and DOC during the summer, exporting only 5.1, 3.8, and 2.5% of the annual  $\text{NO}_3^-$ , DON, and DOC, respectively (Figures 3.7D and 3.8D). During baseflow, LMF exported  $\text{NO}_3^-$  at twice the rate of the other main West Fork tributaries (Figure 3.6).

Seasonal differences in the relative abundance of DIN and DON and TDN and DOC export were observed across the West Fork watershed. In the winter,  $\text{NO}_3^-$  was the most abundant form of TDN exported from all subwatersheds; median DIN:DON ratios were 2.25, ranging from 4.3 at LMF to 1.4 at LNF (Figure 3.7B). During summer and snowmelt, DON constituted the majority of TDN in all tributaries except for LMF (Figures 3.7C and 3.7D). At LMF, the DIN:DON ratio was greater than one throughout the year and was consistently higher than other tributaries (Figures 3.7B, 3.7C, and 3.7D). DOC:TDN ratios were highest during snowmelt in all streams except for the West Fork (WF), driven by high DOC concentrations (Figure 3.8C), and lowest during the dormant season (Figure 3.8D). DOC:TDN ratios were lowest at LMF throughout the year caused by high concentrations of TDN.

### Annual Watershed N Loading and Watershed N Retention

Estimated N loads to the West Fork watershed were  $3.85 \text{ kg ha}^{-1} \text{ yr}^{-1}$ , with subwatershed N loads ranging from  $3.41 \text{ kg ha}^{-1} \text{ yr}^{-1}$  to the South Fork (SF) to  $4.66 \text{ kg ha}^{-1} \text{ yr}^{-1}$  at UMF (Figure 3.9, Table 3.4). The highest N loads at UMF corresponded with highest watershed TDN and DON export but not the highest watershed  $\text{NO}_3^-$  export (Table 3). Instead, the highest watershed  $\text{NO}_3^-$  export corresponded to the highest wastewater N loads at LMF (Table 3.5). Across the West Fork watershed, atmospheric deposition was by far the greatest contributor to watershed N loads (Figure 3.9, Table 3.5); wet deposition N loads varied between  $2.66$  to  $3.14 \text{ kg ha}^{-1} \text{ yr}^{-1}$  because of elevation differences in precipitation, while dry deposition N loads were estimated as  $0.26 \text{ kg ha}^{-1} \text{ yr}^{-1}$  across subwatersheds. Septic loads varied from  $0.005 \text{ kg ha}^{-1} \text{ yr}^{-1}$  at UNF to  $1.74 \text{ kg ha}^{-1} \text{ yr}^{-1}$  at UMF. Only two subwatersheds received wastewater N loading, which contributed about five percent of the N load to LMF and only two percent of the N load to WF.

Estimates of watershed N retention ranged from 81 to 89% for TDN, 92 to 96% for  $\text{NO}_3^-$ , and 87 to 93% for DON (Table 3.4). The relationships between N loading and watershed TDN,  $\text{NO}_3^-$ , and DON retention were best described by linear models (Figure 3.10). Thus, according to the Michaelis-Menten kinetic model, the streams of the West Fork watershed grouped together were well below N saturation [Earl, 2006]. The linear relationships between N loading and watershed  $\text{NO}_3^-$ , DON, and TDN were highly significant with adjusted R squares of 0.93, 0.92, and 0.92, respectively. As expected in

an N limited system, the slope of the relationship between watershed N loading and watershed N retention for  $\text{NO}_3^-$  (0.93) was highest, indicating  $\text{NO}_3^-$  was retained at a higher rate than TDN (0.83) or DON (0.90).

### Isotopic Separation of Streamwater $\text{NO}_3^-$ Sources

Spatial and seasonal isotopes of streamwater  $\text{NO}_3^-$  identified variability of streamwater  $\text{NO}_3^-$  sources and the influence of anthropogenic N on streamwater  $\text{NO}_3^-$  (Figure 3.11, 3.12, 3.13, 3.14, and Table 3.7). The wastewater effluent endmember (+12.2, -2) and the atmospheric endmember (-2, +76.5) were in the range of widely documented wastewater (-2 to +10‰, 0 to +25‰) and precipitation values (+20 to +70‰, -3 to +10‰) [Kendall and McDonnell, 1998]. The mineral weathering endmember (+2.1, +5.25) [Ackerman *et al.*, in prep.] was similar to values found by Goodale *et al.* [2009]. Summer synoptic  $\delta^{15}\text{N}$  of  $\text{NO}_3^-$  values ranged from +0.56 to +10.92‰ and  $\delta^{18}\text{O}$  of  $\text{NO}_3^-$  values ranged from -6.94 to +0.61‰ (Figure 3.11 and 3.12B). Winter synoptic  $\delta^{15}\text{N}$  of  $\text{NO}_3^-$  values were similar to summer  $\delta^{15}\text{N}$  of  $\text{NO}_3^-$  values (+0.2 to +9.75‰), while winter synoptic  $\delta^{18}\text{O}$  of  $\text{NO}_3^-$  values were lower than summer values, ranging from -3.7 to -12.02‰ (Figure 3.12A).  $\delta^{15}\text{N}$  of  $\text{NO}_3^-$  values were enriched at sites located downgradient from Meadow Village during summer and winter baseflow (+7.6 - +10.9‰), indicating a wastewater influence on the streamwater  $\text{NO}_3^-$  concentrations observed at these sites (Figure 3.11, 3.12, and 3.13). On the other hand, at sites draining Lone Mountain  $\delta^{15}\text{N}$  of  $\text{NO}_3^-$  values ranged from +0.55 to +1.6‰ indicating that observed elevated streamwater  $\text{NO}_3^-$  concentrations at these sites were not influenced by wastewater (Figure 3.12).

$\text{NO}_3^-$  isotopic data from the main West Fork tributaries illustrated seasonal variability of streamwater  $\text{NO}_3^-$  sources (Figure 3.13 and 3.14).  $\delta^{15}\text{N}$  of  $\text{NO}_3^-$  values at LMF varied from  $+5.8\text{‰}$  during snowmelt to  $+9.2\text{‰}$  during winter and  $+10.9\text{‰}$  in the summer, signifying a greater wastewater contribution to summer and winter baseflow  $\text{NO}_3^-$ . Wastewater also contributed more to  $\delta^{15}\text{N}$  of  $\text{NO}_3^-$  values at SF during baseflow, when  $\delta^{15}\text{N}$  of  $\text{NO}_3^-$  values varied from  $+2.5\text{‰}$  during snowmelt to  $+4.5\text{‰}$  during winter and  $+6.5\text{‰}$  in the summer. There was no significant variability in the  $\delta^{15}\text{N}$  of  $\text{NO}_3^-$  values at the pristine site, LNF.  $\delta^{18}\text{O}$  of  $\text{NO}_3^-$  was enriched for all tributaries during snowmelt indicating an increase in an atmospheric  $\text{NO}_3^-$  source (Figure 3.13).

A three-component mixing model determined streamwater  $\text{NO}_3^-$  sources at LMF, SF, and LNF (Equations 1 thru 3, Figure 3.13, Figure 3.14, and Table 3.7). Since  $\delta^{15}\text{N}$  and  $\delta^{18}\text{O}$  values of soil water  $\text{NO}_3^-$  were not directly measured, the soil water endmember was assumed to be the average  $\delta^{15}\text{N}$  and  $\delta^{18}\text{O}$  values at sites with no wastewater influence ( $+3.5 \pm 15\text{‰}$ ,  $-6 \pm 6\text{‰}$ ), which fell in the range of typical soil water values [Kendall and McDonnell, 1998]. Soil water was the biggest contributor to streamwater  $\text{NO}_3^-$  across seasons at SF and LNF. At SF, soil water contributed 77% of streamwater  $\text{NO}_3^-$  in the winter, 92% during snowmelt, and 61% in the summer. At LNF, soil water contributed 100% of streamwater  $\text{NO}_3^-$  in the winter, 87% during snowmelt, and 100% in the summer. At LMF soil water was the biggest contributor of streamwater  $\text{NO}_3^-$  only during snowmelt (73%). During winter and summer baseflow, wastewater was the largest source of streamwater  $\text{NO}_3^-$  (summer = 87% and winter = 68%). Although the overall amount of wastewater contributions was less than LMF, the same pattern was

observed at SF, where wastewater contributed 22, 16, and 0% of summer, winter, and snowmelt  $\text{NO}_3^-$  concentrations, respectively. Atmospheric  $\text{NO}_3^-$  contributed 6, 8, and 13% of streamwater  $\text{NO}_3^-$  at LMF, SF, and LNF, respectively during spring runoff.

### Discussion

This research combined spatial snapshots (synoptic) and weekly sampling at multiple catchments of  $\text{NO}_3^-$ , DON, DOC and  $\text{NO}_3^-$  isotopes to provide insight into the internal processes controlling nutrient dynamics. Few studies have simultaneously considered spatial and time series data to assess watershed solute export. Results revealed that within the West Fork watershed, subwatersheds exhibited considerable variability in 1) the annual and seasonal magnitude of  $\text{NO}_3^-$ , DON and DOC export, 2) seasonal  $\text{NO}_3^-$  and DON concentration patterns, 3) the relative abundance of DIN and DON and DOC and TDN, 4) watershed N saturation status, and 5) N sources.

Does Anthropogenic N loading Influence the Spatio-Temporal Patterns of  $\text{NO}_3^-$ , DON and DOC Export, Concentrations and Stoichiometric Ratios?

Annual  $\text{NO}_3^-$ , DON and DOC Export: The magnitude of  $\text{NO}_3^-$ , DON and DOC exported annually from the West Fork watershed was comparable to other mountainous watersheds in western U.S.  $\text{NO}_3^-$  export from the West Fork watershed varied from 0.14 - 0.48  $\text{kg ha}^{-1}\text{yr}^{-1}$ , while three subwatersheds of the Blue River in Summit County, Colorado of mixed land use varied from 0.26 – 0.45  $\text{kg ha}^{-1}\text{yr}^{-1}$  [Kaushal and Lewis, 2003; Kaushal and Lewis, 2006] and two undeveloped headwater watersheds in the

Sierra Nevada mountains were 0.45 and 0.56 kg ha<sup>-1</sup>yr<sup>-1</sup> [Lewis *et al.*, 1999] (Table 3.3, Table 3.6). While NO<sub>3</sub><sup>-</sup> export from the West Fork watershed was considerably less than values recorded at two high-elevation Colorado Rocky watersheds: the Loch Vale watershed in Rocky Mountain National Park (1.7 – 3.9 kg ha<sup>-1</sup>yr<sup>-1</sup>) [Baron and Campbell, 1997; Campbell *et al.*, 2000] and just south, at the Green Lakes Valley watershed, (1.62 – 2.13 kg ha<sup>-1</sup>yr<sup>-1</sup>) [Williams *et al.*, 2001]. These comparisons support past research indicating that watersheds receiving greater anthropogenic N loads can export more NO<sub>3</sub><sup>-</sup> than other watersheds [Aber *et al.*, 1989; Williams *et al.*, 1996; Gundersen *et al.*, 1998b]. N deposition at the Loch Vale and Green Lakes Valley on the eastern slope of the Rocky Mountain Front is greater than watersheds in Summit Valley, the Sierra Nevadas, or the southwestern Montana [NADP, 2010].

Annual NO<sub>3</sub><sup>-</sup> exports within the West Fork watershed were higher in developed watersheds compared to undeveloped watersheds (Figure 3.7A). Higher NO<sub>3</sub><sup>-</sup> export with anthropogenic development has been well documented [Boyer *et al.*, 2002; Whitehead *et al.*, 2002; Groffman *et al.*, 2004; U.S.G.S., 2006]. Since NO<sub>3</sub><sup>-</sup> is highly soluble in water, additional inputs from anthropogenic development can be readily transported to streamwater [Gunderson *et al.*, 1998].

Compared to annual NO<sub>3</sub><sup>-</sup> export, less research has documented DON and DOC export from mountainous watersheds in the western U.S. (Table 3.6). Of the DON export data that has been reported, DON export values from the West Fork watershed (0.23 – 0.63 kg ha<sup>-1</sup>yr<sup>-1</sup> – Table 3.3) were within the range reported from subwatersheds of the Blue River in Colorado (0.3 – 0.7 kg ha<sup>-1</sup>yr<sup>-1</sup>) [Kaushal and Lewis, 2003; Kaushal and

Lewis, 2006] and Green Lakes Valley, Colorado (0.36 - 0.61 kg ha<sup>-1</sup>yr<sup>-1</sup>) [Williams et al., 2001] (Table 3.6). Of studies that did report DOC export, the magnitude of DOC exported annually from the West Fork watershed (5.91 – 14.12 kg ha<sup>-1</sup>yr<sup>-1</sup> – Table 3.3) was within the reported range of DOC export from the Salmon River, Idaho (7.2 – 11.4 kg ha<sup>-1</sup>yr<sup>-1</sup> – Table 3.6) [Moeller et al., 1979], the North Fork and South Platte watersheds in southwest Colorado (10.3 – 12.9kg ha<sup>-1</sup>yr<sup>-1</sup>)[Ward et al., 1976], and Stringer watershed in central Montana (9.6 kg ha<sup>-1</sup>yr<sup>-1</sup>)[Pacific et al., 2009].

Few studies have examined the impacts of anthropogenic N loading on DON and DOC export. Some research has found anthropogenic N loading to increase DON concentrations. Stanley and Maxted [2008] found significantly higher DON concentrations in human dominated watersheds as compared to forested watersheds, however the increase in DON was much less than NO<sub>3</sub><sup>-</sup>. A few studies have shown increasing DON concentrations with agricultural land uses [Stedmon et al., 2006; van Kessel et al., 2009]. Elevated DON and DOC concentrations can also occur downstream of point sources of wastewater [Servais et al., 1999]. Other research did not find a significant relationship between urban or agricultural land and DON concentrations [Pellerin et al., 2004; Mattsson et al., 2009]. In the West Fork watershed, annual DON and DOC export was elevated in developed subwatersheds compared to undeveloped watersheds (Figures 3.7A and 3.8A and Table 3.3); however, synoptically sampled spatial DON and DOC concentration plots showed no clear relationship between development and DON or DOC. In addition to anthropogenic impacts, elevated DOC and DON export evident in Figures 3.7, and 3.8 and Table 3.3 from more developed

subwatersheds could result from: 1) more developed soils and vegetation at lower elevations [*Williams et al., 2001*] and/or 2) a longer time period of hydrologic connectivity between riparian and wetland areas, which generally have higher concentrations of organic matter [*Fiebig et al., 1990; Dosskey and Bertsch, 1994; Pacific et al., 2009*].

Research has shown that the extent of hydrologic connectivity between streams and riparian areas [*Pacific et al., 2009*] and wetlands [*Pellerin, 2004; Stanley and Maxted, 2008; Mattson et al., 2009; Pacific et al., 2009*] can drive the magnitude of DON and DOC export. Shallow flowpaths through riparian and wetland soils rich in organic matter can transport DON and DOC directly to streams [*McGlynn et al., 1999; McGlynn and McDonnell, 2003*] bypassing mineral soils, which tend to retain DON and DOC [*Qualls and Haines, 1991*]. Within the West Fork watershed, DON and DOC export was highest at UMF (Figures 3.7A and 3.8A). Although UMF received the greatest magnitude of N loading, it is also located downstream of an extensive wetland complex. Therefore, we are unable to resolve the degree to which landscape properties and land use change/ nutrient loading explain the increased DON and DOC export from this site.

Because of anthropogenic influence on DIN, anthropogenic N loads also influenced annual stoichiometric ratios of DIN:DON and DOC:TDN. DON was the most abundant form of N exported from the subwatersheds, except for LMF (Table 3.3). Greater proportions of DON (60% to 90%) compared to DIN in streamwater have been reported across all regions of the United States [*Scott et al., 2007*] including the western mountains of the Sierra Nevada [*Coats and Goldman, 2001*], and the Colorado Rockies

[*Campbell et al.*, 2000b; *Kaushal and Lewis*, 2005]. Since anthropogenic N loading generally lead to increased DIN but not DON in this study, DIN:DON ratios were higher in watersheds with greater anthropogenic N loading (Figure 3.3B and 3.7A). Annual DIN:DON was greatest at LMF, which was the only site where DIN dominated annual export (DIN:DON = 1.6). Few studies have examined the watershed distribution of streamwater DIN:DON ratios. In a high-elevation Colorado Rocky Mountain watershed, higher DIN:DON ratios were observed in the alpine headwaters compared to subalpine forest and were suggested to represent a shift in the watershed N status from N saturated (high DIN:DON) to N limited (low DIN:DON) [*Williams et al.*, 2001; *Hood et al.*, 2003a].

High DIN concentrations also drove annual DOC:TDN to be lowest at LMF (Figure 3.8). C:N ratios have been suggested as a useful tool in characterizing watershed N status [*Campbell et al.*, 2000b]. The main biological processes that connect the N and C cycles, and thus C:N ratios, in soil environments are microbial respiration and denitrification. When C limits microbial growth, microbes will mineralize DON and release DIN [*Chapin*, 2002] reducing soil C:N ratios.

With relatively high DIN:DON and DOC:TDN ratios at LMF, watershed N retention appears to have been compromised. Although watershed N retention at LMF was comparable to the other developed watersheds (83% compared to 83% at UMF, 82% at SF, and 81% at WF – Table 3.4), it plots below the linear trend between N loading and  $\text{NO}_3^-$  retention in the West Fork watershed (Figure 3.10). Across the West Fork watershed, watershed TDN,  $\text{NO}_3^-$ , and DON retention increased linearly with watershed

N loading (Figure 3.10) suggesting that when considered as a whole, the West Fork watershed appears to be well below N saturation, according to Michaelis-Menten kinetics [Earl, 2006]. If the West Fork watershed was approaching N saturation, one would expect watershed N retention to increase asymptotically to plateau.

In addition to over predicting watershed  $\text{NO}_3^-$  retention at LMF, the linear trend between N loading and  $\text{NO}_3^-$  retention under predicted  $\text{NO}_3^-$  retention at UMF, while the linear trend between N loading and DON retention was over predicted. The wetland complex upstream of this site is most likely altering instream N dynamics by immobilizing more inorganic N and releasing more organic N [Dosskey and Bertsch, 1994; Pellerin, 2004, Stanley and Maxted, 2008; Mattson et al., 2009].

Seasonal  $\text{NO}_3^-$ , DON and DOC Export: Snowmelt dominated the annual export budget for  $\text{NO}_3^-$ , DON and DOC (Figures 3.6, 3.7, and 3.8). Similar behavior has been observed in other snowmelt dominated systems [Hornberger et al., 1994; Boyer et al., 1997; Hood et al., 2003b; Kaushal and Lewis, 2005; Sebestyen, 2008]. Though much less than snowmelt, at LMF winter  $\text{NO}_3^-$  export was considerably higher than summer  $\text{NO}_3^-$  export (Figures 3.7B and 3.7D). Although summer discharge is generally higher than winter discharge,  $\text{NO}_3^-$  concentrations were considerably lower in the summer than the winter because of higher rates of biological N retention (Figures 3.3A and 3.4A) [Gardner and McGlynn, 2009; McNamara, 2010].  $\text{NO}_3^-$  was the most abundant form of N exported from all catchments during the winter when groundwater flowpaths low in DON dominated streamflow and biological demand was relatively low.

During the summer growing season there were differences among subwatersheds in the relative abundance of DIN and DON. DIN:DON ratios were less than 1 at all sites except for LMF, where the DIN:DON ratio was 4.42 (Figure 3.7D). Other research in the Rocky Mountain West has shown DON to account for the majority of TDN during the growing season [*Kaushal and Lewis, 2003*]. The high ratios at LMF during the growing season are an additional piece of evidence suggesting anthropogenic N loading has exceeded the systems ability to retain N.

DIN:DON ratios were also high at alpine sites draining both pristine and developed areas during the summer growing season (Figure 3.3B). In these alpine areas, DIN was consistently high throughout the year, while DON lowest in the summer (just above detection limits) resulting in high DIN:DON ratios during the summer synoptic sampling event (August). In addition, these alpine areas contained relatively low concentrations of DOC. The combination of low DOC and DON concentrations suggests that flowpaths dominating streamflow intersected little flushable organic matter during the mid summer. September synoptic sampling data did reveal increasing amounts of DON in the alpine areas. *Williams et al., [2001]* found DON concentrations increasing in the late summer and hypothesized that the source of DON changed with time from allochthonous sources to autochthonous sources in the late summer and early fall. Autochthonous sources of organic matter have been shown to have a higher N content than allochthonous sources corresponding to lower C:N ratios [*McKnight, et al., 1994*].

Unlike DIN:DON ratios, the seasonal pattern of DOC:TDN ratios did not appear to be affected by anthropogenic N loading (Figures 3.3C and 3.8). The only discernable

seasonal DOC:TDN pattern was lower DOC:TDN in the valley-bottom stream reaches of the South Fork and West Fork during the summer growing season (Figure 3.3C). Since high levels of algal growth have been noted in these stream segments [*PBS&J*, 2005], autochthonous sources of N could be responsible for the observed low DOC:TDN ratios. Watershed-wide, DOC:TDN was highest during the summer and lowest during the winter (Figures 3.3C and 3.8). These patterns were most likely due to the seasonal fluctuation in biological uptake of DIN. Unlike TDN, DOC export during the winter and summer was comparably low and therefore did not play part in the seasonal variability of DOC:TDN ratios. The absence of strong seasonal fluctuations in DOC, suggests that biological growth in the West Fork watershed is more limited by N than C.

#### Seasonal $\text{NO}_3^-$ , DON and DOC Concentrations Patterns: Anthropogenic N

loading did alter spatial and seasonal streamwater  $\text{NO}_3^-$  concentration patterns (Figures 3.3A, 3.4A) [*Gardner and McGlynn*, 2009]. The seasonal peak in winter  $\text{NO}_3^-$  concentrations downstream of anthropogenic N loading sources were two to three times greater than streamwater  $\text{NO}_3^-$  concentrations in pristine areas (Figure 3.3A). Though not nearly as noticeable, summer baseflow  $\text{NO}_3^-$  concentrations at LMF were just slightly higher than other sites (Figures 3.3A, 3.4A, and 3.6F). No seasonal pattern in streamwater  $\text{NO}_3^-$  concentrations was observed at sites draining Lone Mountain (Figure 3.3A), where concentrations were consistently high. Elevated  $\text{NO}_3^-$  at these sites could be from other human influences (i.e. vegetation removal, fertilizer inputs) or low levels of biologic uptake in high-elevation alpine/subalpine environments [*Gardner and McGlynn*, 2009]. Elevated inorganic N concentrations draining talus and scree fields have been

noted in other research [*Williams and Tonnessen, 2000; Clow and Sueker, 2000; Hood et al., 2003a; Seastedt et al., 2004*].

Although not as obvious as  $\text{NO}_3^-$ , anthropogenic N loading did impact DON concentrations. Across the three main tributaries, DON concentrations were twice as high at LMF during baseflow compared to SF and NF ( $0.06$  vs.  $0.03 \text{ mg L}^{-1}$ ) (Figure 4B). Our results are consistent with those of *Stanley and Maxted [2008]*, who reported that anthropogenic N can increase DON concentrations but not to the same magnitude as  $\text{NO}_3^-$  concentrations.

The major control of DON and DOC appeared to be water transport (hydrology) instead of anthropogenic impacts or biological demand; highest concentrations and export of DON and DOC occurred during spring runoff (Figures 3.4B, 3.4C, 3.5B, 3.5C, 3.7, and 3.8). DOC concentrations peaked earlier than DON on the ascending limb of the hydrograph leading to peak DOC:TDN during this time (Figures 3.4B, 3.4C, and 3.4E). Other research in snowmelt dominated systems has documented peak C:N ratios on the ascending limb of the hydrograph that decrease along descending limb [*Williams et al., 2001; Petrone et al., 2007*]. This behavior suggests flowpath or water source shifts indicative of another organic carbon source or flushing behavior [*McGlynn and McDonnell, 2003*]. During the onset of snowmelt, near stream and shallow flowpaths that contain freshly leached terrestrial organic matter that is less biologically available could be activated, leading to higher C:N ratios in streamflow. Later in the snowmelt hydrograph, lower streamwater C:N ratios reflect activation of deeper flowpaths and

upland source areas with lower C:N ratios [McGlynn and McDonnell, 2003; Pacific *et al.*, 2010].

Concentration-discharge relationships during snowmelt do not indicate anthropogenic influence on the timing of peak  $\text{NO}_3^-$ , DON or DOC concentrations (Figure 3.5).  $\text{NO}_3^-$  concentration peaked during the winter period prior to the onset of snowmelt and declined with increasing discharge, suggesting biological control of the  $\text{NO}_3^-$  - discharge relationship instead of mobilization (Figure 3.5A). This is contrary to research in other snowmelt-dominated systems that has shown mobilization control of the  $\text{NO}_3^-$  discharge relationship.  $\text{NO}_3^-$  flushing behavior has been observed on the rising limb of the snowmelt hydrograph when shallow flowpaths flush  $\text{NO}_3^-$  from upland soils in the Rocky Mountain West [Williams and Melack, 1991; Baron and Campbell, 1997; Campbell *et al.*, 2000a], the Sierra Nevadas [Sickman *et al.*, 2003] and in other snowmelt dominated systems [Creed and Band, 1998; Sebestyen *et al.*, 2008].

A difference in the timing of peak  $\text{NO}_3^-$  concentrations in the West Fork watershed could be result of less atmospheric N deposition in southwestern Montana compared to the Rocky Mountain Front, the Sierra Nevadas and northeastern U.S [NADP, 2010]. Although the majority of streamwater N during snowmelt in these watersheds has been shown to be associated with a soil water source [Campbell *et al.*, 2000a; Sickman *et al.*, 2003; Sebestyen *et al.*, 2008], chronic historical additions of spatially distributed N from atmospheric deposition can increase soil N [Aber *et al.*, 1993], which would then be flushed to streams during snowmelt.

The timing of peak DON and DOC concentrations on the ascending limb of the hydrograph in the West Fork watershed (Figures 3.4B, 3.4C, 3.5B, and 3.5C) was similar to other snowmelt-dominated systems [*Hornberger, 1994; Boyer et al. 1997; Williams, 2001; Hood et al., 2003b; Sebestyen et al., 2008*]. The rise in DOM that occurs during the rising limb of the snowmelt hydrograph has been hypothesized to be flushing of shallow soil flowpaths that are rich in organic matter [*Hornberger, 1994; Boyer et al., 1997*]. A large proportion of runoff at this time originates from riparian areas [*McGlynn et al., 2003; Pacific et al., 2010*]. As discussed previously, DOC concentrations did peak earlier than DON concentrations in the West Fork watersheds.

Although there was no difference in the timing of peak DON concentrations at LMF and UNF, the direction of the DON concentration discharge loops differed (Figure 3.5B). At LMF, DON gradually increased to peak concentrations sustaining high DON concentration for a longer time period during snowmelt until gradually decreasing. This could be attributed to high DON concentrations that persist with depth and distance to the stream. High concentrations of DON in both short and shallow (riparian) and longer and deeper (hillslope) flowpaths suggest that watershed soils had surpassed their adsorptive capacity. Contrarily, a sustained high groundwater table could exist at LMF after snowmelt so that shallow flowpaths dominated streamflow throughout the summer. On the other hand, the counterclockwise DON loop at UNF is indicative of the flushing of shallow riparian flowpaths activated at the onset of snowmelt switching to longer deeper flowpaths on the descending limb of the hydrograph. There are few examples of DON hysteresis loops in the literature. In the Sierra Nevadas, DON concentration – discharge

relationships did not exhibit a hysteresis pattern [Sickman *et al.*, 2003], while clockwise hysteresis was noted during storm events in upstate New York [Inamadar *et al.*, 2008], northern Virginia [Buffam *et al.*, 2001], and northeastern Japan [Jiang *et al.*, 2010]. Counterclockwise hysteresis of DON discharge relationship was documented in one watershed in northeastern Japan [Jiang *et al.*, 2010], while three other watersheds exhibited clockwise hysteresis. This difference was attributed to differences in hydrologic conductivity and antecedent moisture conditions; the watershed with areas of lower hydraulic conductivity and drier antecedent moisture conditions required more time to connect to variable N source areas.

Also notable in the DON concentration – discharge relationships, was the increase in DON concentrations at both LMF and UNF on the descending limb of snowmelt. This increase could result from increases in autochthonous sources of organic matter [McKnight *et al.*, 1994]. Following snowmelt, DON and DOC concentrations were relatively low for the rest of the year as groundwater flowpaths dominated (Figure 3.4B and 3.4C). Aside from high concentrations at snowmelt, there were no apparent seasonal patterns in DON or DOC, suggesting that biologic demand did not control DON concentrations and that there was ample DIN supply to support biologic demand, since DIN is preferentially consumed over DON; however, DON has been shown to be a significant source of N if DIN is severely limited [Kaushal and Lewis, 2005].

In summary, anthropogenic N loading was correlated with: 1) increased magnitude of annual  $\text{NO}_3^-$  export, 2) higher annual DIN:DON ratios, 3) lower annual DOC:TDN ratios, 4) amplified seasonal  $\text{NO}_3^-$  peaks, 5) higher DIN:DON ratios during

winter baseflow, 6) slightly elevated summer DON concentrations, 7) higher summer DIN:DON ratios at one site exhibiting signs of N saturation, and 8) sustained DON concentrations though snowmelt and into summer baseflow.

Do Localized Inputs of Anthropogenic N Lead to Similar Stages of Watershed Saturation Observed at the Watershed Outlet as Spatially Distributed Inputs from Atmospheric Deposition?

Studies across the U.S. and northern Europe have demonstrated long-term, equally distributed inputs (e.g. atmospheric deposition) of anthropogenic N have moved ecosystems towards N saturation [*Aber et al.*, 1989; *Murdoch and Stoddard*, 1992; *Lovett et al.*, 2000; *Magill et al.*, 2000; *Baron et al.*, 2000; *Burns*, 2003]. Related to the accepted catchment-wide N saturation concept, localized saturation may occur from N inputs from development (e.g. septic systems and wastewater disposal). Since mountain ecosystems can be particularly susceptible to N enrichment, modest inputs of N from development can have disproportionately large effects on the N dynamics of headwater ecosystems [*Gardner and McGlynn*, in review]. Results from this analysis confirm conclusions from the Big Sky Nutrient (BiSN) modeling analysis that localized anthropogenic N loading occurring “hydrologically close” to the stream in the West Fork watershed exhibits the same watershed N saturation characteristics as spatially distributed N loading [*Gardner et al.*, in review].

According to *Aber et al.* [1989], a sequence of four recognizable stages emerges in response to long-term loading, leading to altered seasonal patterns of streamwater  $\text{NO}_3^-$  concentrations. Stage characteristics range from Stage 0, in which there is a slight

seasonal pattern in streamwater  $\text{NO}_3^-$  to Stage 3, in which chronic year-long elevated streamwater  $\text{NO}_3^-$  concentrations persist with no recognizable seasonal pattern. Streamwater  $\text{NO}_3^-$  concentrations at UNF, draining a relatively pristine subwatershed, exhibit slight winter peaks and low concentrations at baseflow (Stage 0) (Figure 3.4A). In the absence of disturbance, concentrations of  $\text{NO}_3^-$  in this region are typically near or below detection limits ( $<0.05 \text{ mg L}^{-1}$ ) during the growing season. Slightly amplified streamwater  $\text{NO}_3^-$  winter peaks at SF are characteristic of Stage 1, while amplified winter and summer streamwater  $\text{NO}_3^-$  concentrations at LMF suggest Stage 2 conditions (Figure 3.4A). Absence of seasonal patterns at alpine sites draining Lone Mountain are indicative of Stage 3 N saturation status (Figure 3.3A).

In addition to altered streamwater  $\text{NO}_3^-$  concentration patterns, our results suggest that the relative abundance of DIN and DON may serve as an indicator of watershed N saturation status. *Williams et al.*, [2001] proposed the idea that the annual DIN:DON ratio can serve as an index to evaluate watershed N status. Our results agree that the annual DIN:DON ratio does provide insight on N saturation status; however, depending on the saturation stage, the annual ratio can mask early signs of N enrichment. We suggest that seasonal DIN:DON ratios better capture watershed N saturation status. The seasonal DIN:DON ratio will identify seasonally elevated DIN:DON ratios to aid in identification of N saturation state; whereas, the annual ratio may mask seasonal differences in the DIN:DON ratios. For example, the slightly elevated annual DIN:DON ratio at LMF could indicate Stage 1, 2, or 3 N saturation stage, but the large differences observed between summer, winter and snowmelt DIN:DON ratios eliminate N saturation

Stage 1 and 3 and suggest Stage 2.

Aside from the seasonal DIN:DON, we propose other metrics to assess watershed N saturation status. These metrics include the slope of the cumulative  $\text{NO}_3^-$  flux curve (Figure 3.6) and the location of a subwatershed along the linear trend between watershed N loading and watershed  $\text{NO}_3^-$  retention (Figure 3.9). The slope of the cumulative  $\text{NO}_3^-$  flux curve was steeper during baseflow at LMF (Stage 2) compared to the slope of SF (Stage 1) or NF (Stage 0) (Figure 3.6F). A steeper slope of the cumulative  $\text{NO}_3^-$  flux signified that LMF was leaking  $\text{NO}_3^-$  at a faster rate than other subwatersheds, a noted sign of watershed N saturation [Gunderson *et al.*, 1998]. Another sign of a later watershed N saturation stage was LMF's location along the linear trend between watershed N loading and watershed  $\text{NO}_3^-$  retention (Figure 3.10B). The West Fork watershed as a whole appears to be well below N saturation according to Michaelis-Menten kinetics, demonstrated by the linear increase of watershed  $\text{NO}_3^-$  retention and watershed N loading [Earl, 2006]; however, since LMF sits below the linear trend of watershed N loading and watershed  $\text{NO}_3^-$  retention, it was leaking more  $\text{NO}_3^-$  than the modeled trend across the West Fork watersheds and may be at a later stage of watershed N saturation than other West Fork subwatersheds.

The seasonal amplification of streamwater  $\text{NO}_3^-$  concentration patterns, DIN:DON ratios, and baseflow streamwater  $\text{NO}_3^-$  export of streams in Stage 1 or Stage 2 of watershed N saturation could alternatively be viewed as demonstrating “seasonal N saturation”. In watersheds experiencing Stage 1 or 2 N saturation, flowpaths may not

saturate during the growing season, but in the winter dormant season, flowpaths become more saturated at a much lower  $\text{NO}_3^-$  concentration because lower biologic demand.

In addition to seasonal (temporal) heterogeneity of watershed N saturation state, the West Fork watershed exhibited spatial heterogeneity in watershed N saturation status. High-elevation subwatersheds draining Lone Mountain exhibited Stage 3 saturation signs by elevated streamwater  $\text{NO}_3^-$  concentrations persisting throughout the year (Stage 3). Although the synoptic sampling N snapshots occurred at a low temporal resolution, they did capture a range of hydrological conditions and potential for biological activity across six seasonal sampling campaigns and were adequate to identify watershed N saturation state.

The spatial variability of watershed N saturation status present in the West Fork watershed provided the opportunity to explore factors promoting watershed N saturation. Utilizing multiple approaches to explore N dynamics in the West Fork watershed, which include this empirical data analysis, geostatistical modeling [*Gardner et al., 2009*] and a hybrid mechanistic N export model [*Gardner et al., in review*], we propose N saturation dynamics are controlled by more than just the magnitude of N loading but also by the spatial location of N loading and whether N loading is localized versus spatially distributed. First, localized N loading that occurred in areas with quick transport times to streams (wastewater loading in Meadow Village) had greater ramifications for stream N saturation state than localized loading occurring in areas with longer flowpaths to streams (septic effluent). The second apparent driver of watershed N saturation status, spatial distribution of N loading, was demonstrated by the smaller amounts of localized

anthropogenic N loading to areas of the LMF watershed that had more impact on observed streamwater N patterns than greater amounts of spatially distributed N loading to the UNF watershed. The spatially distributed N loading to the UNF watershed did not saturate flowpaths to the stream, while localized N loading to the LMF watershed likely saturated flowpaths, providing direct transport of  $\text{NO}_3^-$  to the stream. At LMF, both of these factors driving N saturation state were likely significant. Localized wastewater N loading occurred “hydrologically close” to the stream exacerbated N loading impacts on streamwater  $\text{NO}_3^-$ .

This research provides evidence that documentation of the spatial and seasonal heterogeneity of watershed N status and consideration of the spatial location of N loading along hydrological flowpaths are critical to effectively assess and manage watershed N. Without seasonal monitoring of streamwater N, watershed managers would not be aware of amplified  $\text{NO}_3^-$  peaks in the winter. Streams with low  $\text{NO}_3^-$  concentrations in the growing season may still be exhibiting signs of N enrichment observable as amplified winter peaks. Knowledge of an amplified seasonal N pattern, would inform watershed managers of the early stages of N enrichment, and the potential consequences of continued or increased N loading. In addition to seasonal water quality sampling, we believe spatial snapshots of water quality to be extremely useful to characterize watershed N status. Instead of just sampling at the stream outlet, additional samples along the stream network may reveal spatial variability in watershed N status. Knowledge of spatio-temporal variability in watershed N status would help watershed

managers develop a variety of N management strategies across a watershed tailored to address variability in watershed N saturation status.

Are there Spatial and/or Seasonal Variations  
in the Impact of Anthropogenic N Loading on  
Streamwater NO<sub>3</sub><sup>-</sup>?

Spatio-temporal NO<sub>3</sub><sup>-</sup> isotopic data provided valuable insight on spatial and seasonal variability of anthropogenic impacts on streamwater NO<sub>3</sub><sup>-</sup> patterns (Figures 3.11, 3.12, 3.13, and 3.14) that was not possible from N concentration data alone (Figures 3.3 and 3.4). In particular, we were interested in: 1) identifying the sources of elevated N concentrations draining Lone Mountain and Meadow Village, and 2) quantifying seasonal shifts in NO<sub>3</sub><sup>-</sup> sources to streamwater.

Spatio-Temporal Sources of Streamwater NO<sub>3</sub><sup>-</sup>: Spatial NO<sub>3</sub><sup>-</sup> isotopic data allowed for the comparison of NO<sub>3</sub><sup>-</sup> sources across land use and environmental gradients. February and August spatial snapshots of  $\delta^{15}\text{N}$  and  $\delta^{18}\text{O}$  of NO<sub>3</sub><sup>-</sup> values illustrated that sampling sites downgradient of wastewater loading in Meadow Village had isotopically distinct  $\delta^{15}\text{N}$  of NO<sub>3</sub><sup>-</sup> streamwater signatures similar to the wastewater signature (Figure 3.12) signifying wastewater loading was partially responsible for elevated streamwater NO<sub>3</sub><sup>-</sup> concentrations at LMF during both summer and winter baseflow. The enriched  $\delta^{15}\text{N}$  of NO<sub>3</sub><sup>-</sup> values during summer and winter baseflow suggest a groundwater source of wastewater. Potential sources of wastewater to groundwater at LMF include wastewater irrigation infiltrating through soils to groundwater or leaky sewer or irrigation pipes.

In contrast,  $\delta^{15}\text{N}$  of  $\text{NO}_3^-$  values corresponding to elevated streamwater  $\text{NO}_3^-$  concentrations draining Lone Mountain were not similar to the wastewater end-member (Figure 3.12), indicating another source responsible for elevated streamwater  $\text{NO}_3^-$  concentrations. The isotopic signature at these sites was isotopically distinct (depleted  $\delta^{15}\text{N}$  of  $\text{NO}_3^-$  values and enriched  $\delta^{18}\text{O}$  of  $\text{NO}_3^-$  values) compared to wastewater and other sites. Depleted  $\delta^{15}\text{N}$  of  $\text{NO}_3^-$  values could be indicative of shallow flowpath sources since enrichment of  $\delta^{15}\text{N}$  with soil depth has been attributed to denitrification [*Sickman et al.*, 2003]. The relatively high  $\delta^{18}\text{O}$  of  $\text{NO}_3^-$  values at Lone Mountain sites were also suggestive of shorter and/or shallower flowpath contribution. With shorter and/or shallower flowpaths, there is less potential for  $\text{NO}_3^-$  cycling resulting in greater contribution from atmospheric  $\text{NO}_3^-$ . Even though the  $\delta^{18}\text{O}$  of  $\text{NO}_3^-$  values at Lone Mountain sites were enriched compared to other sites across the West Fork watershed, they were still isotopically distinct from atmospheric  $\text{NO}_3^-$  implying that most precipitation released from seasonal snowpack storage infiltrated and underwent biogeochemical processing or mixing before contributing to streamwater  $\text{NO}_3^-$ . This supports past research in alpine areas documenting substantial processing of precipitation  $\text{NO}_3^-$  before entering surface waters [*Campbell et al.*, 2002; *Sickman et al.*, 2003; *Nanus*, 2008].

A few other small but noticeable differences were present in the spatial patterns of  $\delta^{15}\text{N}$  and  $\delta^{18}\text{O}$  of  $\text{NO}_3^-$  during winter and summer baseflow signifying changes in streamwater  $\text{NO}_3^-$  sources. There was more variability in summer  $\delta^{15}\text{N}$  of  $\text{NO}_3^-$  values downgradient of wastewater loading in Meadow Village (Figure 3.11B and 3.12B)

compared to the winter  $\delta^{15}\text{N}$  of  $\text{NO}_3^-$  values (Figure 3.11A and 3.12A). The more enriched values of  $\delta^{15}\text{N}$  values during the summer may be caused by direct N loading of wastewater irrigation into streams or quick transport of N loading from areas hydrologically connected to the stream. The more depleted  $\delta^{15}\text{N}$  values during the summer could be due to small increases in precipitation contribution and high-elevation snowmelt to streamflow as compared to the middle of the winter season when deeper groundwater flowpaths dominated streamflow. Finally, another small but noticeable difference between summer and winter baseflow was more depleted  $\delta^{18}\text{O}$  values in the winter, likely from less contribution from atmospheric  $\text{NO}_3^-$  sources in the winter.

Seasonal Sources of Streamwater  $\text{NO}_3^-$ : Mixing analysis of summer, winter, and snowmelt  $\delta^{15}\text{N}$  and  $\delta^{18}\text{O}$  values of streamwater  $\text{NO}_3^-$  from the three main tributaries of the West Fork indicated seasonal shifts in the influence of anthropogenic N loading on streamwater  $\text{NO}_3^-$  concentrations (Figures 3.12, 3.13 and 3.14, Table 3.7). Wastewater contribution to LMF and SF was greatest during winter (68% and 16% respectively) and summer (87% and 33%) baseflow (Figure 3.13). Greater wastewater contribution during the summer could be attributed to summer wastewater irrigation on the golf course, increased septic use, or increased hydrologic connectivity between N source areas and the stream. The considerably lower wastewater contributions at SF than LMF throughout the year corresponded to less wastewater N loading in the SF watershed compared to the LMF watershed (Figure 3.9). Potential wastewater sources in the SF watershed are primarily septic effluent and leaking sewer lines, while in the LMF watershed has the addition of wastewater irrigation on the golf course.

Previous research in the West Fork watershed quantified statistical relationships between land use and spatial stream network  $\text{NO}_3^-$  concentrations that also suggested seasonal shifts in anthropogenic influences on streamwater  $\text{NO}_3^-$  [Gardner and McGlynn, 2009]. Specifically, Gardner and McGlynn [2009] found wastewater N loading influenced streamwater  $\text{NO}_3^-$  concentrations only during winter baseflow when groundwater flowpaths dominated and biological potential was limited. The results presented here, provide evidence that wastewater effluent also contributed to summer and snowmelt streamwater  $\text{NO}_3^-$  concentrations. The wastewater contributions may not have been detected through statistical methods because of relatively low streamwater  $\text{NO}_3^-$  concentrations. This difference in detection/ attribution highlights the importance of multiple methods and approaches to increase system understanding and the particular usefulness of streamwater  $\text{NO}_3^-$  isotopes and the limitations of statistical inference to elucidate streamwater  $\text{NO}_3^-$  sources. These results have important implications for streamwater management. Low concentrations of streamwater  $\text{NO}_3^-$  measured during the summer growing season does not necessarily equate to less anthropogenic N loading to aquatic ecosystems. Since, biological assimilation can potentially mask signs of anthropogenic impacts, streams should either be monitored for  $\text{NO}_3^-$  during the dormant winter season, when the potential for biological assimilation is low, for algae/biomass during the growing season, or ideally, for  $\text{NO}_3^-$  and  $\text{NO}_3^-$  isotopes simultaneously so that watershed managers can quantify spatial and seasonal shifts in N sources.

While wastewater dominated streamwater  $\text{NO}_3^-$  concentrations during winter and summer baseflow at LMF, soil water was the main contributor to streamwater  $\text{NO}_3^-$

concentrations at UNF and SF throughout the year (Figure 13) and to streamwater  $\text{NO}_3^-$  concentrations at LMF during snowmelt. Other studies have shown the majority of streamwater  $\text{NO}_3^-$  during snowmelt derived from catchment soils [*Spoelstra et al.*, 2001; *Burns and Kendall*, 2002; *Campbell et al.*, 2002; *McHale et al.*, 2002; *Sickman et al.*, 2003; *Ohte*, 2004; *Sebestyen et al.*, 2008]; although, higher frequency sampling has demonstrated that contribution from atmospheric N can vary substantially during the course of snowmelt [*Ohte*, 2004; *Sebestyen*, 2008]. The high percentage of soil water contribution during snowmelt suggests substantial biological cycling of atmospherically  $\text{NO}_3^-$  occurred prior to watershed export. N may be stored in the watershed for months or even years before transport to the stream.

As demonstrated above, isotopic analysis of streamwater  $\text{NO}_3^-$  can provide critical information for watershed management of anthropogenic N loads. First, as previously discussed, low  $\text{NO}_3^-$  concentrations during the summer growing season does not necessarily mean that anthropogenic N loading is not having an impact on streamwater N. Secondly, anthropogenic N loads can have the greatest impacts on aquatic ecosystems during the summer growing season by promoting excess algae and potentially altering stream trophic structure. Finally, even though peak runoff may dilute anthropogenic N loads corresponding to less impact in the immediate area, these high N loads exported from headwater watersheds during spring runoff could have downstream impacts (e.g. eutrophication in the Gulf of Mexico). In the West Fork watershed,  $\text{NO}_3^-$  isotopic data was an essential line of evidence for Total Maximum Daily Loads (TMDL) development in two areas of the watershed: 1) sites draining Lone Mountain, where isotopic analysis

eliminated wastewater as a potential source, and 2) sites downstream of Meadow Village, where despite relatively low streamwater  $\text{NO}_3^-$  concentrations, isotopic data pinpointed wastewater as the primary source of streamwater  $\text{NO}_3^-$  and ruled out significant influence from fertilizer in this relatively high-density residential development.

### Conclusion

This research analyzed multiple sources of contemporary field data, including synoptic and temporal sampling for N and C species and isotopic ratios of  $\text{NO}_3^-$  to examine the effects of anthropogenic N loading on the timing, magnitude and speciation of watershed N export and retention. This analysis allowed for deeper process understanding by drawing upon the strengths of each data set. Our results highlight the seasonal and spatial variability of anthropogenic impacts on streamwater  $\text{NO}_3^-$ , DON, and DOC export and concentration patterns, stoichiometric ratios and watershed N saturation status. Impacts from anthropogenic N loading manifested in increased streamwater  $\text{NO}_3^-$  export and concentrations, elevated DIN:DON ratios, lower DOC:TDN ratios, enriched  $\delta^{15}\text{N}$  of  $\text{NO}_3^-$  values, and sustained DON concentrations through snowmelt; however, in some areas biological uptake masked these enrichment signs during the summer growing season when  $\text{NO}_3^-$  concentrations were low.

Our research suggests that localized anthropogenic N loading from development can lead to similar watershed saturation characteristics as spatially distributed N loading from atmospheric deposition. Like anthropogenic N loading patterns, watershed N saturation characteristics exhibited spatial and seasonal heterogeneity across the

watershed. Anthropogenic N loading that occurred in areas with quick transport and hydrologic connections to the stream were more apt to demonstrate N enrichment signals than those areas disconnected or connected to streams via longer flowpaths for only a small portion of the year. Watershed N retention estimates confirmed that it is not necessarily the amount of N loading that controls watershed N export but where on the landscape it occurs and what time of year. Therefore, it is imperative that water quality managers include such knowledge in developing flexible strategies across a watershed to minimize N loading to surface waters.

A three-component mixing model demonstrated that  $\delta^{15}\text{N}$  and  $\delta^{18}\text{O}$  values of  $\text{NO}_3^-$  can add critical information about streamwater  $\text{NO}_3^-$  sources beyond what is possible from statistical inference of land use and concentration data alone. Despite observed low  $\text{NO}_3^-$  concentrations and loads in the summer, wastewater influence was most evident during summer and winter baseflow, but still contributed to streamwater  $\text{NO}_3^-$  during snowmelt at some sites. In pristine watersheds, the majority of streamwater  $\text{NO}_3^-$  was derived from watershed soils throughout the year. The high percentage of soil  $\text{NO}_3^-$  contribution even during peak snowmelt suggests substantial biological cycling of N loading occurred prior to watershed export and further suggests that N may be stored in the watershed for months or even years before being transported to the stream.

Better understanding of how anthropogenic N inputs affect watershed N enrichment will be critical as development pressure continues in this region and other sensitive mountain areas of the world. In particular, there is need for more research on the coupling of watershed hydrology and biogeochemical processes and their interwoven

controls on the spatial heterogeneity of watershed N export and retention. Developing creative multi-analysis approaches, such as the one presented here can be an attractive, inexpensive approach to gain new insights on complex processes controlling streamwater N export at the watershed scale.

#### Acknowledgements

Financial support was provided by the Environmental Protection Agency (EPA) STAR Grant #R832449, EPA 319 funds administered by the Montana Department of Environmental Quality, the U.S. National Science Foundation BCS 0518429, and the USGS 104(b) Grant Program administered by the Montana Water Center. K.K.G. acknowledges support from the EPA STAR Fellowship and NSF GK-12 Fellowship programs.

References Cited

- Aber, J.D. McDowell, W., Nadelhoffer, K., Magill, A., Berntson, G., Kamakea, M., McNulty, S., Currie, W., Rustad, L., and I. Fernandez (1998). N saturation in temperate forest ecosystems Hypothesis revisited. *BioScience*, 48(11): 921-933.
- Aber, J.D. , A. Magill, R. Boone, J.M. Melillo, P.A. Steudler, and R. Bowden (1993). Plant and soil responses to three years of chronic nitrogen additions at the Harvard Forest, Petersham, MA. *Ecological Applications*, 3: 156-166.
- Aber, J.D., Nadelhoffer, K.J., Steudler, P., and J.M. Melillo (1989). Nitrogen saturation in northern forest ecosystems: excess nitrogen from fossil fuel combustion may stress the biosphere. *BioScience*. 39(60): 378-385.
- Ackerman, G., B.L. McGlynn, S. Montross, and K.K. Gardner (In preparation). Rock nitrogen weathering relationships to mountain streamwater N variability.
- Aitkenhead-Peterson, J.A., R.P. Smart, M.J. Aitkenhead, and M.S. Cresser (2007). Spatial and temporal variation of dissolved organic carbon export from gauged and ungauged watersheds of the Dee Valley, Scotland: Effect of land cover and C:N. *Water Resources Research*, 43, W05442, doi:10.1029/2006WR004999.
- Alexander, R.B., R.A. Smith, G.E. Schwarz (2000). Effect of stream channel size on the delivery of nitrogen to the Gulf of Mexico. *Nature*, 403: 758-761.
- Alt, D., and D.W. Hyndman (1986). *Roadside geology of Montana*. Mountain Press Publishing Company. Missoula MT.
- Arango, C.P, J.L. Tank, J.L. Schaller, T.V. Royer, M.J. Bernot, and M.B. David (2007). Benthic organic carbon influences denitrification in streams with high nitrate concentrations. *Freshwater Biology*, 52: 1210-1222.
- Aravena, R.M., M.L. Evans, and J.A. Cherry (1993). Stable isotopes of oxygen and nitrogen in source identification of nitrate from septic systems. *Ground Water*, 31: 180-186.
- Barnes, R.T., P.A. Raymond, and K.L. Casciotti (2008). Dual isotope analyses indicate efficient processing of atmospheric nitrate by forested watersheds in the northeastern U.S. *Biogeochemistry*, 90: 15-27.
- Baron, J.S. (2002). *Rocky Mountain Futures, an Ecological Perspective*. Island Press, Washington.

- Baron, J.S., Rueth H.M., Wolfe, A.M., Nydick, K.R. Alstott, E.A., Minear, J.T. and B. Moraska (2000). Ecosystem response to nitrogen deposition in the Colorado Front Range. *Ecosystems* 3: 352-368.
- Baron, J.S. and D.H. Campbell (1997). Nitrogen fluxes in a high elevation Colorado rocky Mountain basin. *Hydrological Processes*, 11: 783- 799.
- Bisson, P. A. and R. E. Bilby (2001). Organic Matter and Trophic Dynamics. In Naiman, Robert J. and Robert E. Bilby, eds. *River Ecology and Management: Lessons from the Pacific Coastal Ecoregion*. Springer, New York. p 373-398.
- Boyer, E.W., C.L. Goodale, N.A. Jaworski and R.W. Howarth (2002). Anthropogenic nitrogen sources and relationships to riverine nitrogen export in the northeastern U.S.A. *Biogeochemistry*, 57/58: 99-136.
- Boyer, E.B., Hornberger, G.M., Bencala, K.E., and D.M. McKnight (1997). Response characteristics of DOC flushing into an alpine catchment stream. *Hydrological Processes* 11(12):1635-1647.
- Brookshire, E.N.J, H.M. Valett, S.A. Thomas, and J.R. Webster (2005). Cycling of dissolved organic nitrogen and carbon in a forest stream. *Ecology*, 86(9): 2487-2496.
- Buffam, I., J.N. Galloway, L.K. Blum & K.J. McGlathery (2001). A stormflow/ baseflow comparison of dissolved organic matter concentrations and bioavailability in an Appalachian stream. *Biogeochemistry*, 53: 269-306.
- Burns, D.A., E.W. Boyer, E.M. Elliot, and C. Kendall (2009). Sources and Transformations of Nitrate from Streams Draining Varying Land Uses: Evidence from Dual Isotope Analysis. *Journal of Environmental Quality*, 38: 1149-1159.
- Burns, D.A. (2003). The effects of atmospheric nitrogen deposition in the Rocky Mountains of Colorado and southern Wyoming, USA – a critical review. *Environmental Pollution*, 127: 257-269.
- Burns, D.A. (1998). Retention of NO<sub>3</sub><sup>-</sup> in an upland stream environment: A mass balance approach. *Biogeochemistry*, 40: 73-96.
- Burt, J.W., and K.J. Rice (2009). Not all ski slopes are created equal: Disturbance intensity affects ecosystem properties. *Ecological Applications*, 19(8): 2242-2253.
- Campbell, D.H. Kendall, C., Chang C.C.Y., Silva, S.R., and K.A. Tonnessen (2002). Pathways for nitrate release from an alpine watershed: determination using  $\delta^{15}\text{N}$  and  $\delta^{18}\text{O}$ . *Water Resources Research*, 38: 1052-1071.

- Campbell, D.H., Baron, J.S., Tonnessen, K.A., Brooks, P.D., and P.F. Schuster (2000a). Controls on nitrogen flux in alpine/subalpine watersheds of Colorado. *Water Resources Research*, 36(1): 37-47.
- Campbell, J.L., and M. Mitchell, and B. Mayer (2006). Isotopic assessment of NO<sub>3</sub>- and SO<sub>4</sub><sup>2-</sup> mobility during winter in two adjacent watersheds in the Adirondack Mountains, New York. *Journal of Geophysical Research*, 111, G04007, doi: 10.1029/2006JG000208.
- Campbell, J.L., J.W. Hornbeck, W.H. McDowell, D.C. Buso, J.B. Shanley, and G.E. Likens (2000b). Dissolved organic nitrogen budgets for upland forested ecosystems in New England. *Biogeochemistry*, 49: 123-142.
- Casciotti, K.L., D.M. Sigman, M.G. Hastings, J.K. Bohlke, and A. Hilkert (2001). Measurement of the oxygen isotopic composition of nitrate in seawater and freshwater using the denitrifier method. *Analytical Chemistry*, 74(19): 4905-4912.
- Chang, C.C.Y., C.K. Kendall, S.R. Silva, W.A. Battaglin, and D.H. Campbell (2002). Nitrate stable isotopes: Tools for determining nitrate sources among different land uses in the Mississippi River basin: *Canadian Journal of Fisheries and Aquatic Sciences*, 59 (12): 1874-1885.
- Chapin III, S.F., P.A. Matson, and H.A. Mooney (2002). *Principles of Terrestrial Ecosystem Ecology*. Springer, New York, New York.
- Claessens, L., C.L. Tague, L.E. Band, P.M. Groffman, and S.T. Kenworthy (2009). Hydro-ecological linkages in urbanizing watersheds: An empirical assessment of in-stream nitrate loss and evidence of saturation kinetics. *Journal of Geophysical Research*, 114, G04016, doi:10.1029/2009JG001017.
- Clow, D. W. and J.K. Sueker (2000). 'Relations between basin characteristics and stream-water chemistry in alpine/subalpine basins in Rocky Mountain National Park, Colorado, *Water Resources Research* 36, 49-61.
- Coats, R.N. and C.R. Goldman (2001). Patterns of nitrogen transport in streams of the Lake Tahoe basin, California-Nevada. *Water Resources Research*, 37(2):405-415.
- Cole, D.W. and M. Rapp (1981). In *Dynamic Properties of Forest Ecosystems*. Reichle, D.E., Ed. Cambridge University Press: New York.
- Creed, I.F. and L.E. Band (1998). Exploring functional similarity in the export of nitrate-N from forested catchments: A mechanistic modeling approach. *Water Resources Research*, 34(11): 3079-3093.

- Creed, I.F., Band, L.E., Foster, N.W, Morrison, I.K., Nicolson, J.A., Semkin, R.S. and D.S. Jeffries (1996). Regulation of nitrate-N release from temperate forests: a test of the N flushing hypothesis. *Water Resources Research*, 32: 3337-3354.
- DeWalle, D.R., B.R. Swistock, and W.E. Sharpe (1988). Three-component tracer model for stormflow on a small Apalachian forested catchment. *Journal of Hydrology*, 104: 301-310.
- Dodds W.K., E. Marti E, J.L. Tank, J. Pontius, S.K. Hamilton, N.B. Grimm, W.B. Bowden, W.H. McDowell, B.J. Peterson, H.M. Valett, J.R. Webster, and S. Gregory (2004). Carbon and nitrogen stoichiometry and nitrogen cycling rates in streams. *Oecologia*, 140: 458-467.
- Dodds, W.K., M.A. Evans-White, N.M. Gerlanc, L. Gray, D.A. Gudder, M.J. Kemp, A.L. Lopez, D. Stagliano, E.A. Straus, J.L. Tank, M.R. Whiles, and W.M Wolheim (2000). Quantification of the nitrogen cycle in a prairie stream, *Ecosystems*, 3: 574-589.
- Dosskey, M.G., and P.M. Bertsch (1994). Forest sources and pathways of organic matter transport to a blackwater stream: a hydrologic approach. *Biogeochemistry*, 24(1): 1-19.
- Earl, S. R., H. M. Valett, and J. R. Webster (2006). Nitrogen saturation in streams. *Ecology*, 87(12): 3140-3151.
- Edwards, R. (2007). Personal Communications. Big Sky Water and Sewer District Operations General Manager Big Sky Water and Sewer District.
- Elliot, E.M., C. Kendall, W.W. Boyer, D.A. Burns, S.D. Wankel, K.J. Bain, K. Harlin, T.J. Butler, and R. Carlton (2007). An isotopic tracer of stationary source NO<sub>x</sub> emissions across the Midwestern and northeaster United States. *Environmental Science & Technology*, 41: 7661-7667.
- Fiebig, D.M., M.A. Lock, and C. Neal (1990). Soil water in the riparian zone as a source of carbon for a headwater stream. *Journal of Hydrology*, 116: 217-237.
- Findlay, S., and R. L. Sinsabaugh (1999). Unraveling the sources and bioavailability of dissolved organic matter in lotic aquatic ecosystems. *Marine Freshwater Resources*, 50:781-790.
- Folke, C., S. Carpenter, T. Elmqvist, L. Gunderson, C.S. Holling, B. Walker, J. Bengtsson, F. Berkes, J. Colding, K. Danell, M. Falkenmark, L. Gordon, R. Kasperson, N. Kautsky, A. Kinzig, L Simon, K. Mäler, F. Moberg, L. Ohlsson, P.

- Olsson, E. Ostrom, W. Reid, J. Rockström, H. Savenije, and U. Svedin (2002). Resilience and Sustainable Development: Building Adaptive Capacity in a World of Transformations. Scientific Background Paper on Resilience for the process of the World Summit on Sustainable Development on behalf of The Environmental Advisory council to the Swedish Government URL: <http://www.sou.gov.se/mvb/pdf/resiliens.pdf>.
- Gardner, K.K., B.L. McGlynn, and L.A. Marshall (in preparation). All nitrogen loading is not created equal: localized inputs have disproportionate impacts on modeled streamwater nitrogen.
- Gardner, K.K. and B.L. McGlynn (2009). Seasonality in spatial variability and influence of land use/land cover and watershed characteristics on streamwater nitrate concentrations in the Northern Rocky Mountains. *Water Resources Research*, 45, W08411, doi:10.1029/2008WR007029.
- Generoux, D. (1998). Quantifying uncertainty in tracer-based hydrograph separations, *Water Resources Research*, 34(4): 915-919.
- Goodale, C.L., S.A. Thomas, G. Fredriksen, E.M. Elliot, K.M. Flinn, T.J. Butler, and M.T. Walter (2009). Unusual seasonal patterns and inferred processes of nitrogen retention in forested headwater of the Upper Susquehanna. *Biogeochemistry*, 93: 197-218.
- Goodale, C.L., J.D. Aber, P.M. Vitousek, and W.H. McDowell (2005). Long-term decreases in stream nitrate: successional causes unlikely; possible links to DOC. *Ecosystems*, 8:334-337.
- Goodale, CL, JD Aber, and WH McDowell (2000). The long-term effects of disturbance on organic and inorganic nitrogen export in the White Mountains, New Hampshire. *Ecosystems*, 3(5):433-450.
- Groffman, P.M., N.L. Law, K.T. Belt, L.E. Band, and G.T. Fisher (2004). Nitrogen fluxes and retention in urban watershed ecosystems. *Ecosystems*, 7: 393-403.
- Gundersen, P., I. Callensen, and W. deVries (1998a). Leaching in forest ecosystems is related to forest floor C/N ratios. *Environmental Pollution*, 102(51): 403-407.
- Gunderson, P., Emmett, B.A., Kjonaas, O.J., Koopmans, C.J., and A. Tietema (1998b). Impact of nitrogen deposition on nitrogen cycling in forests: a synthesis of NITREX data. *Forest Ecology and Management*, 101: 37-55.
- Hill, A. R. (1996). Nitrate removal in stream riparian zones, *Journal of Environmental Quality*, 25, 743-755.

- Holloway, J.M., R.A. Dahlgren, B. Hansen, and W.H. Casey (1999). Contribution of bedrock nitrogen to high nitrate concentrations in streamwater. *Nature*, 395, 785-788.
- Holloway, J.M., R.A. Dahlgren, and W.H. Casey (2001). Nitrogen release from rock and soil under simulated field conditions. *Chemical Geology*, 174, 403-413.
- Hope, D., M.F. Billett, and M.S. Cresser (1994). A review of the export of carbon in river water: fluxes and processes. *Environmental Pollution*, 84: 301-324.
- Hood, E.W., M.W. Williams; and N. Caine (2003a). Landscape controls on organic and inorganic nitrogen leaching across an alpine/Subalpine ecotone, Green Lakes Valley, Colorado Front Range. *Ecosystems*, 6: 31-45.
- Hood, E., D.M. McKnight, and M.W. Williams (2003b). Sources and chemical character of dissolved organic carbon across an alpine/subalpine ecotone, Green Lakes Valley, Colorado Front Range, United States. *Water Resources Research*, 39(7): HWC3.1-HWC3.12.
- Hornberger, G.M., Bencala, K.E. and D.M. McKnight (1994). Hydrological controls on the temporal variation of dissolved organic carbon in the Snake River near Montezuma, Colorado. *Biogeochemistry* 25:147-16.
- Inamdar, S., J. Rupp, and M. Mitchell (2008). Differences in dissolved organic carbon and nitrogen responses to storm-even and ground-water condition in a forested, glaciated watershed in western New York. *Journal of Environmental Quality*, 44(6): 1458-1473.
- Jencso, K. J., B. L. McGlynn, M. N. Gooseff, S. M. Wondzell, and K. E. Bencala (2009). Hydrologic connectivity between landscapes and streams: Transferring reach and plot scale understanding to the catchment scale, *Water Resources Research*. W04428, doi:10.1029/2008WR007225.
- Jiang, R., K.P. Woli, K. Kuramochi, A. Hayakawa, M. Shimizu, and R. Hatano (2010). Hydrological process controls on nitrogen export during storm events in an agricultural watershed. *Soil Science and Plant Nutrition*, 56: 72-85.
- Judd, K.E., G.E. Likens, and P.M. Groffman (2007). High nitrate retention during winter in soils of the Hubbard Brook experimental forest. *Ecosystems*, 10(2): 217-255.
- Kaushal, S.S., W.M. Lewis, and J.H. McCutchan (2006). Land use change and nitrogen enrichment of a Rocky Mountain Watershed. *Ecological Applications*, 16(1):299-312.

- Kaushal, S.S. and W.M. Lewis (2005). Fate and transport of organic nitrogen in minimally disturbed montane streams of Colorado, USA. *Biogeochemistry*, 74: 303-321.
- Kaushal, S.S. and W.M. Lewis (2003). Patterns in the chemical fractionation of organic nitrogen in Rocky Mountain Streams. *Ecosystems*, 6: 483-492.
- Kellog, K.S. and V.S. Williams (2005). *Geologic Map of the Ennis 30' X 60' Quadrangle, Madison and Gallatin counties, Montana and Park County, Wyoming*. Montana Bureau of Mines and Geology Open File No. 529.
- Kendall, C and J.J. McDonnell (1998). *Isotope Tracers in Catchment Hydrology*. Elsevier, New York.
- Lewis, W.M., J.M. Melack, W.H. McDowell, M. McClain, and J.E. Richey (1999). Nitrogen yields from undisturbed watersheds in the Americas. *Biogeochemistry*, 46: 149-162.
- Likens, G.E., F.H. Bormann, N.M. Johnson, D.W. Fisher, and R.S. Pierce (1970). Effects of Forest Cutting and Herbicide Treatment on Nutrient Budgets in the Hubbard Brook Watershed-Ecosystem. *Ecological Monographs*, 40 (1): 23-47.
- Lovett, G. M., Weathers, K. C., & Arthur, M. A. (2002). Control of nitrogen loss from forested watersheds by soil carbon: Nitrogen ratio and tree species composition, *Ecosystems*, 5, 712– 718.
- Lovett, G.M., Weathers, K.C., and W.V. Sobczak (2000). Nitrogen saturation and retention in forested watersheds of the Catskill Mountains, New York. *Ecological Applications*, 10(1): 73-84.
- Magill, A.H., Aber, J.D, Berntson, G.M, McDowell, W.H., Nadelhoffer, K.J., Melillo, J.M., and P. Steudler (2000). Long-term nitrogen additions and nitrogen saturation in two temperate forests. *Ecosystems*, 3: 238-253.
- Mattsson, T. P. Kortelainen, A. Laubel, D. Evans, M. Pujo-Pay, A. Raike, and P. Conan (2009). Export of dissolved organic matter in relation to land use along a European climatic gradient. *Science of the Total Environment*, 407: 1967-1976.
- McGlynn, B.L., and J.J. McDonnell (2003). The role of discrete landscape units in controlling catchment dissolved organic carbon dynamics. *Water Resources Research*, 39(4), 1090, doi:10.1029/2002WR001525.

- McGlynn, B.L., J.J. McDonnell, J.B. Shanley, and C. Kendall (1999). Riparian zone flowpath dynamics during snowmelt in a small headwater catchment. *Journal of Hydrology*, 222(75-92).
- McHale, M.R., McDonnell, J.J., Mitchell, M.J., and C. Cirimo (2002). A field based study of soil and groundwater nitrate release in an Adirondack forested watershed. *Water Resources Research*, 38: 1029-1038.
- McKnight, D.M., E.D. Andrews, S.A. Spaulding, and G.R. Aiken (1994). Aquatic fulvic acids in algal-rich Antarctic ponds. *Limnology and Oceanography*, 36: 998-1006.
- McNamara, R.M. (2010). Stream nitrogen uptake dynamics from ambient to saturation across development gradients, stream network position, and seasons. Master's Thesis, Montana State University, Bozeman, MT.
- Messerli, B. and J.D. Ives (1997). *Mountains of the world: a global priority*. Carnforth, UK and New York, USA. Parthenon Publishing Group.
- Moller, J.R., Minshall, G.W., Cummins, K.W., Petersen, R.C. Cushing, C.E., Sedell, J.R., Larson, R.A., and R.L. Vannote (1979). Transport of total dissolved carbon in streams of differing physiographic characteristics, *Organic Geochemistry*, 1: 139-150.
- Murdoch, P.S., and J.L. Stoddard (1992). The role of nitrate in the acidification of streams in the Catskill Mountains of New York. *Water Resources Research*, 28(10): 2707-2720.
- Nanus, L., MW. Williams, D.H. Campbell, E.M. Elliott, and C. Kendall (2008). Evaluating regional patterns in nitrate sources to watersheds in national parks of the rocky mountains using nitrate isotopes. *Environmental Science & Technology*, 42: 6487-6493.
- National Atmospheric Deposition Program (NADP) (2010). <http://nadp.sws.uiuc.edu/>. NADP Program Office, Illinois State Water Survey, Champaign, IL.
- National Science Foundation (NSF) (1976). *Impacts of Large Recreational Development Upon Semi-Primitive Environments*. NSF RANN Program Final Report.
- Ohte, N., S.D. Sebestyen, J.B. Shanley, D.H. Doctor, C. Kendall, S.D. Wankel, and E.W. Boyer (2004). Tracing sources of nitrate in snowmelt runoff using a high-resolution isotopic technique. *Geophysical Research Letters*, 31, 21506, doi:10.1029/2004GL020908.

- Pabich, W.J., Valiela, I., and H.F. Hemond (2001). Relationship between DOC concentration and vadose zone thickness and depth below water table in groundwater of Cape Cod, USA, *Biogeochemistry*, 55: 247-268.
- Pacific, V., K. Jencso, and B.L. McGlynn. (2010). Variable flushing mechanisms and landscape structure control stream DOC export during snowmelt in a set of nested catchments. *Biogeochemistry*. DOI: 10.1007/s10533-009-9401-1.
- Pacific, V.J., Jencso, K.J., and B.L. McGlynn (2009). Variable flushing mechanisms and landscape structure control stream DOC export during snowmelt in a set of nested catchments. *Biogeochemistry*. DOI: 10.1007/s10533-009-9401-1.
- Pellerin, B.A., W.M. Wolheim, C.S. Hopkinson, W.H. McDowell, M.R. Williams, C.J. Vorosmarty, and M.L. Daley (2004). Role of Wetlands and developed land use on dissolved organic nitrogen concentrations and DON? TDN in Northeastern rivers and streams. *Limnology and Oceanography*, 49(4): 910-918.
- Peterson, B. J., W. M. Wolheim, P. J. Mulholland, J. R. Webster, J. L. Meyer, J. L. Tank, E. Marti, W. B. Bowden, H. M. Valett, A. E. Hershey, W. H. McDowell, W. K. Dodds, S. K. Hamilton, S. Gregory, and D. D. Morrall (2001). Control of nitrogen export from watersheds by headwater streams. *Science*, 292:86-90.
- Petrone, K., I. Buffam, and H. Laudon (2007). Hydrologic and biotic control of nitrogen export during snowmelt: A combined conservative and reactive tracer approach. *Water Resources Research*, 43, W06420, doi:10.1029/2006WR005286.
- Post, Buckley, Schuh, and Jernigan, Inc. (PBS&J) (2005). *2005 Biological Monitoring Chlorophyll A Data Summary Upper Gallatin Water Quality Restoration Planning Areas*. TMDL Report prepared for the Montana Department of Environmental Quality.
- Puckett, L.J. (1994). Nonpoint and point sources of nitrogen in major watersheds of the United States. *U.S. Geological Survey Water Resources Investigations Report*, 94-4001.
- Qualls, R.G. and B.L. Haines (1992). Biodegradability of dissolved organic matter in forest throughfall, soil solution, and streamwater. *Soil Science Society of America Journal*, 56:578-586.
- Scott, D., J. Harvey, R. Alexander, and G. Schwarz (2007). Dominance of organic nitrogen from headwater streams to large rivers across the conterminous United States. *Global Biogeochemical Cycles*, 21, GB1003, doi:10.1029/2006GB002730.

- Seastedt, T.R., W.D. Bowman, N. Caine, D. McKnight, A. Townsend and M.W. Williams (2004). The landscape continuum: A model for high-elevation ecosystems. *BioScience*, 54(2): 111-120.
- Sebestyen, S.D., E.W. Boyer, J.B. Shanley, C. Kendall, D.H. Doctor, G.R. Aiken, and N. Ohte. (2008). Sources, transformations, and hydrological processes that control stream nitrate and dissolved organic matter concentrations during snowmelt in an upland forest. *Water Resource Research*, 44, W12410, doi:10.1029/2008WR006983.
- Seitzinger, S.P., R.V. Styles, E.W. Boyer, R.B. Alexander, G. Billen, R.W. Howarth, B. Mayer, and N. Van Breemen (2002). Nitrogen retention in rivers: model development and application to watersheds in the northeastern U.S.A. *Biogeochemistry*, 57/58: 199-237.
- Servais, P., J. Garnier, N. Demarteau, N. Brion, and G. Billen (1999). Supply of organic matter and bacteria to aquatic ecosystems through waste water effluents. *Water Research*, 33(16): 3521-3531.
- Sickman, J.O., A. Leydecker, and J.M. Melack (2003). Mechanisms underlying export of N from high-elevation catchments during seasonal transitions. *Biogeochemistry*, 64(1): 1-24.
- Sickman, J.O. , Leydecker, A., and J.M. Melack (2001). Nitrogen mass balances and abiotic controls on N retention and yield in high-elevation catchments of the Sierra Nevada, California, United States. *Water Resources Research*, 37(5): 1445-1461.
- Sigman, D.M., K.L. Casciotti, M. Andreani, C. Barford, M. Galanter, and J.K. Bohlke (2001). A bacterial method for the nitrogen isotopic analysis of nitrate in seawater and freshwater. *Analytical Chemistry*, 73 (17): 4145-4153.
- Simon, K.S., C.R. Townsend, and B.J.F. Biggs, and W. B. Bowden (2005). Temporal variation of N and P uptake in 2 New Zealand streams. *Journal of the North American Benthological Society*, 24(1): 1-18.
- Sobota, D.J. J.A. Harrison, and R.A. Dahlgren (2009). Influences of climate, hydrology, and land use on input and export of nitrogen in California watersheds. *Biogeochemistry*, 94:43-62.
- Spoelstra, J., S.L. Schiff, R.J. Elgood, R.G. Semkin, and D.S. Jeffries (2001). Tracing the sources of exported nitrate in the Turkey Lakes Watershed using  $^{15}\text{N}/^{14}\text{N}$  and  $^{18}/^{16}\text{O}$  isotopic ratios. *Ecosystems*, 4: 536-544.

- Stanley E.H. and J.T. Maxted (2008). Changes in dissolved nitrogen pool across land cover gradients in Wisconsin streams. *Ecological Applications*, 18(7): 1579-1590.
- Stedmon, C.A., S. Markager, M. Sondergaard, T. Vang, A. Laubel, N.H. Borch, and A. Windelin (2006). Dissolved Organic Matter (DOM) Export to a Temperate Estuary: seasonal variations and implications of land use. *Estuaries and Coasts*, 29(3): 388-400.
- Sterner, R.W. and J.J. Elser (2002). *Ecological Stoichiometry: The Biology of Elements from Molecules to the Biosphere*. Princeton University Press, Princeton, NJ.
- U.S. Department of Agriculture (USDA) Forest Service (FS) (1994). *Ecoregions of the United States*: <http://www.fs.fed.us/land/pubs/ecoregions/>.
- USDA FS (2004). *Gallatin National Forest: Streams* <http://www.fs.fed.us/r1/gallatin/?page=resources/fisheries/streams>.
- USDA Natural Resource Conservation Service (NRCS) (2008). Snotel Precipitation Data. <http://www.wcc.nrcs.usda.gov/cgi-bin/wygraph-multi.pl?stationidname=11D19S-LONE+MOUNTAIN&state=MT&wateryear=2008>.
- USDA Soil Conservation Service (USDA SCS) (1982). Soils of Montana, Bulletin 744, November, Montana State University, Bozeman, MT.
- USDA S.C.S. (1978). General Soil Map, Montana, Ext. Misc. Publication No. 16.
- U.S. Environmental Protection Agency (EPA) (2002). *Onsite Wastewater Treatment System Manual*. EPA/625/R-00/008. U.S. Environmental Protection Agency, Office of Water, Washington, DC, and Office of Research and Development, Cincinnati, OH.
- U.S. Geological Survey (U.S.G.S.) (2006). *Nutrients in Streams and Rivers Across the Nation 1992-2001*. Scientific Investigations Report 2006-5107.
- van Kessel, C., T. Clough, and J.W. van Groenigen (2009). Dissolved Organic Nitrogen: an overlooked pathway of nitrogen loss from agricultural systems. *Journal of Environmental Quality*, 38: 393-410.
- Vitousek, P.M., Aber, J., Howarth, R.W., Likens, G.E., Matson, P.A., Shindler, D.W., Schlesinger, W.H., and D.G. Tilman (1997). Human Alterations of the Global Nitrogen Cycle: Sources and Consequences. *Ecological Applications*, 7(3): 737-750.

- Vitousek, P.M., and R.W. Howarth (1991). Nitrogen limitation on land and in the sea.: How does it occur? *Biogeochemistry*, 13: 87-115.
- Vitousek, P.M. and J.M. Melillo (1979). Nitrate losses from disturbed forests – patterns and mechanisms. *Forest Science*, 25(4): 605-619.
- Ward, J.V. (1976). Comparative limnology of differentially regulated sections of a Colorado mountain river. *Archiv fur Hydrobiologie*, 78: 319-342.
- Wemple, B., J. Shanley, J. Denner, D. Ross, and K. Mills (2007). Hydrology and Water Quality in Two Mountain Basins of the Northeastern US: assessing baseline conditions and effects of ski area development. *Hydrological Processes*, 21(12): 1639-1650.
- Whitehead, P.G., P.J. Johnes, and D. Butterfield (2002). Steady state and dynamic modelling of nitrogen in River Kennet: Impacts of land use change since 1930s. *The Science of the Total Environment*, 282: 417-434.
- Williams, M.W., E. Hood, and N. Caine (2001). Role of organic nitrogen in the nitrogen cycle of a high-elevation catchment, Colorado Front Range. *Water Resources Research*, 37(10): 2569-2581.
- Williams, M.W. and K.A. Tonnessen (2000). Critical loads for inorganic nitrogen deposition in the Colorado Front Range, USA. *Ecological Applications*, 10: 1648-1665.
- Williams, M.W., J.S. Baron, N. Caine, R. Sommerfeld, and R. Sanford Jr. (1998). Nitrogen saturation in the Rocky Mountains. *Environmental Science & Technology*, 30: 640-646.
- Williams, M.W, and J.M. Melack (1991). Solute Chemistry of Snowmelt and Runoff in an Alpine Basin, Sierra Nevada. *Water Resources Research*, 27: 1576-1588.

Table 3.1: Watershed characteristics of the West Fork watershed and five subwatersheds. Location of subwatersheds is illustrated in Figure 3.1B.

<b>Subwatershed</b>	<b>Area</b>	<b>Stream Order</b>	<b>Outlet Elevation (m)</b>	<b>Median Elevation (m)</b>	<b>Median Slope (deg)</b>	<b>N Loading (kg ha<sup>-1</sup>yr<sup>-1</sup>)</b>
<b>Upper North Fork (UNF)</b>	2106	2	2162	2614	25.79	3.41
<b>Lower North Fork (LNF)</b>	2407	2	1956	2617	26.19	3.39
<b>South Fork (SF)</b>	11917	3	1854	2487	15.85	3.41
<b>West Fork (WF)</b>	20700	4	1828	2453	17.27	3.85
<b>Upper Middle Fork (UMF)</b>	3982	2	1941	2388	16.02	4.66
<b>Lower Middle Fork (LMF)</b>	8528	3	1849	2416	19.02	4.42

Table 3.2: Median C and N concentrations and ratios from three synoptic campaigns representing a range in hydrological conditions and biological activity potential. Location of subwatersheds is illustrated in Figure 3.1B.

<b>Synoptic Event</b>	<b>Date</b>	<b>Median NO<sub>3</sub><sup>-</sup> mg L<sup>-1</sup> N</b>	<b>Median TDN mg L<sup>-1</sup> N</b>	<b>Median DON mg L<sup>-1</sup> N</b>	<b>Median DOC mg L<sup>-1</sup></b>	<b>Median DIN:DON Ratio</b>	<b>Median DOC:TDN Ratio</b>
<b>Winter Dormant Season</b>	2/12/06	0.17	0.3	0.14	0.75	1.31	2.26
<b>Snowmelt</b>	6/11/06	0.04	0.25	0.19	2.49	0.22	9.89
<b>Summer Growing Season</b>	8/7/07	0.03	0.06	0.03	1.29	0.53	24.55

Table 3.3: Annual streamwater N and C export in the West Fork watershed and five subwatersheds. Location of subwatersheds is illustrated in Figure 3.1B.

<b>Subwatershed</b>	<b>NO<sub>3</sub><sup>-</sup> kg ha<sup>-1</sup>yr<sup>-1</sup></b>	<b>DON kg ha<sup>-1</sup>yr<sup>-1</sup></b>	<b>TDN kg ha<sup>-1</sup>yr<sup>-1</sup></b>	<b>DOC kg ha<sup>-1</sup>yr<sup>-1</sup></b>	<b>DIN:DON Ratio</b>	<b>DOC:TDN Ratio</b>
<b>Upper North Fork</b>	0.15	0.23	0.39	6.50	0.66	16.85
<b>Lower North Fork</b>	0.14	0.23	0.37	5.91	0.60	15.96
<b>South Fork</b>	0.27	0.34	0.60	8.70	0.80	14.45
<b>West Fork</b>	0.31	0.42	0.73	10.76	0.73	14.68
<b>Upper Middle</b>	0.18	0.63	0.81	14.12	0.29	17.41
<b>Lower Middle Fork</b>	0.48	0.30	0.77	9.30	1.60	12.03
<b>Average</b>	0.25	0.36	0.61	9.21	0.78	15.23
<b>Maximum</b>	0.48	0.63	0.81	14.12	1.60	17.41
<b>Minimum</b>	0.14	0.23	0.37	5.91	0.29	12.03

Table 3.4: N loading and export, and retention in the West Fork watershed and five subwatersheds. Location of subwatersheds is illustrated in Figure 3.1B.

Subwatershed	Total N	TDN		NO <sub>3</sub> <sup>-</sup>		DON	
	Loading kg ha <sup>-1</sup> yr <sup>-1</sup>	Export %	Retention %	Export %	Retention %	Export %	Retention %
Upper North Fork	3.41	11	89	5	95	7	93
Lower North Fork	3.39	11	89	4	96	7	93
South Fork	3.41	18	82	8	92	10	90
West Fork	3.85	19	81	8	92	11	89
Upper Middle Fork	4.66	17	83	4	96	13	87
Lower Middle Fork	4.42	18	83	11	89	7	93

Table 3.5: Estimated N loading to West Fork watershed and five subwatersheds. Table 3.1 describes subwatershed abbreviations. Location of subwatersheds is illustrated in Figure 3.1B.

N Loading (kg ha <sup>-1</sup> yr <sup>-1</sup> )	Reference	Subwatershed					
		UNF	LNF	UMF	LMF	SF	WF
Wet Deposition	NADP, 2010*	3.140	2.900	2.660	2.690	2.770	2.730
Dry Deposition	NADP, 2010*	0.260	0.260	0.260	0.260	0.260	0.260
Septic	EPA, 2002*	0.005	0.230	1.740	1.270	0.380	0.770
Wastewater	Big Sky Water & Sewer Unpublished data*	0.000	0.000	0.000	0.200	0.000	0.090

\* For more details see *Gardner et al.*, in review.

Table 3.6: Comparison of NO<sub>3</sub><sup>-</sup>, DON, and DOC export from Rocky Mountain watersheds

Site	Hectares	Elevation range m	NO <sub>3</sub> <sup>-</sup> kg ha <sup>-1</sup> yr <sup>-1</sup>	DON kg ha <sup>-1</sup> yr <sup>-1</sup>	DOC kg ha <sup>-1</sup> yr <sup>-1</sup>	Reference
Green Lake 4, CO	220	(3,515-4,000)	1.62 - 2.13	0.36 - 0.61	NA	Williams et al. [2001]
McCullough Gulch, CO	1295	(3,200-4,250)	0.37 - 0.45	0.42-0.70	5.82-11.94	Kaushal and Lewis [1999]
Blue River, CO	32020	(2,750-4,250)	0.26	0.3	NA	Kaushal et al. [2006]
Spruce Creek, CO	1585	(3,200-4,250)	0.36 - 0.42	0.47 - 0.60	5.78 - 11.98	Kaushal and Lewis [1999]
Loch Vale, CO	660	(3,050-4,026)	1.7-3.9	NA	NA	Baron and Campbell [1997] Campbell et al. [2000]
North Fork, CO	1241	(2000 - 3518)	NA	NA	12.9	Ward et al. [1976]
South Platte, CO	6680	(1,737-3,518)	NA	NA	10.3	Ward et al. [1976]
Salmon River, ID	123800	(400-3153)	NA	NA	7.2-11.4	Moeller et al. [1979]
Stringer Creek, MT	540	(1,840-2,400)	NA	NA	9.6	Pacific et al. [2009]
Emerald Lake, CA	120	(2,800 - 3,416)	0.56	NA	NA	Lewis et al. [1999]
Spuller Lake, CA	84	(3,121-3,658)	0.45	NA	NA	Lewis et al. [1999]

Table 3.7: Sources of streamwater NO<sub>3</sub><sup>-</sup> (soil, atmospheric (ATM), and wastewater (WW)) and their uncertainty estimated from a three-component mixing model. Location of subwatersheds is illustrated in Figure 3.1B.

Subwatershed	Winter			Snowmelt			Summer		
	% Soil	% ATM	% WW	% Soil	% ATM	% WW	% Soil	% ATM	% WW
LMF	28 ±4	4 ±0.8	68 ±2	73 ±7	6 ±2	21 ±13	9 ±16	4 ±5	87 ±14
SF	77 ±16	7±5.5	16±14	92±20	8±7	0	61±13	6±4	33±11
UNF	1±24	0±8.4	0	87	13	0	1±23	0±8	0

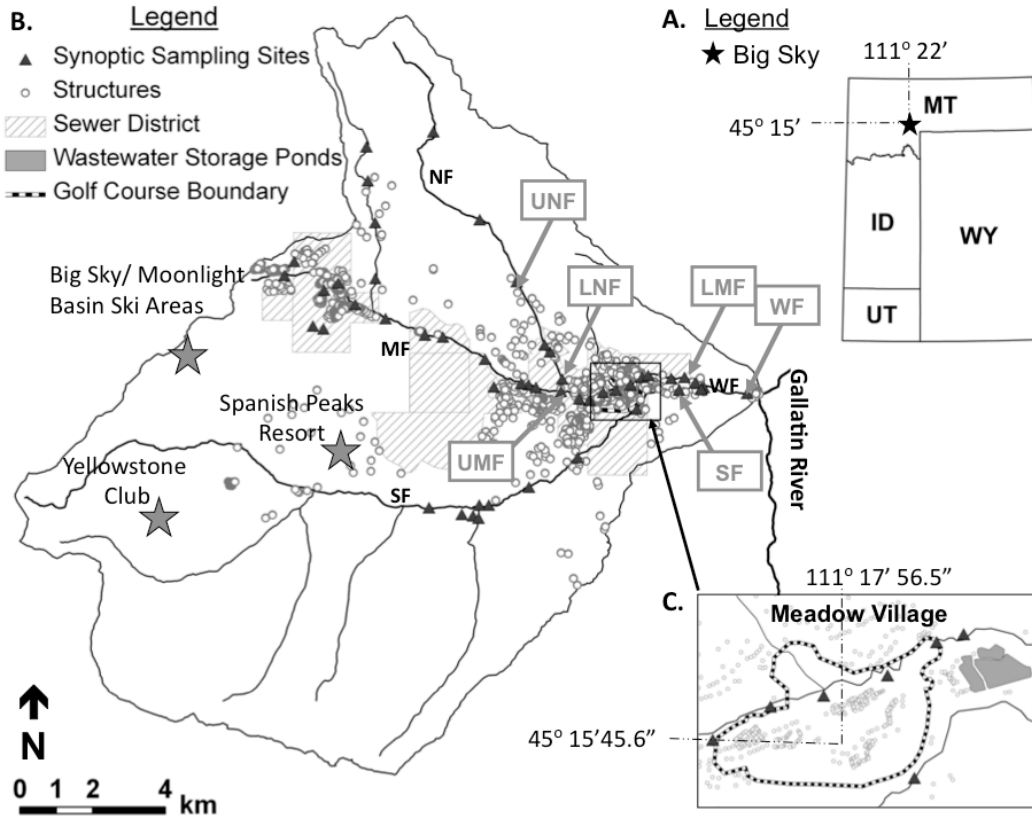


Figure 3.1: (A) Location of the West Fork watershed (212 km<sup>2</sup>) in southwestern Montana, with locations of the atmospheric deposition data sites. (B) Map of the West Fork watershed showing locations of 50 synoptic sampling sites, 6 weekly sampling sites, building structures, and the Big Sky Water and Sewer District boundaries. The West Fork (WF) drains into the Gallatin River (a tributary of the Upper Missouri River) and is comprised of three main tributaries: the Middle Fork (MF), the North Fork (NF), and the South Fork (SF). (C) An expanded view of Meadow Village with wastewater storage ponds and the Big Sky Resort Golf Course. Wastewater effluent is stored in the ponds and irrigated onto the golf course from mid-May through early October.

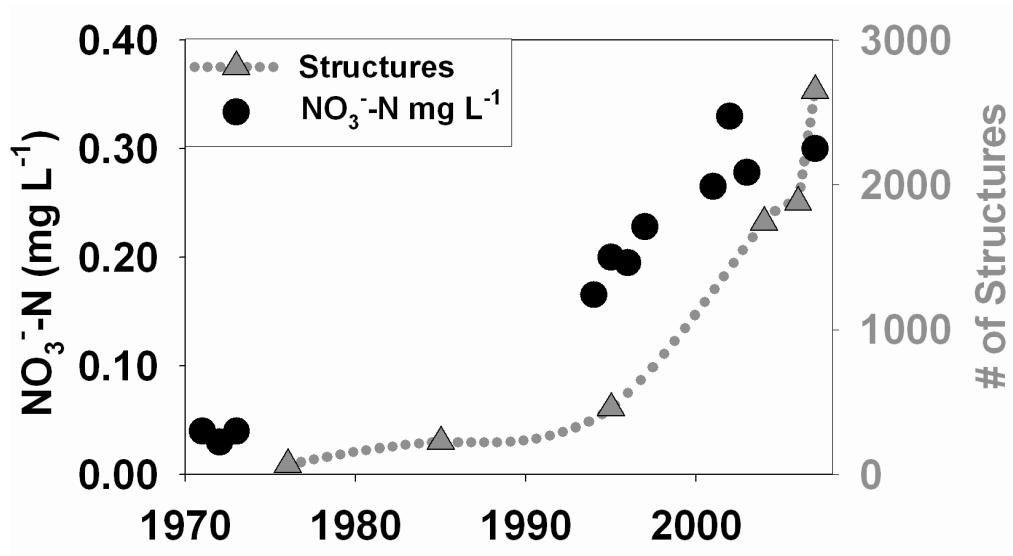


Figure 3.2: In the West Fork watershed, residential development and annual average streamwater  $\text{NO}_3^- \text{-N}$  concentrations in the West Fork have followed a similar upward trend since resort development. [NSF, 1976; Blue Water Task Force, and Big Sky Water and Sewer District, unpublished data].

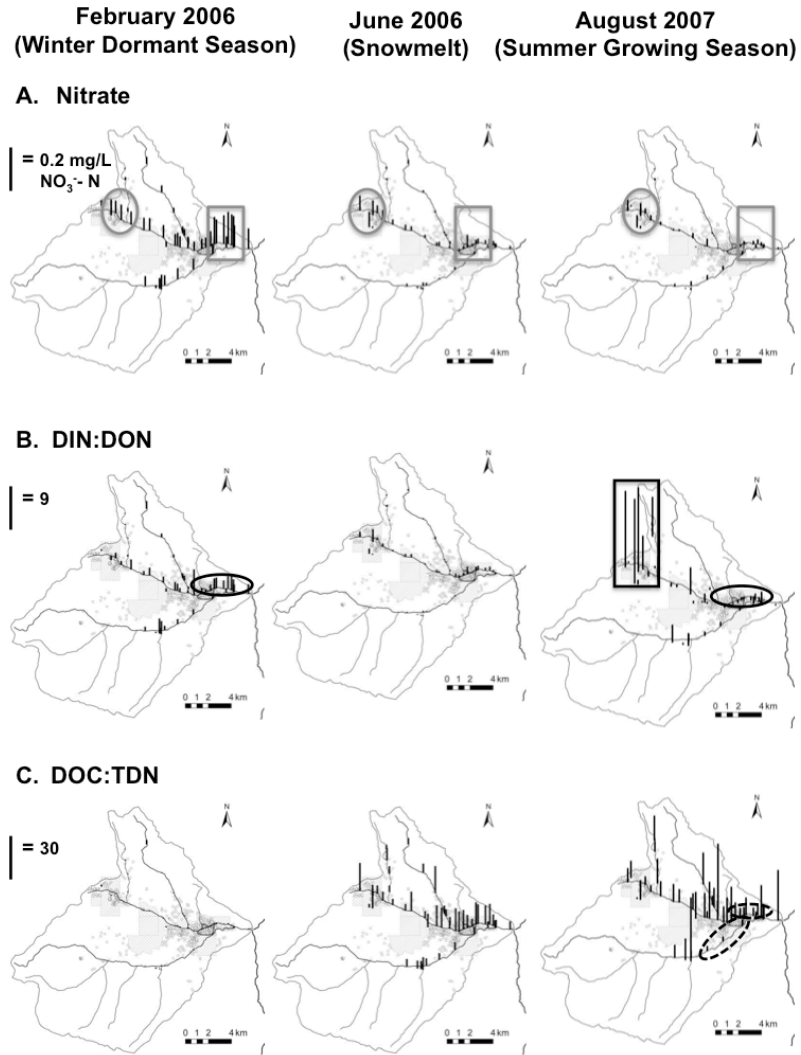


Figure 3.3: Streamwater  $\text{NO}_3^-$  concentrations and DIN:DON and DOC:TDN ratios for 3 synoptic sampling campaigns capturing a range of seasonal hydrological and biological conditions (Table 3.2). (A) Elevated  $\text{NO}_3^-$  concentrations persist in streams draining Lone Mountain across seasons (grey ovals), while elevated concentrations downgradient of Meadow Village are elevated only in the winter months during periods of low potential biologic activity (grey rectangles). (B) DIN:DON ratios were highest during the summer at sites draining alpine areas (black rectangles), and lowest during snowmelt corresponding with peak DON concentrations. DIN:DON was elevated downstream of Meadow Village during winter and snowmelt (black ovals) (C) DOC:TDN ratios were smallest during the winter when groundwater flowpaths dominate. During the summer, DOC:TDN ratios were smaller in the lower reaches of the South Fork and West Fork (black-dashed ovals) suggesting an instream sources of DOM. Otherwise, the West Fork watershed exhibited a high degree of spatial variability in DOC concentrations across seasons.

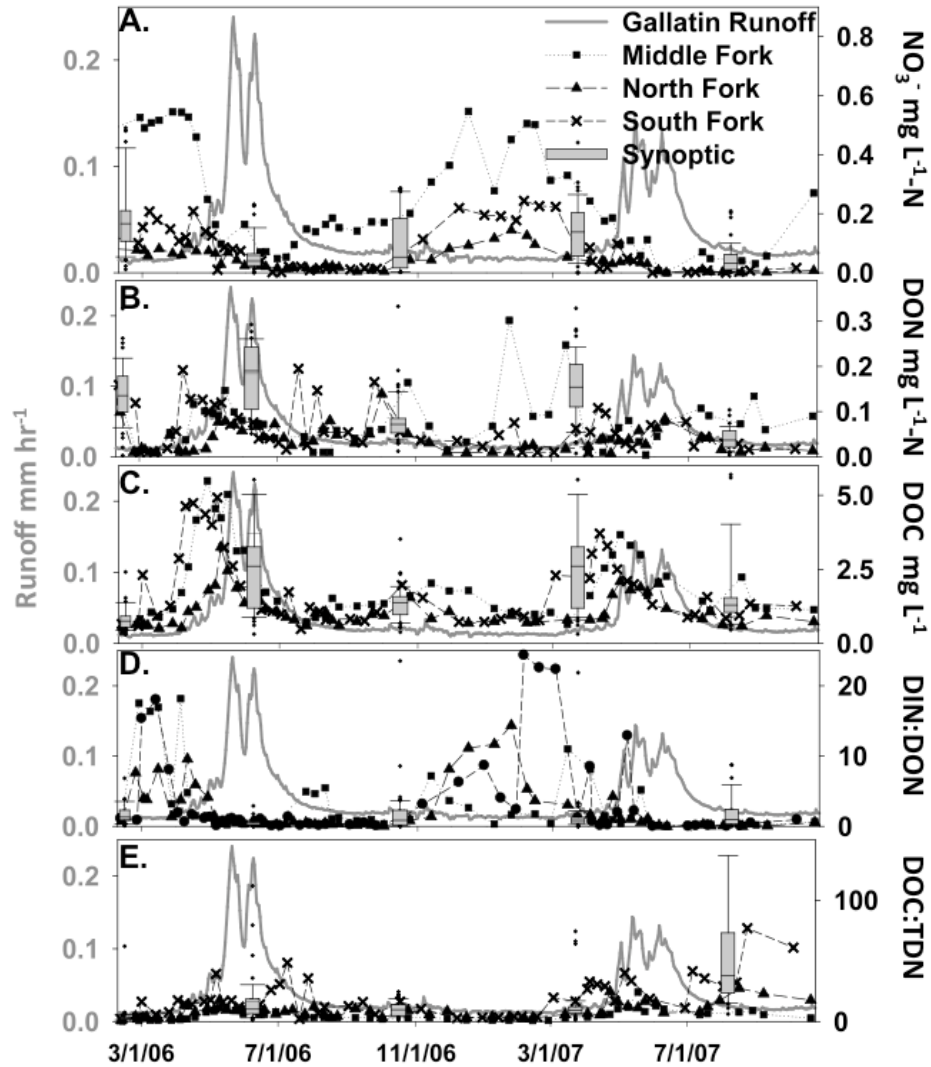


Figure 3.4: Weekly time series for the main tributaries of the West Fork (WF) represented by squares at the lower Middle Fork (LMF), crosses at the South Fork (SF), and triangles at the lower North Fork (LNF). Locations are illustrated in Figure 3.1B. Grey boxplots illustrate synoptic  $\text{NO}_3^-$ , DOC, and DON concentrations and DIN:DON and DOC:DON ratios for the 6 synoptic sampling campaigns conducted between September 2005 and August 2007. Each boxplot consists of 46-50 data points. (A) Streamwater  $\text{NO}_3^-$  concentrations and variability are highest during late fall, winter, and early spring during periods of low streamflow and limited biologic activity. (B) Streamwater DON and (C) DOC concentrations peaked on the ascending limb of the hydrograph and exhibited a high degree of variability the rest of the year. (D) Streamwater DIN:DON ratios are highest during the winter when biological activity is at a minimum. (E) Streamwater DOC:DON ratios are highest just prior to snowmelt, corresponding to peak DOC concentrations and otherwise, exhibit a high degree of variability the rest of the year.

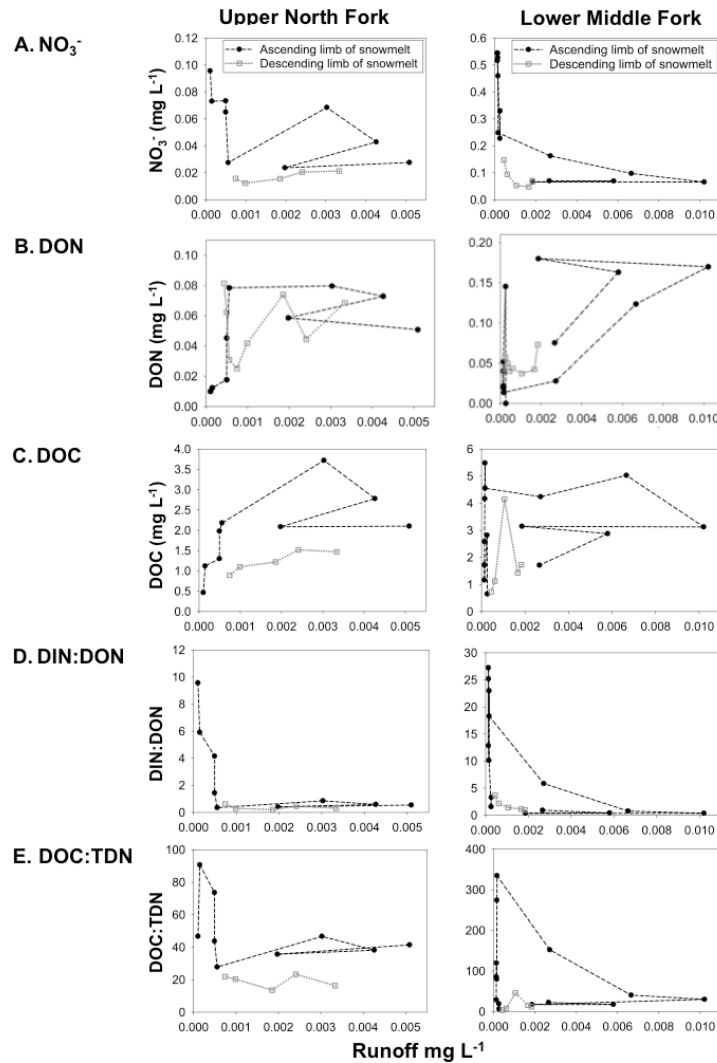


Figure 3.5: Concentration-discharge relationships for the lower Middle Fork (LMF) and the Upper North Fork (UNF), two streams with contrasting land use and watershed characteristics (Table 3.1). Locations are illustrated in Figure 3.1. Relationships between discharge and (A)  $\text{NO}_3^-$ , (C) DOC, (D) DIN:DON, and (E) DOC:TDN exhibit clockwise hysteresis at both sites, while the relationship between (B) DON concentration and discharge exhibited clockwise hysteresis at UNF and counterclockwise hysteresis at LMF. (A)  $\text{NO}_3^-$  concentration and (D) DIN:DON sharply declined with initial increase in discharge followed by a gradual decline until discharge reached a near minimum when concentration began to rise suggesting biological control of the concentration-discharge relationship. DOC concentration (C) and DOC:TDN (E) increased with discharge and peaked prior to peak snowmelt indicating a flushing mechanism controlling the concentration-discharge relationship. The magnitude of  $\text{NO}_3^-$ , DON, and DOC concentrations and DIN:DON DOC:TDN ratios were greater at LMF than UNF throughout snowmelt.

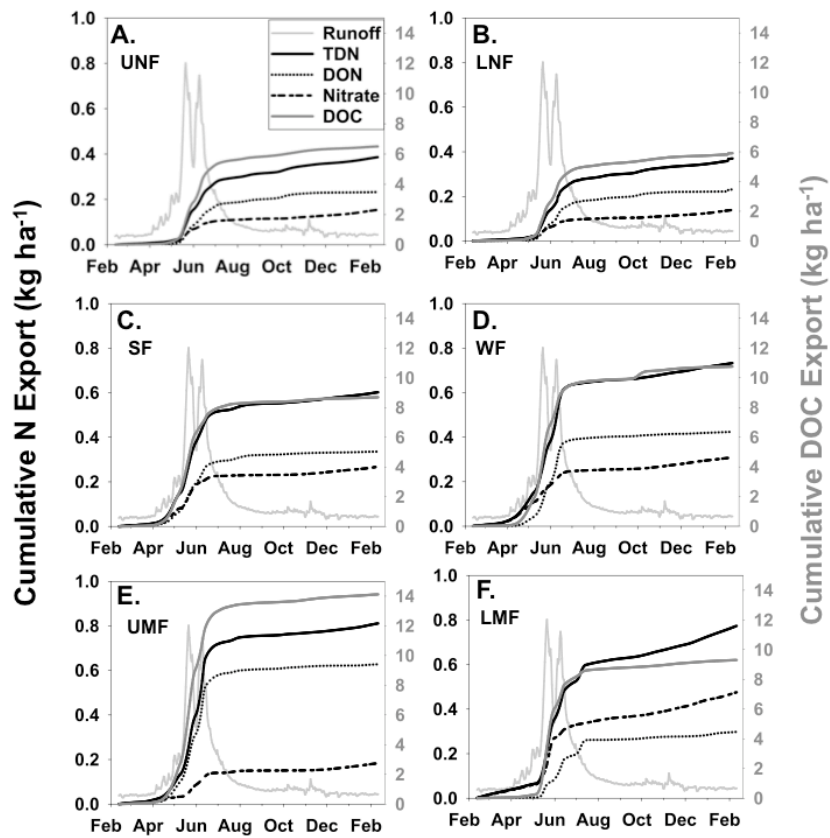


Figure 3.6: Cumulative flux of TDN, DON,  $\text{NO}_3^-$ , and DOC for 6 stream reaches in the West Fork watershed: (A) upper North Fork (UNF), (B) lower North Fork (LNF), (C) South Fork (SF), (D) West Fork (WF), (E) upper Middle Fork (UMF) and the (F) lower Middle Fork. Locations are illustrated in Figure 3.1B. The majority of C and N flux occurs at snowmelt during the months of May and June. (B) LMF exported  $\text{NO}_3^-$  at twice the rate of the other main West Fork tributaries on the descending limb of the snowmelt hydrograph.

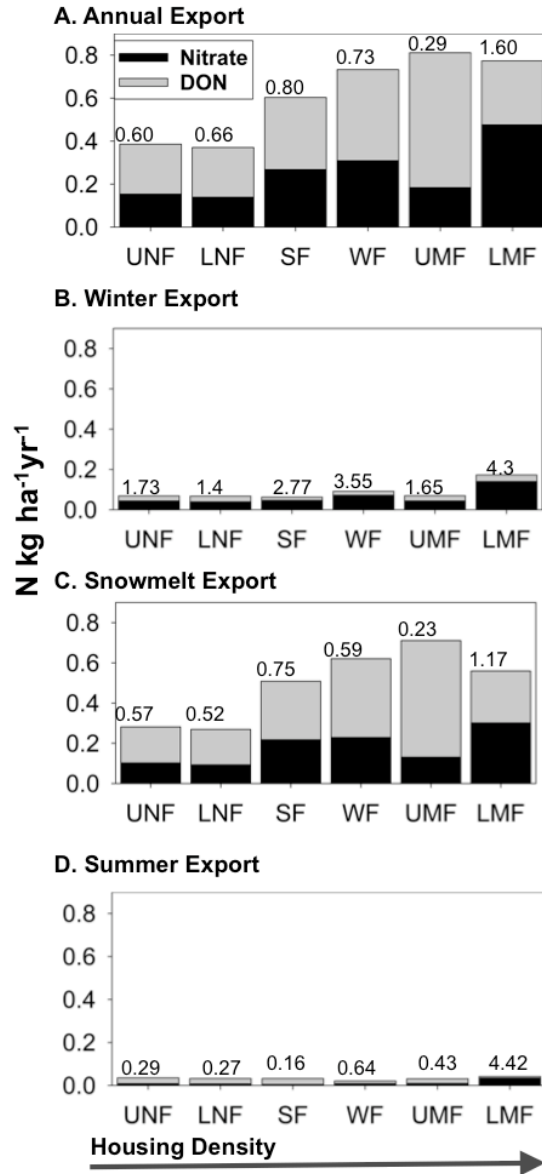


Figure 3.7: Annual and seasonal streamwater export of  $\text{NO}_3^-$  and DON with corresponding DIN:DON ratios on top of each stacked column. (A) DON was the dominant form of N exported from all subwatersheds, except for LMF. (B)  $\text{NO}_3^-$  was the most abundant form of TDN exported in the winter for all subcatchments, while DON dominated TDN during snowmelt (C) and summer (D), except for LMF, where  $\text{NO}_3^-$  was more abundant throughout the year. Locations are illustrated in Figure 3.1B.

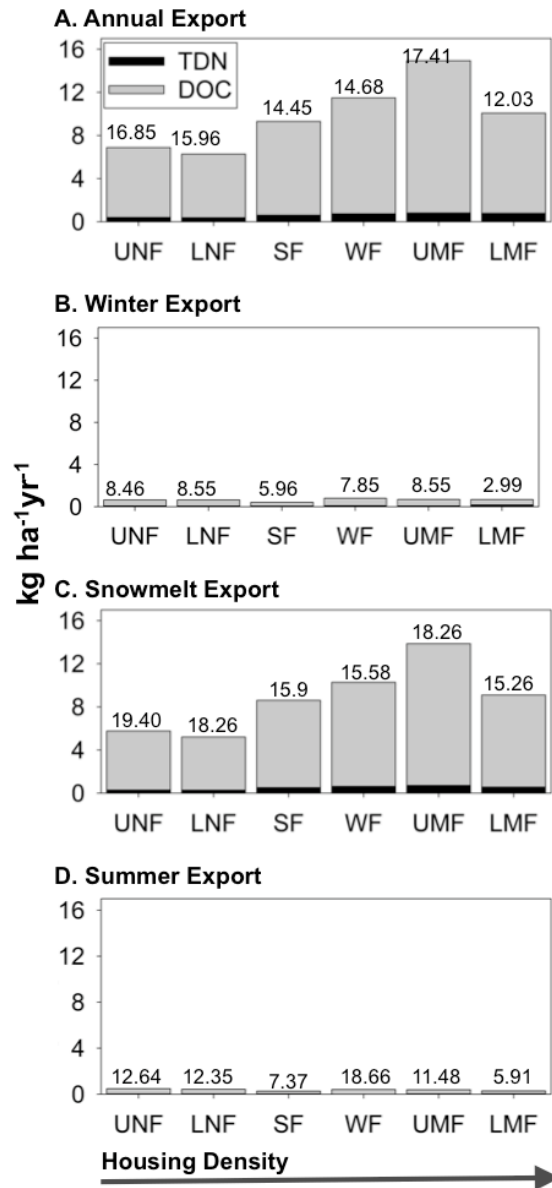


Figure 3.8: Annual and seasonal export of TDN and DOC from the West Fork and 5 subwatersheds with corresponding DOC:TDN ratios on top of each stacked column. Locations are illustrated in Figure 3.1B.(C) The majority of DON and DOC export occurred during snowmelt. (A) Annual DON and DOC export was highest at LMF, just downstream from an extensive wetland complex. (D) Generally, DOC:TDN ratios were lowest during the summer except for LMF and the WF.

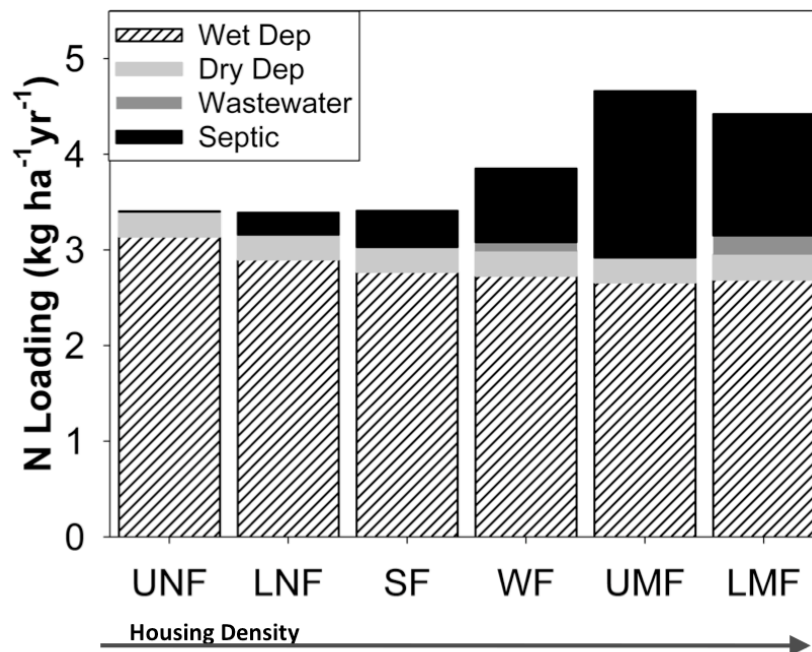


Figure 3.9: Estimated sources of N loading to the West Fork watershed and five subwatersheds. Atmospheric deposition was the biggest source of N to all subwatersheds. Total N loading varied from 3.39 kg ha<sup>-1</sup>yr<sup>-1</sup> at LNF to 4.46 kg ha<sup>-1</sup>yr<sup>-1</sup> at UMF. The highest N loading (UMF) corresponded with the highest TDN and DON export (Table 3.3), while the highest wastewater loading corresponded to the highest NO<sub>3</sub><sup>-</sup> export.

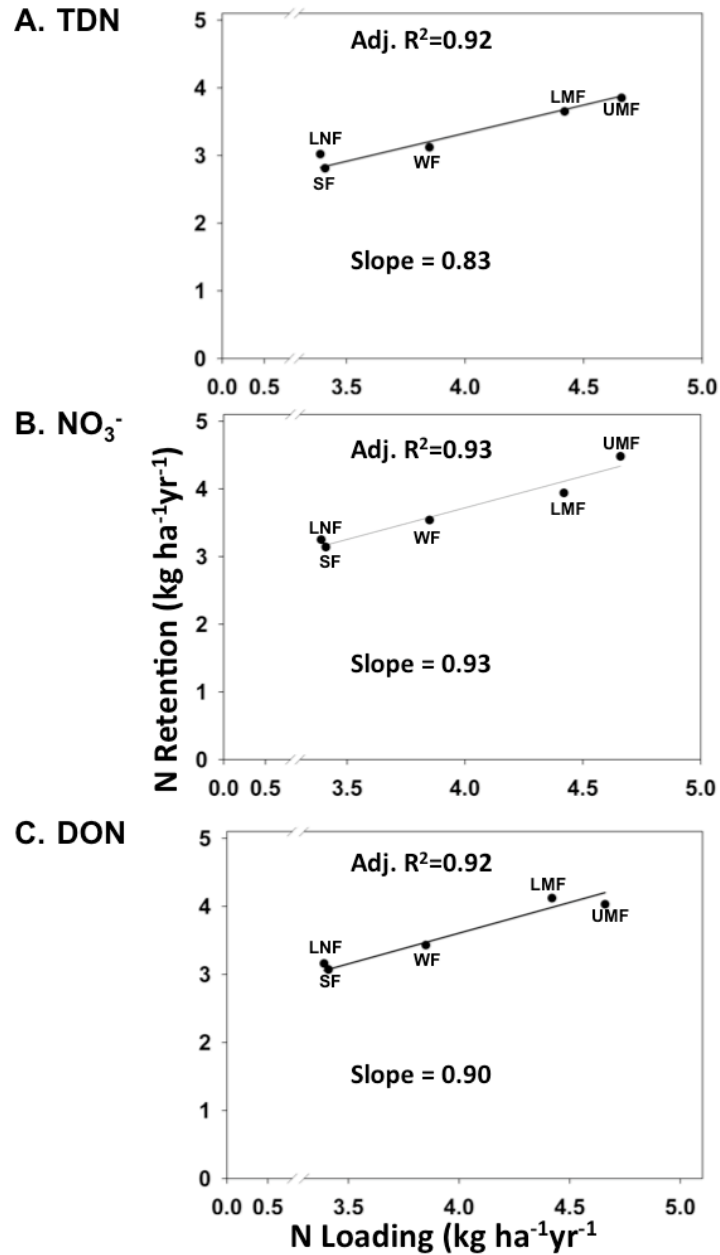


Figure 3.10: Watershed retention of (A) TDN, (B) NO<sub>3</sub><sup>-</sup>, and (C) DON increased linearly with N loading. The linear relationship was significant and signified that the West Fork watershed was well below N saturation according to the Michaelis-Menten kinetics model [Earl *et al.*, 2006]. As expected in an N limited system, watershed NO<sub>3</sub><sup>-</sup> retention increased at a higher rate than retention of TDN or DON as evident by the slope of the regression line; the slope of NO<sub>3</sub><sup>-</sup> = 0.93 versus 0.83 for TDN and 0.90 for DON. Locations are illustrated in Figure 3.1B.

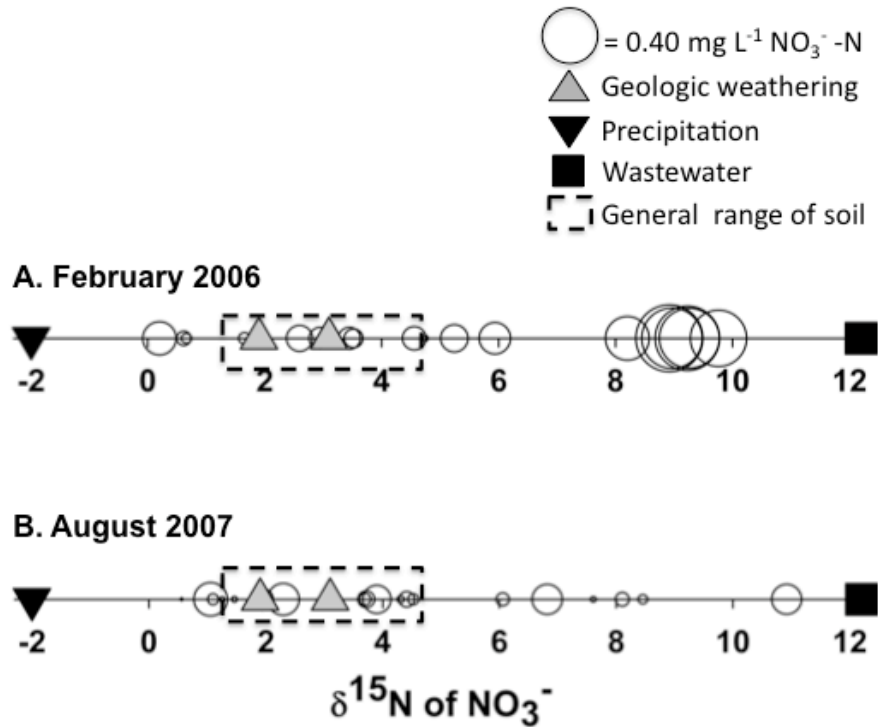
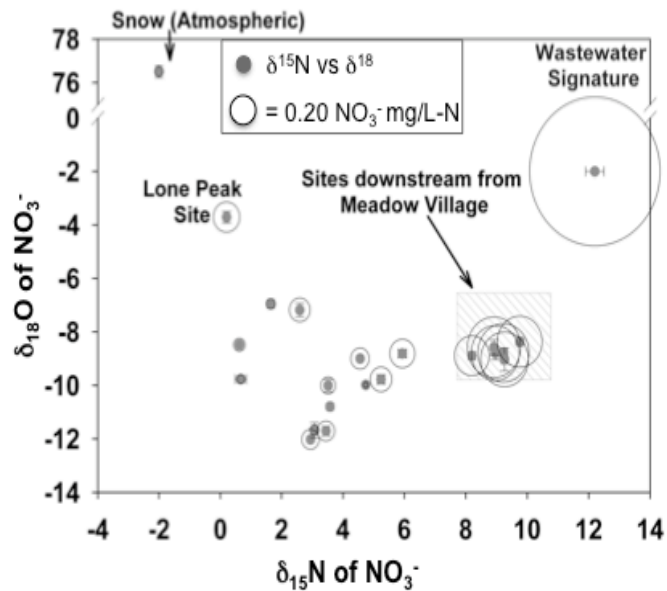


Figure 3.11:  $\delta^{15}\text{N}$  of  $\text{NO}_3^-$  of snow (black triangles), wastewater effluent (black squares), mineral weathering experiment slurries (grey triangles [Ackerman et al., in review], and a subset of the (A) February and (B) August synoptic samples from the West Fork watershed (black outlined circles) (Figure 3.4A). Streamwater  $\text{NO}_3^-$  concentration represented by circle size, ranged from  $0.04 \text{ mg L}^{-1}$  to  $0.045 \text{ mg L}^{-1}$  in February and  $0.01 \text{ mg L}^{-1}$  to  $0.21 \text{ mg L}^{-1}$  in August.  $\delta^{15}\text{N}$  of  $\text{NO}_3^-$  values at sites located downgradient from Meadow Village had enriched  $\delta^{15}\text{N}$  of  $\text{NO}_3^-$  values in August and February, indicating a significant contribution from wastewater. Other sites appeared to be more influenced by a mixture of geologic weathering, soil water, or precipitation [Kendall and McDonnell, 1998].

## A. February



## B. August

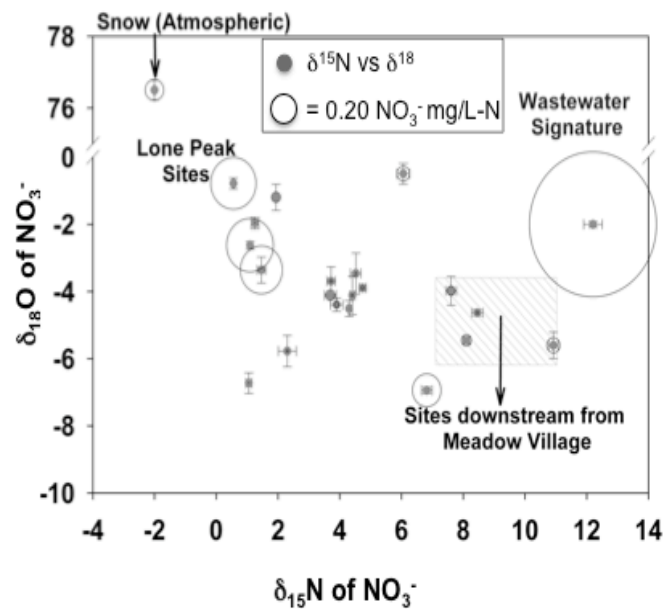


Figure 3.12:  $\delta^{15}\text{N}$  and  $\delta^{18}\text{O}$  of  $\text{NO}_3^-$  values for a subset of August (A) and February (B) synoptic streamwater samples.  $\delta^{15}\text{N}$  of  $\text{NO}_3^-$  values at sites located downgradient from Meadow Village had enriched  $\delta^{15}\text{N}$  of  $\text{NO}_3^-$  values in August and February, indicating a significant contribution from wastewater. Light  $\delta^{15}\text{N}$  of  $\text{NO}_3^-$  values indicated that sites draining Lone Mountain with high  $\text{NO}_3^-$  concentrations were not influenced by wastewater. Median  $\delta^{18}\text{O}$  of  $\text{NO}_3^-$  was lower in February (-8.9) versus August (-4) suggesting less contribution from atmospheric  $\text{NO}_3^-$  [Kendall and McDonnell, 1998].

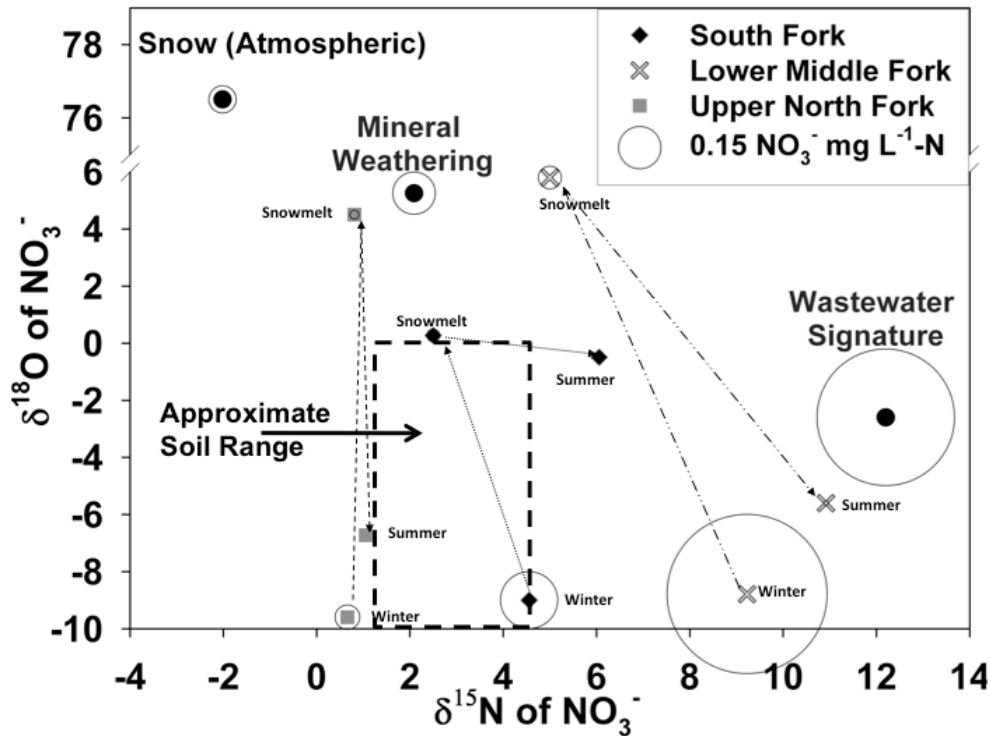


Figure 3.13:  $\text{NO}_3^-$  isotope data from the main West Fork tributaries illustrated seasonal variability in the sources of streamwater  $\text{NO}_3^-$ . During snowmelt, enriched  $\delta^{18}\text{O}$  of  $\text{NO}_3^-$  values at all sites pointed to higher contributions of atmospheric  $\text{NO}_3^-$  than other times of year; however, contributions from atmospheric  $\text{NO}_3^-$  were less than soil water contributions as evident from  $\delta^{18}\text{O}$  of  $\text{NO}_3^-$  signatures more similar to soil water  $\text{NO}_3^-$ . During summer and winter baseflow,  $\delta^{15}\text{N}$  of  $\text{NO}_3^-$  values indicated a significant contribution from wastewater to streamwater  $\text{NO}_3^-$  concentrations in the Middle Fork and to a lesser degree during snowmelt. In the South Fork, small wastewater contributions were evident in winter and summer baseflow.

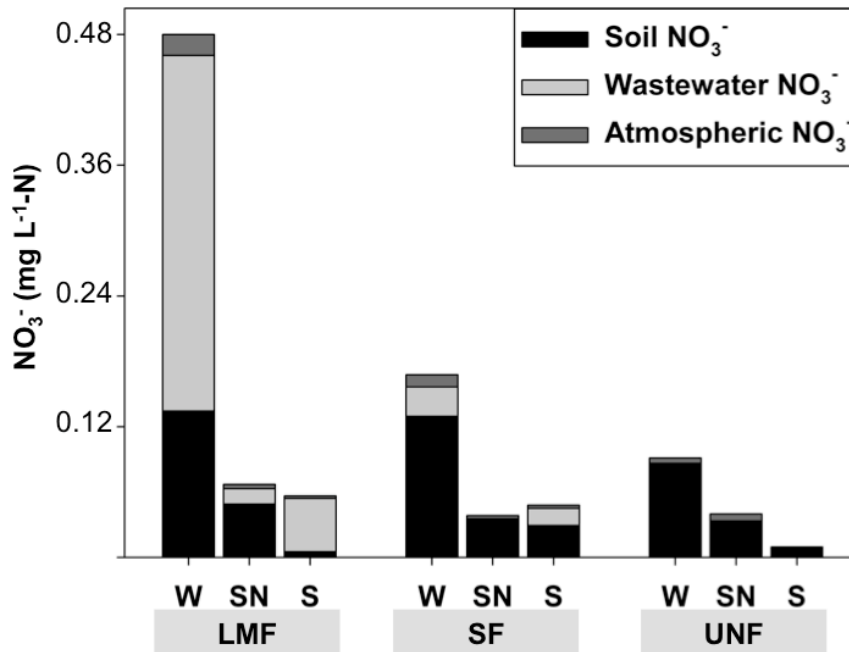


Figure 3.14: Seasonal variability of streamwater  $\text{NO}_3^-$  sources to the three main tributaries of the West Fork estimated through endmember mixing model analysis of  $\delta^{15}\text{N}$  and  $\delta^{18}\text{O}$  of  $\text{NO}_3^-$  values. Seasonal fluctuations occurred in the influences of anthropogenic N on streamwater  $\text{NO}_3^-$ . Wastewater influence on streamwater  $\text{NO}_3^-$  concentrations was most evident in developed streams during summer (“S”) and winter (“W”) baseflow. Even though streamwater  $\text{NO}_3^-$  concentrations were low relative to other times of the year, wastewater was the biggest contributor to streamwater  $\text{NO}_3^-$  at LMF during summer growing season, when it contributed 85% of streamwater  $\text{NO}_3^-$ . Soil water  $\text{NO}_3^-$  was the biggest contributor to streamwater  $\text{NO}_3^-$  at UNF and SF year-round and at LMF only during snowmelt. Atmospheric  $\text{NO}_3^-$  contributed only 6, 8, and 13% of streamwater  $\text{NO}_3^-$  at LMF, SF, and UNF, respectively during spring runoff suggesting substantial biological cycling of atmospherically  $\text{NO}_3^-$  occurred prior to watershed export

Contribution of Authors and Co-Authors

Manuscript in Chapter 4: Quantifying Watershed Sensitivity to Spatially Variable Nitrogen Loading and the Relative Importance of Nitrogen Retention Mechanisms

Author: Kristin K. Gardner

Contributions: co-developed and implemented the project, collected and analyzed output data, and wrote the manuscript.

Co-author: Dr. Brian L. McGlynn

Contributions: co-developed the study, discussed the results and implications and commented on the manuscript at all stages.

Co-author: Dr. Lucy A. Marshall

Contributions: aided in model development, discussed the results and implications and commented on the manuscript at all stages.

Manuscript Information Page

Kristin K. Gardner, Brian L. McGlynn, and Lucy A. Marshall

Journal Name: Water Resources Research

Status of Manuscript:

Prepared for submission to a peer-reviewed journal

Officially submitted to a peer-reviewed journal

Accepted by a peer-reviewed journal

Published in a peer-reviewed journal

Publisher: American Geophysical Union

Date submitted: July 12, 2010

## CHAPTER 4

QUANTIFYING WATERSHED SENSITIVITY TO SPATIALLY VARIABLE  
NITROGEN LOADING AND THE RELATIVE IMPORTANCE OF  
NITROGEN RETENTION MECHANISMSAbstract

The link between nitrogen (N) loading and watershed nitrate ( $\text{NO}_3^-$ ) export is poorly understood yet critical to addressing the growing problem of anthropogenic N enrichment in developing watersheds across the United States and world. We introduce the Big Sky Nutrient Export model (BiSN), which incorporates spatial streamwater chemistry, data from instream N uptake and geological weathering experiments, and terrain and land use analysis to quantify the spatial variability of watershed sensitivity to N loading and the relative importance of upland, riparian and instream N retention across land use/ land cover and landscape positions. Bayesian Markov chain Monte Carlo (MCMC) methods were used for model specification and were helpful in assessing model and parameter uncertainty and advancing understanding of the primary processes governing watershed  $\text{NO}_3^-$  export. Modeling results revealed that small amounts of wastewater loading occurring in watershed areas with short travel times to the stream had disproportionate impacts on watershed  $\text{NO}_3^-$  export compared to spatially distributed N loading or N loading in watershed areas with longer travel times. In contrast, spatially distributed N inputs of greater magnitude (soil storage release and septic) had little influence on  $\text{NO}_3^-$  export. During summer baseflow conditions, 98-99 percent of

watershed N retention occurred in the uplands most likely from biological uptake and/or a lack of hydrologic transport to the stream network. Relative instream N retention increased with loading downstream through the stream network. This work demonstrates the importance of characterizing the spatial variability of watershed N loading, export and retention mechanisms, and considering landscape position of N sources to effectively manage watershed N.

### Introduction

Human activities have greatly increased the bioavailability of watershed nitrogen (N), primarily from the addition of fertilizers, human and animal waste, and the burning of fossil fuels [Vitousek *et al.*, 1997]. With increasing amounts of bioavailable N, watershed biotic demand can become saturated, potentially resulting in excess N delivered to surface waters [Aber *et al.*, 1989]. N enrichment of aquatic resources can have profound impacts on ecosystem function by stimulating primary production, which can alter biological communities and expedite eutrophication [Allen, 1995].

Minimizing the influence of anthropogenic N on aquatic ecosystems is one of watershed management's biggest challenges. This is because the relationship between anthropogenic N loading and stream N export is complicated; N is not conservatively transported and there is potential for N retention to occur in terrestrial and stream ecosystems. Mechanisms for N retention include: (1) microbial denitrification [Brooks *et al.*, 1996; Burt *et al.*, 1999], (2) plant or microbial assimilation [Hadas, 1992; Nadelhoffer *et al.*, 1999], (3) physical sorption [Qualls and Haines, 1992; Triska *et al.*,

1994], and (4) biotic and abiotic retention through iron and sulfur reduction [*Brunet and Garcia-Gil, 1996; Davidson et al., 2003*]. N retention can alter the timing, magnitude, and form of N transported creating complex spatial and temporal patterns in streamwater N.

For effective management of streamwater N, it is critical to identify and quantify the spatial distribution of watershed N loading and retention. For this, environmental managers often rely upon water quality models. A water quality model is a set of equations that can be used to describe the processes that determine instream N concentrations or loads. Watershed models range in their complexity from simple empirical models with minimal data requirements to complex mechanistic models that require enormous amounts of data. Selecting the level of model complexity should depend on the: 1) goals or objectives of the model, 2) available data, 3) computational efficiency, 4) budgetary constraints [*U.S EPA, 1976*], 5) spatial scale [*Soulsby et al., 2006*], and 6) level of predictive and parameter uncertainty [*Perrin et al., 2001*].

Overly complex models can lead to problems of over parameterization and equifinality [*Beven, 1993; Beven, 2006*], which may in turn result in large predictive uncertainty. High model uncertainty is common in water quality applications as a result of spatial variability of environmental variables, parameter uncertainty, measurement error, and conceptual uncertainty [*Beven, 2001*]. Simple watershed models are an attractive approach to reduce model uncertainty and can be suitable for some watersheds processes, like describing an integrated watershed response [*Savenije, 2001*]. Ideally, a model should have a small number of parameters with a high enough level of mechanistic

detail to represent the major processes controlling the modeled phenomena or the model may lead to misrepresentative conclusions and poor land management decisions [Young *et al.*, 1996].

Export coefficient models represent a simple modeling approach that has been applied in many catchments to predict nutrient loads [Beaulac and Reckhow, *et al.*, 1982; Rast and Lee, 1983; Johnes, 1996; Worrall and Burt, 1999; McFarland and Hauck, 2001; Endreny and Wood, 2003; Zobrist and Reichert, 2006]. The basic export coefficient model assumes that land use is a major driver of catchment nutrient export. These models calibrate nutrient export coefficients, which represent the amount of nitrogen or phosphorus exported from a specific land use over a specific time period. Several studies have introduced process representation into the basic export coefficient model by adding: 1) export coefficients weighted within a threshold distance from rivers [Johnes and Heathwaite, 1997], 2) soil nitrogen reserves [Worrall and Burt, 1999], 3) monthly runoff data to capture seasonal variability [Hanrahan *et al.*, 2001], 4) export coefficients weighted by the topographic index and buffer index to represent transport and retention processes [Endreny and Wood, 2003], and 5) an erosion index as a surrogate for hydrologic variability in modeling phosphorus export [Khadam and Kaluarachchi, 2004].

This paper introduces the Big Sky Nitrogen Export Model (BiSN), which predicts watershed nitrate ( $\text{NO}_3^-$ ) export by incorporating terrestrial, riparian, and instream retention process representation to a basic export coefficient model. The spatial network structure of BiSN allows for exploration of watershed N loading and retention and  $\text{NO}_3^-$  export patterns at the watershed scale. This approach can provide valuable insight into N

spatial dynamics to formulate more focused research questions or to aid development of effective land use planning to minimize N loading to streams. We consider the uncertainty in the BiSN output and its parameters by applying a Bayesian Markov Chain Monte Carlo (MCMC) approach. Bayesian MCMC methods, which put emphasis on the posterior distribution of model parameters, can provide a detailed description of parameter uncertainty leading to better quantification of model error and information for model diagnostics.

We apply BiSN to summer synoptic streamwater  $\text{NO}_3^-$  data collected in a developing mountain watershed to: 1) determine the model's ability to characterize the spatial heterogeneity of streamwater  $\text{NO}_3^-$  export, 2) identify the primary drivers of the spatial heterogeneity of streamwater  $\text{NO}_3^-$  export, and 3) quantify how the spatial distribution of N loading and retention and  $\text{NO}_3^-$  export vary with land use and landscape position.

### Study Area

The West Fork of the Gallatin River in the northern Rocky Mountains of southwestern Montana (Figure 4.1A) drains Big Sky, Moonlight Basin, Yellowstone Club, and Spanish Peaks resort areas (Figure 4.1B). The West Fork watershed (212 km<sup>2</sup>) is characterized by well-defined steep topography and shallow soils. Elevation in the drainage ranges from approximately 1800 to 3400 meters and average annual precipitation exceeds 1270 millimeters (mm) at higher elevations and is less than 500 mm near the watershed outlet. Sixty percent of precipitation falls during the winter and

spring months [USDA NRCS, 2008]. Hydrographs of the West Fork River indicate peak flows during spring snowmelt typically occurring in late May and early June followed by a general recession throughout the summer, autumn, and winter months.

Streams in the West Fork watershed range from first-order, high gradient, boulder dominated mountain streams in the upper elevations to fourth-order, alluvial streams near the watershed outlet. Stream productivity is generally low due to cold temperatures and short growing seasons [USDA FS, 2004], however in recent years, increased algal growth has been noted in streams draining developed subwatersheds near the watershed outlet. The increased algal growth in streams draining development may be signs of the beginning stages of N enrichment. Chlorophyll *a* data collected in September 2005 suggest that algal growth is elevated above natural background levels in streams draining developed subwatersheds. Median Chlorophyll *a* ranged from 2.5 mg m<sup>-2</sup> in pristine low order streams, 20 mg m<sup>-2</sup> in pristine higher order streams to 360 mg m<sup>-2</sup> in higher order streams draining more developed watersheds [PBS&J, 2005].

Diverse geologic materials are present in the West Fork watershed, including metamorphosed volcanics of Archean age, sedimentary and meta-sedimentary formations of various ages, and colluvium and glacial deposits that dominate the surficial geology in valley bottoms. Carbonaceous minerals such as limestones and shales are present in the mineralogy of some but not all headwater catchments, and quartzite, biotite, gneiss, gabbros, and sandstones are also present [Alt and Hyndman, 1986; Kellog and Williams, 2006]. Vegetation below tree line consists of coniferous forest (lodgepole pine, blue and Engelmann spruce, and Douglas-fir), grasslands, shrublands, and willow and aspen

groves in the riparian areas. The watershed has a brief growing season from mid-June through mid-September (75 – 90 frost free days), decreasing with elevation [*USDA FS*, 1994].

Big Sky Resort was established in the early 1970s and since then, the West Fork watershed has seen a rapid increase in growth with the addition of three new ski resorts and golf courses with associated residential development. Since resort development, streamwater  $\text{NO}_3^-$  concentrations in the West Fork of the Gallatin River have followed a similar upward trend to development as represented by the number of building structures in the 212 km<sup>2</sup> watershed (Figure 4.2). The Big Sky Water and Sewer District services the two village areas with public water supply and sewer in the West Fork watershed (Figure 4.1B). Public wastewater receives secondary treatment and is released into three lined sewer detention ponds and stored until mid-spring when it is released as irrigation water onto the Big Sky Golf Course (Figure 4.1C). Golf course irrigation begins in mid-spring when the ground thaws and continues through mid-fall, when the ground again freezes. Areas outside of the sewer district are on individual or community septic systems and private wells [*R. Edwards*, personal comm., 2007].

### Methods

The BiSN model uses a traditional export coefficient modeling approach but additionally incorporates spatially explicit observations of land and stream attributes. The BiSN modeling framework then allows for representation of spatially distributed N processes whilst retaining relative model parsimony. We describe here the data collection and

construction of BiSN. Model inputs included: 1) field data collected to describe the spatial variability in streamwater  $\text{NO}_3^-$ , instream  $\text{NO}_3^-$  retention, atmospheric inorganic N deposition, stream discharge, and mineral release of N, 2) terrain indices associated with rates of transport through the watershed and with riparian buffering potential, and 3) land use/land cover acting as principal sources or sinks of watershed N.

#### Streamwater Sampling and Chemistry Analysis

The spatial distribution of watershed  $\text{NO}_3^-$  export was measured through synoptic, or “snapshot-in-time,” sampling in which streamwater was collected in 250 mL high-density polyethylene (HDPE) bottles from 50 sites across the West Fork watershed within 2-3 hours time (Figure 4.1B). Synoptic sampling sites were selected to represent a range of subwatershed characteristics including: land use/land cover (LULC), number of wastewater disposal units, geology, stream order, elevation, and discharge (Figure 4.1B). Six repeated synoptic sampling campaigns were conducted across a range of hydrological and biological activity [*Gardner and McGlynn, 2009*]. BiSN implementation for this study was based on data from the August 8, 2009 synoptic campaign. The summer synoptic campaign was used for the following reasons: 1) abundant summer instream  $\text{NO}_3^-$  uptake data was available, and 2) modeling results were used for Total Maximum Daily Load development, which in Montana is primarily concerned with summer low flow conditions.

Instream  $\text{NO}_3^-$  uptake experiments were conducted in six stream reaches representing a range of watershed and land use characteristics [*McNamara et al., in prep. McNamara, 2010*]. Two tracer addition methods were followed: constant-rate tracer

additions using modified methods from *Webster and Valett* [2006] and instantaneous tracer additions using the newly developed TASC method (Tracer Additions for Spiraling Curve Characterization) accomplished as part of this project and related research by the MSU Watershed Hydrology Laboratory [*Covino et al.* in press A, *Covino et al.*, in press B]. N, chloride, and specific conductance data collected during the tracer addition experiments were used to estimate total  $\text{NO}_3^-$  retention, Michaelis-Menten kinetic model parameters (including ambient uptake), and spiraling parameters for each of 6 stream reaches [*McNamara et al.*, in prep; *Covino et al.*, in press A].

Continuous stage data was collected on the West Fork and its three tributaries [*PBSJ*, 2008]. Stream discharge was calculated from stage-discharge rating curves developed from measurements over the full range of discharge. Stream discharge was measured with a Marsh McBirney Flo-Mate 2000™ current velocity meter and standard USGS area-velocity method [*Gardner and McGlynn*, 2006]. For reaches in which no discharge data was collected, watershed area was used to scale discharge. During the summer baseflow period, the relationship between watershed area and stream discharge measured at four locations in the West Fork watershed was strongly correlated ( $R^2=0.99$ ) and significant ( $p<0.05$ ).

Streamwater samples from the synoptic campaigns and the tracer additions were chilled to 0-4°C and transported to the laboratory where they were filtered within 24 hours of collection with 0.45  $\mu\text{m}$  Millipore Isopore Polycarbonate membranes. Filtered water samples were preserved in HDPE bottles and frozen until analysis. Dissolved aqueous nitrogen species analyzed included nitrite ( $\text{NO}_2^-$ ),  $\text{NO}_3^-$ , ammonium ( $\text{NH}_4^+$ ), and

organic N. For this study, we examined inorganic N (for more details on organic N, see *Gardner et al.*, in review), but since most samples contained  $\text{NO}_2^-$  and  $\text{NH}_4^+$  levels near or below detection limits (0.005-0.01  $\text{mg L}^{-1}$ ), we focused on  $\text{NO}_3^-$ .  $\text{NO}_3^-$  was analyzed by ion-exchange chromatography (IC) using a Metrohm Peak model 820 interface equipped with a 4-mm anion-exchange column [Metrohm, Herisau, Switzerland]. The detection limit for  $\text{NO}_3^-$  was 0.01  $\text{mg L}^{-1}$ -N. Accuracy was within 10% for certified 0.09  $\text{mg L}^{-1}$   $\text{NO}_3^-$ -N standards ( $0.09 \pm 0.009 \text{ mg L}^{-1} \text{ NO}_3\text{-N}$ ), as measured every 11<sup>th</sup> sample. Coefficients of variation (CVs) for  $\text{NO}_3^-$  standard peak areas were 2% or less.

#### Geologic Weathering Experiments

Research has shown that modeling N export purely dependent on land use tends to underestimate N export [*Worrall and Burt, 1999*]. Consequently, *Worrall and Burt* [1999] introduced a soil reserve parameter representing the release of inorganic N from soil organic matter, which can be a significant pool of watershed N [*Post et al., 1985*]. In BiSN, we defined this parameter as soil storage release (*SSR*). *SSR* is the release of N from soil storage, which is the accrual of N in soils from historic N loading (i.e. atmospheric N deposition, wastewater), plant and microbial immobilization, and soil adsorption. Release of inorganic N from soil occurs through mineralization, fixation, geologic weathering, and dissolution. Laboratory geologic weathering experiments supported other research that has demonstrated geology to be a substantial source of watershed N [*Holloway et al., 1998; 2001*]. Specifically, *Ackerman et al.* [in prep.] found that Cretaceous carbonate rocks produced enough N to be considered an important source of inorganic N to certain streams in the watershed; 10 times more total N was weathered

from cretaceous carbonate rocks as compared to other rock types found in the study area. This information from the geologic weathering experiments partially informed the *SSR* parameter. *SSR* was computed as a relative amount of inorganic N released from soil storage. This means that watershed areas consisting of geology with greater potential to weather inorganic N were assumed to have 10 times more inorganic N in soil storage and therefore, release ten times more N than other grid cells consisting of geology with less potential to weather inorganic N. To incorporate this information into BiSN, the *SSR* parameter in grid cells with geology less prone to weather inorganic N (which was the majority of the grid cells) was multiplied by 0.1.

#### Atmospheric Deposition

Inputs of inorganic N ( $\text{NO}_3^-$  and  $\text{NH}_4^+$ ), from atmospheric dry and wet deposition can be a significant source of watershed N loading [Aber *et al.*, 1989; Burns, 2003]. The atmospheric dry deposition inorganic N load was assumed equivalent to the average dry deposition inorganic N load measured between 2000 and 2007 in the northwestern corner of Yellowstone National Park (Figure 4.1A) [US EPA CMAD, 2009]. This site is located at 2400 m, 100 km from the West Fork watershed and was presumed to have similar dry N deposition rates. No discernable temporal trend in inorganic N deposition occurred across this time period. Atmospheric dry deposition inorganic N load was assumed to be constant across the study area. The atmospheric wet deposition inorganic N load was computed from average wet deposition inorganic N concentrations measured at Tower Falls in Yellowstone National Park between 2000 and 2007 (Figure 4.1A) [NADP, 2009]. Tower Falls is 40 km north of the dry deposition site in Yellowstone National Park at

1900 m, 70 km southeast of the West Fork watershed and was presumed to have similar wet inorganic N depositional rates as lower elevations. There was no observed trend in inorganic N concentration of atmospheric wet deposition across this time period. The atmospheric wet deposition load for each modeled grid cell in the study area was calculated by multiplying inorganic N concentration by elevation scaled precipitation. Elevation scaled precipitation was determined by a statistical relationship developed between precipitation and elevation data from two weather stations in the study area (Appendix A): 1) the Lone Mountain SNOTEL station located in the headwaters of the North Fork watershed (Figure 4.1B) at 2706 m in a subalpine environment, and 2) the Lone Mountain Ranch weather station, located towards the valley bottom at 2100 m.

### Watershed Characteristics

Terrain Analysis:  $\text{NO}_3^-$  transport in watersheds along hydrologic flowpaths is partially controlled by landscape characteristics [Dunne, 1978; Newson, 1997]. Definition of hydrological flowpaths, potential travel times along each flowpath and the concomitant spatial pattern of N loading across the West Fork watershed are necessary to explain variability in streamwater  $\text{NO}_3^-$ . To explicitly characterize the spatial distribution of N loading by various sources, the BiSN model includes the discretization of the landscape to units representing different hydrologic and land use conditions. The West Fork watershed has steep slopes and predominately thin soils with high hydraulic conductivities [USDA SCS, 1978; USDA SCS, 1982]. These conditions often promote shallow subsurface runoff pathways that can result in rapid  $\text{NO}_3^-$  delivery to riparian

zones and streams. Consequently, hydrological flowpaths are likely to be well represented by surface topography. For this study, the  $MD_{\infty}$  flow accumulation algorithm [Seibert and McGlynn, 2007] was used to define the hydrological flowpaths in the West Fork watershed using a 10m digital elevation model (DEM) developed by parsing a 1-m resolution Airborne Laser Swath Mapping data set. The spatial resolution of the 1-m DEM was reduced to improve computational time and to prevent the terrain analysis software from terminating before completion.

Terrain analysis extracted relevant terrain characteristics from the 10m DEM to model streamwater  $\text{NO}_3^-$  concentrations. First, an approximation of water transit time for each grid cell was calculated [McGuire *et al.*, 2005] and referred to as water travel time (*TT*).  $\text{NO}_3^-$  export has been shown to be inversely related to watershed residence time due to increased reaction time for immobilization [Seitzinger *et al.*, 2002]. For each grid cell, *TT* is the topographically derived flowpath distance to the stream divided by the gradient over the flowpath. *TT* is an estimate of the relative travel time from a grid cell to the stream channel (For more details, see Gardner and McGlynn [2009]).

In addition to *TT*, a riparian buffering index (*RBI*) was computed from the 10m DEM by an automated method in which the delineated riparian zone area associated with each stream pixel is divided by the local contributing area (lateral upslope inflows) [McGlynn and Seibert, 2003; Jencso *et al.*, 2010; Grabs *et al.*, 2010] (For more details see Gardner and McGlynn [2009]). Stream reach to stream reach assessment of riparian buffering potential of lateral hillslope inputs is pertinent in LULC change-water quality analyses because it allows for assessment of potential riparian buffering down-gradient

(along each flowpath) of  $\text{NO}_3^-$  inputs.

The stream network was delineated into reaches approximately 500m in length. A 500 m reach length was chosen because 97% of measured  $\text{NO}_3^-$  uptake lengths were less than 500m [McNamara *et al.*, in prep., McNamara, 2010]. A total of 231 nested subwatersheds were delineated, ranging in area from 0.01 to 207  $\text{km}^2$ . Upstream subwatersheds were subtracted from downstream subwatersheds to create non-nested subwatersheds so that each land pixel contributed to only 1 stream reach. Non-nested subwatersheds ranged in area from 0.01  $\text{km}^2$  to 3.7  $\text{km}^2$  (Figure 4.3A).

Land Cover Analysis: Natural and human altered LULC can have direct bearing on streamwater  $\text{NO}_3^-$  export [Likens *et al.*, 1970; Chang *et al.*, 2002; Wong *et al.*, 2004; Gardner and McGlynn, 2009]. Here, LULC was delineated from a cloud-free QuickBird scene acquired on July 21, 2005 [Campos, in press] for input into BiSN. Delineated land use classes included forest, impervious surface, grass, golf, soil, and sewer ponds. Septic locations were mapped by masking the Big Sky Water and Sewer District boundary GIS layer over a 2006 structure layer supplied by the Gallatin County Planning District. Geologic maps, acquired from the Montana Bureau of Mines and Geology [Kellog and Williams, 2005] were used to determine the percent of geology with higher potential for N weathering in each subwatershed [Ackerman *et al.*, in prep]. Subwatershed land use and terrain characteristics were then extracted as model parameters in BiSN.

The model parameters identified from land use/ land cover and terrain analysis included forest, impervious surface, grass, golf, soil, septic, sewerponds, geology, and relative travel time. Since initial model simulations resulted in poor convergence and

high parameter correlations, model parameter classes were lumped [Bates and Campbell *et al.*, 2001] so that “vegetation” consisted of grass and forest, “non-vegetation” consisted of impervious surface and soil, and “wastewater” consisted of the golf courses and sewerponds. Additional model simulations demonstrated that  $\text{NO}_3^-$  export was insensitive to the “non-vegetation” parameter illustrated by a uniform posterior distribution across the entire prior distribution. Furthermore, the vegetation Markov chain did not converge despite relatively long model runs and low correlations with other parameters. For these reasons, the “non-vegetation” parameter was not included in the model (Equation 4.1). The insensitivity of “non-vegetation” parameter suggests that “non-vegetation” was not a primary driver of streamwater concentrations during the summer growing season. Other research has shown impervious surface to be most associated with watershed  $\text{NO}_3^-$  export during high runoff events [Lunetta *et al.*, 2005; Shields *et al.* 2008], while having less influence on watershed  $\text{NO}_3^-$  export during drier periods [Lunetta *et al.*, 2005]. In addition, impervious surface has been shown to exhibit threshold behavior in its influence on watershed  $\text{NO}_3^-$  export [Carle *et al.*, 2005; Lunetta *et al.*, 2005; Clausen *et al.* 2008]. Since BiSN modeled watershed  $\text{NO}_3^-$  export during a dry period and “non-vegetation” occurred at a low density in the West Fork watershed, one might expect “non-vegetation” parameter not to be a major driver of watershed  $\text{NO}_3^-$  export.

#### Big Sky Nutrient Export Model (BiSN)

The relationship between LULC, watershed characteristics, and  $\text{NO}_3^-$  export was determined by BiSN, whose modeling framework was adapted from the hybrid

mechanistic and spatial modeling approaches used by [Worrall and Burt, 1999] and [Endreny and Wood, 2003]. BiSN introduces process representation by incorporating terrestrial, riparian, and instream retention to the basic export modeling approach. We believe characterizing the spatial patterns in these retention processes is critical to capturing the spatial heterogeneity of watershed  $\text{NO}_3^-$  export.  $\text{NO}_3^-$  export to the downstream end of stream reach  $i$  ( $NE_i$  in  $\text{kg d}^{-1}$ ) was modeled as a function of: 1) lateral  $\text{NO}_3^-$  loading from the incremental drainage  $i$  decayed along terrestrial flowpaths and half of the stream reach  $i$ , and 2)  $\text{NO}_3^-$  loading from one or more adjacent upstream reaches decayed along the length of stream reach  $i$  ( $N_{up}$ ) (Equation 4.1, Figure 4.3B):

$$NE_i = \left( \sum_{j=1}^n (VEG_j * b_v + WW_j * b_{ww} + S_j * b_s + SSR_j * b_{ssr} + WD_j * b_{wd} + DD) * \frac{b\beta}{TT_j(b\alpha - 1)} \right) - (RBI_i * b_r) - (0.5 * decay) + (NE_{up} - decay) + e_i \quad (4.1)$$

where,  $NE_i$  is the  $\text{NO}_3^-$  export to the downstream end of stream reach  $i$ ,  $n$  is the number of grid cells contributing to stream reach  $i$  (i.e. the size of the BiSN modeling unit  $i$ ), and  $e_i$  is the model residual or error. Upland lateral loading of N was calculated via indicator variables representing vegetation ( $VEG$ ), wastewater application ( $WW$ ), the number of septic systems ( $S$ ), and soil storage release of  $\text{NO}_3^-$  ( $SSR$ ), which occurred in all grid cells but was 10 times greater in grid cells consisting of geology with a higher potential to release N [Ackerman et al., in prep]. Wet inorganic deposition,  $WD$ , was scaled by precipitation (varied by elevation) (Appendix A), while dry inorganic N deposition,  $DD$ ,

was constant across the watershed.  $b_v$ ,  $b_w$ ,  $b_s$ ,  $b_{SSR}$ , and  $b_{wd}$  are calibrated nitrogen export coefficients associated with the model parameters  $VEG$ ,  $W$ ,  $S$ ,  $SSR$ , and  $WD$ , respectively.

Terrestrial retention occurring in the uplands and the riparian area is described by two terrain indices, watershed travel time ( $TT$ ) and riparian buffering potential ( $RBI$ ). The N load from each pixel is modeled to follow a power law decay as it travel along hydrological flowpaths to the stream as a function of  $TT_j$ , the  $TT$  index for each grid cell  $j$ . Therefore, upland retention for subwatershed  $i$  is computed as N loading inputs from  $WW$ ,  $S$ ,  $DD$ ,  $WD$ ,  $SSR$  minus  $\text{NO}_3^-$  exported from the uplands (N loading inputs \*  $f(TT)$ ).  $\text{NO}_3^-$  exported from the uplands is subject to immobilization in the riparian area from  $RBI_i$ , a riparian buffer index ratio for each subwatershed  $i$ .  $b_\alpha$  and  $b_\beta$  are the calibrated shape and scale parameters of the power law function associated with  $TT_j$ , and  $b_r$  is the calibrated  $RBI$  parameter.

N loading that is exported from the riparian area is subject to instream retention, which is modeled as a decay component formulated from field data acquired from instream  $\text{NO}_3^-$  uptake experiments. In addition to upland loading,  $NE_i$  is a function of  $\text{NO}_3^-$  export from one or more upstream reach(es) ( $NE_{up}$ ) (Figure 4.3B).  $NE_{up}$  and the decayed upland lateral loading are subject to instream  $\text{NO}_3^-$  loss,  $decay$ , (areal uptake,  $\text{kg d}^{-1}\text{m}^2$ ) which was inferred from instream  $\text{NO}_3^-$  experiments conducted in the West Fork watershed during the study period [McNamara et al., in prep.] (Appendix B).  $\text{NO}_3^-$  export was computed for each of the 231 stream reaches and compared to the observed  $\text{NO}_3^-$  export at 50 stream reaches. The total watershed export for the West Fork watershed

is the  $NE$  calculated for the most downstream reach in the watershed and represents the integrated watershed response.

### BiSN Model Specification and Parameter Estimation

BiSN Inference and Markov Chain Monte Carlo Methods: Bayesian methods allow for “expert knowledge” of system behavior to be incorporated with observed data into model structure through the Bayes rule [*Gelman et al.*, 2004]:

$$P(\theta|NE) = \frac{P(\theta) * P(NE|\theta)}{P(NE)} \quad (4.2)$$

where,  $P(\theta|NE)$  is the posterior distribution or the probability of the unknown model parameters  $\theta$  given the observed data ( $NE$ ),  $P(\theta)$  is the prior distribution or the current knowledge of the model parameters,  $P(NE|\theta)$  is the likelihood or the probability of the observed data given the parameters values, and  $P(NE)$  is the prior probability of the observed data which acts as a normalizing constant.

Recent research in hydrologic modeling has shown Bayesian statistical inference to provide a powerful framework for assessing parameter uncertainty and subsequent uncertainty in applications such as rainfall-runoff model simulations [*Bates and Campbell*, 2001; *Marshall et al.*, 2004], groundwater flow [*Hassan et al.*, 2009], and solute export [*Qian*, 2005; *Zobrist and Reichert*, 2006; *Shrestha*, 2008]. This is because uncertainty in the model parameters can easily be assessed through the posterior distribution; instead of a single fit to the data, Bayesian methods estimate a distribution of possible parameter values.

The Bayesian approach provides an attractive framework for inference in nutrient export modeling. This is especially true given the uncertainties in the export model parameters and processes, and the comparative lack of available data with which to constrain model results. Rather than give a deterministic “best” simulation, the full range of parameter uncertainty and interactions may be determined and their impacts on subsequent model simulations assessed.

Computation of the posterior distribution,  $P(\theta|NE)$ , for most non-linear models and models with a high dimensional parameter space can be prohibitively difficult [Gelman *et al.*, 2004]. For these cases,  $P(\theta|NE)$  can be generated using a sampling algorithm. MCMC simulation methods are commonly used in Bayesian inference to estimate the posterior distribution by generating a sample from a distribution. BiSN was fit using an adaptive MCMC method for estimation of model parameters. The adaptive Metropolis algorithm (AM) [Haario, 2001] is a modification of the standard Metropolis algorithm, and has been shown to be advantageous for hydrologic modeling [Marshall *et al.*, 2004; Hassan, *et al.*, 2009]. A major advantage of the AM algorithm is that the entire parameter set is updated simultaneously, which reduces computational time and complexity.

Following other hydrologic studies such as Bates and Campbell [2001], Marshall *et al.* [2004], Zobrist and Reichert [2006], Hassan *et al.* [2009], Smith and Marshall [2010], the likelihood function assumed homoscedastic, uncorrelated error terms:

$$P(NE|\theta) = (2\pi\sigma^{-n/2}) \prod_t \left\{ -\frac{[NE_{observed(t)} - NE_{predicted(t)}]^2}{2\sigma^2} \right\} \quad (4.3)$$

where,  $n$  is number of observed data points ( $NE_{\text{observed}}$ ), and  $\sigma^2$  is the error variance.

### BiSN Implementation

*Prior Densities:* The prior probability distribution represents the modeler's knowledge of system behavior. Prior knowledge of vegetation, non-vegetation, septic, and riparian export coefficients was based on literature values (Table 4.1) [*Rast and Lee, 1984; Burt et al., 1999; McFarland et al., 2001; US EPA, 2002; Maitre et al., 2003; Zobrist and Reichert, 2006; Alexander et al., 2008; NADP, 2009*]. Recognizing that literature values were based on studies conducted in watersheds with varying climatic and physical characteristics, prior bounds were loosely constrained by literature values. In general, prior bounds were within a order of magnitude of given literature values.

The soil storage release, wastewater, and atmospheric deposition parameters were constrained by empirical data collected in the study area (Table 4.1). The wastewater prior distribution was constrained by unpublished wastewater N concentration and discharge data acquired from the Big Sky Water and Sewer District. Data from geologic weathering experiments loosely bound the soil storage release prior probability distribution [*Ackerman et al., in prep*]. Inorganic N concentration data from Yellowstone National Park loosely constrained the atmospheric wet deposition parameter. For the travel time parameter, the power law scale parameter,  $\beta$ , and the shape parameter,  $\alpha$ , were constrained between 0 and 1. During initial model runs,  $\beta$  was unstable, so the

parameter was fixed at its most probable value 0.035 from initial model runs [*Bates and Campbell, 2001*].

Expert knowledge informed the shape of each parameter's prior probability distributions (Table 4.1, Figure 4.8). Uninformative uniform prior probability distributions were applied for the travel time, wastewater, soil storage release, and vegetation parameters. The uniform distribution applies equal probability to all values between the prior bounds. The septic and atmospheric deposition parameters priors were assumed to be a generalized trapezoid distribution [*Seibert and McDonnell, 2002*], while the riparian parameter prior distribution was assumed to be a triangular distribution [*Hession and Storm, 2000*].

*Model Convergence:* To ensure that the simulated posterior distribution was representative of the true posterior distribution, chain convergence was assessed by the Gelman-Rubin convergence diagnostic test [*Gelman and Rubin, 1992*]. The Gelman-Rubin diagnostic test is based on running multiple chains with starting points widely dispersed throughout the posterior distribution. The Gelman-Rubin approach diagnoses convergence by calculating the estimated potential scale reduction (R), which compares the variance within and between the multiple chains. At convergence, R should be close to 1.

For this project, model simulations were performed in Matlab. Each model simulation was run for 200,000 iterations. Pretuning runs were used to determine parameter values of high posterior density to help initialize MCMC runs. Based on these runs, multiple chains were run with starting values chosen across the simulated posterior

distribution to compute the Gelman-Rubin statistic and diagnose convergence to the posterior distribution.

*Model Uncertainty:* Total predictive uncertainty included uncertainties in the parameter values and the residual variance of the model output. We estimated total predictive uncertainty in our model simulations via MCMC parameter samples incorporating the effect of the model residual term.

## Results

Observed streamwater  $\text{NO}_3^-$  concentrations varied between 0.001 and 0.21  $\text{mg L}^{-1}$  (Figure 4.4A) and were generally highest in the most developed areas in the watershed (Figure 1b). Streamwater  $\text{NO}_3^-$  export across the West Fork watershed varied within three orders of magnitude, from 1.06  $\text{kg yr}^{-1}$  to 1245  $\text{kg yr}^{-1}$  (Figure 4.4B) and generally increased in a downstream direction. Streamwater  $\text{NO}_3^-$  export was generally highest in the lower reaches of the South Fork and the West Fork, which flow through the most developed areas in the watershed (Figure 4.1), while streamwater  $\text{NO}_3^-$  export was lowest in headwater subwatersheds (Beehive, Upper Middle Fork, and North Fork). Although we modeled streamwater  $\text{NO}_3^-$  in  $\text{kg d}^{-1}$ , we chose to report yearly export values so that comparisons could easily be made with export values in the literature. We emphasize that reporting yearly  $\text{NO}_3^-$  export based on summer  $\text{NO}_3^-$  export underestimates yearly  $\text{NO}_3^-$  export since the West Fork data was collected during summer low flow when  $\text{NO}_3^-$  export is small compared to  $\text{NO}_3^-$  export during the winter and snowmelt [*Gardner and McGlynn*, in prep.].

Normalized to watershed area, observed streamwater  $\text{NO}_3^-$  export ranged from 0.0002 to 0.24  $\text{kg ha}^{-1}\text{yr}^{-1}$ . In the headwaters of the Middle Fork (Figure 4.1), streams draining Lone Mountain exported the highest amounts of streamwater  $\text{NO}_3^-$  (Figure 4.4B). Lone Mountain is an alpine environment above treeline with steep slopes, consisting mainly of talus and scree. Inorganic N entering this environment with shallow soils, steep talus/scree slopes and little riparian area could easily be transported through the system. Unfortunately, no data exists in the headwaters of the South Fork due to inaccessibility of private land. Normalized  $\text{NO}_3^-$  export was elevated in the lower reaches of the South Fork and the West Fork. Both of these streams are alluvial streams draining areas of significant human development in the lower elevations of the watershed.

#### Model Performance and Model Uncertainty

BiSN converged after 100,000 iterations (the Gelman Rubin Diagnostic  $R \sim 1$ ) for all parameters, therefore the subsequent results are based on iterations 100,001 to 200,000. Modeled versus observed streamwater  $\text{NO}_3^-$  export with 90% prediction intervals are illustrated in Figure 4.5. The 90% prediction intervals included uncertainties in the parameter values and the residual variance of the model. Overall, the spatial variability of observed streamwater  $\text{NO}_3^-$  export was well captured by the BiSN model structure over a wide range of environmental and land use gradients (Figures 4.5 and 4.6); the Nash-Sutcliffe model efficiency coefficient was 0.90 (Figure 4.6). Model residuals were normally distributed, and did not appear to be homoscedastic (Figure 4.6) or spatially correlated (Figure 4.7). Since 93% of the observed data fell between the 90%

prediction intervals (Figure 4.5) and there was no pattern in the model residuals, we can assume that the likelihood assumptions were appropriate.

### Parameter Estimates

The parameter distributions produced by the MCMC sampling algorithm are illustrated in Figure 4.8. Parameter identifiability refers to the ability to constrain a parameter by a set of data and identify maximum likelihood values of the parameters [Luo *et al.*, 2009]. Parameters for the BiSN model parameters varied in their identifiability.  $b_w$ , the wastewater parameter (Figure 4.8B), and  $b_{\alpha}$ , the travel  $\alpha$  parameter (Figure 4.8E), were most identifiable; their posterior distributions were constrained by the observed data and show a clear peak in their distributions. The wastewater posterior distribution peaked at approximately  $10 \text{ kg ha}^{-1}\text{yr}^{-1}$ , while the travel  $\alpha$  was most likely between 0 and  $0.4 \text{ kg ha}^{-1}\text{yr}^{-1}$ .  $b_{SSR}$ , the soil storage release parameter (Figure 4.8D), and  $b_r$ , the riparian buffer parameter (Figure 4.8G), had regions of their parameter space that were more likely than others. Soil storage release was most likely to be at the lower end of the prior distribution, between  $100$  and  $500 \text{ kg ha}^{-1}\text{yr}^{-1}$  (Figure 4.8D) for grid cells with geology more prone to weather N; however, most of the watershed consisted of geology less prone to weather N, which corresponded to SSR export values of  $0.1 * \text{SSR}$  or between  $10$  and  $50 \text{ kg ha}^{-1}\text{yr}^{-1}$ . These large export values suggest that soil storage release of  $\text{NO}_3^-$  was a significant source of watershed  $\text{NO}_3^-$ . Riparian buffer was most likely greater than zero, which indicated that the riparian buffer was a net sink for of watershed  $\text{NO}_3^-$  (Equation 4.1).

The posterior distributions of  $b_v$ , the vegetation parameter (Figure 4.8A),  $b_s$ , the septic parameter (Figure 4.8C), and  $b_{ad}$ , the wet deposition parameter (Figure 4.8F), were not well constrained by the observed data, meaning their posterior distributions were relatively flat across the entire prior distribution. A flat/uniform posterior distribution signifies that any value between the upper and lower bound of the prior distribution has an equal probability of occurrence. Even though streamwater  $\text{NO}_3^-$  export was less sensitive to N inputs from vegetation, septic, or wet deposition, there were a few general observations that could be made about their posterior distributions: 1) vegetation was most likely an N sink, 2) septic export value had the highest probability of being close to  $500 \text{ kg ha}^{-1}\text{yr}^{-1}$ , and 3) wet deposition concentration was most likely between  $1.0$  and  $1.2 \text{ mg L}^{-1}$ .

The parameter values that produced the maximum likelihood and minimum variance are presented with their 90 percent confidence intervals in Table 4.2. The maximum likelihood parameter values assessed the capability of BiSN to estimate observed streamwater  $\text{NO}_3^-$  export (Figure 4.4A.) and were employed to calculate N loading, retention, and export by subwatershed. The maximum likelihood estimates of the parameters indicated that loading from septic and soil storage were highest at  $336.5$  and  $297 \text{ kg ha}^{-1}\text{yr}^{-1}$ , respectively. Soil storage release of  $\text{NO}_3^-$  from areas consisting of geology with high potential to weather  $\text{NO}_3^-$  was  $297 \text{ kg ha}^{-1}\text{yr}^{-1}$ , while soil storage release of  $\text{NO}_3^-$  from areas consisting of geology with low potential to weather  $\text{NO}_3^-$  was a  $29.7 \text{ kg ha}^{-1}\text{yr}^{-1}$  ( $0.1 * \text{SSR}$ ). Although their export parameter values are quite similar, N loading from septic effluent and soil storage release are quite different and have

ramifications for streamwater  $\text{NO}_3^-$  export. Septic systems export effluent to a localized area, but the actual loading value appears smaller because it is normalized across a hectare. Localized highly concentrated septic loading has the potential to saturate the immediate disposal area and be quickly transported to streams. On the other hand, inorganic N released from soil storage is evenly dispersed across a hectare. Consequently, there is more opportunity for plant and microbial immobilization of  $\text{NO}_3^-$  leading to less  $\text{NO}_3^-$  transported to streams.

Vegetated land exported the least amount of N at  $2.73 \text{ kg ha}^{-1}\text{yr}^{-1}$  (Table 4.2); however, this value is highly uncertain. Based on the 90% confidence intervals, vegetation could be a net sink or source of N. The maximum likelihood estimate for wet deposition inorganic N concentration was  $1.15 \text{ mg L}^{-1}$ , with an upper and lower 90% confidence limit of 0.5 and  $1.34 \text{ mg L}^{-1}$ . The riparian buffer was estimated to be a net sink of  $\text{NO}_3^-$ , removing  $270 \text{ kg ha}^{-1}\text{yr}^{-1}$ , which was towards the upper end of the confidence interval [ $4 \text{ kg ha}^{-1}\text{yr}^{-1}$  to  $286 \text{ kg ha}^{-1}\text{yr}^{-1}$ ]. The power law shape parameter,  $\alpha$ , was estimated to be 0.619, while the power law scale parameter,  $\beta$ , was fixed at 0.035.

#### Drivers of the Spatial Heterogeneity of Streamwater $\text{NO}_3^-$ Export

The spatial network structure of BiSN allows for exploration of N loading, export and retention patterns at the watershed scale.  $\text{NO}_3^-$  contribution from each source for each subwatershed was calculated by multiplying the maximum likelihood parameter estimates by the source area and then dividing by the total subwatershed area (Table 4.3). Total N loading is presented in Figures 4.9A and 4.9C and Table 4.3, while  $\text{NO}_3^-$

exported from the uplands (i.e. N loading decayed by relative travel time) is presented in Figures 4.9B and 4.9D and Table 4.3. Soil storage release of  $\text{NO}_3^-$ , which is the release of  $\text{NO}_3^-$  in storage that has accrued from historic N loading (e.g. atmospheric deposition, wastewater), plant and microbial immobilization, and soil adsorption, dominated N loading across the watershed (Figure 4.9A). Excluding soil storage release of  $\text{NO}_3^-$  to illuminate other source contributions, the relative N loading across the watershed was very similar with the exception of a high septic load in the upper Middle Fork (MFHW1) (Figure 4.9C). Very little  $\text{NO}_3^-$  was exported from the uplands except for in the mainstem West Fork, where wastewater contributions to  $\text{NO}_3^-$  export were high (Figure 4.9D, Table 4.4). Although the wastewater load was relatively small compared to other sources, it had a disproportionately greater contribution to upland  $\text{NO}_3^-$  export (Figure 4.9D).

Watershed N retention was divided into its three main components (uplands, riparian, and instream) and depicted in Figure 4.10 and Table 4.4. The majority of  $\text{NO}_3^-$  (98-99 %) was retained in the uplands as either a function of biological uptake or a lack of physical transport (i.e. hydrologic connectivity) between source areas and the stream (Figure 4.10A, Table 4.4). Instream  $\text{NO}_3^-$  removal was substantially greater than riparian  $\text{NO}_3^-$  removal in the South Fork, the lower Middle Fork, and the West Fork (Figure 4.10B). In headwaters of the South Fork, the Middle Fork and the North Fork, there were differences in the relative amounts of riparian and instream  $\text{NO}_3^-$  removal. In the headwaters of the South Fork watershed, instream processes generally immobilized more  $\text{NO}_3^-$  than the riparian area. Conversely, in the Middle Fork and North Fork the riparian area generally immobilized more  $\text{NO}_3^-$  than instream processes. In addition, the

magnitude of riparian and instream retention was significantly higher in the South Fork than the Middle and North Forks. Presumably, this was a result of higher  $\text{NO}_3^-$  loading to the riparian area occurring through most of the South Fork watershed (Figure 4.9B).

## Discussion

### Model Performance and Model Uncertainty

BiSN integrated stream chemistry from spatial sampling and  $\text{NO}_3^-$  tracer additions, terrain and land use analysis in a Bayesian framework to estimate watershed N loading,  $\text{NO}_3^-$  export and retention. As a relatively simple model with the goal of minimizing model parameters and predictive uncertainty, BiSN's minimal data requirements included: observed streamwater  $\text{NO}_3^-$  concentrations, a DEM, information on wastewater sources (i.e. septic location and wastewater irrigation location and load) and maps of land use/cover and geology.

Despite model simplicity (7 calibrated parameters), BiSN fit the observed streamwater  $\text{NO}_3^-$  data well ; the Nash Sutcliffe model efficiency coefficient was 0.90 (Figure 4.6) and 93% of the observed data fell between the 90% prediction intervals (Figure 4.5). Although the prediction intervals, which include uncertainties in parameter values and model residuals, were fairly wide, they did capture the general patterns of streamwater  $\text{NO}_3^-$  export of streams ranging from pristine first-order streams draining high-elevation alpine-subalpine watersheds (Beehive) to a fourth-order alluvial bottom stream draining substantial human development (West Fork).

Analysis of predictive uncertainty, which incorporated parameter uncertainty (Figure 4.6), is a real advancement in our analysis approach compared to other export coefficient modeling approaches. In BiSN, parameter uncertainty implied that the exact allocation of each  $\text{NO}_3^-$  source/sink is unknown. The degree of uncertainty for each parameter was reflected in the full range and shape of the parameter posterior distributions. The majority studies applying export coefficient models have judged model performance solely by stating some goodness of fit measure that compares observed and predicted observations (i.e.  $R^2$ , Nash-Sutcliffe, percent error etc.) [Worrall and Burt, 1999; 2001, Johnes, 1996; Whitehead et al., 2002]. Some studies have attempted to account for uncertainty in export coefficient parameters by surveying the full range of export coefficient values observed across a range of watersheds [Reckhow et al., 1980; Griffin, 1995; McFarland and Hauck, 2001; Wickham and Wade, 2002; Endreny and Wood, 2003]; however, this representation reflects the variability in export coefficients not their uncertainty [Khadam and Kaluarachchi, 2006]. Other studies have recognized the high uncertainty inherent in export coefficients [Zobrist and Reichert, 2006; Khadam and Kaluarachchi, 2006]; however, these studies did not report how parameter uncertainty impacted model predictions of watershed nutrient export. Effects of parameter uncertainties on model performance can be substantial and should be evaluated to ensure the precision and reliability of the predicted results [Beck, 1987].

In addition to predictive uncertainty, other model diagnostics important to model evaluation include examination of model residuals. BiSN model residuals were normally distributed (Figure 4.6), homoschedastic (Figure 4.5) and did not appear to be spatially

correlated (Figure 4.7). Recent research has shown the existence of spatial dependency in water quality data [*Dent and Grimm, 1999; Peterson et al., 2006; Gardner and McGlynn, 2009*]. Spatial processes governing  $\text{NO}_3^-$  export were implicitly incorporated within the BiSN network structure: each reach had  $\text{NO}_3^-$  inputs from upstream reaches and  $\text{NO}_3^-$  outputs that influenced downstream reaches (Figure 4.3B). Instream processing further defined the spatial relationship between upstream and downstream reaches.

#### Drivers of the Spatial Heterogeneity of Streamwater $\text{NO}_3^-$ Export

BiSN's output provided insight into the main drivers of streamwater  $\text{NO}_3^-$  export in the West Fork watershed during the summer growing season. Specifically, the shape and range of the parameter posterior distributions reflect the relative influence of each parameter on streamwater  $\text{NO}_3^-$  export.

Model parameters had a wide range of influence on modeled streamwater  $\text{NO}_3^-$  export (Figure 4.8), as demonstrated by their posterior distributions. Modeled streamwater  $\text{NO}_3^-$  export was most sensitive to the wastewater and travel  $\alpha$  parameters. Wastewater loading occurs on the Big Sky Resort Golf Course, which drains into the lower Middle Fork, just before the confluence with the South Fork (Figure 4.1). Although the amount of N loading to the Big Sky Golf Course is relatively small (Figures 4.9A and 4.9C, Table 4.2), it had a disproportionately large impact on streamwater  $\text{NO}_3^-$  export (Figure 4.9B and 4.9D, Table 4.3). Golf course irrigation with treated wastewater occurs over a short time period (approximately May through October) onto an area with very short relative travel times to the stream. Consequently, there is limited potential for

biological immobilization of  $\text{NO}_3^-$  and the majority of N loading is readily transported through shallow groundwater to the lower Middle Fork.

The travel time parameter, travel  $\alpha$ , was strongly identifiable and had significant influence on modeled streamwater  $\text{NO}_3^-$  export. Travel  $\alpha$ , the power law distribution shape parameter, describes the rate at which N loading is immobilized as it moves through the landscape. Under most circumstances, N loading occurring “hydrologically close” to the stream (short relative travel times) should have greater impact on streamwater  $\text{NO}_3^-$  than N loading occurring “hydrologically farther away” (longer relative travel times). This is because of the increased time and distance for  $\text{NO}_3^-$  immobilization [Seitzinger *et al.*, 2002]. Other simple N export models have also found improved model performance by adding parameters that describe hydrologic transport times [Smith, 1997; Johnes and Heathwaite, 1997; Frateriggo and Downing, 2008; Gardner and McGlynn, 2009].

Although not as sensitive as the wastewater and travel time parameters, the soil storage release and riparian parameters did have regions of their modeled parameter space that were more likely than others (Figures 4.8D and 4.8G). Soil storage release of N was most probable between 100 and 500  $\text{kg ha}^{-1}\text{yr}^{-1}$ , as illustrated by the soil storage posterior distribution (Figure 4.8D). Therefore, soils in areas associated with mineralogy more prone to weather N exported between 100 and 500  $\text{kg ha}^{-1}\text{yr}^{-1}$ , while soil in areas associated with mineralogy less prone to weather N exported 10 to 50  $\text{kg ha}^{-1}\text{yr}^{-1}$  (0.1 \* SSR, see Section 3.2 for more details). Soil storage of N occurs from the buildup of N in soils from historic N loading (e.g. atmospheric deposition, wastewater), soil adsorption,

and plant and microbial immobilization. Soil storage has been estimated to be anywhere from 2000 kg ha<sup>-1</sup> in warm deserts to 20,000 kg ha<sup>-1</sup> in wet tropical systems [Post *et al.*, 1985]. SSR includes releases of N from soil storage through geologic N weathering, N fixation, mineralization, and dissolution.

Although N fixation and mineralization were not directly included as a parameter in BiSN, their contributions to watershed N were incorporated into the SSR parameter. Studies have shown that N fixation from terrestrial [Fahey *et al.*, 1985; Cleveland *et al.*, 1999; Vitousek *et al.*, 2002; Jacot *et al.*, 2009] and aquatic [Meyer *et al.*, 1981; Grimm and Petrone, 1997; Triska, 1984] ecosystems can be substantial sources of watershed N. In addition to N fixation, mineralization of organic matter can be a significant contributor to watershed N export [Bormann, 1977; Fisk and Schmidt, 1995; Brooks *et al.*, 1996]. Mineralization is the release of inorganic N from the microbial break down of organic matter. Research has shown watershed net mineralization rates to highly variable, from <1 to 37 kg ha<sup>-1</sup>yr<sup>-1</sup>, which is similar to the soil storage release of sites with low potential for geologic release of N. Mineralization rates can depend on soil temperature, soil moisture [Hong *et al.*, 2004; Miller *et al.*, 2009], soil C:N ratios [Janssen, 1996; Springob and Kirchmann, 2003], snowcover [Brooks *et al.*, 1996; Miller *et al.*, 2009], and vegetation and soil type [Hart and Firestone, 1991]. In addition to mineralization, soil disturbance from freeze thaw cycles can destroy fine roots and disturb microbiological communities decreasing N immobilization thereby releasing more inorganic N [Groffman *et al.*, 2001].

Similar to the soil storage release parameter, the riparian buffer posterior distribution illustrated a range of values that were more likely than others. The riparian buffer parameter was most likely greater than zero, meaning a net sink of watershed  $\text{NO}_3^-$  (Figure 4.8G, Equation 4.1). As the interface between the terrestrial and aquatic ecosystems, riparian ecosystems can be hot spots for  $\text{NO}_3^-$  immobilization. However the riparian buffer's ability to remove  $\text{NO}_3^-$  can be highly variable depending on 1) the proximity of the water table to the root zone, 2) the groundwater flow rate, 3) the width of the riparian zone, 4) temperature, and 5) the labile carbon supply for microbial denitrification [Burt *et al.*, 1999; Lowrance *et al.*, 1984; Hill, 1996; Maitre *et al.*, 2003; Dent *et al.*, 2007]. Conversely, riparian areas can also be significant sources of organic N [Schade *et al.*, 2002]. Therefore, at the watershed scale, in which many of these factors controlling the storage and release of N in the riparian area are highly variable, we might expect  $\text{NO}_3^-$  removal occurring in riparian buffers to be difficult to identify since BiSN generalizes riparian control of N through the terrain index, *RBI*.

The remaining model parameters (septic system, wet deposition, and vegetation) had modeled posterior distributions that were less identifiable than other parameters. These parameters may have been less identifiable because their informative priors were tightly bound by prior knowledge. The septic system posterior distribution illustrated septic system N loading was most likely to be between 275 and 1000  $\text{kg ha}^{-1}\text{yr}^{-1}$  (Figure 4.8C). Variability in septic system N loading is expected due to the seasonality of second home use and the variability in the number of people using each system.

Although septic effluent has high concentrations of inorganic N [EPA, 2002], septic systems contributed very little to upland  $\text{NO}_3^-$  across the West Fork watershed (Figures 4.9B and 4.9D). There are two plausible explanations for their limited impact on upland  $\text{NO}_3^-$  export: 1) the septic systems are relatively few and widely dispersed across the 212 km<sup>2</sup> West Fork watershed and the effluent is either diluted and/or readily immobilized before it reaches the stream, or 2) the septic systems have a limited or nonexistent hydrological connectivity to the stream. Previous research showed distinct seasonality in the influence of septic systems on streamwater  $\text{NO}_3^-$  concentrations in the West Fork watershed [Gardner and McGlynn, 2009]. During the growing season, septic system effluent may be quickly immobilized along hydrological pathways before it reaches the stream network. While in the dormant season, septic effluent may leach into shallow, cold soil that has little or no capacity to transform and assimilate nutrients or retain large inputs of subsurface water; N may then directly enter shallow groundwater and be readily transported to streams. Other research has shown that increased septic system distance from surface water could increase septic  $\text{NO}_3^-$  removal thus minimizing N enrichment from septic systems [Meile *et al.*, 2010]; however, septic  $\text{NO}_3^-$  removal can be limited if carbon is limiting microbial denitrification [Colman *et al.*, 2004]. In addition to biological uptake diminishing septic influence on streamwater, it is possible there was limited or nonexistent hydrologic connectivity between septic systems and the streams. Recent work in the northern Rocky Mountains has shown that hydrologic connectivity between most uplands and the stream exists for only small fraction of the

year during snowmelt [Jencso, 2009]. Without hydrologic transport, septic effluent would remain in upland soils and not be delivered to the stream.

The wet deposition parameter had a relatively informative prior distribution and its posterior distribution was slightly more constrained than the septic posterior distribution by observed data. The posterior distribution suggested that wet deposition inorganic N concentration was most probable between 1.0 and 1.2 mg L<sup>-1</sup>. The only modestly improved identifiability of the wet deposition parameter could be because: 1) similar to septic effluent, during the growing season at these low concentrations, wet deposition onto an N limited environment is either readily immobilized and/or lacking a transport mechanism to the stream, or 2) BiSN did not accurately characterize the high spatial and seasonal variability of inorganic N deposition in mountainous regions due to varying slope, aspect, elevation, and N sources [Nanus, 2003] (Appendix A).

The vegetation posterior distribution was also relatively flat across the prior distribution (Figure 4.8A). Though most likely a sink of watershed N, the posterior distribution indicated that the vegetation parameter could have been modeled as a sink or source of watershed N, as supported by past studies. This is not surprising as studies have shown vegetation as both an N sink and N source at the watershed scale. Forest disturbance by fire or clear-cutting has been shown to increase streamwater NO<sub>3</sub><sup>-</sup> immediately following the disturbance followed by decreasing NO<sub>3</sub><sup>-</sup> as new growth takes over the burned/cut area [Bormann *et al.*, 1968; Vitousek, 1979]. Residential grass areas could be a source of N by fertilizer addition. Some types of vegetation are N fixers and can be a significant source of ecosystem NO<sub>3</sub><sup>-</sup> [Postage, 1998]. Even within non-N

fixers, there is variability in the amount of  $\text{NO}_3^-$  exported from different types of vegetation [Lovett *et al.*, 2002]. Aside from vegetation type, vegetation age can greatly influence streamwater  $\text{NO}_3^-$  export. Early to mid-successional N limited forests retain N strongly, while older stands are less retentive of N most likely because of lower productivity rates [Vitousek and Reiners, 1975; Goodale and Aber, 2001].

As demonstrated above, modeled streamwater  $\text{NO}_3^-$  export was highly sensitive to some model parameters (e.g. wastewater, travel  $\alpha$ ) and less sensitive to others (e.g. vegetation, wet deposition). We believe that there is great value in exploring model parameter sensitivities to understand system behavior. Although the parameter sensitivities and even parameters may be completely different in other locations, the methods and general model structure presented here can transfer to other watersheds to explore the primary controls of watershed  $\text{NO}_3^-$  export. For example, in the West Fork watershed, there is no agricultural land, however in other watersheds, agriculture may be the major control of streamwater  $\text{NO}_3^-$  [Omernik, 1981] and can be added as a parameter to BiSN. Or, the travel time parameter may not be influential in a watershed in which hydrologic flowpaths are not well represented by topography (e.g. watershed with poorly drained soils, confined aquifers or groundwater in fractured bedrock). In addition to different parameters, parameter sensitivities could be different in another watershed. For example, in a watershed that is experiencing a higher level of N enrichment than the West Fork watershed, there could be increased model sensitivity to N loading from the septic or wet deposition parameter [Aber *et al.*, 1998].

Spatial Distribution of  $\text{NO}_3^-$  Loading,  
Retention and Export Across Land Use/  
Land Cover and Landscape Positions.

Maximum likelihood estimates were applied to calculate watershed N loading, export, and retention across a range of land use/ land cover and landscape positions. Spatial patterns in N loading (Figure 4.9A, 4.8C, and Table 4.3), upland export (Figures 4.9B, 4.9D and Table 4.4), and retention (Figures 4.10A, 4.10B, and Table 4.4) provided insight into the relative importance of hydrologic and biological processes influencing streamwater  $\text{NO}_3^-$  export in the West Fork watershed.

For most subwatersheds in West Fork watershed, soil storage release was the main source of  $\text{NO}_3^-$  exported from the uplands (Figure 4.9B). Upland export was greatest in South Fork and West Fork, though the  $\text{NO}_3^-$  originated from a different source. The relatively high levels of  $\text{NO}_3^-$  export in the South Fork were geologic in origin, which is incorporated into the soil storage release parameter; a significant portion of the South Fork watershed is comprised of surface minerals that exude elevated levels of  $\text{NO}_3^-$  compared to other minerals found throughout the West Fork watershed [Ackerman *et al.*, in prep]. On the other hand, upland export from the lower Middle Fork was relatively high as a result of wastewater inputs (Figure 4.9D and Table 4.4). After the confluence with the South Fork, upland export from the West Fork was an equal mixture of soil storage release and wastewater  $\text{NO}_3^-$ .

As demonstrated by relatively high wastewater N export from the West Fork, the spatial location and pattern of N loading may have ramifications on the magnitude and patterns of streamwater  $\text{NO}_3^-$  export. For example, the spatial pattern of anthropogenic N

loading distributed by septic and wastewater effluent is quite different: N input from septic systems is sparsely distributed across the watershed, while N input from wastewater is localized to an area with very short transit times to the stream. Even though the septic effluent export is approximately an order of magnitude higher than the wastewater effluent export (Table 4.2), longer travel times may allow the majority of septic  $\text{NO}_3^-$  to be immobilized along hydrological flowpaths to the stream. Conversely, wastewater  $\text{NO}_3^-$  applied to a large contiguous area with short times to the stream may surpass the ecosystem's ability to cycle N. Consequently, much of the wastewater  $\text{NO}_3^-$  is readily transported to the stream and manifests itself in higher levels of streamwater  $\text{NO}_3^-$  export (Figure 4.9D).

This retention of N loading occurring in the uplands from either biological immobilization or a lack of hydrologic connectivity is by far the largest  $\text{NO}_3^-$  sink in the West Fork watershed (Figure 4.10A, Table 4.4) removing 98-99 percent of N loading across the watershed. This high retention rate suggests that the West Fork watershed is highly N limited in the summer growing season. We recognize that the retention rate may be overestimated on an annual basis because retention rates were estimated from summer synoptic chemistry and instream  $\text{NO}_3^-$  uptake data when biological activity was at a peak and the extent of the uplands hydrologically connected to the stream was waning. There is an abundance of evidence that N is the most limiting nutrient for growth in most terrestrial systems [Vitousek and Howarth, 1995]. N inputs to an N limited system are quickly immobilized by biota [Gundersen *et al.*, 1995]. The retention rate in the West Fork seems reasonable for a highly N limited system. For example, in

other N enriched watersheds in the eastern United States and Northern Europe watershed retention rates have been shown to vary between of 95-100% of total N inputs [Gundersen *et al.*, 1995; Magill *et al.*, 1996].

Aside from biological immobilization,  $\text{NO}_3^-$  may be immobilized from a lack of hydrological connectivity between the uplands and the stream as a hydrologic connection between the uplands and the stream most likely exists for only small fraction of the year during snowmelt or large rain events [McGlynn and McDonnell, 2003; Jencso *et al.*, 2009]. This seasonal timing of hydrologic connectivity may drive the seasonal patterns of nutrient export exhibited in the West Fork watershed [Pacific *et al.*, 2010; Jencso *et al.*, 2010; Gardner and McGlynn, in prep.]. In other systems, in which the uplands are hydrologically connected for a longer periods during the year, N loading may have more severe impacts on streamwater quality [Ocampo *et al.*, 2006].

Masking upland retention from the retention calculation provided insight into the relative importance of  $\text{NO}_3^-$  removal in stream and riparian areas (Figure 4.10B and Table 4.4). Across the West Fork, the variation in the land use/land cover and watershed characteristics most likely drove the spatial heterogeneity present in both the magnitude and relative importance of riparian and instream  $\text{NO}_3^-$  removal. Additional characteristics which are highly variable across the West Fork watershed that could influence riparian  $\text{NO}_3^-$  removal and are not included in BiSN are: 1) the proximity of the water table to the root zone, 2) the groundwater flow rate, 3) riparian vegetation, 4) temperature, and 5) the labile carbon supply for microbial denitrification. Characteristics which are highly variable across the West Fork watershed that would influence instream

$\text{NO}_3^-$  removal include but are not limited to: 1)  $\text{NO}_3^-$  concentration, 2) sunlight, 3) benthic biomass, 4) stream metabolic rates, 5) temperature, and 6) hyporheic and groundwater exchange. All of the factors described above which control instream and riparian uptake are highly variable across the land use/ land cover and landscape position in the West Fork watershed and therefore, may be responsible for some of the spatial heterogeneity in riparian and instream removal of watershed N.

Despite this spatial heterogeneity, patterns in riparian and instream N removal are apparent (Figure 4.10B and Table 4.4). In the headwaters of the South Fork and West Fork, there were differences in relative N removal. In the South Fork headwaters, instream processes generally immobilized more  $\text{NO}_3^-$  than the riparian areas, while in the headwaters of the West Fork (Middle Fork, Beehive, and North Fork) more  $\text{NO}_3^-$  was removed in the riparian areas than in instream processes. There are two plausible explanations for this phenomenon. First the South Fork generally has incised stream channels and limited riparian areas thus decreasing potential for biological removal [McGlynn and Seibert, 2003; Vidon and Hill, 2006; Jencso et al., 2010]. Secondly, the riparian and instream areas located in the headwaters of the South Fork received considerably greater N loads than the headwaters of the West Fork, primarily from mineral weathering [Ackerman et al, in prep.]. Research has shown the increasing role of instream removal with increasing N inputs [Mulholland et al., 2008; Covino et al., In press A, B].

Another interesting spatial pattern across the West Fork watershed was that the relative importance of instream  $\text{NO}_3^-$  removal increased in a downstream direction in the

stream network. In some headwater streams, instream retention has been shown to play less of a role in overall watershed  $\text{NO}_3^-$  retention than higher order streams because of low N inputs. In these systems, as N loading increased downstream higher-order streams have the opportunity to remove more  $\text{NO}_3^-$  and thus instream N removal appears to play a larger role in overall watershed N retention [Mulholland *et al.*, 2008; Covino *et al.*, in press A, B; McNamara *et al.*, in prep.].

Finally, there are a few stream reaches with a noticeably high percentage of N export (Table 4.4). Streamwater N export from MFHW1 was exceptionally large: 64 percent of  $\text{NO}_3^-$  transported from the uplands was exported from the stream. This site had the highest density of septic loading ( $\text{kg ha}^{-1}\text{yr}^{-1}$ ) that may be overwhelming the watershed's ability to retain  $\text{NO}_3^-$ . Confounding the problem, this site drains Lone Mountain, which is an alpine environment above treeline with steep slopes, consisting mainly of talus and scree. Inorganic N enters an area with shallow soils, steep talus/scree slopes, and little riparian area with limited potential for  $\text{NO}_3^-$  processing and is readily transported to the stream. Increased  $\text{NO}_3^-$  export from talus springs has been noted in other research [Campbell *et al.*, 2002].

Downstream, from MFHW1,  $\text{NO}_3^-$  export gradually decreased until the Middle Fork joins the North Fork (Figure 4.1). There is a spike in streamwater  $\text{NO}_3^-$  export at LMF (Table 4.4). As previously discussed, N loading at this site is in excess of N retention as a result of localized wastewater loading. As the system is overloaded with N, it is no longer able to immobilize subsequent inputs of N. Consequently  $\text{NO}_3^-$  bypasses through the uplands and the riparian buffer, and is readily exported downstream.

## Conclusion

This research introduced BiSN, a modified nitrogen export coefficient model, to identify primary drivers in watershed  $\text{NO}_3^-$  export and to explore the spatial patterns of N loading, retention, and export across a developing mountain watershed. Export coefficient models can be an attractive modeling approach due to limited data requirements and applicability to land use and management practices.

We used Bayesian MCMC methods to estimate model parameters and found them extremely useful in assessing model and parameter uncertainty and advancing understanding of the primary processes governing watershed  $\text{NO}_3^-$  export. Modeled parameter posterior distributions identified wastewater loading and relative travel time, which represents the hydrologic transport time between N inputs and the stream channel, as being the most important controls of watershed  $\text{NO}_3^-$  export. Our results highlight the importance of: 1) the spatial location of N loading, and 2) localized N loading versus spatially distributed N loading. This implies that not all anthropogenic N loading equally impacts stream  $\text{NO}_3^-$  concentrations and export. Localized N loading occurring in watershed areas with fast travel times to the stream may have disproportionate effects on water quality. Under these conditions, the systems ability to retain  $\text{NO}_3^-$  is overwhelmed, resulting in excess  $\text{NO}_3^-$  readily exported from the system.

Spatial patterns in watershed retention processes revealed that most watershed  $\text{NO}_3^-$  removal occurred in the terrestrial ecosystem either by biological uptake or from a lack of physical transport (i.e. hydrologic connectivity) between the uplands and the

stream channel. Excluding upland retention, our results show the increasing role of instream retention with increasing N loading going downstream in the stream network. The modeling approach used here can be adapted for other watersheds to increase understanding of the primary drivers of watershed  $\text{NO}_3^-$  export and to determine the spatial patterns of watershed N loading, retention and export with a goal of minimizing N loading impacts on surface waters.

#### Acknowledgements

Financial support was provided by the Environmental Protections Agency (EPA) STAR Grant #R832449, EPA 319 funds administered by the Montana Department of Environmental Quality, the U.S. National Science Foundation BCS 0518429, and the USGS 104(b) Grant Program administered by the Montana Water Center. K.K.G. acknowledges support from the EPA STAR Fellowship and NSF GK-12 Fellowship programs.

References Cited

- Aber, J.D., K.J. Nadelhoffer, P. Steudler, and J.M. Melillo (1989). Nitrogen saturation in northern forest ecosystems: excess nitrogen from fossil fuel combustion may stress the biosphere. *BioScience*, 39(6): 378-385.
- Ackerman, G., B.L. McGlynn, S. Montross, and K. Gardner (In prep.) Rock nitrogen weathering relationships to mountain streamwater N variability.
- Alexander, R.B., R.A. Smith, G.E. Schwarz, E.W. Boyer, J.V. Nolan, and J.W. Brakebill (2008). Differences in Phosphorus and Nitrogen Delivery to the Gulf of Mexico from the Mississippi River Basin. *Environmental Science & Technology*, 42: 822-830.
- Allen, J.D. (1995). *Stream Ecology, Structure and function of running waters*. Kluwer Academic Publishers, Dordrecht, The Netherlands.
- Alt, D., and D.W. Hyndman (1986). *Roadside geology of Montana*. Mountain Press Publishing Company. Missoula MT.
- Baron, J.S., D.S. Ojima, and E.A. Holland. (1994). Analysis of nitrogen saturation potential in Rocky-Mountain tundra and forest – implications for aquatic system. *Biogeochemistry*, 27 (10): 61-82.
- Bates, B.C., and E.P. Campbell (2001). A Markov chain Monte Carlo scheme for parameter estimation and inference in conceptual rainfall-runoff modeling, *Water Resources Research*, 37(4), 937-947.
- Beaulac, M.N. and K.M. Reckhow (1982). An examination of land use-nutrient export relationships. *Water Resources Bulletin*, 18: 1013-1024.
- Beck, M.B. (1987). Water Quality Modeling: A Review of the Analysis of Uncertainty. *Water Resources Research*, 23(8): 1393-1442.
- Beven, K. (2006). A manifesto for the equifinality thesis. *Journal of Hydrology*, 320, 18 – 36.
- Beven, K.J. (2001). *Rainfall-Runoff Modelling, The Primer*. John Wiley & Sons Ltd., West Sussex, England.
- Beven, K. (1993). Prophecy, reality and uncertainty in distributed hydrological modeling, *Advances in Water Resources*, 16, 41 – 51, doi:10.1016/0309-708(93)90028-E.

- Beven, K.J. and M.J. Kirkby (1979). A physically-based variable contributing area model of basin hydrology. *Hydrological Sciences Bulletin*, 24(1): 43-69.
- Bormann, F.H., G.E. Likens, J.M. Melillo (1977). Nitrogen Budget for an aggrading northern hardwood forest ecosystem. *Science*, 196 (196): 981-983.
- Bormann, F.H., G.E. Likens, D.W. Fisher, and R.S. Pierce (1968). Nutrient Loss Accelerated by Clear-Cutting of a Forest Ecosystem. *Science*, 159 (3817): 882-884.
- Brooks, P.D., M.W. Williams, S.K. Schmidt (1996). Microbial Activity under Alpine Snowpacks, Niwot Ridge, Colorado. *Biogeochemistry*, 32(2): 93-113.
- Brunet, R.C. and L.J. Garcia-Gil (1996). Sulfide-induced dissimilatory nitrate reduction to ammonia in anaerobic freshwater sediments, *FEMS Microbiology Ecology*, 21: 131-138.
- Burns, D.A. (2003). Atmospheric nitrogen deposition in the Rocky Mountains of Colorado and southern Wyoming -- A review and new analysis of past study results. *Atmospheric Environment*, 37 (7): 921-932.
- Burt, T.P., L.S. Matchett, K.W.T. Goulding, C.P. Webster, and N.E. Haycock (1999). Denitrification in riparian buffer zones: the role of floodplain hydrology. *Hydrological Processes*, 13: 1451-1463.
- Campbell, D.H. Kendall, C., Chang C.C.Y., Silva, S.R., and K.A. Tonnessen (2002). Pathways for nitrate release from an alpine watershed: determination using  $\delta^{15}\text{N}$  and  $\delta^{18}\text{O}$ . *Water Resources Research*, 38: 1052-1071.
- Campos, N., R., Lawrence, B.L. McGlynn, and K.K. Gardner (In press). Effects of Lidar-QuickBird fusion on object oriented classification of mountain resort development, *Journal of Applied Remote Sensing*.
- Carle, M.V., P.N. Halpin, and C.A. Stow (2005). Patterns of watershed urbanization and impacts on water quality. *Journal of the American Water Resources Association*, 41(3): 693-708.
- Chang, C.C.Y., C. Kendall, S.R. Silva, W.A. Battaglin, and D.H. Campbell. (2002). Nitrate stable isotopes: tools for determining nitrate sources among different land uses in the Mississippi River Basin. *Groundwater*, 59: 1874-1885.
- Cleveland, C.C., A.R. Townsend, D.S. Schimel, H. Fisher, R.W. Howarth, L.O. Hedin, S.S. Perakis, E.F. Latty, J.C. Von Fischer, A. Elseroad, and M.F. Wasson (1999).

Global patterns of terrestrial biological nitrogen (N<sub>2</sub>) fixation in natural ecosystems. *Global Biogeochemical Cycles*, 13 (2): 623-645.

Colman, J.A., J.P. Masterson, W.J. Pabich and D.A. Walter (2004). Effects of aquifer travel time on nitrogen transport to a coastal embayment. *Groundwater*, 42(7): 1069-1078.

Covino, T.P., B.L. McGlynn, R.A. McNamara (In press A). Quantifying stream nutrient uptake kinetics from ambient to saturation: Tracer Additions for Spiraling Curve Characterization. *Limnology and Oceanography: Methods*.

Covino, T.P., B.L. McGlynn, and M.A. Baker. (In press B). Separating physical and biological nutrient retention and quantifying uptake kinetics from ambient to saturation in successive mountain stream reaches. *Journal of Geophysical Research - Biogeosciences*.

Davidson, E.A., J. Chorover, and D.B. Dail (2003). A mechanism of abiotic immobilization of nitrate in forest ecosystems: the ferrous wheel hypothesis. *Global Change Biology*, 9: 228-236.

Dent, C.L., N.B Grimm, E. Marti, J.W. Edmonds, J.C. Henry, and J.R. Welter (2007). Variability in surface-subsurface hydrologic interactions and implications for nutrient retention in an arid-land stream. *Journal of Geophysical Research*, 112, G04004, doi:10.1029/2007JG000467.

Dent, C.L. and N.B. Grimm (1999). Spatial heterogeneity of stream water nutrient concentrations over successional time. *Ecology*, 80: 2283-2298.

Dietz, M/E., and J.C. Clausen (2008). Stormwater runoff and export changes with development in a traditional and low impact subdivision. *Journal of Environmental Management*, 87: 560-566.

Dunne, T. (1978). *Field studies of hillslope processes*. In: *Hillslope Hydrology*, Kirkby MJ (ed.). John Wiley and Sons, Ltd: New York: 227– 289.

Earl, S. R., H. M. Valett, and J. R. Webster (2006). Nitrogen saturation in streams. *Ecology*, 87(12): 3140-3151.

Edreny T.A., and E.F. Wood (2003). Watershed weighting of export coefficients to map critical phosphorous loading areas. *Journal of the American Water Resources Association*, 39(1): 165-181.

Edwards, R. (2007). Personal Communications. Big Sky Water and Sewer District Operations General Manager Big Sky Water and Sewer District.

- Fahey, T.J., J.B. Yavitt, J.A. Pearson, and D.H. Knight (1985). The nitrogen cycle in lodgepole pine forests, southeastern Wyoming. *Biogeochemistry*, 1(3): 257-275.
- Fraterrigo, J.M., and J.A. Downing (2008). The influence of land use on lake nutrients varies with watershed transport capacity. *Ecosystems*, 11: 1021-1034.
- Gardner, K.K., B.L. McGlynn (In Review). Seasonal and spatial variability of nitrogen saturation dynamics across environmental and land use gradients in a developing mountain watershed.
- Gardner, K.K. and B.L. McGlynn (2009). Seasonality in spatial variability and influence of land use/land cover and watershed characteristics on streamwater nitrate concentrations in the Northern Rocky Mountains. *Water Resources Research*, 45, W08411, doi:10.1029/2008WR007029.
- Gelman, A., J.B. Carlin, H.S. Stern, and D.B. Rubin (2004). *Bayesian Data Analysis*. 2<sup>nd</sup> ed., Chapman and Hall, New York.
- Gelman, A., and D.B. Rubin (1992). Inference from iterative simulation using multiple sequences. *Statistical Science*, 7:457-511.
- Goodale, C.L and J.D. Aber (2001). The long-term effects of land-use history on nitrogen cycling in northern hardwood forests. *Ecological Applications*, 11(1): 253-267.
- Grabs, T., K.J. Jencso, B.L. McGlynn, J. Seibert (2010). Calculating terrain indices along streams - a new method for separating stream sides. *Water Resources Research*.
- Griffin, C.B. (1995). Uncertainty analysis of BMP effectiveness for controlling nitrogen from urban nonpoint sources. *Water Resources Bulletin*, 31(6), 1041-1050.
- Grimm, N.B. and K.C. Petrone (1997). Nitrogen fixation in a desert stream ecosystem. *Biogeochemistry*, 37: 33-61.
- Groffman, P.M., C.T. Driscoll, T.J. Fahey, J.P. Hardy, R.D. Fitzhugh and G.L. Tierney (2001). Effects of mild winter freezing on soil nitrogen and carbon dynamics in a northern hardwood forest. *Biogeochemistry*, 56: 191-213.
- Gundersen, P., and L. Rasmussen (1995). Nitrogen mobility in a nitrogen limited forest at Klosterhede, Denmark, examined by  $\text{NH}_4\text{NO}_3$  addition. *Forest Ecology and Management*, 71: 75-58.
- Haario, H., E. Saksman, and J. Tamminen (2001). An adaptive Metropolis algorithm. *Bernoulli*, 7(2), 223-242.

- Hadas, A., M. Sofer, J.A. E. Molina, P. Barak, and C.E. Clapp (1992). Assimilation of nitrogen by soil microbial population:  $\text{NH}_4$  versus organic N. *Soil Biology & Biochemistry*, 24: 137-143.
- Hanrahan, G., M. Gledhill, W.A. House, and P.J. Worsfold (2001). P loading in the Frome catchment, UK: Seasonal refinement of the coefficient modeling approach. *Journal of Environmental Quality*, 30(5): 1738-1746.
- Hart, S.C. and M.K. Firestone (1991). Forest-Mineral soil interactions in the internal nitrogen cycle of an old-growth Forest. *Biogeochemistry*, 12(2): 103-127.
- Hassan, A.E., H.M. Bekhit, and J.B. Chapman (2009). Using Markov Chain Monte Carlo to quantify parameter uncertainty and its effect on predictions of a groundwater flow model. *Environmental Modelling & Software*, 24: 749-763.
- Hession, W.C. and D.E. Storm (2000). Watershed-level uncertainties: Implications for phosphorus management and eutrophication. *Journal of Environmental Quality*, 29(4): 1172-1179.
- Hill, A. R. (1996). Nitrate removal in stream riparian zones. *Journal of Environmental Quality*, 25, 743-755.
- Holloway, J.M., R.A. Dahlgren, and W.H. Casey (2001). Nitrogen release from rock and soil under simulated field conditions. *Chemical Geology*, 174, 403-413.
- Holloway, J.M., R.A. Dahlgren, B. Hansen, and W.H. Casey (1998). Contribution of bedrock nitrogen to high nitrate concentrations in streamwater. *Nature*, 395, 785-788.
- Hong, B., D.P. Saney, P.B. Woodbury, and D.A. Weinstein (2004). Long-term nitrate export pattern from Hubbard Brook 6 watershed driven by climatic variation. *Water, Air, and Soil Pollution*, 160: 293-326.
- Jacot, K.A., A. Luscher, J. Nosberger, and U.A. Hartwig (2000). The relative contribution of symbiotic  $\text{N}_2$  fixation and other nitrogen sources to grassland ecosystems along an altitudinal gradient in the Alps. *Plant and Soil*, 225: 201-211.
- Janssen, B.H. 1996. Nitrogen mineralization in relation to C:N ratio and decomposability of organic materials. *Plant and Soil*, 181: 39-45.
- Jencso, K.J., B.L. McGlynn, M.N. Gooseff, K.E. Bencala. and S.M. Wondzell (2010). Hillslope hydrologic connectivity controls riparian groundwater turnover:

Implications of catchment structure for riparian buffering and stream water sources. *Water Resources Research*.

- Jencso, K. J., B. L. McGlynn, M. N. Gooseff, S. M. Wondzell, and K. E. Bencala (2009). Hydrologic connectivity between landscapes and streams: Transferring reach and plot scale understanding to the catchment scale, *Water Resources Research*, W04428, doi:10.1029/2008WR007225.
- Johnes P.J. (1996). Evaluation and management of the impact of land use change on the nitrogen and phosphorus load delivered to surface waters: the export coefficient modeling approach. *Journal of Hydrology*, 183: 323–349.
- Johnes, P.J and A.L Heathwaite (1996). Modeling the impact of land use change on water quality in agricultural catchments. *Hydrological Processes*, 11: 269-286.
- Kellog, K.S. and V.S. Williams (2005). *Geologic Map of the Ennis 30' X 60' Quadrangle, Madison and Gallatin counties, Montana and Park County, Wyoming*. Montana Bureau of Mines and Geology Open File No. 529.
- Khadam, I.M. and J.J. Kaluarachchi (2006). Water quality modeling under hydrologic variability and parameter uncertainty using erosion-scaled export coefficients, *Journal of Hydrology*, 330: 354-367.
- Likens, G.E., F.H. Bormann, N.M. Johnson, D.W. Fisher, and R.S. Pierce (1970). Effects of Forest Cutting and Herbicide Treatment on Nutrient Budgets in the Hubbard Brook Watershed-Ecosystem. *Ecological Monographs*, 40 (1): 23-47.
- Lovett, G.M., K.C. Weathers, and M.A. Arthur (2002). Control of nitrogen loss from forested watersheds by soil carbon:nitrogen ratio and tree species composition. *Ecosystems*, 5:712-718.
- Lowrance, R., R. Todd, J. Fail, Jr., O. Hendrickson, Jr., R. Leonard, and L Asmussen (1984). Riparian forests as nutrient filters in agricultural watersheds. *Bioscience*, 34: 374-377.
- Lunetta, R.S., R.G. Greene, and J.G. Lyon (2005). Modeling the distribution of diffuse nitrogen sources and sinks in the Neuse River Basin of North Carolina, USA. *Journal of the American Water Resources Association*, 41(5): 1129-1147.
- Luo, Y., E., Weng, X. Wu, C. Gao, Z. Zhou, and L. Zhang (2009). Parameter identifiability, constraint, and equifinality in data assimilation with ecosystem models. *Ecological Applications*, 19(3): 571-574.

- Magill, A.H., M.R. Downs, K.J. Nadelhoffer, R.A. Hallet and J.D. Aber (1996). Forest ecosystem response to four years of chronic nitrate and sulfate additions at Bear Brooks Watershed, Maine, USA. *Forest Ecology and Management*, 84: 29-37.
- Maitre, V., A. Cosandey, E. Desagher, and P. Parriaux (2003). Effectiveness of groundwater nitrate removal in a river riparian area: the importance of hydrogeological conditions. *Journal of Hydrology*, 278 (1-4): 76 – 93.
- Marshall, L., D. Nott, and A. Sharma (2004). A comparative study of Markov chain Monte Carlo methods for conceptual rainfall-runoff modeling. *Water Resources Research*, 40, W02501, doi:10.1029/2003WR002378.
- McFarland A.M.S and L.M. Hauck (2001). Determining nutrient export coefficients and source loading uncertainty using in-stream monitoring data. *Journal of the American Water Resources Association*, 37(1): 223-236.
- McGlynn, B.L. (2005). *The role of riparian zones in steep mountain watersheds*. in Global Change and Mountain Regions. “Advances in Global Change Research book series”, Martin Beniston (ed), Kluwer.
- McGlynn, B.L., and J.J. McDonnell (2003). Quantifying the relative contributions of riparian and hillslope zones to catchment runoff and composition. [Water Resources Research](#). Vol. 39, No. 11, 1310 10.1029/2003WR002091.
- McGlynn, B.L., and J. Seibert (2003). Distributed assessment of contributing area and riparian buffering along stream networks. *Water Resources Research*, 39(4), 1082, doi:10.1029/2002WR001521.
- McGuire, K. J., J. J. McDonnell, M. Weiler, C. Kendall, B. L. McGlynn, J. M. Welker, and J. Seibert (2005). The role of topography on catchment-scale water residence time. *Water Resources Research*, 41, W05002, doi:10.1029/2004WR003657.
- McNamara, R., B.L. McGlynn, T.C. Covino, K. Gardner (In preparation). The kinetics of instream N immobilization across space and time in a developing mountain watershed.
- McNamara, R.A. Stream nitrogen uptake dynamics from ambient to saturation across development gradients, stream network position, and seasons. Master Thesis, Montana State University, Bozeman, Montana.
- Meyer, J.L., M.J. Pal, and W.K. Taulbee (2005). Phosphorous nitrogen, and organic carbon flux in a headwater stream. *Achiv fur Hydrobiologie*, 91: 28-44.

- Miele, C., W.P. Porubsky, R.L. Walker, K. Payne (2010). Natural attenuation of nitrogen loading from septic effluents: spatial and environmental controls. *Water Research*, 44: 1399-1208.
- Miller, A.E., J.P. Schimel, J.O. Sickman, K. Skeen, T. Meixner, and J. M. Melack (2009). Seasonal variation in nitrogen uptake and turnover in two high-elevation soils: mineralization responses are site-dependent. *Biogeochemistry*, 93: 253-270.
- Nadelhoffer, K. J., M. R. Downs, and B. R. Fry (1999). Sinks for <sup>15</sup>N-enriched additions to an oak forest and a red pine plantation. *Ecological Applications* 9:72-86.
- Nanus, L., D.H. Campbell, G.P. Ingersoll, D.W. Clow, and M.A. Mast (2003). Atmospheric deposition maps for the Rocky Mountains. *Atmospheric Environment*, 37: 4881-492.
- National Atmospheric Deposition Program (NADP) (2010). <http://nadp.sws.uiuc.edu/>. NADP Program Office, Illinois State Water Survey, Champaign, IL.
- National Science Foundation (NSF) (1976). *Impacts of Large Recreational Development Upon Semi-Primitive Environments*. NSF RANN Program Final Report.
- Newson, M.D. (1997). *Land, Water and Development: Sustainable Management of River Basin Systems*. Routledge: London.
- Ocampo, C.J. M. Sivapalan, C. Oldham (2006). Hydrological connectivity of upland-riparian zones in agricultural catchments: Implications for runoff generation and nitrate transport. *Journal of Hydrology*, 331: 643-658.
- Omernik, J.M., A.R. Abernathy, and L.M. Male (1981). Stream nutrient levels and proximity of agricultural and forest land to streams: Some relationships. *Journal of Soil and Water Conservation*, 36(4): 227-231.
- Pacific, V., K. Jencso, and B.L. McGlynn (2010). Variable flushing mechanisms and landscape structure control stream DOC export during snowmelt in a set of nested catchments. *Biogeochemistry*. DOI: 10.1007/s10533-009-9401-1.
- Peterson, E.E., A.A. Merton, D.M. Theobald, and N.S. Urquhart (2006). Patterns of Spatial Autocorrelation in Stream Water Chemistry. *Environmental Monitoring and Assessment*, 121 (1): 569-594.
- PBS&J, Inc. (2005). *2005 Biological Monitoring Chlorophyll A Data Summary Upper Gallatin Water Quality Restoration Planning Areas*. TMDL Report prepared for the Montana Department of Environmental Quality.

- PBS&J, Inc. (2008). West Fork Gallatin River Streamflow Study 2007-2008. TMDL Report prepared for the Montana Department of Environmental Quality.
- Post, W.M., J. Pastor, P.J. Zinke, and A.G. Stangenberger (1985). Global patterns of soil nitrogen storage. *Nature*, 317 (17): 613-616.
- Postage, J. (1998). *Nitrogen Fixation*. Third Edition. Cambridge University Press, Cambridge, United Kingdom.
- Qian, S.S., K.H. Reckhow, Zhai, J., and G. McMahon (2005). Nonlinear regression modeling of nutrient loads in streams: A Bayesian approach. *Water Resources Research*, 41, W07012, doi:10.1029/2005WR003986.
- Qualls, R.G. and B.L. Haines (1992). Biodegradability of dissolved organic matter in forest throughfall, soil solution, and streamwater. *Soil Science Society of America Journal*, 56:578-586.
- Rast, W. and G.F. Lee (1983). Evaluation of nutrient loading estimates for lakes. *Journal of Environmental Engineering*, 109: 502-517.
- Reckhow, K.H., Beaulac, M.N., and Simpson, J.T. (1980). *Modeling P loading and lake response under uncertainty: A manual and compilation of export coefficients*. U.S. Environmental Protection Agency Report No: EPA-440/5-80-011. Office of Water Regulations and Standards, Criteria and Standards Division, U.S. Environmental Protection Agency, Washington, DC.
- Savenije, H. H. G. (2001). Equifinality, a blessing in disguise?, *Hydrological Processes*, 15, 2835 – 2838, doi:10.1002/hyp.494.
- Schade, J.D., E. Marti, J.R. Welter, S.G. Fisher, and N. B. Grimm (2002). Sources of nitrogen to the riparian zone of a desert stream: implications for riparian vegetation and nitrogen retention. *Ecosystems*, 5: 68-69.
- Seibert, J. and McDonnell (2002). On the dialog between experimentalist and modeler in catchment hydrology: Use of soft data for multicriteria model calibration. *Water Resources Research*, 38(11), 1241, doi:10.1029./2001WR000978.
- Seibert, J. and B.L. McGlynn (2007). A new triangular multiple flow-direction algorithm for computing upslope areas from gridded digital elevation models. *Water Resources Research*, 43, W04501, doi:10.1029/2006WR005128.
- Seitzinger, S.P., R.V. Styles, E.W. Boyer, R.B. Alexander, G. Billen, R.W. Howarth, B. Mayer, and N. Van Breemen (2002). Nitrogen retention in rivers: model

development and application to watersheds in the northeastern U.S.A.  
*Biogeochemistry*, 57/58: 199-237.

Shields, C.A, L.E. Band, N. Law, P.M. Groffman, S.S. Kaushal, K. Savas, G.T. Fisher, and K.T. Belt (2008). Streamflow distribution of non-point source nitrogen export from urban-rural catchments in the Chesapeake Bay watershed. *Water Resources Research*, 44, W09416, doi: 10.1029/2007WR006360.

Shrestha, S., F. Kazama, and L.T.H. Newham (2008). A framework for estimating pollutant export coefficients from long-term in-stream water quality monitoring data. *Environmental Modelling & Software*, 23: 182-194.

Smith, R.A., G.E. Schwarz, and R.B. Alexander (1997). Regional interpretation of water quality monitoring data. *Water Resources Research*, 33: 2781-2798.

Smith, T.J. and L.A. Marshall (2010). Exploring uncertainty and model predictive performance concepts via a modular snowmelt-runoff modeling framework. *Environmental Modelling & Software*, 25: 691- 701.

Soulsby C, D. Tetzlaff, S.M. Dunn, and S. Waldron (2006). Scaling up and out in runoff process understanding —insights from nested experimental catchment studies. *Hydrological Processes*, 20: 2461 – 2465.

Springob, G. and H. Kirchmann (2003). Bulk soil C to N ratio as a simple measure of net N mineralization from stabilized soil organic matter in sandy arable soil. *Soil, Biology & Biochemistry*, 35: 629-632.

Triska, F.J., A.P. Jackman, J.H. Duff, and R.J. Avanzino (1994). Ammonium sorption to channel and riparian sediments: A transient storage pool for dissolved inorganic nitrogen. *Biogeochemistry*, 26: 67-83.

Triska, F.J., J.R. Sedell, K. Cromack, S.V. Gregory, and F.M. McCorison (1984). Nitrogen budget for a small coniferous forest stream. *Ecological Monographs*, 54: 119-140.

U.S. Department of Agriculture (USDA) Forest Service (FS) (1994). *Ecoregions of the United States*: <http://www.fs.fed.us/land/pubs/ecoregions/>.

U.S. Environmental Protection Agency Clean Market Air Division (USEPA CMAD) (2009). Clean Air Status and Trends Network (CASTN). <http://www.epa.gov/castnet/>.

- U.S. EPA (2002). *Onsite Wastewater Treatment System Manual*. EPA/625/R-00/008. U.S. Environmental Protection Agency, Office of Water, Washington, DC, and Office of Research and Development, Cincinnati, OH.
- U.S. EPA (1976). *Areawide assessment procedures manual*, volumes I, II, and III. EPA/600/9-76/014 (NTIS PB-271863). USEPA Office of Research and Development.
- USDA Forest Service (FS) (2004). *Gallatin National Forest: Streams* <http://www.fs.fed.us/r1/gallatin/?page=resources/fisheries/streams>.
- USDA Natural Resource Conservation Service (NRCS) (2008). Snotel Precipitation Data. <http://www.wcc.nrcs.usda.gov/cgi-bin/wygraph-multi.pl?stationidname=11D19S-LONE+MOUNTAIN&state=MT&wateryear=2008>.
- USDA Soil Conservation Service (USDA SCS) (1982). *Soils of Montana*, Bulletin 744, November, Montana State University, Bozeman, MT.
- USDA S.C.S. (1978). *General Soil Map*, Montana, Ext. Misc. Publication No. 16.
- Vidon, P.G. and A.R. Hill (2006). A landscape approach to estimate riparian hydrological and nitrate removal functions. *Journal of the American Water Resources Association*, 42(4): 1099-1112.
- Vitousek, P.M., K. Cassman, C. Cleveland, T. Crews, C.B. Field, N.B. Grimm, R.W. Howarth, R. Marino, L. Martinelli, E.B. Rastetter and J.I. Sprent (2002). Towards an ecological understanding of biological nitrogen fixation. *Biogeochemistry*, 57/58: 1-45.
- Vitousek, P.M., Aber, J., Howarth, R.W., Likens, G.E., Matson, P.A., Shindler, D.W., Schlesinger, W.H., and D.G. Tilman (1997). Human Alterations of the Global Nitrogen Cycle: Sources and Consequences. *Ecological Applications*, 7(3): 737-750.
- Vitousek, P.M. (1979). Nitrate losses from disturbed forests – patterns and mechanisms. *Science*, 25(4): 605-619.
- Vitousek, P.M. and W.A. Reiners (1975). Ecosystem Succession and Nutrient Retention: A Hypothesis. *BioScience* (25)6: 376-381.
- Webster, J. R. & H. M. Valett (2006). Solute Dynamics. In, F. R. Hauer & G. A. Lamberti (Ed.). *Methods in Stream Ecology*. (pp169-185). Burlington, MA: Elsevier.
- Wetzel R.G. (2001). *Limnology*. 3rd ed. San Diego: Academic Press.

- Whitehead, P.G., P.J. Johnes, and D. Butterfield (2002). Steady state and dynamic modelling of nitrogen in River Kennet: Impacts of land use change since 1930s. *The Science of the Total Environment*, 282: 417-434.
- Wickham, J.D. and T.G. Wade (2002). Watershed level risk assessment of nitrogen and phosphorus export. *Computers and Electronics in Agriculture*, 37: 15-24.
- Wong, J.W.C, C.W.Y. Chan, and K.C. Cheung (1998). Nitrogen and phosphorus leaching from fertilizer applied on golf course: lysimeter study. *Water, Air & Soil Pollution*, 107 (1-4): 335-345.
- Worrall, F., and T.P. Burt (1999). The impact of land-use change on water quality at the catchment scale: The use of export coefficients and structural models. *Journal of Hydrology*, 221 (1-2): 75-90.
- Young, P., S. Parkinson & Matthew Lees (1996). Simplicity out of complexity in environmental modeling: Occam's razor revisited. *Journal of Applied Statistics*, 23(2&3): 165-210.
- Zobrist, J. and P. Reichert (2006). Bayesian estimation of export coefficients from diffuse and point sources in Swiss watersheds. *Journal of Hydrology*, 329: 207-223.

Table 4.1: Prior distributions of BiSN parameters and corresponding references used to determine the range of possible prior values.

<b>Model Parameter</b>	<b>Calibrated Coefficient</b>	<b>Prior Distribution</b>	<b>Prior Distribution Parameters</b>	<b>Units</b>	<b>Reference</b>
<i>Vegetation (VEG)</i>	$b_v$	Uniform	a = -3.65 b = 3.65	kg ha <sup>-1</sup> yr <sup>-1</sup>	Alexander et al., 2008 McFarland et al., 2001 Rast and Lee, 1983 Zobrist and Reichert, 2006
<i>Wastewater (WW)</i>	$b_w$	Uniform	a = 0 b = 3650	kg ha <sup>-1</sup> yr <sup>-1</sup>	Big Sky Water and Sewer District Unpublished Data
<i>Septic (S)</i>	$b_s$	Trapezoidal	a = 0, b = 365 c = 1825, d = 2190	kg ha <sup>-1</sup> yr <sup>-1</sup>	USEPA, 2002
<i>Soil Storage Release (SSR)</i>	$b_{ssr}$	Uniform	[0, 3650]	kg ha <sup>-1</sup> yr <sup>-1</sup>	Ackerman et al., in prep.
<i>Travel a (TT<sub>a</sub>)</i>	$b_a$	Uniform	[0, 1]	na	na
<i>Travel b (TT<sub>b</sub>)</i>	$b_b$	Uniform	[0, 1]	na	na
<i>Wet Deposition (WD)</i>	$b_{wd}$	Trapezoidal	a = 0.34, b = 0.55 c = 1.1, d = 1.36	mg/L	NADP, 2009
<i>Riparian Buffer (RBI)</i>	$b_r$	Triangular	a = -36.5, b = 182.5 c = 36.5	kg yr <sup>-1</sup>	Burt et al., 1999 Maitre et al., 2003

Table 4.2: The 5th and 95<sup>th</sup> percentile of sampled parameter values and the parameter values corresponding to the maximum log-likelihood of BiSN runs. Abbreviations for parameters are described in Table 4.1.

<b>Parameter</b>	<b>5th Percentile</b>	<b>Maximum Likelihood</b>	<b>95th Percentile</b>	<b>Units</b>
<i>VEG</i>	-3.307	2.734	3.157	kg ha <sup>-1</sup> yr <sup>-1</sup>
<i>WW</i>	4.052	10.439	12.082	kg ha <sup>-1</sup> yr <sup>-1</sup>
<i>S</i>	289.080	336.530	2107.875	kg ha <sup>-1</sup> yr <sup>-1</sup>
<i>SSR</i>	244.550	297.402	3412.750	kg ha <sup>-1</sup> yr <sup>-1</sup>
<i>TT<sub>a</sub></i>	0.048	0.619	0.596	na
<i>TT<sub>b</sub></i>	0.035	0.035	0.035	na
<i>WD</i>	0.500	1.150	1.340	mg L <sup>-1</sup>
<i>RBI</i>	41.245	270.427	286.525	kg ha <sup>-1</sup> yr <sup>-1</sup>

Table 4.3: Modeled sources of N loading for subwatersheds corresponding to Figures 4.9 and 4.10. Map codes correspond to sites depicted in Figure 4.10A. Abbreviations for N sources are described in Table 4.1.

Map Code	Subwatershed	Hectares	VEG kg ha <sup>-1</sup> yr <sup>-1</sup>	WW kg ha <sup>-1</sup> yr <sup>-1</sup>	S kg ha <sup>-1</sup> yr <sup>-1</sup>	SSR kg ha <sup>-1</sup> yr <sup>-1</sup>	WD kg ha <sup>-1</sup> yr <sup>-1</sup>	DD kg ha <sup>-1</sup> yr <sup>-1</sup>	Total N Inputs kg ha <sup>-1</sup> yr <sup>-1</sup>
1	<i>Upper Beehive (UB)</i>	299	1.79	0	0	30.22	3.18	0.26	35.46
2	<i>Beehive (BH)</i>	833	2.28	0.00	0.71	44.90	2.94	0.26	51.09
3	<i>MF Headwaters 1 (MFHW1)</i>	88	1.91	0.00	9.36	29.97	2.86	0.26	44.37
4	<i>MF Headwaters 2 (MFHW2)</i>	380	2.51	0.00	0.39	33.11	2.81	0.26	39.08
5	<i>Upper Middle Fork (UMF)</i>	1280	2.09	0.00	2.44	31.31	2.80	0.26	38.89
6	<i>Middle Middle Fork1 (MMF1)</i>	2773	2.16	0.00	1.45	44.02	2.78	0.26	50.67
7	<i>Middle Middle Fork2 (MMF2)</i>	4786	2.27	0.00	1.74	37.93	2.66	0.26	44.87
8	<i>Upper North Fork (UNF)</i>	378	1.65	0.00	0.00	29.87	3.14	0.26	34.92
9	<i>Middle North Fork (MNF)</i>	1077	2.02	0.00	0.00	37.49	3.00	0.26	42.77
10	<i>Lower North Fork (LNF)</i>	2319	2.23	0.00	0.23	35.58	2.90	0.26	41.20
11	<i>Lower Middle Fork (LMF)</i>	8412	2.24	0.20	1.27	38.84	2.69	0.26	45.49
12	<i>South Fork Headwaters (SFH)</i>	1898	2.15	0.00	0.02	29.86	2.98	0.26	35.27
13	<i>Upper South Fork (USF)</i>	2565	2.12	0.00	0.33	41.38	2.93	0.26	47.02
14	<i>Upper Muddy Creek (UMC)</i>	1913	2.17	0.00	0.00	49.91	3.00	0.26	55.34
15	<i>Third Yellow Mule (3YM)</i>	633	2.24	0.00	0.00	124.52	3.02	0.26	130.04
16	<i>Lower Muddy Creek (LMC)</i>	3577	2.19	0.00	0.03	59.08	2.94	0.26	64.50
17	<i>Second Yellow Mule (2YM)</i>	1148	2.46	0.00	0.00	160.53	2.90	0.26	166.15
18	<i>Middle South Fork1 (MSF1)</i>	8020	2.20	0.00	0.20	66.53	2.88	0.26	72.07
19	<i>Upper Yellow Mule (UYM)</i>	464	2.26	0.00	0.00	186.03	2.97	0.26	191.52
20	<i>Lower Yellow Mule (LYM)</i>	1101	2.51	0.00	0.00	115.04	2.81	0.26	120.62
21	<i>Middle South Fork2 (MSF2)</i>	11068	2.27	0.00	0.16	68.71	2.82	0.26	74.23
22	<i>Lower South Fork (LSF)</i>	11971	2.29	0.00	0.38	66.00	2.77	0.26	71.71
23	<i>Lower West Fork (WF)</i>	20617	2.27	0.09	0.77	54.41	2.73	0.26	60.52

Table 4.4: Relative importance of upland, riparian, and instream N retention for subwatersheds listed in Table 4.2. Percent retention excluding upland retention is in parenthesis. Map codes correspond to sites depicted in Figure 4.10A.

Map Code	Subwatershed	Total N Inputs kg ha <sup>-1</sup> yr <sup>-1</sup>	Upland N Retention kg ha <sup>-1</sup> yr <sup>-1</sup>	Riparian N Retention kg ha <sup>-1</sup> yr <sup>-1</sup>	Instream N Retention kg ha <sup>-1</sup> yr <sup>-1</sup>	NO <sub>3</sub> <sup>-</sup> -N Export kg ha <sup>-1</sup> yr <sup>-1</sup>
1	<i>Upper Beehive (UB)</i>	35.46	34.93 (99)	0.26 (49)	0.26 (50)	0.003 (1)
2	<i>Beehive (BH)</i>	51.09	50.72 (99)	0.26 (71)	0.10 (26)	0.011 (3)
3	<i>Middle Fork Headwaters 1 (MFHW1)</i>	44.37	44.02 (98)	0.08 (23)	0.05 (13)	0.226 (64)
4	<i>Middle Fork Headwaters 2 (MFHW2)</i>	39.08	38.80 (98)	0.04 (16)	0.19 (67)	0.050 (17)
5	<i>Upper Middle Fork (UMF)</i>	38.89	38.62 (99)	0.15 (55)	0.09 (34)	0.030 (11)
6	<i>Middle Middle Fork 1 (MMF1)</i>	50.67	50.36 (99)	0.19 (60)	0.124 (39)	0.006 (1)
7	<i>Middle Middle Fork 2 (MMF2)</i>	44.87	44.46 (99)	0.18 (44)	0.23 (55)	0.001 (1)
8	<i>Upper North Fork (UNF)</i>	34.92	34.77 (99)	0.09 (62)	0.05 (33)	0.006 (4)
9	<i>Middle North Fork (UNF)</i>	42.77	42.59 (99)	0.094 (52)	0.085 (47)	0.0002 (<1)
10	<i>Lower North Fork (LNF)</i>	41.20	40.89 (99)	0.13 (43)	0.17 (56)	0.003 (2)
11	<i>Lower Middle Fork (LMF)</i>	45.49	44.78 (98)	0.21 (29)	0.44 (63)	0.059 (11)
12	<i>South Fork Headwaters (SFH)</i>	35.27	35.11 (99)	0.12 (72)	0.045 (27)	0.0002 (<1)
13	<i>Upper South Fork (USF)</i>	47.02	46.79 (99)	0.12 (49)	0.12 (50)	0.0003 (<1)
14	<i>Upper Muddy Creek (UMC)</i>	55.34	54.89 (99)	0.097 (22)	0.35 (78)	0.002 (1)
15	<i>Third Yellow Mule (3YM)</i>	130.04	129.62 (99)	0.12 (29)	0.24 (57)	0.05 (13)
16	<i>Lower Muddy Creek (LMC)</i>	64.50	64.04 (99)	0.11 (24)	0.35 (76)	0.0002 (<1)
17	<i>Second Yellow Mule (2YM)</i>	166.15	164.56 (98)	0.082 (5)	1.45 (91)	0.06 (4)
18	<i>Middle South Fork1 (MSF1)</i>	72.07	71.26 (98)	0.12 (15)	0.65 (83)	0.040 (2)
19	<i>Upper Yellow Mule (UYM)</i>	191.52	189.82 (99)	0.15 (9)	1.40 (82)	0.16 (9)
20	<i>Lower Yellow Mule (LYM)</i>	120.62	119.55 (99)	0.18 (17)	0.88 (82)	0.012 (1)
21	<i>Middle South Fork2 (MSF2)</i>	74.23	73.15 (98)	0.14 (13)	0.87 (80)	0.080 (7)
22	<i>Lower South Fork (LSF)</i>	71.71	70.40 (98)	0.15 (11)	1.13 (86)	0.035 (3)
23	<i>Lower West Fork (WF)</i>	60.52	59.39 (98)	0.18 (15)	0.96 (82)	0.035 (3)

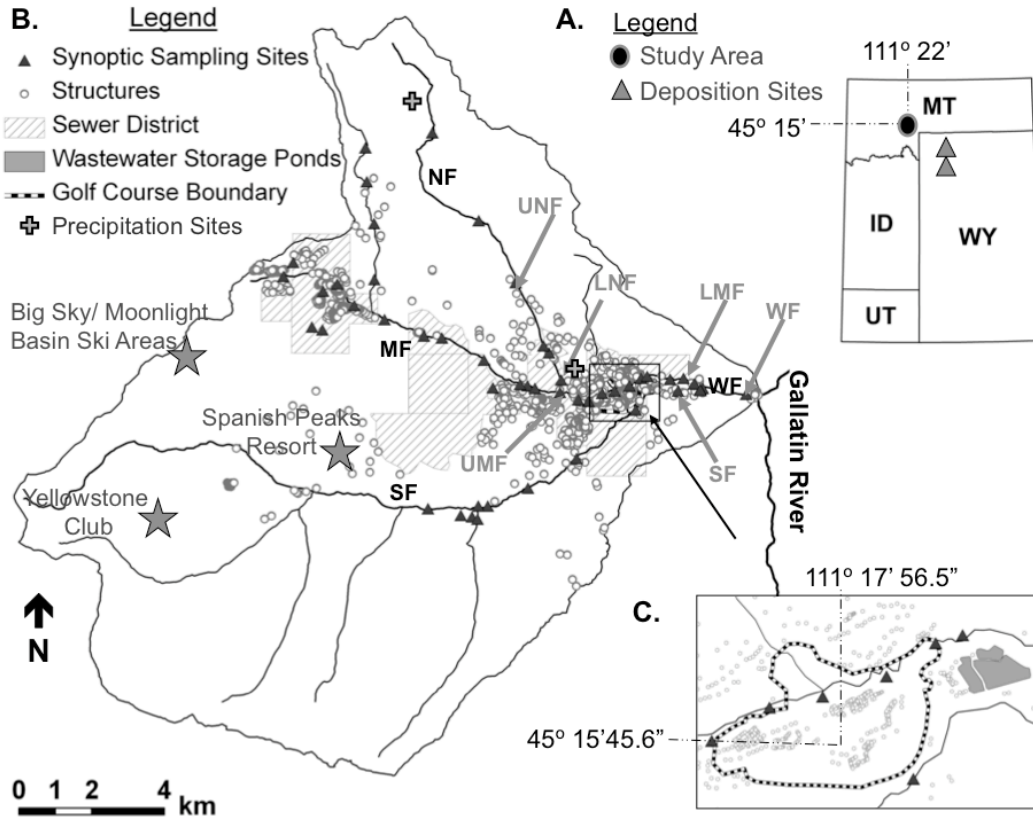


Figure 4.1: (A) Location of the West Fork watershed (212 km<sup>2</sup>) in southwestern Montana, with locations of atmospheric deposition data collection sites. (B) Map of the West Fork watershed showing locations of 50 synoptic sampling sites (black triangles), building structures (grey circles), and the Big Sky Water and Sewer District boundaries (grey hatched lines). The West Fork (WF) drains into the Gallatin River (a tributary of the Upper Missouri River) and is comprised of three main tributaries: the Middle Fork (MF), the North Fork (NF), and the South Fork (SF). (C) An expanded view of the wastewater storage ponds and the Big Sky Resort Golf Course. Wastewater effluent is stored in the ponds and irrigated onto the golf course from mid-May through early October.

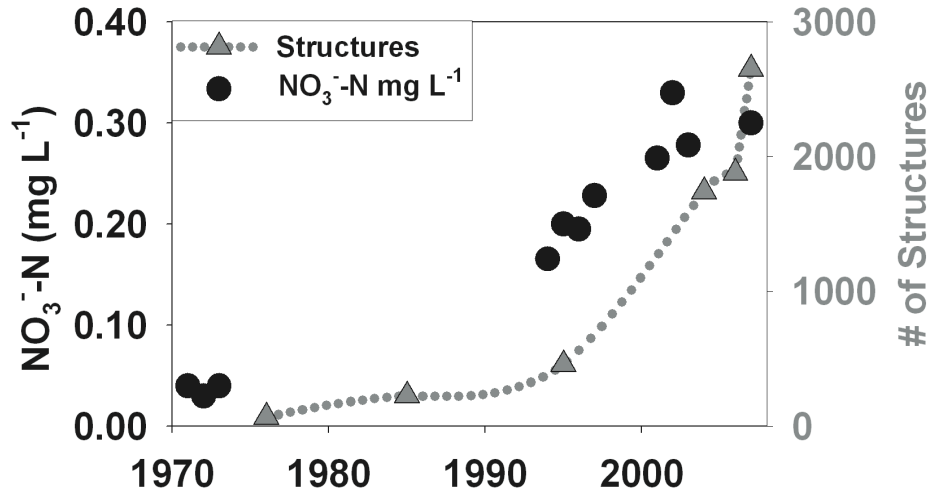


Figure 4.2: In the West Fork watershed, residential development and annual average streamwater  $\text{NO}_3^-$  concentrations in the West Fork have followed a similar upward trend since resort development. [NSF, 1976; Blue Water Task Force, and Big Sky Water and Sewer District, unpublished data].

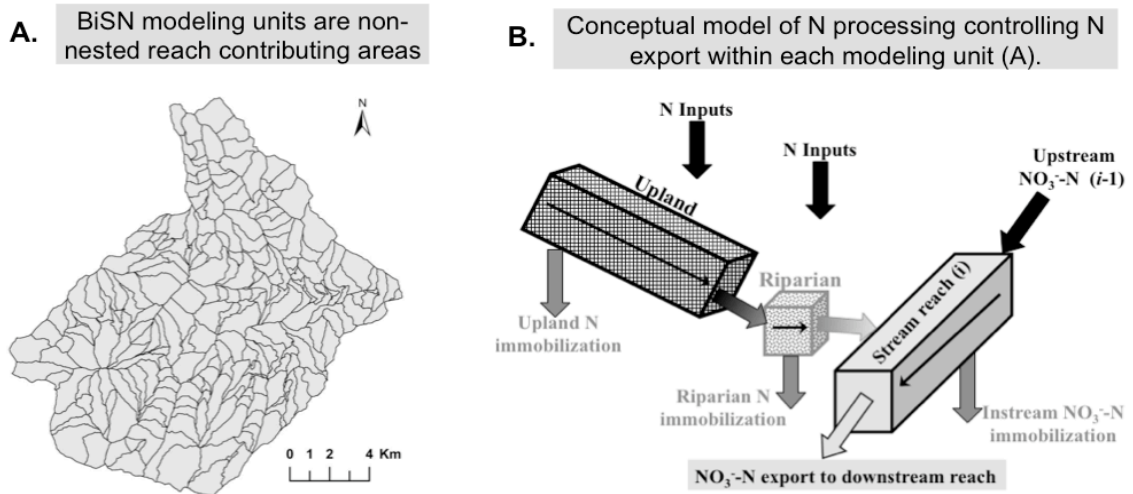


Figure 4.3: (A) Watershed modeling units of the Big Sky Nutrient Model (BiSN) were 231 non-nested stream reach contributing areas ranging in size from  $0.01 \text{ km}^2$  to  $3.7 \text{ km}^2$ . The stream network was delineated into stream reaches of approximately 500m in length. A 500 m stream reach length was chosen because 97% of measured  $\text{NO}_3^-$  uptake lengths were less than 500m [McNamara et al., in prep.]. (B) Conceptual model of processes controlling N loading and retention West Fork watershed. Stream reach  $\text{NO}_3^-$  is as function of upstream  $\text{NO}_3^-$  inputs and lateral loading from the reach contributing area (A).

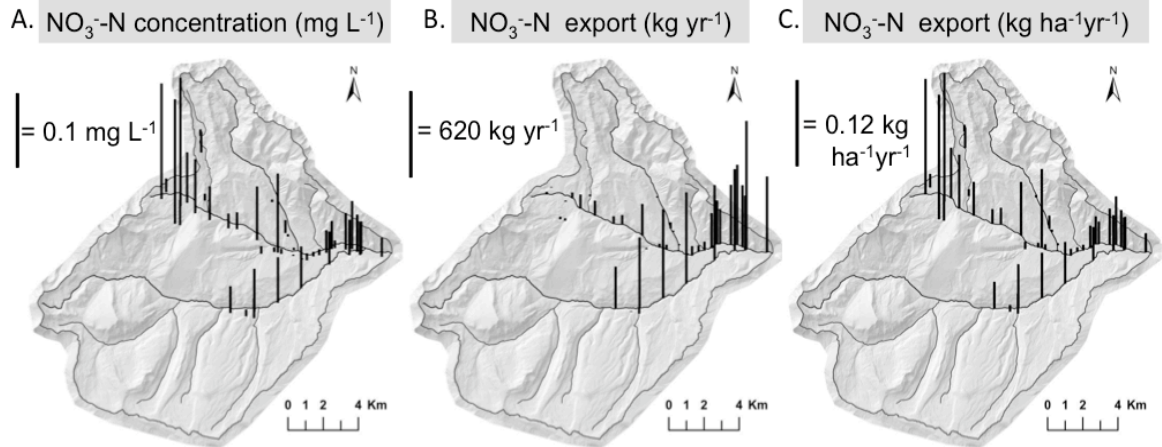


Figure 4.4: (A) Observed spatial  $\text{NO}_3^-$  concentrations (black bars) from August 7, 2007.  $\text{NO}_3^-$  concentration is greatest in the headwaters of the Middle Fork and elevated in the South Fork and West Fork compared to other streams. (B) Observed streamwater  $\text{NO}_3^-$  export (black bars) generally increased in a downstream direction. (C) When N export is normalized for watershed area,  $\text{NO}_3^-$  export pattern mirrors the patterns of concentrations;  $\text{NO}_3^-$  export is greatest in the headwaters of the Middle Fork and elevated in the South Fork and West Fork compared to other streams. Height of the black bars corresponds to  $\text{NO}_3^-$  export values. There is no data from the headwaters of the South Fork due to landowner refusal for access.

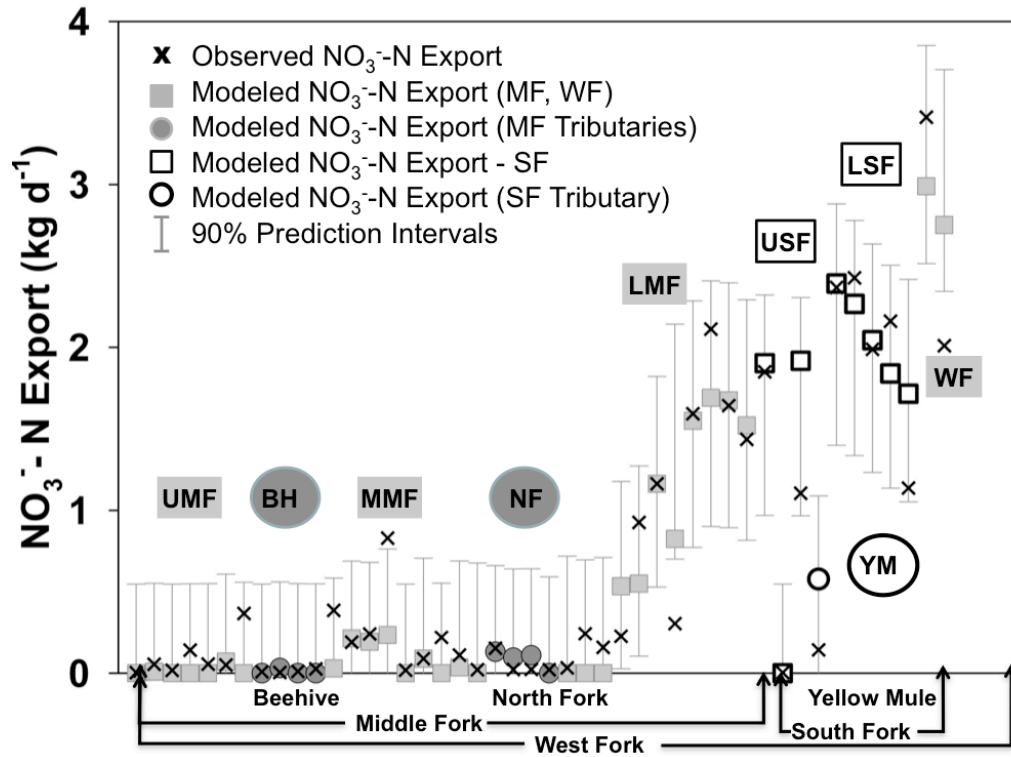


Figure 4.5: The spatial variability of observed streamwater  $\text{NO}_3^-$  export (black x's) was well captured by BiSN over a wide range of land use/ land cover and landscape positions with 90% prediction intervals (grey lines). 93% of observed data falls within the 90% prediction intervals. Data is ordered to depict network organization. From the headwaters, the Middle Fork flows into the West Fork (grey squares). Tributaries to the Middle Fork and West Fork include the South Fork and Beehive (grey circles). Yellow mule is a tributary to the South Fork (black outlined circle).

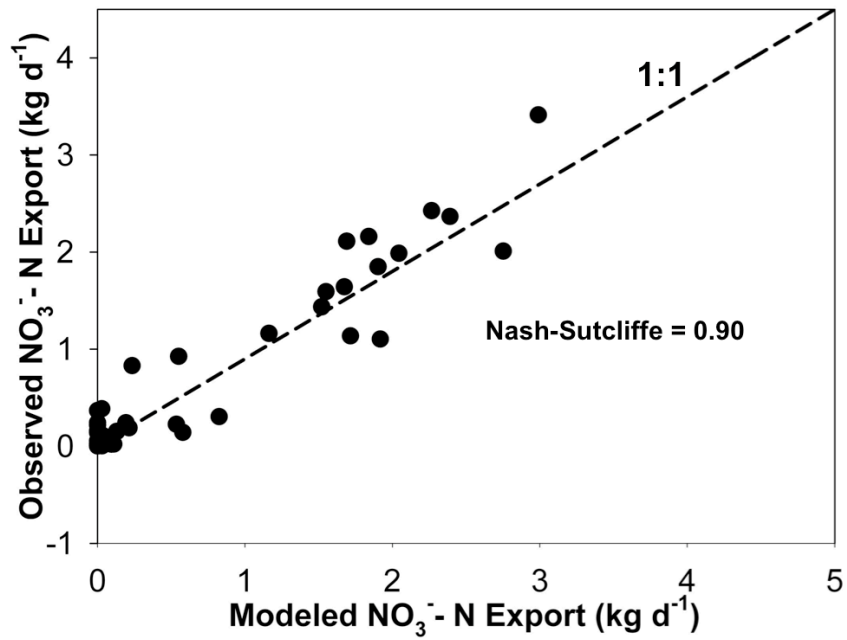


Figure 4.6: BiSN was a good predictor of streamwater  $\text{NO}_3^-$  export (Nash-Sutcliffe model efficiency coefficient = 0.90). Model residuals were normally distributed and did not appear to have a pattern about the 1:1 line or to be spatially correlated (Figure 4.7).

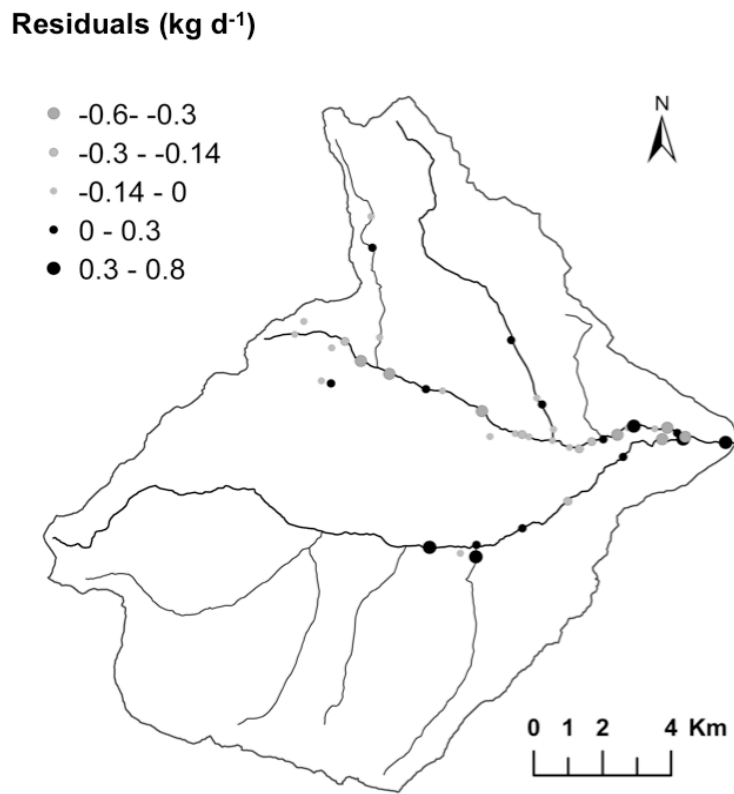


Figure 4.7: Spatial distribution of  $\text{NO}_3^-$  export model residuals. Model residuals do not exhibit spatial correlation: Model under-predictions (grey circles) and over-predictions (black circles) appear to be randomly dispersed across the West Fork watershed. The spatial variability of streamwater  $\text{NO}_3^-$  export was well captured by the N export model over a wide range of land use/ land cover and landscape positions.

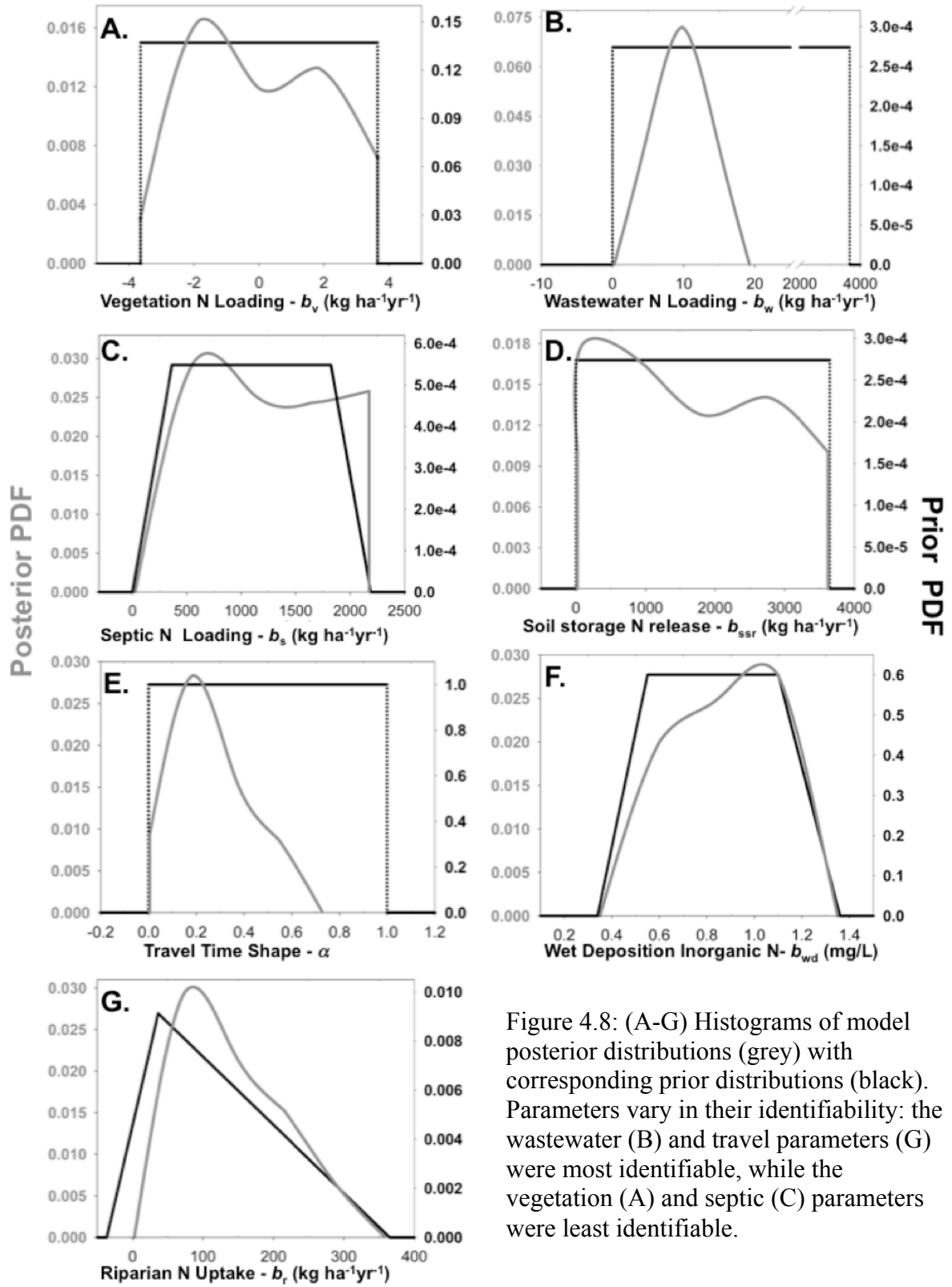


Figure 4.8: (A-G) Histograms of model posterior distributions (grey) with corresponding prior distributions (black). Parameters vary in their identifiability: the wastewater (B) and travel parameters (G) were most identifiable, while the vegetation (A) and septic (C) parameters were least identifiable.

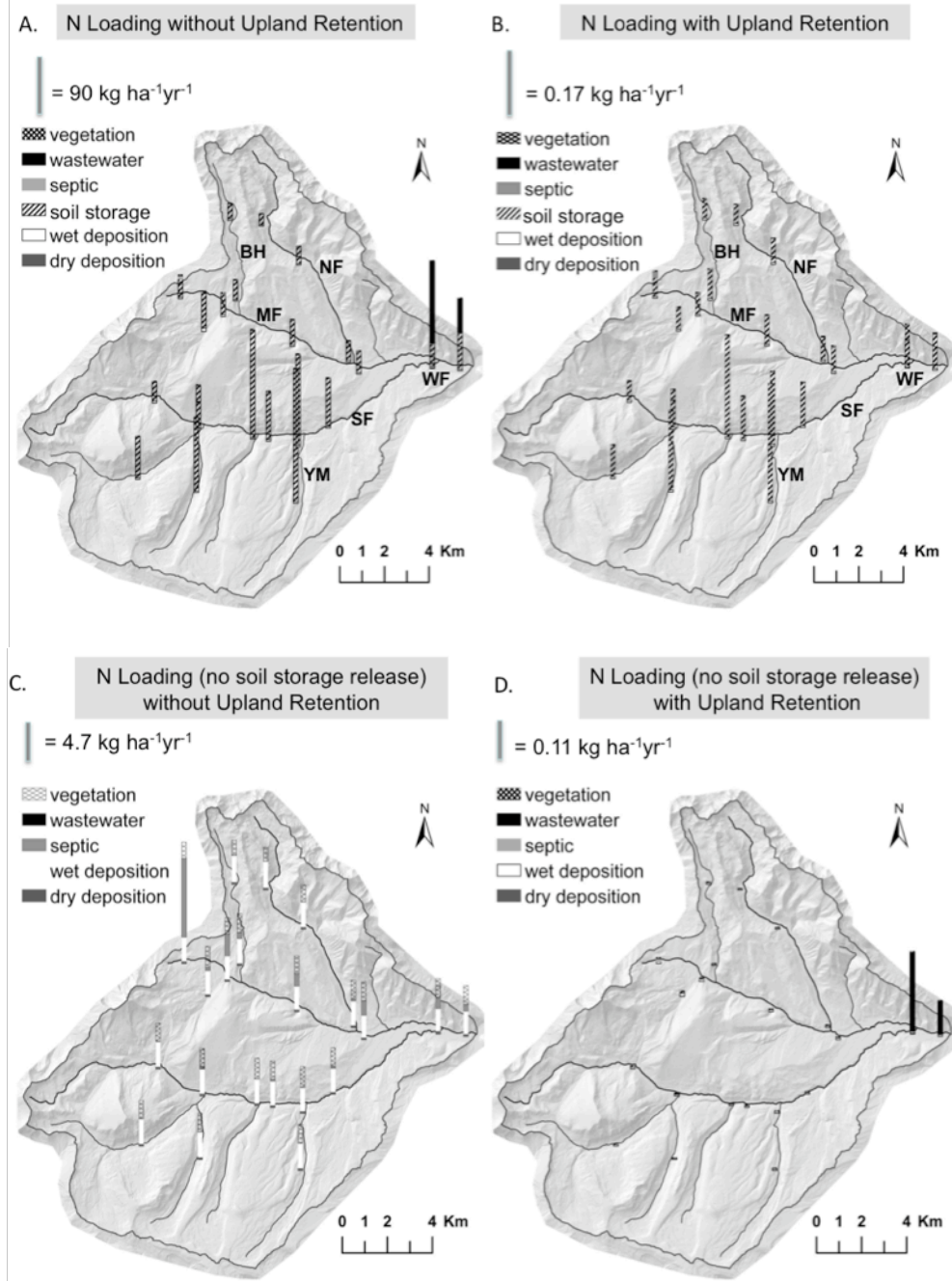


Figure 4.9: Modeled N loading across the West Fork watershed (A) compared to N loading after travel time decay is applied (B). N originating from soil storage release dominated the  $\text{NO}_3^-$  signal. Excluding N loading from soil storage release (C, D), localized small inputs of anthropogenic N from wastewater were responsible for elevated streamwater  $\text{NO}_3^-$  export in the lower section of the West Fork (D). Wastewater inputs, which occurred “hydrologically close” to the stream and were smaller relative to other N inputs, had a disproportionate impact on watershed  $\text{NO}_3^-$  export.

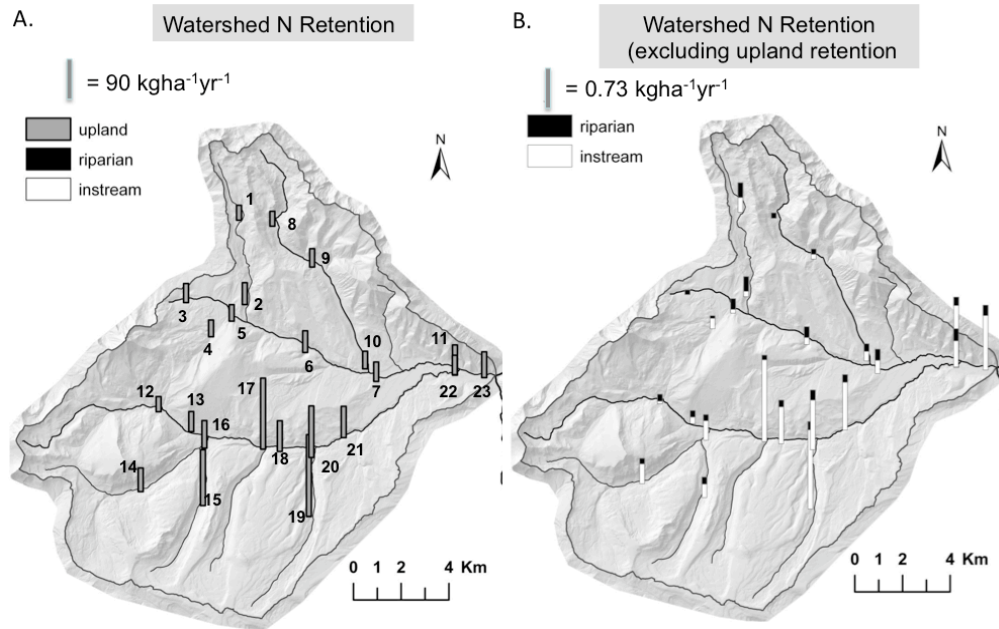


Figure 4.10: Modeled upland, instream, and riparian  $\text{NO}_3^-$  retention across the West Fork watershed. (A) Most N loading was retained in the upland (by either biological processes or lack of a physical transport mechanism (hydrological connectivity)). (B) Excluding upland retention, instream processes were responsible for more  $\text{NO}_3^-$  immobilization than riparian areas in the majority of the watershed. Numbers correspond to Map codes in Tables 4.3 and 4.4.

## CHAPTER 5

## SUMMARY

With changes in land use occurring at an accelerated rate, watershed nitrogen (N) enrichment is a growing concern due to its association with human development. Watershed N enrichment can lead to nuisance algal growth, changes in biological community structure, and in the most extreme cases, eutrophication of surface waters. One such example is the hypoxic zone in the Gulf of Mexico. Because of the potentially detrimental consequences of watershed N enrichment, much work has focused on the impacts of land use/ land cover (LULC) change on watershed N export. Despite the abundance of research on this topic, there is still a notable lack of understanding of LULC impacts on the spatial and seasonal heterogeneity present in watershed N export.

Historically, knowledge of anthropogenic N impacts on watershed N export generally has been drawn from two types of studies: studies, which have examined increased nitrate ( $\text{NO}_3^-$ ) export from spatially distributed inputs of atmospheric deposition N, and other studies, which have developed statistical relationships between percentages of LULC and watershed  $\text{NO}_3^-$  export during low flow summer conditions. The research sought to improve knowledge of the linkages between anthropogenic N inputs and the spatial and seasonal variable patterns of watershed N export by examining the roles of landscape position and the spatial distribution of N loading on watershed N export and retention. These roles were explored across seasons and watersheds that varied in development densities, stream order, residence times, and riparian buffering potential.

In Chapter 2, an exploratory spatial analysis suggested that watershed biological processing was a primary driver of spatial and seasonal variability of streamwater  $\text{NO}_3^-$  concentrations. Spatial snapshots of streamwater  $\text{NO}_3^-$  concentrations collected across time periods of varying potential of hydrologic and biological activity illustrated spatial and seasonally variable patterns of streamwater  $\text{NO}_3^-$  concentrations. In lower elevation alluvial streams,  $\text{NO}_3^-$  concentrations peaked during the dormant season and remained relatively low the rest of the year. In addition, streamwater nitrate concentrations were spatially correlated for longer distances in the winter dormant season compared the summer growing season. Both of these results suggests that during periods of high biological potential, N immobilization lead to a break down of spatial streamwater  $\text{NO}_3^-$  patterns, therefore masking LULC impacts on streamwater  $\text{NO}_3^-$  concentrations (see also, *McNamara* [2010]). Seasonal patterns in streamwater  $\text{NO}_3^-$  concentrations were absent in high-elevation alpine environments, with sparse vegetation, limited riparian areas, and shallow, undeveloped soils, where streamwater  $\text{NO}_3^-$  concentrations and remained elevated yearlong. Biological processing in these alpine environments did not appear to be a major control on seasonal streamwater  $\text{NO}_3^-$  concentration patterns.

In this chapter, geostatistical models also conveyed the importance of biologic retention on the spatial patterns of streamwater  $\text{NO}_3^-$  concentrations during the growing season when biological variables (riparian buffering potential and percent forest) most strongly influenced streamwater  $\text{NO}_3^-$ ; however, in the dormant season, N loading variables explained the most variability in streamwater  $\text{NO}_3^-$  concentrations. Important implications for future research and management of watershed N from Chapter 2 include

the importance of: 1) incorporating spatial relationships into water quality modeling, and 2) investigating streamwater chemistry across seasons to gain a more complete understanding of development impacts on streamwater quality.

The empirical analysis of spatial and seasonal streamwater chemistry presented in Chapter 3 highlighted the seasonal and spatial variability of anthropogenic impacts on watershed  $\text{NO}_3^-$ , dissolved organic nitrogen (DON) and dissolved organic carbon (DOC) export and concentration patterns, stoichiometric ratios and watershed N saturation status. Impacts for anthropogenic N loading were manifested in increased streamwater  $\text{NO}_3^-$  export and concentrations, elevated DIN:DON ratios, lower C:N ratios, and sustained DON release during snowmelt. Biological uptake masked these N enrichment signs during the summer growing season when  $\text{NO}_3^-$  concentrations were relatively low.

Similar to Chapter 2, this chapter revealed seasonal variability in anthropogenic N influences on streamwater N export; however, endmember mixing analysis of  $\delta^{15}\text{N}$  and  $\delta^{18}\text{O}$  values of  $\text{NO}_3^-$  provided evidence of anthropogenic influence of streamwater  $\text{NO}_3^-$  during the summer growing season. This was not captured from statistical inference from land use and concentration data presented in Chapter 2. Specifically,  $\delta^{15}\text{N}$  and  $\delta^{18}\text{O}$  isotopic ratios of  $\text{NO}_3^-$  demonstrated that wastewater influence was most significant during summer and winter baseflow, but still contributed to streamwater  $\text{NO}_3^-$  during snowmelt in some streams. This has major ramifications for watershed management in that low N concentrations do not necessarily equate to no human impacts.

Also in Chapter 3, the idea of localized N saturation was introduced. N saturation dynamics were exhibited in the West Fork watershed as a result of localized inputs of

anthropogenic N, which is contrary to the widely accepted N saturation dynamics occurring from spatially distributed N loading. Like anthropogenic N loading patterns, watershed N saturation characteristics exhibited spatial and seasonal heterogeneity across the West Fork watershed. Anthropogenic N loading that occurred in areas with quick transport times to the stream were more apt to lead to N enrichment signals than N source areas connected to streams via longer flowpaths that may have limited hydrologic connection to the stream. Watershed N retention estimates confirmed that it is not necessarily the amount of N loading that controls watershed N export but where on the landscape it occurs and what time of year. These findings should be implemented into land use planning strategies to minimize N loading impacts on surface waters.

In Chapter 4, the Big Sky Nutrient Model (BiSN), a hybrid mechanistic nutrient export model run with a Bayesian framework, was introduced. Modeling results supported results from the empirical analysis in Chapter 3 that showed localized N loading occurring in watershed areas with fast travel times to the stream having disproportionate effects on water quality. BiSN's output provided insight into the main drivers of streamwater  $\text{NO}_3^-$  export in the West Fork watershed during the summer growing season. Modeled parameter posterior distributions identified wastewater loading and relative travel time, which represents the hydrologic transport time between N inputs and the stream channel, as being the most important controls of watershed  $\text{NO}_3^-$  export. These results agree with conclusions from the  $\text{NO}_3^-$  isotopic analysis in Chapter 3, that wastewater was a significant contributor to summer  $\text{NO}_3^-$  concentrations.

Lastly, Chapter 4 revealed that most watershed  $\text{NO}_3^-$  removal occurred in the terrestrial ecosystem as a result of biological uptake or a lack of physical transport (i.e. hydrologic connectivity) between the uplands and the stream channel. This again provides evidence that careful consideration of watershed N sources can minimize N loading to surface waters. Excluding upland retention, results agree with network patterns observed in other studies that have shown increasing role of instream N removal with increasing N loading going downstream in the stream network.

Collectively, through a multi-analysis approach this dissertation increased understanding of the influences of anthropogenic N loading on emergent patterns of watershed N export and retention. Based on the insight gained from this research, I offer the following recommendations for future research:

- 1) The linkages between carbon, nitrogen, and phosphorous cycles and watershed nitrogen export and how these linkages may vary seasonally across landscape position (hillslope, riparian area, and stream), soil/groundwater/stream transitions, N loading gradients, and the stream network. This will lead to further understanding on how N saturation/limitation dynamics vary in space and time in relation to carbon and phosphorous availability and could be useful to predict impacts from land use or climate change scenarios.
- 2) Further exploration of how spatial and seasonal patterns of streamwater  $\text{NO}_3^-$  export, loading and retention vary along the stream network from the

headwaters to the catchment outlet by applying the BiSN model to winter, spring runoff and annual  $\text{NO}_3^-$  export data.

- 3) Watershed DON dynamics and how they may be altered by anthropogenic influence. Limited research has focused on DON and the studies that have focused on DON have contrasting results. Recent advances in the analysis of DON isotopes [*Ros et al.*, 2010] could allow for better tracking of DON sources, especially if used in combination with other geochemical tracers. In addition, I suggest applying the BiSN framework for DON to gain insight into the controls of DON export.
- 4) Avalanche control explosives as a potential source of watershed N. Although elevated levels of inorganic N draining alpine areas have been documented in other research, I have suspicion that explosives used for avalanche control may be contributing to elevated inorganic N observed at sites draining Lone Mountain. The explosives used for avalanche control contain ammonium nitrate. Perhaps the byproducts have isotopically distinct signatures and can be traced through the isotopic analysis of  $^{15}\text{N}$  and  $^{18}\text{O}$  of  $\text{NO}_3^-$ . I am not aware of any studies that have examined avalanche bombs as a potential source of watershed N.
- 5) Downstream impacts of Stage 1 or Stage 2 N saturation dynamics in headwater streams. State agencies put emphasis on summer N concentrations and loads because they can promote nuisance algal growth; however, research that quantifies the downstream effects of high winter  $\text{NO}_3^-$  concentrations in

headwater streams is warranted. Increased N loads from headwater watersheds in the winter may have cascading impacts on downstream ecosystem health and function, including exacerbating coastal eutrophication (e.g. Gulf of Mexico).

- 6) The legacy of historical N loading. At the daily time step, BiSN results indicated that soil storage release of N was a primary driver of summer export of watershed  $\text{NO}_3^-$  (Chapter 4). How long is N stored in watershed soils? Manipulation field studies could be designed to focus on what happens to watershed N export when high levels of N loading decline over time. This is a critical question to answer in the face of monitoring the success of stream and watershed restoration projects.
- 7) Terrain analysis algorithms that include: 1) realistic flowpaths and travel times in human impacted watersheds, and 2) more precise definition of riparian buffering potential. First, human structures and alteration of the natural environment can greatly modify hydrologic flowpaths and water transport times (e.g. impervious surface, surface compaction, vegetation removal). Incorporating hydrologic flowpaths in land use change research may significantly improve accuracy of water and N transport in spatial models. Secondly, riparian buffering potential estimates could be improved by incorporating the probability of the riparian area intersecting hillslope flowpaths, which can drive N processing. In addition, the combination of terrain and remote sensing data could illuminate the presence or absence and

density of riparian vegetation. Given potential importance of riparian areas to watershed N retention and export, these changes in approximating riparian buffering potential could considerably improve quantification of the relative importance of watershed N retention mechanisms.

As described above, this dissertation sets the stage for more process based and applied research questions on the interactions between human development, hydrology, landscape characteristics, and the N and C biogeochemical cycles, and how these interactions may affect watershed N export. The nitrogen cycle is a complex biogeochemical cycle. To accurately quantify and predict the extent to which human activities disrupt the nitrogen cycle at the landscape scale remains to be one of the biggest challenges of the 21<sup>st</sup> century.

References Cited

- McNamara, R.M. (2010). *Stream nitrogen uptake dynamics from ambient to saturation across development gradients, stream network position, and seasons*. Master's Thesis, Montana State University, Bozeman, MT.
- Ros, G.H, E.J.M. Temminghoff, and J.W. van Groenigen (2010). Isotopic analysis of dissolved organic nitrogen in soils. *Analytical Chemistry*, doi:10.1021/ac1018183.

APPENDICES

APPENDIX A

ATMOSPHERIC DEPOSITION CALCULATION FOR THE BIG SKY  
NUTRIENT EXPORT MODEL (BISN)

Precipitation in the drainage varies significantly across elevation gradients; annual precipitation exceeds 1270 mm at higher elevations (3400 m) and is less than 500 mm near the watershed outlet (1800 m). The West Fork watershed has two year round weather stations, which measure precipitation (Figure 4.1B): 1) the Lone Mountain SNOTEL station is located in Bear Basin in the headwaters of the North Fork at 2706 m in a subalpine environment, and 2) the Lone Mountain Ranch station located in the valley bottom at 2100 m. There were six years that both stations recorded data (2002-2007). Linear regression developed a relationship to the average precipitation and elevation data and this relationship was used to scale precipitation. Calibrated wet N deposition concentration was multiplied by precipitation to calculate wet deposition N loading for each grid cell.

APPENDIX B

INSTREAM NITROGEN DECAY MODEL DESCRIPTION

Multiple regression determined the relationship between measured areal uptake ( $\text{g m}^{-2} \text{d}^{-1}$ ) of  $\text{NO}_3^-$  and potential explanatory variables. Potential explanatory variables to predict areal uptake included: watershed area, nitrate concentration, and stream order. Watershed area and stream order for each reach was determined through terrain analysis and measured  $\text{NO}_3^-$  concentration. A significant linear relationship ( $R^2 = 0.74$ ) was found between areal uptake, watershed area, and measured streamwater  $\text{NO}_3^-$ . Instream areal  $\text{NO}_3^-$  uptake increased with watershed area and  $\text{NO}_3^-$  concentration.

In the N export model (Equation 4.1) areal  $\text{NO}_3^-$  uptake for each stream reach was computed by applying the regression relationship between watershed area and nitrate concentration. The computed areal uptake was multiplied by the reach length (m) and reach width (m) to determine total N immobilization ( $\text{kg d}^{-1}$ ). The upland N load from the incremental subwatershed  $i$  (Figure 4.3) was assumed to travel on average half the reach length. Therefore, stream *decay* function was applied for only half the distance of stream reach  $i$ :

$$\text{Upland Load} = (0.5 * \text{reach length}_i * \text{reach width}_i^1 * \text{decay}) \quad (4.A1)$$

For the upstream load ( $\text{NE}_{\text{up}}$ ), N immobilization (*decay*) occurs throughout the entire length of the downstream reach  $i$ :

$$\text{NE}_{\text{up}} = (\text{reach length}_i \times \text{reach width}_i^1 * \text{decay}) \quad (4.A2)$$

<sup>1</sup>Stream width assumptions were dependent on stream order. Based on field observations, a first, second, third and fourth order streams were assumed to have a stream width.